The fate of nitrogen after grassland renewal and grassland conversion to maize cropping – An investigation of N_2O processes and mineral N dynamics at the field scale

Von der

Fakultät Architektur, Bauingenieurwesen und Umweltwissenschaften

der Technischen Universität Carolo-Wilhelmina

zu Braunschweig

zur Erlangung des Grades einer

Doktorin der Naturwissenschaften (Dr. rer. nat.)

genehmigte

Dissertation

von

Caroline Buchen

geboren am 03.06.1987

aus Siegen

Eingereicht am: 23. November 2016

Disputation am: 27. Januar 2017

Berichterstatter: Prof. Dr. R. Nieder, Technische Universität Braunschweig

Prof. Dr. H. Flessa, Georg August Universität Göttingen

2017

Summary

Across Europe, an increasing demand for biomass production forces famers to optimise their grassland management. In order to improve forage quality and sward composition of unproductive grasslands, the management technique of grassland renewal is a common practice. Furthermore, large areas of grassland were converted to arable land during the last decades. The break-up of permanent grassland is associated with the release of large amounts of carbon (C) and nitrogen (N) caused by an increased mineralisation due to decomposition of soil organic matter (SOM) and the old grass sward. This additional supply of mineral N can cause enhanced N losses either in gaseous form as nitrous oxide (N_2O), an important greenhouse gas and/or as nitrate (NO_3^-) leaching. Until now, information about the persistence of this effect by using different renewal techniques (e.g. resowing, chemical and/or mechanical sward destruction) is scarce, even though this knowledge might be important for national greenhouse gas inventories. Moreover, there is an increasing need for a better understanding of processes and identification of sources of N_2O turnover following grassland break-up in order to devise mitigation options.

For this purpose, a field trial with different renewal techniques in comparison to permanent grassland and grassland conversion to maize cropping, was set up on two grassland sites (soil types: Histic Gleysol and Plaggic Anthrosol) with different SOM content and drainage regime in the north-western part of Germany. Grassland renewal was done in September 2013, while grassland conversion to maize cropping was conducted in April 2014 according to local agricultural practice.

In the first part of the study, N_2O fluxes and mineral N dynamics (0-30 cm) following grassland break-up were studied for a period of two years. In addition mineral N profiles (0-90 cm) were used to estimate the risk of NO_3^- leaching over winter. Although, no effect of the different renewal treatments on the annual N_2O emissions was obtained, grassland renewal caused elevated N_2O fluxes for a short period of two months (e.g. cumulative N_2O fluxes in the *Mechanical* treatment: 5.6±4.1 kg N ha^{-1} 2 $month^{-1}$). The risk of NO_3^- leaching however, was particularly enhanced during the first winter following grassland break-up (difference between pre-winter N_{min} and post-winter N_{min}: -80 %) especially for the sandy Plaggic Anthrosol. Grassland renewal did not lead to the potential positive yield effect.

To investigate N_2O production processes and in particular N_2O reduction to N_2 (i.e. the main end product of denitrification), the ^{15}N gas-flux method was applied *in situ*, during summer period in 2014 in the second part of the study. A fertiliser enriched in ^{15}N was injected to the soil for homogenous ^{15}N label distribution. In the following, N_2O fluxes, N_2 fluxes, mineral N and their ^{15}N enrichment were measured. High denitrification rates (N_2O+N_2 fluxes up to 83 kg N ha^{-1} within 44 days) were obtained for the Histic Gleysol while the $N_2O/(N_2+N_2O)$ ratio was mostly below 0.2. The identification of other pathways of N_2O production and consumption was uncertain, as water-saturation of the Histic Gleysol lead to heterogeneity in ^{15}N label distribution. For the Plaggic Anthrosol a higher nitrification potential (percentage of N_2O emitted from NH_4^+ oxidation per unit NO_3^- produced ranged between 0.4 to 1.8 %), along with general lower gaseous losses was obtained.

In the third part of the study, natural abundance stable isotope signatures of soil-emitted N_2O ($\delta^{15}N^{bulk}_{N2O}$, $\delta^{18}O_{N2O}$ and $\delta^{15}N^{SP}_{N2O}$ = intramolecular distribution of ^{15}N in the N_2O molecule) were used to identify sources of N_2O emission during the first year after grassland renewal (2013-2014). By using a novel isotopocule mapping approach (plotting $\delta^{15}N^{SP}_{N2O}$ vs. $\delta^{18}O_{N2O}$), the magnitude of N_2O reduction to N_2 and the fraction of microbial N_2O sources could be estimated simultaneously. Both sites indicated bacterial denitrification (heterotrophic bacterial denitrification and/or nitrifier denitrification) as the main source of N_2O production, while a significant contribution of N_2O reduction to N_2 was confirmed. Moreover, nitrification and/or fungal denitrification also contributed to N_2O fluxes to some extent. As both, the isotopocule approach and the ^{15}N tracing study were conducted simultaneously a comparison of the isotopocule approach was possible for two single samplings, as conditions of soil moisture, NO_3^- availability and N_2O flux were similar.

It was shown, that the persistence of the grassland renewal effect on N_2O fluxes did not last for a period longer than two months for the two investigated sites. For that period, isotopocule data indicated that N_2O emissions were mainly driven by bacterial denitrification with partial N_2O reduction to N_2. A potential risk of NO_3^- leaching was present for the sandy soil, in particular during the first winter following grassland break-up. With respect to N_2O mitigation and the prevention of NO_3^- leaching, a rapid development of the new grass sward (i.e. acting as a considerable N sink) is recommended to avoid N losses. However expenses, consequences and necessity of grassland renewal should be carefully considered.

Zusammenfassung

Grünlandflächen werden in Europa immer intensiver genutzt, um dem erhöhten Bedarf an Biomasse gerecht zu werden. Dies ist nur durch eine Verbesserung des Grünlandmanagements zu erreichen. Grünlanderneuerung ist eine weit verbreitete Maßnahme, die zu einer Verbesserung der Grünlandzusammensetzung, der Beseitigung von Narbenschäden und zur Steigerung der Futterqualität in unproduktiven Grünländern angewendet wird. Des Weiteren wurde in den vergangenen Jahren vermehrt Dauergrünland für den Energiepflanzenanbau umgebrochen. Die mechanische Bearbeitung von Grünlandböden kann jedoch hohe Kohlenstoff- und Stickstoffverluste (C- und N-Verluste) zur Folge haben. Gesteigerte Mineralisation durch den Abbau organischer Bodensubstanz und der alten Grasnarbe begünstigt vor allem N-Verluste in Form des klimarelevanten Treibhausgases Lachgas (N_2O) und/oder Nitratauswaschung (NO_3^-). Bisher gibt es jedoch über die Dauer des beschriebenen Effektes, sowie den Einfluss unterschiedlicher Techniken der Grünlanderneuerung (z.B. Nachsaat, chemische und/oder mechanische Zerstörung der Grasnarbe) nur wenige Informationen. Insbesondere für die nationale Treibhausbilanzierung ist es jedoch von Bedeutung, die Prozesse der N_2O Umsetzung und ihre Quellen zu kennen und zu erfassen, da sich nur so Maßnahmen zur Emissionsminderung ableiten lassen.

Zu diesem Zweck wurde in Norddeutschland ein Feldversuch angelegt, bei dem verschiedene Grünlanderneuerungstechniken mit Dauergrünland und Grünlandumbruch mit anschließender Maisnutzung verglichen wurden. Dafür wurden zwei Grünlandflächen mit unterschiedlichen Bodentypen (Plaggenesch und Anmoorgley) gewählt. Diese unterscheiden sich im Gehalt an organischen Bodensubtanz und dem Grundwassereinfluss. Die Grünlanderneuerung wurde im September 2013 durchgeführt, der Umbruch zu Mais erfolgte zum Zeitpunkt der nächsten Maisaussaat (April 2014).

Im ersten Teil der Studie wurden N_2O Flüsse und die Dynamik des mineralischen N (0-30 cm) über einen Zeitraum von zwei Jahren untersucht. Zusätzlich wurden N_{min} Profile (0-90 cm) genutzt, um den N-Verlust über Winter zu quantifizieren und das Risiko für eine mögliche NO_3^- Auswaschung abzuschätzen. Obwohl die N_2O Flüsse für einen kurzen Zeitraum (2 Monate) nach der Grünlanderneuerung erhöht waren (z.B. kumulative N_2O Flüsse in der *Mechanische* Variante: 5.6±4.1 kg N ha^{-1} 2 $Monate^{-1}$), konnte kein Jahreseffekt festgestellt werden. Im ersten Winter nach dem Aufbrechen der alten Grasnarbe trat jedoch insbesondere für den Plaggenesch ein erhöhtes Risiko für NO_3^- Auswaschung auf, welches sich im N_{min} Verlust über Winter (Differenz zwischen Frühjahr und Herbst N_{min}: -80%) zeigte. Eine mögliche Ertragssteigerung infolge der Grünlanderneuerung blieb hingegen auf beiden Standorten aus.

Die Untersuchung der N_2O Produktionswege und der N_2O Reduktion zu N_2 (dem Endprodukt der Denitrifikation), erfolgte unter Anwendung der ^{15}N Gasflussmethode im Feld, ab Sommer 2014 (zweiter Teil der Studie). Der ^{15}N angereicherte Dünger wurde in den Boden injiziert, um eine möglichst homogene Verteilung zu erreichen. Nach der ^{15}N Applikation wurden N_2O und N_2 Flüsse sowie der mineralische N-Gehalt und die jeweilige ^{15}N Anreicherung gemessen. Auf dem Anmoorgley konnten große N-Verluste (bis zu 83 kg N ha^{-1} innerhalb von 44 Messtagen) durch den Prozess der Denitrifikation bestimmt werden, insbesondere wenn das $N_2O/(N_2+N_2O)$

Verhältnis gering (unter 0.2) war. Die Bestimmung weiterer N_2O Produktionswege war auf dem häufig wassergesättigten Boden aufgrund der heterogenen ^{15}N Markierung mit Unsicherheiten behaftet. Für den Plaggenesch konnte ein höheres Nitrifikationspotential (Anteil des emittiertes N_2O aus der NH_4^+ Oxidation pro Einheit produziertes NO_3^- schwankte zwischen 0.4 und 1.8 %), festgestellt werden, obwohl gasförmige Verluste an diesem Standort generell geringer waren.

In der dritten Studie, wurden natürlich vorhandene stabile Isotopensignaturen im bodenbürtigen N_2O ($\delta^{15}N^{bulk}_{N2O}$, $\delta^{18}O_{N2O}$ und $\delta^{15}N^{SP}_{N2O}$ = intramolekulare Verteilung von ^{15}N im N_2O Molekül) genutzt, um Quellen der N_2O Bildung im ersten Jahr nach Grünlanderneuerung (2013-2014) zu ermitteln. Unter Anwendung eines neuen Isotopen-Mapping Ansatzes (Darstellung von $\delta^{15}N^{SP}_{N2O}$ vs. $\delta^{18}O_{N2O}$) konnten gleichzeitig die Anteile der N_2O Reduktion und der bakteriellen N_2O Bildung abgeschätzt werden. Für beide Standorte wurden bakterielle Denitrifikation (heterotrophe bakterielle Denitrifikation / Nitrifizierer Denitrifikation) als N_2O Quelle identifiziert. Es zeigte sich jedoch, dass ein hoher Anteil des emittierten N_2O zu N_2 reduziert wurde, während sich weitere Anteile auf die Prozesse der Nitrifikation und der pilzlichen Denitrifikation zurückführen lassen. Die zeitgleiche Durchführung des Isotopen-Mapping Ansatzes und des ^{15}N Markierungsversuchs, ermöglichte den ersten Vergleich des Isotopen-Mapping Ansatzes für zwei Proben im Feld bei denen ähnlichen Bodenbedingungen (Bodenfeuchte, NO_3^- Verfügbarkeit und N_2O Fluss) vorlagen.

Für die untersuchten Standorte gilt, dass Grünlanderneuerungseffekte nicht länger als zwei Monate auf N_2O Emissionen wirkten. Die Isotopendaten zeigten, dass die N_2O Emissionen vornehmlich durch den Prozess der Denitrifikation, mit teilweiser N_2O Reduktion zu N_2 gesteuert wurden. Ein potentielles Risiko für NO_3^- Auswaschung bestand besonders im ersten Jahr nach dem Aufbrechen der alten Grünlandnarbe auf den sandigen Standort. Dies zeigt, dass eine schnelle Entwicklung des neuen Pflanzenbestandes notwendig ist (Wirkung als N-Senke), um N-Verluste zu vermeiden. Daher sollte der Landwirt Aufwand, Folgen und Notwendigkeit einer Grünlanderneuerung gut abwägen.

Table of contents

Summary i

Zusammenfassung iii

Table of contents v

List of figures ix

List of tables xi

List of abbreviations xiv

Chapter 1: General Introduction 1

1.1 Grassland renewal 1

1.2 Grassland conversion to arable land 2

1.3 Impact of grassland management on N transformation processes with emphasis on N_2O production and reduction 3

1.4 Environmental variables controlling N losses soil 8

1.5 Quantification of N transformation processes at the field scale 10

1.6 Scope of this thesis and research questions 14

1.6.1 Soil mineral N dynamics and N_2O emissions following grassland renewal 15

1.6.2 Fluxes of N_2 and N_2O and contributing processes in summer after grassland renewal and grassland conversion to maize cropping on a Plaggic Anthrosol and a Histic Gleysol 16

1.6.3 Estimating N_2O processes during grassland renewal and grassland conversion to maize cropping using N_2O isotopocules 17

Chapter 2: Soil mineral N dynamics and N_2O emissions following grassland renewal 19

2.1 Introduction 20

2.2 Material & methods 24

2.2.1 Field sites and management 24

2.2.2 Measurements of site characteristics 26

2.2.3 Soil sampling and analysis 27

2.2.4 Gas sampling and analysis 28

2.2.5 Plant sampling and analysis 29

2.2.6 Unaccounted-for N of the N budget 29

2.2.7 Data treatment and statistical analysis 30

2.3 Results 33
2.3.1 Meteorological and hydrological data 33
2.3.2 Soil mineral nitrogen 34
2.3.3 N_2O emissions 38
2.3.4 Response of N_2O fluxes to soil variables 41
2.3.5 Plant growth, nitrogen uptake and yield-related N_2O emissions 42
2.3.6 Unaccounted-for N of the N budget 45
2.4 Discussion 46
2.4.1 N_2O emissions 46
2.4.2 Environmental controls and involved processes of N_2O emissions 48
2.4.3 Mineral N dynamics 50
2.4.4 Yields and plant-available nitrogen 53
2.5 Conclusions 54

Chapter 3: Fluxes of N_2 and N_2O and contributing processes in summer after grassland renewal and grassland conversion to maize cropping on a Plaggic Anthrosol and a Histic Gleysol 55
3.1 Introduction 56
3.2 Materials & methods 59
3.2.1 Study site 59
3.2.2 Experimental design and ^{15}N application 60
3.2.3 Soil sampling and analysis 61
3.2.4 Gas sampling and analysis 62
3.2.5 Data treatment and statistical analysis 67
3.3 Results 69
3.3.1 Meteorological data and environmental parameters 69
3.3.2 N_2O and N_2 fluxes and ^{15}N enrichment 70
3.3.3 Partial correlation of N_2O and N_2 emissions with soil variables 74
3.3.4 Contributing processes 75
3.4 Discussion 76
3.4.1 Impact of grassland disturbance on N_2O and N_2 fluxes 76
3.4.2 Treatment effects on type and magnitude of N_2O processes 77
3.4.3 Impact of controlling factors on N_2, N_2O fluxes and contributing processes 80

3.5 Conclusions 82

Chapter 4: Estimating N_2O processes during grassland renewal and grassland conversion to maize cropping using N_2O isotopocules 84

4.1 Introduction 85

4.2 Material & methods 88

4.2.1 Site description 88

4.2.2 Soil sampling 89

4.2.3 N_2O sampling and analysis 89

4.2.4 N_2O isotopocule sampling and analysis 90

4.2.5 Determination of precursor compounds 91

4.2.6 Data processing and statistical analysis 92

4.3 Results 98

4.3.1 Isotopocule mapping 98

4.3.2 N_2O reduction and source partitioning 99

4.3.3 N_2O+N_2 fluxes 101

4.3.4 Comparison of mean values from different Scenario variations 102

4.3.5 Partial correlation of N_2O, N_2 fluxes and fractions with soil variables 104

4.3.6 Comparison of r_{N2O} values from the ^{15}N labelling experiments and from the isotopocule mapping approach 105

4.4 Discussion 107

4.4.1 Scenario calculations and the attempt to validate the isotopocule mapping approach 107

4.4.2 Contribution of N_2O reduction to N_2 and the other source processes 110

4.4.3 Controlling factors of soil-emitted N_2O+N_2 fluxes and contributing processes ... 113

4.5 Conclusions 114

Chapter 5: Synthesis and conclusions 115

5.1 Overview of the main findings 115

5.1.1 Soil mineral N dynamics and N_2O emissions following grassland renewal 115

5.1.2 Fluxes of N_2 and N_2O and contributing processes in summer after grassland renewal and grassland conversion to maize cropping on a Plaggic Anthrosol and a Histic Gleysol 116

5.1.3 Estimating N_2O processes during grassland renewal and grassland conversion to maize cropping using N_2O isotopocules 116

5.2 Impact of grassland break-up on N_2O+N_2 fluxes, mineral N dynamics and yield 117
5.2.1 Management effects 117
5.2.2 Environmental drivers 119
5.2.3 Yield effects and famer's potential benefit 121
5.3 Determination of N_2O processes 122
5.3.1 Methodological aspects 122
5.3.2 Impact of heterogeneity at the field scale 124
5.4 Conclusions and further implications 126
References 128
Appendix A2 – Supplementary data: Soil mineral N dynamics and N_2O emissions following grassland renewal 153
Appendix A3 – Supplementary data: Fluxes of N_2 and N_2O and contributing processes in summer after grassland renewal and grassland conversion to maize cropping on a Plaggic Anthrosol and a Histic Gleysol 161
Appendix A4 – Supplementary data: Estimating N_2O processes during grassland renewal and grassland conversion to maize cropping using N_2O isotopocules 169
Danksagung 176
Curriculum vitae 178
Declaration of Authorship 180

List of figures

Figure 1-1: Major microbial N_2O transformation pathways in soil 6

Figure 2-1: Time course of (a) precipitation and air temperature, (b) groundwater level, (c) gravimetric water content and (d) soil temperature for the Histic Gleysol site 33

Figure 2-2: Time course of (a) precipitation and air temperature, (b) groundwater level, (c) WFPS and (d) soil temperature for the Plaggic Anthrosol site 34

Figure 2-3: Time course of soil NO_3^--N and NH_4^+-N content (0-30 cm topsoil layer) in all the treatments at the Histic Gleysol site 35

Figure 2-4: Time course of soil NO_3^--N and NH_4^+-N content (0-30 cm topsoil layer) in all treatments at the Plaggic Anthrosol site 36

Figure 2-5: Pre-winter (October) and post-winter (February) N_{min} contents for all treatments 37

Figure 2-6: Time course of N_2O fluxes in treatments at the Histic Gleysol site 38

Figure 2-7: Time course of N_2O fluxes in treatments at the Plaggic Anthrosol site ... 39

Figure 2-8: Unaccounted-for N of the N budget (i.e. N_{ua}, Eq. 2-1) in kg N ha^{-1} of the Histic Gleysol and of the Plaggic Anthrosol for the periods 2013/2014 and 2014/2015 45

Figure 3-1: (a, b) Soil temperature during gas sampling and daily precipitation, (c) groundwater level and gravimetric water content for the Histic Gleysol, (d) WFPS for the Plaggic Anthrosol, (e, f) NO_3-N concentration and (g, h) NH_4+-N concentration 69

Figure 3-2: (a, b) Daily $N_2fluxes_L$, (c, d) $N_2Ofluxes_{total}$, (e, f) (f_{p_N2O}) from the active labelled NO_3^- pool and (g, h) $N_2O/(N_2+N_2O)$ ratio of denitrification per treatment following ^{15}N label addition at day 0 70

Figure 3-3: ^{15}N enrichment of the labelled N pool emitting N_2 (a_{p_N2}), N_2O (a_{p_N2O}) in headspace samples and ^{15}N enrichment of NO_3^- in soil extracts (a_{NO3}-) per treatment on both soil types 72

Figure 4-1: Isotopocule map illustrating the simultaneous estimation of N_2O reduction to N_2 and other source processes 95

Figure 4-2: Isotopocule values of soil-emitted N_2O plotted per treatment in the isotopocule map ($\delta^{15}N^{SP}_{N2O}$ vs. $\delta^{18}O_{N2O/H2O}$) for a: Histic Gleysol (n=148) and b: Plaggic Anthrosol (n=129) 99

Figure 4-3: Time course of the unreduced, residual N_2O fraction (r_{N2O}) and the N_2O fraction from bacterial denitrification (f_B) based on calculations of Scenario a1 and b1 for the Histic Gleysol and the Plaggic Anthrosol 100

Figure 4-4: Time course of denitrification losses (N_2O+N_2 flux) based on calculations of Scenario a1 and b1 for the Histic Gleysol and the Plaggic Anthrosol 101

Figure 4-5: Comparison of the residual, unreduced N_2O fraction (r_{N2O}) from the ^{15}N labelling experiments (^{15}N) with the isotopocule mapping approach (Scenario a1 and b1) of the Histic Gleysol for the four parallel sampling dates in June 2014 106

Figure 5-1: Assumed N-losses (N_2O emission and NO_3^- leaching), depending on the time between cultivation and sowing of a new grass/crop after grassland break-up in comparison to permanent grassland 118

Figure A2-1: GAM model plots of log-scaled N_2O fluxes and explaining parameters 158

Figure A2-2: GAM model plots of log-scaled N_2O fluxes and explaining parameters 159

Figure A3-1: $N_2O/(N_2+N_2O)$ ratio of denitrification of each block (different colours) and the different treatments (*Control, Renewal, Maize*) over the first 23 sampling days for the Histic Gleysol 165

Figure A3-2: Model plot of the interaction term *s*(groundwater level) for the Histic Gleysol 166

Figure A3-3: Model plot of the interaction terms *s*(nitrate) and *s*(soil temperature) for the three treatments (*Control, Reseed* and *Maize*) on the Plaggic Anthrosol 167

Figure A4-1: Example of scenario variations (Scenario 1-7a and Scenario 1-7b) and the calculated residual, unreduced N_2O fractions or the fractions of N_2O from heterotrophic bacterial denitrification based on one sample of the Maize treatment (September 9, 2014) with a $\delta^{18}O_{N2O/H2O}$ value of 51.5‰ and a $\delta^{15}N^{SP}_{N2O}$ value of 20.0‰ 169

Figure A4-2: Time course of (a, b) N_2O flux from heterotrophic bacterial denitrification / nitrifier denitrification and (c, d) N_2O flux from fungal denitrification / nitrification based on calculations of Scenario a1 and b1 for the Histic Gleysol 171

Figure A4-3: Time course of (a, b) N_2O flux from heterotrophic bacterial denitrification / nitrifier denitrification and (c, d) N_2O flux from fungal denitrification / nitrification based on calculations of Scenario a1 and b1 for the Plaggic Anthrosol 172

List of tables

Table 1-1: Different strategies of grassland improvement 2

Table 1-2: Main advantages and limitations of the different isotope approaches to N_2O source partitioning 14

Table 2-1: Summary of available studies on the effect of grassland renewal on N_2O emissions and NO_3^- leaching within the first year 22

Table 2-2: Soil properties at the two experimental sites 25

Table 2-3a: Cumulative N_2O fluxes of the grassland treatments per year (September 2013 to 2014 and September 2014 to 2015). 40

Table 2-3b: Cumulative N_2O fluxes of the *Maize* treatment per cultivation period (May to October 2014 and 2015) and on an annual basis for the first year following grassland conversion to maize cropping (April 2014 to May 2015) in comparison to permanent grassland (*Control*) 41

Table 2-4: Dry matter yields (DM), plant N removal with harvested biomass, net energy yield for lactation (NEL) and NEL yield-related N_2O fluxes per treatment and year 44

Table 3-1: Mean total N_2O fluxes (N_2Oflux_{total}), N_2O fluxes (N_2Oflux_L) and N_2 fluxes (N_2flux_L) from the active labelled NO_3^- pool and the $N_2O/(N_2+N_2O)$ ratio of denitrification, calculated from the mean fluxes per plot, over a 23-day period for the Histic Gleysol and Plaggic Anthrosol 73

Table 3-2: Partial Spearman's (R^2) correlation of mean total N_2O fluxes (N_2Oflux_{total}), N_2 fluxes (N_2flux_L) and N_2+N_2O fluxes ($(N_2+N_2O)flux_L$) from the active labelled NO_3^- pool, and f_{p_N2O} with potential driving variable 74

Table 3-3: Gross nitrification rates per soil layer and average of the 5 sampling intervals for the Plaggic Anthrosol 76

Table 4-1: $\delta_0{}^{15}N^{SP}{}_{N2O}$ and $\delta_0{}^{18}O_{N2O/H2O}$ values for different N_2O production pathways with the appropriate minimum, maximum and mean of endmember values (adapted from Lewicka-Szczebak et al. (2017)) used in the isotopocule mapping approach 93

Table 4-2: Mean values of the residual, unreduced N_2O fraction (r_{N2O}), the N_2O fraction from bacterial denitrification (f_B), and the N_2O+N_2 flux for the Scenario variations (1-7) and Scenarios (a and b) for the Histic Gleysol and the Plaggic Anthrosol 103

Table 4-3: Partial Spearman's correlation coefficients (R^2) of the residual, unreduced N_2O fraction (r_{N2O}) (Scenario a1 and b1), the N_2O fraction from bacterial denitrification (f_B), (Scenario a1/b1) and the N_2O+N_2 flux and the N_2 flux (Scenario a1 and b1) with potential driving variables for the Histic Gleysol (n=136) and the Plaggic Anthrosol (n=129) 104

Table A2-1: Agricultural management of the treatments on the Histic Gleysol from June 2013 to October 2015 153

Table A2-2: Agricultural management of the treatments on the Plaggic Anthrosol from June 2013 to October 2015 155

Table A2-3a: Cumulative N fertiliser-related N_2O fluxes (N_2O per N fertiliser in %) of the grassland treatments per year (September 2013 to 2014 and September 2014 to 2015) 157

Table A2-3b: Cumulative N fertiliser-related N_2O fluxes (N_2O per N fertiliser in %) of the Maize treatment per cultivation period (May to October 2014 and 2015) and on an annual basis for the first year following grassland conversion to maize cropping (April 2014 to May 2015) in comparison with permanent grassland (*Control*) 157

Table A2-4: ANOVA table of a penalised regression generalised additive model (GAM) of log-transformed N_2O emissions depending on linear effects of treatment and block, an interaction of gravimetric water content and NO_3^- concentration per treatment and a smoother of CO_2 flux for the Histic Gleysol 158

Table A2-5: ANOVA table of a penalised regression generalised additive model (GAM) of log-transformed N_2O emissions depending on linear effects of treatment and block, an interaction of WFPS and NO_3^- concentration per treatment and a smoother of CO_2 flux for the Plaggic Anthrosol 159

Table A2-6: Calculation of the unaccounted-for N of the N budget (i.e. N_{ua}, Eq. 2-1) in kg N ha^{-1} of the Histic Gleysol and of the Plaggic Anthrosol for the periods 2013-2014 (February 2013 to October 2014) and 2014-2015 (February 2014 to October 2015) 160

Table A3-1: Soil characteristics of the studied soils at 0-30 cm depth 161

Table A3-2: Agricultural management practices at the Histic Gleysol site (Ihausen) between June 2013 and July 2014 162

Table A3-3: Agricultural management practices at the Plaggic Anthrosol site (Wehnen) between June 2013 and July 2014 163

Table A3-4: Summary of N_2O and N_2 forming processes, determined by application of the ^{15}N gas flux method *in situ* 164

Table A3-5: Mean total N_2O fluxes (N_2Oflux_{total}), N_2O fluxes (N_2Oflux_L) and N_2 fluxes (N_2flux_L) from the active labelled NO_3^- pool and the $N_2O/(N_2+N_2O)$ ratio of denitrification, calculated from the mean fluxes per plot, over a 44-day period for the Histic Gleysol and Plaggic Anthrosol 165

Table A3-6: ANOVA table of a penalised regression generalised additive model (GAM) of log-transformed $N_2Ofluxes_{total}$ depending on linear effects of treatment, block and nitrate (NO_3^--N) concentration and a smoother of groundwater level for the Histic Gleysol 166

Table A3-7: ANOVA table of a penalised regression generalised additive model (GAM) of log-transformed $N_2Ofluxes_{total}$ depending on linear effects of treatment, block and nitrate (NO_3^--N) concentration and a smoother of groundwater level for the Plaggic Anthrosol 167

Table A3-8: Gross nitrification rates per depth and sampling interval for the Plaggic Anthrosol 168

Table A4-1: Minimum and maximum values of the residual, unreduced N_2O fraction (r_{N2O}) and N_2O fraction from heterotrophic bacterial denitrification (f_B) in each Scenario (a and b) and per Scenario variation (1-7) allowing r_{N2O} or f_B values <0 or >1 170

Table A4-2: Mean values of the residual, unreduced N_2O fraction (r_{N2O}), N_2O fraction from heterotrophic bacterial denitrification (f_B) and the N_2O+N_2 flux for the scenario variations (1-7) and Scenarios (a and b) per treatment of the Histic Gleysol 173

Table A4-3: Mean values of the residual, unreduced N_2O fraction (r_{N2O}), N_2O fraction from heterotrophic bacterial denitrification (f_B) and the N_2O+N_2 flux for the scenario variations (1-7) and Scenarios (a and b) per treatment of the Plaggic Anthrosol 174

Table A4-4: Potential parameters controlling N_2O transformation processes during the ^{15}N labelling experiment (^{15}N study) and the isotopocule sampling (Scenario a1/b1) for the four parallel sampling dates in June 2014 175

List of abbreviations

General terms

Anammox	Anaerobic ammonium oxidation
ANOVA	Analysis of variance
AOA	Ammonia oxidising archaea
AOB	Ammonia oxidising bacteria
bd	Below the detection limit
C	Carbon
C_2H_2	Acetylene
$CaCl_2$	Calcium chloride
CAP	Common Agricultural Policy
CH_4	Methane
CO_2	Carbon dioxide
C_{org}	Organic carbon
DM	Dry matter
DNRA	Dissimilatory nitrate reduction to ammonium
EU	European Union
GAM	Generalised additive model
IPCC	Intergovernmental Panel on Climate Change
IUPAC	International Union of Pure and Applied Chemistry
K	Potassium
LULUCF	Land Use, Land-Use Change and Forestry
ME	Metabolisable energy
n	Sample size
N	Nitrogen
N_2	Molecular nitrogen
N_2O	Nitrous oxide
NA	Not applicable
na	Not available
nd	Not determined
NEL	Net energy for lactation
NFC	Nitrogen conversion factor

NH_2OH	Hydroxylamine
NH_3	Ammonia
NH_4^+	Ammonium
N_{min}	Mineral nitrogen
NO	Nitric oxide
NO_2^-	Nitrite
NO_3^-	Nitrate
N_{org}	Organic nitrogen
N_t	Total nitrogen
N_{ua}	Unaccounted-for N of the N budget of the vegetation period
O_2	Oxygen
P	Phosphorous
SOC	Soil organic carbon
SOM	Soil organic matter
WFPS	Water-filled pore space
WRB	Word reference base

Isotopic analysis

a	^{15}N abundance: $a^{15}N$
a_{bgd}	^{15}N abundance of non-labelled pool (atmospheric background or experimental matrix)
a_m	Measured ^{15}N abundance in total gas mixture
a_{NH4+}	^{15}N abundances in NH_4^+
a_{NO3-}	^{15}N abundances in NO_3^-
a_p	Calculated ^{15}N abundance of the labelled pool
a_{p_N2}	Calculated ^{15}N abundance of the labelled pool producing N_2
a_{p_N2O}	Calculated ^{15}N abundance of the labelled pool producing N_2O
at%	Atom percent of ^{15}N
f_B	N_2O fraction of bacterial denitrification
f_{H_N2}	N_2 fraction originating from hybrid pool
f_{H_N2O}	N_2O fraction originating from hybrid pool
f_{N_N2O}	N_2O fraction originating from non-labelled natural abundance pools, like NH_4^+ or N_{org}
f_{NH_N2}	N_2 fraction originating from non-hybrid pool

f_{NH_N2O}	N_2O fraction originating from non-hybrid pool
f_P	Gas fraction originating from the labelled pool
f_{P_N2}	N_2 fraction originating from the labelled pool
f_{P_N2O}	N_2O fraction originating from the labelled pool
n	Gross nitrification rate pro soil amount and time
N_2flux_L	N_2 flux emitted from the labelled NO_3^- pool
$N_2flux_{L\_H}$	Hybrid N_2 flux emitted from the labelled NO_3^- pool
$N_2flux_{L\_NH}$	Non-hybrid N_2 flux emitted from the labelled NO_3^- pool
N_2Oflux_{bD}	N_2O flux emitted from heterotrophic bacterial denitrification / nitrifier denitrification
N_2Oflux_{fDNi}	N_2O flux emitted from fungal denitrification / nitrification
N_2Oflux_L	N_2O flux emitted from the labelled NO_3^- pool
$N_2Oflux_{L\_H}$	Hybrid N_2O flux emitted from the labelled NO_3^- pool
$N_2Oflux_{L\_NH}$	Non-hybrid N_2O flux emitted from the labelled NO_3^- pool
N_2Oflux_{NL}	N_2O flux emitted from the non-labelled NO_3^- pool
r_{N2O}	Residual, unreduced N_2O fraction
γ_{N2}; γ_{N2O}	Mole fraction of N_2; N_2O in total gas background
δ_0	Initial isotopic signature before N_2O reduction
$\delta^{15}N^{bulk}_{N2O}$	Nitrogen isotopic signature of N_2O - average value for both N atoms
$\delta^{15}N_{NO3-}$	Nitrogen isotopic signature of NO_3^-
$\delta^{15}N^{SP}_{N2O}$	Site preference of nitrogen isotopic signature of N_2O - difference between the central ($\delta^{15}N^{\alpha}_{N2O}$) and peripheral ($\delta^{15}N^{\beta}_{N2O}$) position within the linear N_2O molecule
$\delta^{18}O_{N2O}$	Oxygen isotopic signature of N_2O
$\delta^{18}O_{NO3-}$	Oxygen isotopic signature of NO_3^-
$\delta_{soil\text{-}emitted}$	Isotopic composition ($\delta^{15}N^{bulk}_{N2O}$, $\delta^{18}O_{N2O}$ or $\delta^{15}N^{SP}_{N2O}$) of the soil-emitted N_2O
η_{red}	Net isotope effect associated with N_2O reduction

Chapter 1

General introduction

Permanent grassland refers to the following definition: “a land used to grow grasses or other herbaceous forage naturally (self-seeded) or through cultivation (sown) and that has not been included in the crop rotation of the holding for five years or more; it may include other species such as shrubs and/or trees which can be grazed provided that the grasses and other herbaceous forage remain predominant” (EU-Regulation 1307/2013 of the European Parliament and Council (2013)).

Grassland is an important landscape element throughout Europe and covers 20% of the total land area in the European Union (EU-27) (EUROSTAT, 2013). Grassland dominates the landscape in Ireland (67%), the United Kingdom (40%), and the Benelux countries (38%), while grassland accounts for 23% of the total land cover in Germany. Grasslands in Europe are essential resources of livestock farming and primary managed for feeding domestic herbivores, either directly at grazing or through forage production which is stored as hay or silage (Soussana et al., 2007). Currently, around 4.7 Mio ha of permanent grassland in Germany is used for forage production (40%) and grazing (56%), while 4% are nature conservation areas (DESTATIS, 2016).

1.1 Grassland renewal

Due to an increasing demand for biomass production from grassland systems, grassland renewal is used as a management technique in order to maintain productivity and improve forage quality. A substantial amount of permanent grassland is periodically renewed in intervals of five to ten years in north-western Europe (Velthof and Oenema, 2001; Seidel et al., 2009; Necpalova et al., 2013), but detailed data at the national level are lacking so far. The main reason for a decline in yield and quality of temperate managed grasslands is a progressive decrease during ageing due to botanical deterioration of the grass sward, resulting from either abiotic factors such as frost, drought and flooding or impermeable soil layers, soil compaction due to crossing with heavy machinery or animal trampling during wet periods, inaccurate application of organic and mineral fertilisers or damage by vertebrates or by fungal diseases (Velthof and Oenema, 2001; Reheul et al., 2007). Renewal techniques (Table 1-1) vary from minimal intervention, such as rejuvenation and improving the old sward by resowing, to chemical and/or mechanical destruction of the sward and soil structure by applying herbicide (e.g. glyphosate) followed by ploughing (Tiley and Frame, 1991). Along with an increasing

soil structure and sward destruction, the competition of the old sward decreases and inputs and costs of farmers for the implementation of a new sward increase. Therefore, the economic success of grassland renewal is only given, if the achievable benefit outweighs the involved costs (Tiley and Frame, 1991; Biegemann, 2014). Some further challenges in establishing a new high-yielding grass sward are due to prevailing weather conditions, preferable not too dry and not too moist, as well as soil conditions and sward competition. Depending on soil type, usage, sward quality and nutrient supply, a well-managed grassland can achieve an average dry matter yield (DM) between 7 to 13 t DM ha^{-1} $year^{-1}$ (Velthof et al., 2010) and up to 15 t DM ha^{-1} $year^{-1}$ on high-yielding sites in dominating grassland regions in north-western Europe.

Table 1-1: Different strategies of grassland improvement (adapted from Tiley and Frame (1991))

	Rejuvenation	Resowing	Renewal	Renewal
Old grass sward	Retained	Partially replaced	Completely replaced	Completely replaced
Destruction of old sward	None	Partial/None	Chemical	Mechanical
Soil cultivation	None or surface	None, minimum slots or strips	None or surface	Ploughed
Herbicide	Possibly selective	None or suppressants	Total sward destruction	Weed control, total sward destruction
Methods	Improved management and manuring	Oversowing or direct drilling	Oversowing or direct drilling	Tillage and sowing
Seed	None	Reduced rate	Full rate	Full rate
	Increasing disturbance of sward and soil			
	Decreasing competition from old sward			
	Increasing inputs and costs			

1.2 Grassland conversion to arable land

Apart from the destruction of permanent grassland by grassland renewal, large areas of permanent grassland have been converted to arable land during the last decades in north-western Europe (Vellinga and Hoving, 2011; Nitsch et al., 2012). Arable land was requested in order to cultivate energy maize for use in subsidised biogas production instead of being used as conserved fodder for dairy cattle (Vellinga et al., 2004; Nitsch et al., 2012). Also, farm structural change leads to higher conversion rates when grassland is rented to other farms (Osterburg et al., 2011). Within a 20-year period (1994-2014) in Germany, the area under maize cultivation increased by 74%, while the agricultural land-use of permanent grassland decreased by 10% (DESTATIS, 1995, 2016). In particular, the years after 2005 indicate a

rising pressure for the conversion of grassland to arable land, as a slightly intensified loss of grassland compared to the previous years was determined (Nitsch et al., 2012). Between 2005 and 2007, the grassland losses through grassland conversion into arable land were reported to be 3.5% in Lower Saxony (Osterburg et al., 2010). An analysis of four German federal states (Mecklenburg-Western Pomerania, Lower Saxony, North Rhine-Westphalia and Rhineland-Palatinate) has shown that, considerable grassland losses following grassland conversion to arable land occurred at a rate of -1.3% per year within the years 2005 to 2007 (Osterburg et al., 2011). During this survey, it was also observed that even within environmentally sensitive areas, such as drinking water protection areas, flood plains, peatland, valuable grassland habitats and on slopes, grasslands were converted to arable land. Yet, there are also regions where the grassland area increased during the last decades, in particular in hilly and mountainous areas of western Germany, a fact that might mask net figures on a national level (Osterburg et al., 2011). As a result of decreasing grassland areas, the common agricultural policy (CAP) of the EU extended the permanent grassland protection by cross compliance requirements (Nitsch et al., 2012). Requirements on national scale were introduced, and the ratio of land under permanent grassland in relation to the total agricultural area was permitted not to decrease by more than 5% compared to the reference year 2003 (EU-Regulation 1307/2013 of the European Parliament and Council (2013)).

1.3 Impact of grassland management on N transformation processes with emphasis on N_2O production and reduction

Grassland management practices, such as grassland renewal or even stronger intervention like grassland conversion to arable land affect the soil-water-plant-air system of grasslands in different ways. Further, soil organic matter (SOM) contents are usually higher in grassland soils than in arable soils. A meta-study for temperate regions by Poeplau et al. (2011) attributed a carbon (C) loss of 36±5% of the initial C stock (0-27 cm soil depth) following grassland conversion to arable land, where its variability is mainly driven by soil texture. Further this can be influenced by site conditions, sward age, soil properties and management practices (Hassink, 1994; Velthof and Oenema, 2001; Ammann et al., 2009; Poeplau et al., 2011). The long-term C loss due to grassland conversion to arable land, grassland break-up is associated with a significant short-term increase of nitrogen (N) and C mineralisation (MacDonald et al., 2010), which can be attributed to the physical disruption of aggregates and the destruction of the grass sward. As a consequence previously protected SOM will be decomposed, further driven by the incorporation of the biomass from the old grass sward and stubbles

(Hassink, 1994; Jarvis et al., 1996; Shepherd et al., 2001). If the amount of mineralised C and N exceeds the demand of the succeeding grass or crop, considerable N losses via nitrate (NO_3^-) leaching (Davies et al., 2001) and gaseous emissions of carbon dioxide (CO_2) , methane (CH_4) and nitrous oxide (N_2O) can occur (Velthof et al., 2010; Necpalova et al., 2013; Biegemann, 2014; Krol et al., 2016). In particular in fertilised systems, such N losses are a large environmental risk, regarding soil, water and climate protection, as well as an economical loss for the farmers, while the magnitude of those effects is site-specific.

The contribution of N_2O to the global climate change induced by human activity is well-known, as N_2O is the third most important greenhouse gas besides CO_2 and CH_4. Although the concentration of N_2O in the atmosphere is about one thousand times smaller than that of CO_2, the 100-year warming potential of N_2O is about 298 times that of CO_2 (IPCC, 2013). In addition, N_2O is a major precursor for ozone depletion (Ravishankara et al., 2009), resulting from the photo-oxidation of N_2O to reactive nitrogen (NO_x) in the stratosphere (Ussiri and Lal, 2012). Currently, the atmospheric concentration of N_2O has increased by a factor of 1.2 since the pre-industrial times (IPCC, 2013). Agriculture is the main responsible anthropogenic source of N_2O emissions, resulting from N fertilisation of soil and livestock manure (59%), while aquatic systems, (i.e. rivers, estuaries and coastal zones) contribute to indirect anthropogenic N_2O emissions due to fertiliser NO_3^- leaching and runoff (9%) (Well and Butterbach-Bahl, 2010; IPCC, 2013). Therefore, 4100 Gg N_2O-N $year^{-1}$ are attributed to the anthropogenic emissions of N_2O from agricultural systems (IPCC, 2013), while agricultural soils under grassland management account for 809 Gg N_2O-N $year^{-1}$ to the global annual emissions (Stehfest and Bouwman, 2006). For European grassland, an amount of 99 Gg N_2O-N $year^{-1}$ was calculated (Stehfest and Bouwman, 2006). A recent study evaluating N_2O emissions from European grasslands (6 sites) revealed a wide range of annual N_2O emissions ranging from 0 to 65 kg N_2O-N ha^{-1} $year^{-1}$, where the N input (i.e. N fertilisation) was the accountable driver for the largest annual emissions (Rees et al., 2013).

Until now, consequences of grassland break-up, such as greenhouse gas emissions resulting from land-use change (i.e. grassland conversion to arable land) are reported in the sector of emissions from land use, land use change and forestry (LULUCF) in the German Greenhouse Gas Inventory. However, the impact of grassland renewal is yet not completely assessed, because suitable data on greenhouse gas emissions following grassland renewal in comparison to permanent grassland as a basis for calculation are not available. Until now, only a rough estimation based on a renewal rhythm of ten years, assuming an incorporation of crop/grass

residues by taking the amount of N in below ground residues and in the above ground residues and the application of fixed default values for N_2O emission, is taken into account for calculations in the German Greenhouse Gas Inventory (Rösemann et al., 2015). A more precise estimate will become increasingly important, as the United Nations Framework Convention on Climate Change in Paris (COP 21) defined a reduction of greenhouse gases by 40% until the year 2030 compared to the reference year 1990 as one of their main climate protection goals.

To investigate N_2O emissions and develop mitigation options, it is important to know the processes of N transformation in soil. Microorganisms produce N_2O as intermediate or end product during different microbial transformation processes depending on currently prevailing conditions. Microorganisms, which are capable of N_2O production in soil could be found in various microbial groups, such as ammonia oxidising bacteria, archaea, denitrifying bacteria and fungi (Braker and Conrad, 2011). Major source processes of N_2O are autotrophic nitrification and heterotrophic denitrification (Figure 1-1), which are key transformation processes in the N-cycle (Ussiri and Lal, 2012) and contribute about approximately 70% to the global annual N_2O budgets (Butterbach-Bahl et al., 2013). However, several other processes have to be added to N_2O production pathways in soil (Figure 1-1).

Nitrification is the biological oxidation of reduced N and is favourable under oxic conditions, controlled by O_2 partial pressure, NH_3/NH_4^+ concentrations and pH in soil (Tiedje, 1988). Ammonia (NH_3) or ammonium (NH_4^+) is oxidised to the intermediates hydroxylamine (NH_2OH) and nitrite (NO_2^-) and finally to the end product nitrate (NO_3^-), whereby N_2O can be released as a by-product. This process is primarily carried out by ammonia oxidising bacteria (AOB) and archaea (AOA). More common among fungi and heterotrophic bacteria is the oxidation of inorganic and organic reduced forms of N to NO_3^- (heterotrophic nitrification) with the same intermediates. Generally, heterotrophic nitrification is considered as a less important N_2O production pathway, while under certain environmental conditions (e.g. low pH, high O_2 amount and organic material) its importance may increase (Papen et al., 1989; Wrage et al., 2001). For grassland soils, Müller and Clough (2014) concluded from results of a ^{15}N tracing model, that organic N compounds might contribute up to 50% to the total N_2O emission.

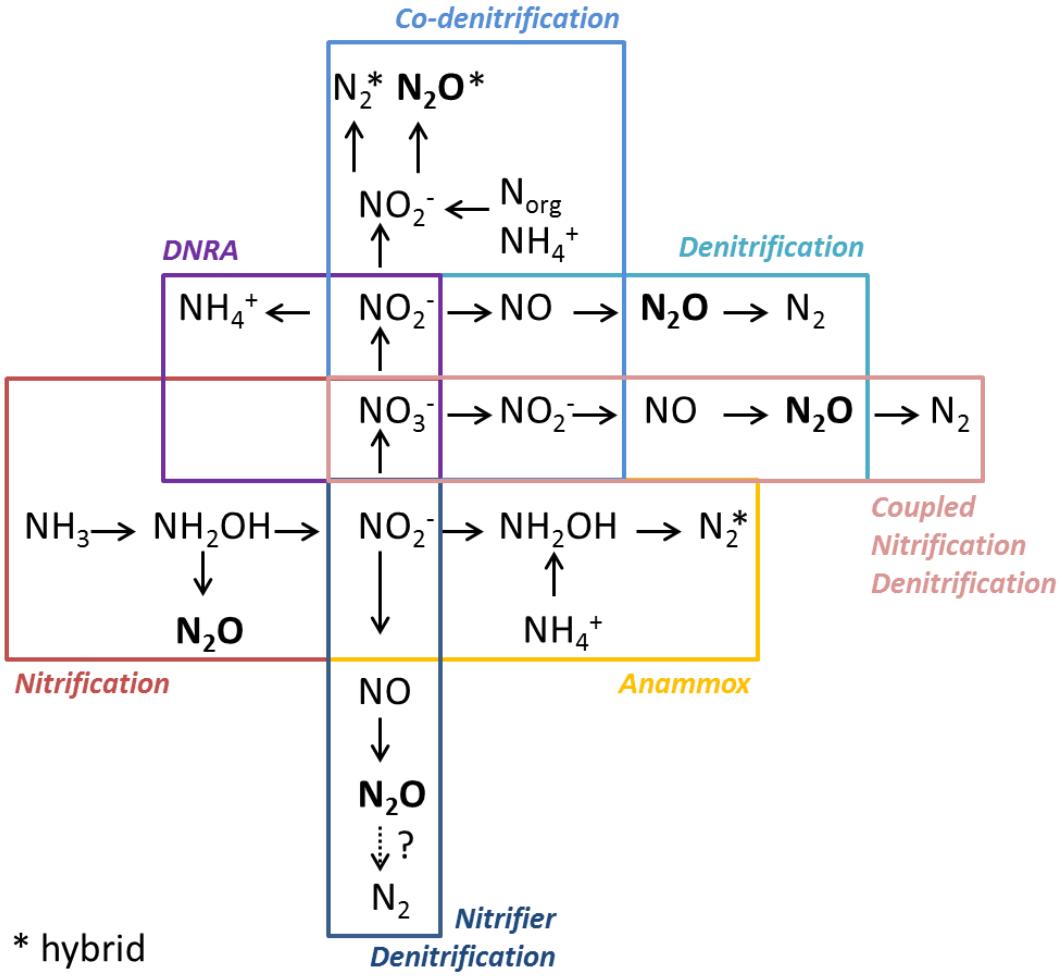

Figure 1-1: Major microbial N_2O transformation pathways in soil (adapted from Wrage et al. (2001); Philippot et al. (2007), Spott and Stange (2007))

Under anoxic conditions, denitrification, i.e. the microbial reduction of NO_3^- or NO_2^- to the gases nitric oxide (NO), N_2O and dinitrogen (N_2) (Knowles, 1982; Tiedje, 1982), is the major N_2O production pathway (Figure 1-1). Denitrification can be performed by a wide range of microorganisms (e.g. *Pseudomonas*, *Bacillus*) (Knowles, 1982), as well as fungi (Bollag and Tung, 1972) and archaea. The contribution of archaeal denitrification is mostly unknown, whereas pure culture studies revealed important insights to the fungal denitrification pathway (Sutka et al., 2006; Rohe et al., 2014), but precise information about the contribution of N_2O emissions from soils is lacking so far. Globally, it has been estimated that the soils of terrestrial ecosystems denitrify approximately 124 Tg N $year^{-1}$, or 35-40% of the total land-based reactive N sources (Seitzinger et al., 2006). For agricultural soils, high N fertiliser application rates and poor soil drainage (Hofstra and Bouwman, 2005), as well as high SOM rates in organic soils and decomposing plant residues in mineral soils (Parkin, 1987) are supposed to create denitrification "hotspots".

Under conditions, which are sub-optimal for denitrification (e.g. suboxic conditions coupled with low SOC contents and low pH values), the pathway of nitrifier denitrification can contribute substantially to the N_2O production pathways in soils (Kool et al., 2011) (Figure 1-1). During the pathway of nitrifier denitrification, NH_3 is oxidised to NO_2^- followed by the reduction to NO, N_2O and/or N_2 (Wrage et al., 2001), although there is still no evidence that ammonia oxidisers can produce N_2 during this process (Baggs and Philippot, 2010). Nitrifier denitrification is carried out by autotrophic nitrifiers and differs from coupled nitrification denitrification, where denitrifiers reduce NO_2^- or NO_3^- that was produced by nitrifiers (Wrage et al., 2001). Coupled nitrification denitrification can occur in micro environments, where conditions are suboptimal for both nitrification and denitrification, or nitrifying and denitrifying microsites are in intermediate vicinity.

Furthermore, fungi and bacteria can produce N_2O and N_2 by a hybrid reaction named co-denitrification from NO_2^- and N from another source (NH_4^+ or organic N) (i.e. co-substrate in Figure 1-1) (Spott and Stange, 2011). So far, Laughlin and Stevens (2002) showed that fungi in grassland soils may be responsible for up to 90% of the N_2O produced, which was confirmed in a recent study by Selbie et al. (2015), showing that co-denitrification can be the major N_2 production pathway in a grazed grassland.

Another anaerobic pathway of the microbial N cycle is dissimilatory NO_3^- reduction to NH_4^+ (DNRA) (Tiedje, 1988), sometimes referred as NO_3^- ammonification, fermentative NO_3^- reduction or fermentative ammonification (Rütting et al., 2011) (Figure 1-1). Redox status and C and NO_3^- availability were found to be most important environmental factors regulating DNRA, while there is prevailing evidence that a variety of soil bacteria and fungi have the ability to perform DNRA (Rütting et al., 2011). Many soil microorganisms conducting DNRA also have the capability to produce N_2O and thus if DNRA and heterotrophic nitrification are coupled, this could be also seen as an alternative pathway providing NH_4^+ production from organic matter to the mineralisation pathway (Rütting et al., 2011). Furthermore, DNRA is capable of transferring NO_3^- to NH_4^+ in the soil, similar to immobilisation und subsequent remobilisation (Rütting et al., 2011). Until know, there is given evidence that DNRA is an important N transformation process in waterlogged soils.

Besides DNRA, the pathway of anaerobic ammonium oxidation (Anammox) (Figure 1-1) where N_2 is formed as a hybrid due to a combination of two single N atoms of two different N species (NH_4^+) combined with nitrite (NO_2^-) (Spott and Stange, 2007), has been found in a number of aquatic ecosystems and waterlogged soils such as permafrost soil, rice paddy soils

and organic soils (Long et al., 2013). Due to the required conditions, anammox is likely to play just a minor role in the terrestrial N-cycle.

Together all these processes and involved microorganisms are essential to maintain the balance of mineral N production and consumption in soil, while during disturbance of grassland ecosystems due to grassland renewal and grassland conversion to maize cropping, conditions are changing and N transformation pathways can be affected. So far, knowledge about changes in underlying N processes during grassland break-up is lacking. Furthermore, N is the limiting nutrient factor for plant growth in many ecosystems, while it is continuously lost by denitrification, N-leaching and NH_3 volatilisation, so that N losses are significant factors that have to be considered in agricultural management strategies to mitigate direct and indirect N_2O emissions.

1.4 Environmental variables controlling N losses soil

For a further understanding of the N losses from soil, it is necessary to also understand the controlling variables, interacting with the above mentioned N transformation processes, as controlling variables, climatic conditions and agricultural management add further complexity.

Soil texture affects N losses in several ways. Mainly total porosity and pore size distribution are directly affected by soil texture, and thereby the diffusive transport of gases (in particular O_2) and solutes (NH_4^+, NO_3^-), as well as pore connectivity. Higher N_2O losses via denitrification and a lower NO_3^- leaching potential are attributed to fine-textured (clay-rich) soils, while NO_3^- leaching is more frequent in coarse-textured (sandy), strongly aerated soils (Velthof and Oenema, 2001).

Anoxic conditions occur, when the oxygen consumption rate exceeds the supply rate, while this rate depends primarily on the amount of available C, it is regulated by soil water availability and soil temperature (Tiedje et al., 1984). In general, the soil water content depends on the amount of water entering the soil through precipitation or irrigation and the combined effect of evapotranspiration and drainage (Ussiri and Lal, 2012), as well as the groundwater regime and thus affecting N transformation processes in soil. Thus, soil water contents can exceed field capacity, which means water movement beyond the rooting zone, so that nutrient losses through leaching can occur, in particular the NO_3^- ion can be leached out. Especially soils with a low water holding capacity, such as sandy soils are favourable to NO_3^- leaching.

Furthermore, soil water controls soil aeration, i.e. the O_2 partial pressure in the gas phase and the O_2 availability in the soil matrix (Ussiri and Lal, 2012). Thus, low N_2O emissions are found in soils with a soil water content below 40% water-filled pore space (WFPS) and good O_2 availability, while emissions increase with increasing soil moisture. Optimal conditions for nitrification are considered within WFPS values up to 50%, while N_2O emissions further increase linearly between 55-65% WFPS (Dalal et al., 2003; Ussiri and Lal, 2012). However, in water logged-soils (>90% WFPS) with low O_2 availability and restricted diffusion, N_2O production is mainly driven by denitrification with a significant contribution of N_2O reduction to N_2 (Wrage et al., 2004b; Ussiri and Lal, 2012). Thus, N_2O emissions are often undetectable, resulting from lower N_2O:N_2 ratios under such conditions. Among environmental drivers, soil moisture is often regarded as the most important one (Butterbach-Bahl et al., 2013).

Soil temperature is another important environmental variable affecting N transformation processes in soil, as microbial process rates depend on soil temperature. For N_2O emissions an exponential increase with raising soil temperatures has been shown and both nitrification and denitrification rates will increase until reaching the temperature optimum of microbial growth (Ussiri and Lal, 2012). Dalal et al. (2003) showed a sharp increase of N_2O emissions between 5 and 20 °C for temperate soils. However, significant N_2O emission peaks have been also observed for soil temperatures below 0 °C during freeze/thaw periods (Müller et al., 2003), in particular Kammann et al. (1998) accounted for 43-52% of the annual N_2O emissions from a high fertilised grassland during winter. Although during denitrification, the N_2O/N_2 ratio has been shown to decrease with increasing temperature (Keeney et al., 1979). Overall, N_2O emissions depend also on the interaction of soil temperature and soil moisture, leading to an increase in N_2O production, which was shown for permanent grasslands across Europe (Flechard et al., 2007).

Soil pH is another key regulator affecting nitrification, denitrification and their product ratio. Furthermore, soil pH affects other N transformation processes, like mineralisation and immobilisation, so that N_2O emission are also indirectly affected by pH altering the NO_3^-/NH_4^+ production and consumption (Ussiri and Lal, 2012) and thus affects nitrification due to changes in substrate availability. The optimum pH range for nitrification and denitrification is 7.0-8.0, while N_2O production is probably enhanced at a pH of 5.5-6.0 (Ussiri and Lal, 2012). Usually, high pH values lead to maximum denitrification rates, while N_2O/N_2 ratio decreases with increasing pH values (Blackmer and Bremner, 1978).

Besides the abovementioned factors, SOM contents affect N transformation processes. Grasslands are C and N rich. SOM stimulates microbial activity and thus affects N_2O emission (Ussiri and Lal, 2012). Organic C (C_{org}) provides the electron donor for N oxide reduction and indirectly affects the O_2 status of aerobic soils, as available C increases microbial respiration in aerobic soils along with a decrease in O_2 and thus creates anaerobic microsites ("hotspots") for denitrifying microorganism (Folorunso and Rolston, 1984; Parkin, 1987; Ussiri and Lal, 2012). Contrary to that, nitrification is more influenced by the availability of NH_4^+ to the nitrifiers in soil (Ussiri and Lal, 2012). Then the C/N ratio (i.e. quality of SOM) determines heterotrophic bacterial populations and their capacity to compete with nitrifiers for NH_4^+ (Ussiri and Lal, 2012).

Apart from the present N in soil, reactive N is added in form of N fertiliser to increase soil fertility in agricultural soils or is naturally derived from atmospheric deposition or N_2 fixation. Generally, N_2O emissions increase with increasing N input (Bouwman, 1996; Bouwman et al., 2002).

Although the influence of the mentioned environmental control variables of N transformation processes have been studied in numerous experiments, the understanding of N_2O turnover and the corresponding production processes at field scale, in particular under different management options (e.g. grassland renewal), where all parameters mutually influence each other, is still incomplete (Butterbach-Bahl et al., 2013).

1.5 Quantification of N transformation processes at the field scale

In the present thesis, quantification of N_2O production and consumption is based on the static closed chamber technique and as methodological considerations are not addressed within the individual research papers (see Chapters 2 to 4); a brief overview is given here.

The principle of the static closed chamber technique is an accumulation of soil-emitted gases (here: N_2O, N_2) using an enclosure within a certain time frame. The concentration increase in the chamber is measured at different time points to further calculate a flux rate, by taking air temperature and pressure into account (Hutchinson and Mosier, 1981). This measurement technique is widely used for quantification of N_2O fluxes in field studies, since it is simple to use, inexpensive and is suitable to determine treatment effects as well as to carry out specific process based studies, if it is combined with stable isotope methods (Butterbach-Bahl et al., 2013). Nevertheless, the static closed chamber technique has several shortcomings. Due to a limited covering of the soil surface with the chamber (usually less than 1 m^2), spatial

heterogeneity is often not sufficiently represented (Butterbach-Bahl et al., 2013). We used four chambers (length: 64 cm, width: 48 cm, height: 30 cm) in a randomised block experiment with five treatments to overcome this problem. Nevertheless, small-scale heterogeneity in soil properties and environmental conditions (e.g. soil moisture, nutrient availability) can result in increased uncertainty in the determination of soil-emitted N_2O and N_2 (Chapter 2 and 3). Furthermore, insertion of the chamber bases (collars) goes along with destruction of living grass and root material. To avoid those, collars remained in the soil as long as management was possible without removing. Only for grassland break-up and grass cut, the collars had to be removed. Moreover, the present spatial and temporal variability of N_2O and N_2 fluxes is hard to cover by manual chamber sampling. Therefore, we sampled weekly and with a higher frequency following grassland break-up and during the ^{15}N tracing study to cover peak emission periods (Flessa et al., 2002), as these periods are often associated with highly variable fluxes (Butterbach-Bahl et al., 2013). Using automatic chamber systems might overcome the problem of temporal resolution, but this technique is quite costly. The use of micrometeorological methods (e.g. Eddy covariance or gradient techniques) in conjunction with laser techniques allow the determination of short-term variability of fluxes and is a useful method to integrate over larger areas and supply much higher time resolution (Butterbach-Bahl et al., 2013). But this technique is not appropriate for plot trials, as large homogeneous surfaces are required and the sample size (n) is only one. Therefore, chamber-based flux measurements remain as the method of choice in research questions with several different treatments.

To understand the contribution of different N_2O processes and sources to the total N_2O flux, analysis of the isotopic composition of N_2O can be a useful tool (i.e. isotope tracing as well as natural abundance stable isotope signatures of soil-emitted N_2O). Stable isotopes are forms of the same element that differ in the number of neutrons in the nucleus and thus in the mass (Fry, 2006). As N_2O contains two elements (N and O) which in turn encompass several stable isotopes, it can be used for isotopic analysis. N naturally occurs with mass 14 (^{14}N, natural abundance of 99.64%) – referred to as light (“light”) isotope, and mass 15 (^{15}N, natural abundance of 0.36%), the high mass (“heavy”) isotope (Fry, 2006). For O, three stable isotopes exist which differ in their natural abundance: ^{16}O (99.76%), ^{17}O (0.04%) and ^{18}O (0.20%) (Fry, 2006). Thus, isotope studies can use the isotopic fractionation resulting from the favouring of ^{14}N and ^{16}O (isotopes with lower mass) relative to ^{15}N and ^{18}O (isotopes with higher mass) during the turnover of N compounds to differentiate between certain biological processes (Baggs, 2008). This means for N_2O isotopes that $^{14}N^{14}N^{16}O$ molecules with lower mass are more reactive and less bonded compared to molecules with higher mass (i.e. $^{14}N^{15}N^{16}O$,

$^{15}N^{14}N^{16}O$ or $^{14}N^{14}N^{18}O$). To differ between N_2O production processes this could be used as fractionation during nitrification is generally higher than for denitrification. In reverse, this means that products that are produced during denitrification are more enriched than N_2O produced during the nitrification processes (Baggs, 2008). The heavy to light isotope ratio of N_2O isotopes ($^{15}N/^{14}N$ or $^{18}O/^{16}O$) is expressed as the relative difference between the molecules of a sample (R_{sample}) compared to the corresponding values of an international accepted standard ($R_{standard}$) (see Eq. 1-1), while these values are reported as delta-values (δ) in parts per thousand (denoted as permil ‰) (Fry, 2006).

$$\boldsymbol{\delta = \frac{R_{sample} - R_{standard}}{R_{standard}} * 1000} \qquad \textbf{Eq. 1-1}$$

In the present thesis, we used preferentially the International Union of Pure and Applied Chemistry (IUPAC) nomenclature for isotope molecules, namely the term isotopocules for "molecular species that only differ in either the number or positions of isotopic substitutions" (Toyoda et al., 2015). Furthermore, it is possible to differentiate the terms: isotopomers, which are "isomers having the same number of each isotopic atom but differing in their positions" and isotopologues which are "a molecular entity that differs only in its number of isotopic substitutions" (Toyoda et al., 2015).

In particular, the intramolecular distribution of ^{15}N in N_2O molecules allows us to differentiate between certain processes (bacterial denitrification and/or nitrifier denitrification and fungal denitrification and/or nitrification) (see Chapter 4, section 4.2.6). The ^{15}N substitution can be either in the central (α) or peripheral beta (β) position within the linear N_2O molecule (Brenninkmeijer and Röckmann, 1999; Toyoda and Yoshida, 1999). The site-specific ^{15}N distribution in N_2O is referred as "site preference" of N_2O ($\delta^{15}N^{SP}{}_{N2O}$).

$$\boldsymbol{\delta^{15}N^{SP}{}_{N2O} = \delta^{15}N^{\alpha}{}_{N2O} - \delta^{15}N^{\beta}{}_{N2O}} \qquad \textbf{Eq. 1-2}$$

Furthermore, the $\delta^{15}N$ variation of bulk N in N_2O ($\delta^{15}N^{bulk}{}_{N2O}$) is used as a parameter to infer the origin and production–consumption mechanisms of N_2O.

$$\boldsymbol{\delta^{15}N^{bulk}{}_{N2O} = \frac{\delta^{15}N^{\alpha}{}_{N2O} + \delta^{15}N^{\beta}{}_{N2O}}{2}} \qquad \textbf{Eq. 1-3}$$

Apart from using natural abundance stable isotope signatures of soil-emitted N_2O, isotope tracing can be used to quantify N transformation processes in soil. In N_2O isotope tracing studies, substrates of N_2O production, which are enriched in ^{15}N (e.g. ^{15}N labelled NO_3^- or NH_4^+) or in ^{18}O (e.g. ^{18}O labelled NO_3^- or H_2O) are applied to the soil and individual N_2O

sources can be measured *in situ* (Baggs, 2008). First of all, Hauck et al. (1958) demonstrated how the ratio of $^{14}N^{15}N$ and $^{15}N^{15}N$ of soil-emitted N_2 reflects the ratio of ^{14}N to ^{15}N in the N_2-emitting source, unless there is a random pairing of N atoms. Furthermore, Hauck and Melsted (1956) developed a method for direct quantification of denitrification in environmental samples, by adding ^{15}N labelled NO_3^- and measuring the production of enriched N_2 and N_2O in the soil. Several years later, Stevens et al. (1993) determined the mixing ratios and distribution of ^{15}N atoms in the N_2O molecule as a means to source partitioning. A random distribution of ^{15}N atoms (at% of ^{15}N in N_2O: $^{45}N_2O/^{46}N_2O = {}^{46}N_2O/^{44}N_2O$) is representative for a single N_2O source, while a non-random distribution refers to at least two sources of N_2O (Stevens et al., 1993). Using a two-source mixing model, Stevens et al. (1997) investigated the contribution of NO_3^- reduction due to denitrification and NH_4^+ oxidation (i.e. autotrophic nitrification) to N_2O emissions. By developing more complex ^{15}N tracing models using triple tracer addition, analytical (Stange et al., 2009) or numerical (Stange et al., 2013; Müller et al., 2014) approaches, the contribution of oxidation of organic N (heterotrophic nitrification) to N_2O production in soils has been shown and further insights in different N transformation pathways were given (Van Groenigen et al., 2015). However, homogenous isotopic labelling is unlikely *in situ* due to temporal and spatial variability, so that the identification of single microbial sources of N_2O production is still challenging and associated with various uncertainties (Groffman et al., 2006).

The aim of using stable isotope approaches is to better constrain the N_2O budget by the identification of sources, as this is necessary in order to develop of mitigation strategies (Baggs, 2008). Currently, stable isotope approaches have several technical and also theoretical constraints; an overview about the main advantages and limitations of the different isotope approaches (natural abundance stable isotope signatures of soil-emitted N_2O and isotope tracing) is given in Table 1-2 (Baggs, 2008).

Table 1-2: Main advantages and limitations of the different isotope approaches to N_2O source partitioning (adapted from Baggs (2008), Behrendt et al. (2015))

	Advantages	Disadvantages
Natural abundance stable isotopes ($\delta^{15}N$, $\delta^{18}O$)	• Non-invasive • Potential for source partitioning over a large scale • Less expensive than isotope enrichment approaches • Quantification of sources	• Lack of quantification • Fractionation not yet known for all processes • Fractionation may differ between different strains
Site preference ($\delta^{15}N^{SP}_{N2O}$)	• Providing greater precision than the determination of $\delta^{15}N$, $\delta^{18}O$ • Offers the potential for estimating DNRA • Possibility to distinguish between fungal and bacterial denitrification	• Lack of quantification • Inability to distinguish between bacterial denitrification and nitrifier-denitrification • Insufficient data for environmentally relevant species and strains • Variation between different microbial strains still uncertain • Limitation of source partitioning due to overlapping of $\delta^{15}N^{SP}_{N2O}$ values • Lack of standard calibration between laboratories
^{15}N tracing	• Emissions can be related to input (e.g. fertiliser) • Potential to link source partitioning to nano-scale imaging • Allows the quantification of co-denitrification • Potential for elucidating interactions with other process and cycles	• Expensive application at plot or field scale • Application of $\delta^{18}O_{H2O}$ not suitable under field conditions, only $\delta^{15}N$ possible (i.e. N fertiliser) • Obtrusive – not suitable for natural (unfertilised) systems → undesirable fertilisation effect

Until now, the quantification of the main microbial N_2O production pathways is possible by the isotope enrichment techniques, but the technical challenge remains to quantify sources at natural abundance levels in natural systems, as well as to overcome their uncertainties in source partitioning (Baggs, 2008). To overcome the limitations of each single approach, we used them simultaneously in the present study (Chapter 3 and 4) to allow a better understanding of N_2O source and turnover processes.

1.6 Scope of this thesis and research questions

Due to the potential N losses following grassland management, i.e. grassland renewal and grassland conversion to arable land, there is an increasing need to evaluate the environmental impact of grassland management practices and also to derive recommendations for actions for farmers. From a farmer's perspective, grassland management has to be beneficial. N losses

such as N_2O emission and NO_3^- leaching are regarded as either an environmental pollution that affects all of us and an economic loss of available N (i.e. soil mineral N) or of added N (i.e. N fertiliser).

The studies within this thesis were set up in cooperation with the Chamber of Agriculture in Lower Saxony in order to be close to practical experience with regard to grassland management. The development of relevant mitigation options of N_2O emission requires the understanding of environmental controls and the complexity of N transformation processes in grassland soils. Until now, knowledge about N_2O production and consumption processes following grassland break-up is rare, in particular process understanding of denitrification (especially N_2O reduction to N_2) is lacking. Moreover, many studies on N transformation in soils were only conducted under laboratory conditions. The present thesis for the first time uses ^{15}N tracing and natural abundance stable isotope signatures of soil-emitted N_2O simultaneously at the field scale to evaluate the impact under natural conditions. Two agricultural sites field differing in environmental controls (i.e. soil type, SOM content and groundwater level) in north-western Germany were chosen to determine N losses and further identify underlying N transformation processes following grassland renewal and grassland conversion to maize cropping. The main objectives of this research were:

- to determine N_2O fluxes and mineral N dynamics, as well as their controlling parameters,
- to investigate the dynamics of N_2O emission, N_2 emission, $N_2O/(N_2+N_2O)$ ratio of denitrification, contributing processes and controls, and
- to quantify soil-emitted N_2O fluxes in order to determine the relevance of N_2O turnover processes.

In the following, the different issues of each study are substantiated in detail by their corresponding hypothesis and research questions.

1.6.1 Soil mineral N dynamics and N_2O emissions following grassland renewal

So far, knowledge about the persistence of the effects of grassland renewal and grassland conversion to maize cropping is still scarce. Therefore, we measured N_2O fluxes and its controlling factors, mineral N (N_{min}) dynamics and yields following grassland renewal and grassland conversion to maize cropping over a two-year period.

- **Does the net release of N_{min} and N_2O emissions increase after grassland renewal compared with permanent grassland?**

Grassland break-up is known to increase N_2O emissions and NO_3^- leaching due to enhanced N mineralisation following decomposition of the old grass sward and stubbles. But it is still unclear, how persistent this effect is and whether an impact on the annual N_2O emissions exists. We hypothesise a long-term effect on N_2O emissions and on net release of N_{min}.

- **Do N_{min} release and N_2O emissions increase with the degree of sward and soil disturbance?**

We hypothesise an increase of N_{min} release and N_2O emissions due to the increase of sward and soil disturbance in the different treatments in the following order: keeping and improving the old sward < renewal by chemical sward destruction and direct sowing < renewal by chemical and mechanical sward destruction.

- **Are the effects of grassland disturbance larger for soils with higher SOC contents than for well-drained mineral soils?**

So far, various studies were conducted on sandy to loamy soils and the impact of important controlling variables such as SOC content and soil moisture were not evaluated. We hypothesise a stronger effect on N_2O emission from the C-rich organic soil than from the well-drained mineral soil, as these conditions are optimal conditions for denitrification.

- **Does grassland renewal lead to higher yields?**

Farmers perform grassland renewal due to botanical degradation of the sward, unfavourable soil conditions or climate based sward damages (drought or frost) to get higher dry matter yields and improved forage quality. Thus, we also expect higher yields from the renewed grasslands.

1.6.2 Fluxes of N_2 and N_2O and contributing processes in summer after grassland renewal and grassland conversion to maize cropping on a Plaggic Anthrosol and a Histic Gleysol

Although, enhanced N_2O emissions following grassland renewal and grassland conversion to maize cropping are known, knowledge about N_2O reduction to N_2 is missing so far. Moreover, the relevance of other processes contributing to N_2O production and consumption and their controls has to be further investigated. To achieve this, we used the ^{15}N gas flux method *in situ*

to quantify N_2O/N_2 fluxes and contributing processes. In addition reference data for the third part of the study (Isotopocules) were thereby produced.

- **Do denitrification losses, in particular N_2O reduction to N_2 increase due to grassland ploughing for maize cropping and renewal of grassland compared to permanent grassland?**

N_2O emissions are known to increase following grassland ploughing, so an increase of N_2O reduction to N_2 – supposed the necessary environmental conditions, such as high soil moisture and low O_2 availability are present – is excepted.

- **Which further processes contribute significantly to the N_2O production in the investigated soils?**

Various N_2O production processes apart from denitrification and nitrification can potentially occur at the investigated sites. Thus, we expect a potential contribution to N_2O fluxes from nitrification, nitrifier denitrification, heterotrophic denitrification and co-denitrification, N_2O reduction and NH_4^+ production by DNRA.

- **Are there different N_2O source processes in the two investigated soils?**

As the two investigated soil sites differ largely in their controlling factors of N transformation processes, such as organic matter content and drainage regime, we hypothesise a larger contribution of heterotrophic denitrification and N_2O reduction to N_2 at the Histic Gleysol than at the Plaggic Anthrosol.

- **Do the formation of hybrid N_2 and/or N_2O contribute to the N transformation processes?**

Formation of hybrid N_2O/N_2 through co-denitrification and/or Anammox has been shown to occur in grassland. Thus, we expect a potential contribution also for our soils, while these results could be further used to evaluate a potential bias, which might occur from non-homogeneous ^{15}N label distribution.

1.6.3 Estimating N_2O processes during grassland renewal and grassland conversion to maize cropping using N_2O isotopocules

Based on the previous applied techniques, we quantified N_2O emissions and N_2O reduction following grassland renewal and grassland conversion to maize cropping at the investigated

sites. Moreover, we were able to conduct isotopic analysis of soil-emitted N_2O to determine the relevance of N_2O turnover processes with a non-invasive method using natural abundance stable isotope signatures.

- **Is it possible to compare the results of the isotopocule mapping approach with the measured data from the ^{15}N tracing study?**

Using a novel isotopocule mapping approach, we were able to simultaneously estimate the magnitude of N_2O reduction to N_2 and the fraction of N_2O originating from the bacterial denitrification pathway. But calculations of the isotopocule mapping approach are based on endmember areas of isotopic values for the N_2O produced from different sources reported in the literature, while our ^{15}N tracing study provided independent reference data. We hypothesise, that, if environmental conditions are similar, results from the isotopocule mapping approach agree very well with results from the ^{15}N tracing study.

- **How large is the contribution of residual, unreduced N_2O fraction and bacterial/fungal denitrification to the total N_2O flux?**

Denitrification turned out to be the dominant process at the Histic Gleysol due to the high groundwater level at this site; thus we expect also a larger contribution of N_2O reduction to N_2 (i.e. residual, unreduced N_2O fraction), which was also shown in the ^{15}N tracing study. For the Plaggic Anthrosol we assume a lower N_2O reduction potential.

- **Are there seasonal changes of N_2O production?**

As seasonal changes of N_2O production due to management events and climatic changes are known, we expect increased N_2O production during the summer period (N fertilisation and grass cuts) and potentially in winter during freeze/thaw periods.

- **Is it possible to determine treatment differences using the isotopocule mapping approach?**

Since N_2O concentrations from the first and the second part of the study do not obtain any treatment differences, we expected the same using natural abundance stable isotope signatures of soil-emitted N_2O.

Applied material and methods for each study are listed in the respective Chapters 2-4. Accepted manuscripts were adapted to the format of the present thesis without changing the content of the original papers.

Chapter 2

Soil mineral N dynamics and N_2O emissions following grassland renewal

Abstract

Managed grasslands are periodically renewed in north-western Europe, primarily in response to a decline in yield and nutritive value or sward damage. Grassland conversion to arable land is also a common agricultural practice on intensively used grassland sites. However, depending on the soil and its management, grassland break-up (i.e. the destruction of the grass sward and soil disturbance) is associated with the mineralisation of soil organic nitrogen (N) and the decomposition of stubbles and roots from the old grass sward, with both leading to enhanced nitrous oxide (N_2O) emissions and nitrate (NO_3^-) leaching. Two sites were set up to investigate the effects of different grassland renewal techniques (keeping and improving the old sward, chemical sward killing and the chemical killing of the sward followed by ploughing) with grassland conversion to maize cropping and permanent grassland as the reference treatments. The sites (Histic Gleysol and a Plaggic Anthrosol) differed in their organic matter content and groundwater level. N_2O fluxes were measured weekly using static closed chambers for a period of two years. The relationship between N_2O fluxes and explanatory/controlling variables was investigated using generalised additive models (GAM). The potential NO_3^- losses *via* NO_3^- leaching were quantified by taking weekly measurements of the soil mineral N (N_{min}) from the topsoil layer (0-30 cm) and from depth profiles (0-90 cm) in the autumn (pre-winter) and spring (post-winter). The aboveground biomass in the different treatments was also measured. Grassland renewal was not a significant source of direct N_2O emissions at either experimental site during the two years of the study. There was only a short two-month period during which there were significantly increased N_2O fluxes (up to a maximum of 1.6 kg N_2O ha^{-1} day^{-1} in the Histic Gleysol) and treatment differences. N fertilisation (as reflected in the N_{min} content in soil), soil moisture, and microbial and plant respiratory activity were identified as important drivers of N_2O emission. The destruction of the old grass sward (i.e. chemical killing by herbicide application and ploughing and conversion to maize cropping) resulted in an increased net N release of N_{min} during the first year, which indicated losses *via* indirect N_2O emission and a higher risk of NO_3^- leaching, especially on the sandy Plaggic Anthrosol. No yield effects were found after grassland renewal at either site. With respect to N_2O mitigation and the prevention of NO_3^- leaching, it is recommended that the new grass sward should be rapidly established as a sink for N_{min} and that the amount of available mineralised N following grassland renewal is taken into account when applying N fertiliser, as mineralisation following sward destruction provides high amounts of plant-available N.

This chapter has been submitted and is currently under review with the reference number AGEE16485 in Agriculture, Ecosystem and Environment with a modified reference style. Authors: Buchen, C., Benke, M., Flessa, H., Fuß, R., Gensior, A., Helfrich, M., Kayser, M., Well, R.

2.1 Introduction

Grassland is one of the most important types of land use in the European Union (EUROSTAT, 2013), and it dominates the landscape in Ireland (67%), the United Kingdom (40%), and the Benelux countries (38%) and accounts for 23% of the land cover in Germany. Most of this grassland is used for livestock farming, either by grazing or cutting. To maintain productivity, many grasslands are periodically renewed at intervals of five to ten years in north-western Europe (Seidel et al., 2009; Necpalova et al., 2013). Renewal techniques vary from minimal intervention, such as improving the old sward by resowing, to the destruction of the sward and soil structure by applying a herbicide (e.g. glyphosate) followed by ploughing in Europe (Tiley and Frame, 1991). Large areas of permanent grassland have also been converted to arable land in north-western Europe during recent decades (Vellinga and Hoving, 2011; Nitsch et al., 2012). The reasons for this conversion are an intensification of dairy farming with the use of ley grass systems and the increasing production of energy crops (Vellinga et al., 2004; Nitsch et al., 2012), which have resulted in land-use changes and often include the conversion of grassland to maize cropping (Osterburg et al., 2011; Taube et al., 2014).

The organic matter and total N content are usually higher in grassland soils than in arable soils; differences in soil C and N stocks are influenced by the site conditions, sward age, soil properties and management practices (Hassink, 1994; Velthof and Oenema, 2001; Ammann et al., 2009; Poeplau et al., 2011). The conversion of grassland to arable land and the grassland renewal can increase C and N mineralisation (MacDonald et al., 2010; Velthof et al., 2010), which promotes nitrification and denitrification. This effect might be greatest for soils with high organic matter content due to the fact that the potential mineralisation is known to be high after disturbances, e.g. drainage (Eickenscheidt et al., 2014) or soil tillage (Höper, 2002). As a result of increased mineralisation, high N losses *via* nitrate (NO_3^-) leaching and gaseous emissions, particularly nitrous oxide (N_2O), can occur (Davies et al., 2001; Velthof and Oenema, 2001). N_2O is a potent greenhouse gas that contributes to global warming (IPCC, 2007). Moreover, it is a precursor to stratospheric ozone depletion (Ravishankara et al., 2009). Apart from direct N_2O emissions resulting from grassland management (i.e. grassland break-up and N fertilisation) (Velthof et al., 2010; MacDonald et al., 2011; Biegemann, 2014), indirect emissions caused by NO_3^- leaching into aquatic systems are also considered to be an important N_2O source (Well and Butterbach-Bahl, 2010). Consequently, direct and indirect N_2O emissions has to be reported in the national greenhouse gas inventories (IPCC, 2006, 2014) and shall be considered in strategies to mitigate greenhouse gas fluxes from managed grasslands.

NO_3^- leaching following grassland renewal or conversion might occur when a period of initial high mineral N (N_{min}) release coincides with no or small N uptake by plants, resulting in large amounts of pre-winter N_{min} content (Smit and Velthof, 2010; Velthof et al., 2010). This pattern may occur when the growth of the newly established swards is delayed and the amount of mineralised N is much higher than the potential plant uptake.

Some studies have already investigated the effect of grassland ploughing on NO_3^- leaching, and they have shown large NO_3^- leaching losses during the first winter following grassland renewal (Scholefield et al., 1993; Shepherd et al., 2001; Seidel et al., 2009; Hansen and Eriksen, 2016). Renewal in autumn in particular has been reported to result in strong NO_3^- leaching, at 36 to 106 kg N ha^{-1} (Francis, 1995; Seidel et al., 2009) during the first winter. Even higher NO_3^- leaching values (28 to 254 kg N ha^{-1}) have been reported after the conversion of grassland to arable land (Lloyd, 1992; Johnston et al., 1994; Francis et al., 1995; McLenaghen et al., 1996; Djurhuus and Olsen, 1997; Kayser et al., 2008), and these losses appear to be positively correlated to the grassland age (Velthof and Oenema, 2001). A summary of available studies on the effect of grassland renewal on N_2O emissions and NO_3^- leaching losses is presented in Table 2-1. Previous studies have evaluated various grassland renewal techniques ranging from either ploughing or chemical killing to chemical killing with the subsequent ploughing of the old grass sward, while there is very little knowledge of minimal procedures such as reseeding (i.e. rejuvenation). Overall, the N_2O fluxes measured within the first year after grassland renewal range between zero emissions to 29.1 kg N ha^{-1} $year^{-1}$. Unfortunately, the highest emissions of 29.1 kg N_2O-N $year^{-1}$ were determined without analysing an undisturbed control grassland treatment (Merbold et al., 2014). Thus, the part of these emissions resulting from grassland ploughing remained unknown.

Knowledge of the persistence of grassland renewal effects and the conversion to arable land on N_2O emissions is still scarce. To date, most studies have concentrated on the initial effect of grassland renewal, and they have covered only a period of less than one year (Table 2-1) (Davies et al., 2001; Pinto et al., 2004; Mori and Hojito, 2007; Cowan et al., 2016; Krol et al., 2016).

Table 2-1: Summary of available studies on the effect of grassland renewal on N_2O emissions* and NO_3^- leaching within the first year (adapted from Biegemann (2014)) (Table is continued on the next page)**

Reference	Location	Soil properties				Sward		Grassland renewal technique	Time of grassland renewal	Subsequent use	N fertilisation rate	Measuring period	N_2O losses	NO_3^- leaching losses
		Soil type	C_{org}	N_t	Soil layer	Type	Age							
			g kg^{-1}	g kg^{-1}	cm		years				kg N ha^{-1}		kg N ha^{-1}	kg N ha^{-1}
Biegemann (2014)	Kiel, Germany	Sandy loam	16	1	0-30	GC GC	16-18	Control Ploughing	S/A	GC GL	0-240	1 year	0.4-1.4 2-24	na [a]
Cowan et al. (2016)	Easter Bush, Scotland	Clay loam	nd	nd	nd	GL	20	Chemical killing, Ploughing	S	GL	70	24 weeks	1.9-2.3	nd
Davies et al. (2001)	Midlothian, Scotland	Clay loam	37-46	2	0-20	GC GC	>7	Control Ploughing	S	GC GC	0	7 weeks	0.1 1.2	nd 1-2 [a]
Krol et al. (2016)	Wexford, Ireland	nd nd nd	42 54 32	4 5 3	0-10	GL GL GL		Ploughing Ploughing Ploughing	A A A	GL GL GL	130	17 weeks	2.1 1.2 1.6	2 [b] 10 [b] 17 [b]
Merbold et al. (2014)	Chamau, Switzerland	Loam	31 [+]	3 [+]	0-10 [+]	GL	10	Ploughing	S	GL	170	1 year	29.1	nd
Mori and Hojito (2007)	Nasu, Japan	Loam	58 53	4 4	0-5	GL GL	6	Control Ploughing	A	GL GL	40	9 weeks	1-2.8 2.1-5.3	nd
Necpalova et al. (2013)	Solohead, Ireland	Clay loam	45 5	38 4	0-30	GL GL	13	Control Ploughing	A	GL GC	0	1 year	1.32 2.49	2-3 [d] 4-6 [d]
Pinto et al. (2004)	Gorliz, Spain	Sandy clay loam	19	2	0-30	GL GL	17	Control Ploughing	S	GL GL	0-15	<1 week	0-0.3 0-0.5	nd

Velthof et al. (2010)	Heino, Netherlands	Sand	22***	1	0-20	GL	10	Control		GL	150-400	1 year	1.3-2.2	73 [c]
						GL		Chemical killing	S/A	GL			4.1-9.8	130 [c]
						GL		Chemical killing, Ploughing	S/A	GL			2.0-8.9	55-130 [c]
	Marheeze Netherlands		24***	1		GL	6	Control		GL			1.0-6.1	60 [c]
						GL		Chemical killing	S/A	GL			4.5-5.3	175 [c]
						GL		Chemical killing, Ploughing	S/A	GL			2.3-7.3	53-137 [c]
	Goutum, Netherlands	Clay	38***	3		GL	8	Control		GL			0.8-3.2	43 [c]
						GL		Chemical killing	S/A	GL			9.7-11.8	106 [c]
						GL		Chemical killing, Ploughing	S/A	GL			7.3-14.4	40-89 [c]
This study	Ihausen, Germany	Peat\ Silty sand	194	14	0-30	GL	>15	Control		GL	280	1 year	3.2-9.4	26-62 [c]
						GL		Chemical killing	A	GL			5.7-10.2	72-105 [c]
						GL		Ploughing	A	GL			5.3-14.4	89-118 [c]
	Wehnen, Germany	Sand	25	2		GL		Control		GL			0.7-2.3	32-36 [c]
						GL		Chemical killing	A	GL			1.3-2.5	92-154 [c]
						GL		Ploughing	A	GL			1.5-3.5	84-132 [c]

* N_2O fluxes are from static chamber measurements with a minimum measurement interval of once per week in the **first year following renewal**, except one study with N_2O fluxes by eddy covariance (Merbold et al., 2014) and one study with N_2O fluxes as an average of static chambers, dynamic chambers and eddy covariance (Cowan et al., 2016).

** NO_3^- leaching results from suction cups [a], lysimeters [b], pre-winter N_{min} content (0-90 cm) as potential NO_3^- leaching [c], or a dense piezometer network. [d]

*** Total C in g kg^{-1}.

GC: *grass clover;* GL*: grassland;* A*: autumn* refers to August, September, and October; S: *spring* refers to March, April and May

Control: permanent grassland as a reference*;* chemical killing by glyphosate.

nd: *not determined*; na: *not available.*

[+]Soil characteristics from Roth (2006).

To evaluate the greenhouse gas impact of grassland renewal and conversion adequately, there is a pressing need for data on N_2O emissions and N losses that cover more than one year. These data are also needed for national greenhouse gas inventories. To fill this knowledge gap, two field plot experiments were set up in north-western Germany to investigate the effects of different grassland renewal techniques and grassland conversion to maize cropping on the soil N_{min} dynamics, N_2O emissions, and yields. Ideally, the timeframe of this study would be a full cycle of typical regular grassland renewal, of 5 to 10 years. In view of the limited resources, we focussed on the first two years after renewal, due to the fact that the impact on N_2O fluxes is expected to decrease with time.

The objectives of this study were as follows:

- to determine the impact of different grassland renewal techniques and grassland conversion to maize cropping on the soil N_{min} dynamics and N_2O emissions in two soils with different organic matter content and groundwater levels,
- to evaluate the impact of different grassland renewal techniques on the dry matter and N yield.

The tested hypotheses were as follows: (1) the net release of N_{min} and N_2O emissions increases after grassland renewal compared with that of continuous grassland and (2) the N_{min} content and N_2O emissions increase with the degree of sward and soil disturbance (keeping and improving the old sward < renewal by chemical sward destruction and direct sowing < renewal by chemical and mechanical sward destruction). In addition, it was hypothesised that (3) the direct N_2O emissions and net N mineralisation induced by grassland disturbance is greater for the soil with higher organic matter content than it is for well-drained mineral soils, and (4) grassland renewal leads to higher yields.

2.2 Material & methods

2.2.1 Field sites and management

Research sites

Investigations were performed on two typical grassland sites in north-western Germany, both of which are located near the city of Oldenburg in Lower Saxony (Ihausen: 53°15’ N, 7°50’ E, 2 m a.s.l. and Wehnen: 53°10’ N, 8°2’ E, 10 m a.s.l.). One site was a plaggen soil (Plaggic Anthrosol, World Reference Base for Soil Resources (WRB), IUSS Working Group (2006)), a

soil type that is characterised by relatively high soil nutrient availability and its storage capacity for water and nutrients (Giani et al., 2014). The other site was a groundwater-influenced and C-rich Histic Gleysol according to WRB (IUSS Working Group, 2006). The two soils differ in terms of their soil organic matter (SOM) content and groundwater level (Table 2-2, Figure 2-1 and Figure 2-2). The 30-year mean air temperature at the Ihausen study site is 9.5 °C and the mean annual precipitation is 752 mm (data were taken from the nearby German Weather Service station at Friesoythe). The mean annual long-term precipitation at the Wehnen site is 760 mm and the mean air temperature is 9.9 °C (data from a nearby station at the Chamber of Agriculture research site, Lower Saxony).

Table 2-2: Soil properties at the two experimental sites. The C_{org}, C/N ratio, pH and bulk density were determined from soil cores on a plot basis (n=20), except for the bulk density in the 60-90 cm layer (n=1). The texture was analysed from a single soil profile per site, but it was not determined (nd) for the organic horizon. Mean ± one standard deviation

Soil type	Depth	Sand	Silt	Clay	C_{org}	C/N ratio	pH*	Bulk density
	cm	%	%	%	g kg^{-1}			g cm^{-3}
Histic Gleysol	0-10	nd	nd	nd	196.9±96.5	13.5±1.2	5.6±0.5	0.6±0.2
	10-20	nd	nd	nd	191.2±120.3	14.3±1.7	5.5±0.3	0.7±0.3
	20-30	70	24	5	56.4±50.7	14.4±2.8	5.6±0.3	0.9±0.3
	30-60	91	6	3	7.0±5.1	15.4±3.9	6.0±0.4	1.5±0.0
	60-90	74	21	5	1.9±1.2	15.9±4.8	6.2±0.4	1.7
Plaggic Anthrosol	0-10	91	6	3	28.1±3.1	14.4±0.8	5.1±0.2	1.3±0.1
	10-20	90	6	4	22.4±3.0	14.4±0.8	5.0±0.4	1.4±0.1
	20-30	91	6	3	18.9±4.3	15.9±2.7	4.9±0.4	1.4±0.1
	30-60	93	5	2	11.5±4.1	15.9±2.3	4.8±0.2	1.4±0.1
	60-90	92	7	1	2.0±0.9	18.9±3.7	4.8±0.2	1.9

*Measured in 0.01 M $CaCl_2$

Treatments

Prior to this study, both study sites had been managed by local farmers as continuous grassland without renewal for at least 15 years. Under conventional management, the grassland in Ihausen had been cut four times per year and was fertilised with approximately 360 kg N ha^{-1} $year^{-1}$, which was provided as a mixture of organic fertiliser, i.e. cattle slurry and biogas residues. By contrast, the grassland in Wehnen had been used for grazing, with substantially less N input of 250 kg N ha^{-1} $year^{-1}$ from both organic and mineral fertiliser. In the summer of 2013, a randomised field experiment with four replicates (blocks) was established at both sites. The plot size was 90 m². The following renewal treatments, which represented common farming practices that varied from minimal intervention to a destruction of the sward and complete disturbance of the soil structure, were implemented: (i) "*Minimum*",

i.e. keeping and improving the old sward by direct sowing at 1 cm depth (100% *Lolium perenne* L.), (ii) "*Chemical*", i.e. chemical sward killing with glyphosate followed by the direct sowing of a new grass mixture (54% *Lolium perenne* L., 20% *Festuca pratensis*, 17% *Phleum pratense* L., and 10% *Poa pratensis* L.), (iii) "*Mechanical*", i.e. the chemical killing of the sward with glyphosate followed by cutting and mixing with a rotary cultivator, mouldboard ploughing (depth of 25 cm), seedbed preparation and the sowing of the new grass mixture. In addition, one further treatment representing grassland conversion to arable land was established to demonstrate the exemplary differences between grassland renewal and grassland conversion due to the different timing and intensity of plant growth, tillage and fertilisation. This treatment was established as follows: (iv) "*Maize*", i.e. the conversion of permanent grassland to maize cropping by the chemical killing of the sward with glyphosate followed by cutting and mixing with a rotary cultivator, mouldboard ploughing (25 cm depth), seedbed preparation and the sowing of *Zea mays* L. Furthermore, the (v) "*Control*" treatment is undisturbed permanent grassland. Grassland conversion to maize cropping was performed in the spring (May 2014), while grassland renewal (treatments: *Minimum*, *Chemical* and *Mechanical*) was performed towards the end of the summer (September 2013) in accordance with local practice. Maize was cultivated during the first (2014) and second (2015) years following grassland ploughing (treatment: *Maize*). In 2015, a second sowing of maize at the Histic Gleysol site was necessary in early June because the young maize plants from the sowing date in May had been damaged by complete water saturation. The *Maize* plots were left to fallow between harvests. The agricultural management at the two sites and for all the treatments was carried out with common field machinery and is given in Table A2-1 and Table A2-2 (Supplementary data). All the grassland treatments (*Control*, *Minimum*, *Chemical* and *Mechanical*) were fertilised manually with 280 kg N ha^{-1} $year^{-1}$ in the form of calcium ammonium nitrate that was split into four dressings (100, 80, 60, and 40 kg N ha^{-1}). The grassland was cut four times each year. The *Maize* plots received 150 kg N ha^{-1} $year^{-1}$ (NPK-fertiliser with 9.5% nitrate N and 15.7% ammonium N) after sowing and were harvested in October of each year.

2.2.2 Measurements of site characteristics

At the Plaggic Anthrosol site, the precipitation (mm) and air temperature (°C) were continuously recorded by a nearby weather station (that was located 500 m from the site), which was operated by the Chamber of Agriculture, Lower Saxony. The Histic Gleysol site was equipped with a weather station with an air temperature sensor at 2 m height, which took measurements at a temporal resolution of 15 minutes, and there was a rain sensor with a

temporal resolution of five minutes. At both sites, the groundwater level was monitored at a temporal resolution of 15 minutes by water level loggers (Type Diver, Eijkelkamp Agrisearch Equipment, The Netherlands) in previously installed groundwater wells. The soil temperature (5 cm depth) was measured at each plot using a hand-held digital thermometer every 20 minutes during the gas sampling procedure.

2.2.3 Soil sampling and analysis

In June 2013 (before the experiment began), the plots were sampled and one soil core was taken from each plot with a motor-driven auger (with a diameter of 8 cm) down to 90 cm depth. Each core was divided into five depths (0-10 cm, 10-20 cm, 20-30 cm, 30-60 cm and 60-90 cm). For a soil analysis of the texture and the C and N content, the samples were dried at 40 °C until reaching a constant weight and sieved to ≤2 mm. The texture was analysed according to DIN ISO 11277 with a combined sieving and sedimentation method. For the C and N analyses, the subsamples were milled and the organic C (C_{org}) and total N (N_{tot}) were measured with a C/N analyser (LECO TruMac, LECO Instruments, Mönchengladbach, Germany). To determine the soil pH, 5 g of fresh soil was shaken in 25 mL of 0.01 M $CaCl_2$ solution for one hour and measured with a pH meter (FE20, Mettler Toledo, Urdorf, Switzerland). The soil samples (0-30 cm) for determining the mineral nitrogen (N_{min}) dynamics were taken weekly to biweekly (during winter) from July 2013 to October 2015 using a Goettinger gouge auger with a diameter of 18 mm and 14 mm slot (Nietfeld GmbH, Quakenbrück, Germany). Additionally, soil samples were taken from 0-30 cm, 30-60 cm and 60-90 cm in October (pre-winter) and February (post-winter) with a Puerkhauer gouge auger (3.5 cm diameter). The pre-winter date was close to the beginning of the leaching period for each year. According to common practice in the agricultural extension services (NLWKN, 2015), the difference between the N_{min} content in the upper 90 cm soil layer pre- and post-winter was used as an indicator for NO_3^- leaching to the groundwater during the winter. Soil extracts for mineral nitrogen (N_{min} = NO_3^--N + NH_4^+-N) analysis were prepared according to VDLUFA (2002) (section 6.1.4) (600 mL of 0.0125 M $CaCl_2$ solution, 150 g of field fresh-sieved soil, shaken for 1 h, MN614 ¼ filters, Macherey and Nagel, Düren, Germany) and photometrically measured with a Nanocolor photometer (Macherey and Nagel, Düren, Germany). The soil moisture content was gravimetrically determined after drying 70 g of soil at 105 °C for 24 h. The water-filled pore space (WFPS) was calculated from the gravimetric water content and the bulk density, which had been determined for each plot from undisturbed soil samples that were taken with stainless steel cylinders (100 cm^3), and by assuming a solid

phase density of 2.65 g cm^{-3} for the Plaggic Anthrosol. The WFPS was also determined for the organic soil (Histic Gleysol), but it could not be used due to the high spatial heterogeneity in the soil organic carbon content (SOC) and uncertainties in the bulk density. Pore space estimates from intact core measurements that were taken prior to the beginning of the field experiment were not representative of samples from weekly water content measurements, and the WFPS calculated from the water content, bulk density and SOC reached values of up to 120% and were therefore considered inaccurate.

2.2.4 Gas sampling and analysis

Chamber sampling

The greenhouse gas fluxes (N_2O and CO_2) were measured weekly for all the experimental plots from July 2013 to October 2015 using the closed chamber method (Hutchinson and Mosier, 1981). The sampling frequency was increased during the first week after grassland renewal and conversion. In the *Maize* treatment, chambers were placed between the plant rows. The opaque PVC chambers (PS-plastic, Eching, Germany) were 30 cm high and covered a surface of 64 x 48 cm. Chamber base frames were permanently installed approximately 8 cm down in the soil, and they were removed only for tillage and harvest events. The chambers were ventilated with small fans to ensure the complete mixing of the gas phase. Vent tubes permitted the equilibration of the air pressure. At each sampling date, gas sampling was performed between 8 a.m. to 1 p.m., when the chambers were closed and sealed to be air-tight for 60 minutes. Chamber air samples were collected at 0, 20, 40, and 60 minutes after chamber closure by flushing the septum capped vials (each had a volume of 20 mL) with air from the chamber. A 50-fold exchange of the vial volume with chamber air was performed, along with the application of overpressure at the end, which was maintained until and checked prior to gas analysis. The chamber temperature was measured at each gas sampling.

Gas analysis

N_2O and CO_2 analyses were performed with two gas chromatographs (GC 2014, Shimadzu, Kyoto, Japan, modified according to Loftfield et al. (1997), and CP-3800 GC, Varian, Walnut Creek, CA, USA) that were equipped with ECD detectors and coupled with autosampler systems. The GC systems were calibrated for each sample run using four standard gases ranging from 300 ppb to 3,000 ppb N_2O and 350 ppm to 4,000 ppm CO_2, while the analytical precision was determined weekly by repeated measurements (ten times) of standard gases (300 ppb N_2O and 350 ppm CO_2), and it was consistently found to be <2%.

2.2.5 Plant sampling and analysis

The aboveground biomass of the grassland treatments was harvested (four cuts per year) from a representative area of 15 m² for each plot. For the *Maize* plots, two rows (>100 plants) were selected. The plant material was dried at 60 °C until reaching a constant weight for plant analysis. To determine the total dry matter (DM), subsamples of plant material were dried at 105 °C. Dry samples were ground and analysed for crude protein, utilisable crude protein, crude fibre, crude fat, crude ash, gas formation, starch content (maize), acid detergent fibre and neutral detergent fibre using near-infrared spectroscopy (NIRS) (Bruker MPA Multi-Purpose FT-NIR analyser, Rheinstetten, Germany) according to VDLUFA (2013) (section 31.2 and 31.3). The metabolisable energy content (ME) and the net energy for lactation (NEL) of the grass and maize were calculated according to GfE (2008) and Weißbach et al. (1996). The N concentration in the biomass was calculated from the crude protein using a nitrogen conversion factor (NFC) of 6.25% (Karman and Van Boeckl, 1986). The plant N removal and energy (NEL) yield in the aboveground biomass per ha were calculated from the yield data and the N and GJ NEL concentrations in the harvested biomass.

2.2.6 Unaccounted-for N of the N budget

To derive indications of the organic N mineralisation following grassland renewal and grassland conversion to maize cropping, the quantity of the initial available N_{min} recovered from the plant harvest and post-harvest in pre-winter in soil was determined. The calculation determined the unaccounted-for N of the N budget (Allison, 1955; Meisinger et al., 2008), i.e. the inputs (A) and outputs (B) from the unaccounted-for N pool including soil N_{min} in the rooting zone and harvested N.

The unaccounted-for N of the N budget for the vegetation period (N_{ua}) was determined by taking the difference between the initial N_{min} plus fertilisation (A) and the final N_{min} plus harvested N (B) as follows:

$$N_{ua} = B - A \qquad \textbf{Eq. 2-1}$$

where A is the initial amount of plant-available N_{min}, i.e. the sum of post-winter soil N_{min} at 0-90 cm depth and the added N fertiliser amount, and B is the sum of the pre-winter soil N_{min} at 0-90 cm depth in autumn and the plant N removal by harvested biomass.

If N_{ua} is positive, i.e. B is greater than A, this sign indicates that the input (e.g. atmospheric deposition and mineralisation of organic N) must exceed the N losses (gaseous fluxes,

leaching, and immobilisation into organic matter) and *vice versa*. To allow this approach, it was assumed that the amount of N stored in the grass sward did not change between spring and autumn. Positive values of N_{ua} are therefore a minimum estimate of atmospheric deposition plus net N mineralisation of organic N (i.e. gross mineralisation minus immobilisation), while negative N_{ua} values indicate unaccounted-for NO_3^- leaching and/or gaseous N losses. It should be noted that this simple estimation of N_{ua} includes a number of uncertainties and gives useful indications regarding mineralisation only if the magnitude of the unknowns can be constrained (Oenema et al., 2003; Meisinger et al., 2008).

2.2.7 Data treatment and statistical analysis

N_2O fluxes

The N_2O fluxes were calculated using linear regression, robust linear regression (Huber and Ronchetti, 1981) and Hutchinson-Mosier regression (Pedersen et al., 2010). The choice of regression method followed an algorithm as described by Leiber-Sauheitl et al. (2014), but it was based on the calculation of standard errors as corrected by the update of the HMR package to version 0.4.1 (Pedersen, 2015). As a result, almost all the N_2O fluxes were calculated linearly (Histic Gleysol: 99% and Plaggic Anthrosol: 98%).

To identify outliers, the distribution of the square roots of the flux standard error was checked (calculated from the regression). The median standard errors were 2.87 µg N_2O m^{-2} h^{-1} for the Histic Gleysol and 2.28 µg N_2O m^{-2} h^{-1} for the Plaggic Anthrosol, demonstrating the adequate accuracy of the flux measurements. Where extreme standard error values appeared, the respective fluxes were checked to verify whether they were related to problems during sampling or an absence of overpressure in the vial by the time of analysis. Because the N_2O concentrations were often near ambient concentration, CO_2 fluxes were used as an additional quality parameter for reliable gas sampling.

Flux rates were expressed as the mean (n=4) with the standard deviation of the replicated field plots. The cumulative annual N_2O emissions were calculated from the N_2O fluxes per plot using linear interpolations between two measurement dates. The period for comparing the N_2O emissions on an annual basis was set from September to September of both years for the grassland treatments (*Control*, *Minimum*, *Chemical* and *Mechanical*) because the renewal began in September 2013. For the *Maize* treatment only, the cultivation period from May to October of each year was actually comparable because the *Maize* plots had been kept as grassland until conversion in April 2014, and they were left fallow after harvest until the next

sowing in April 2015. However, to assess the N_2O losses from grassland conversion to maize cropping as an agricultural system (grassland-maize-fallow), the average losses from April 2014 to May 2015 were calculated. For the same periods, N fertiliser-related N_2O fluxes were also calculated, which was relevant because the N fertilisation was not the same for all the treatments. To compare the N_2O fluxes in relation to the harvested biomass, NEL yield-related N_2O fluxes were calculated because the yield-related emissions are more relevant than area-related fluxes in terms of life cycle assessments of agricultural systems and products (Küstermann et al., 2013). The net energy lactation (NEL) was used as the reference to provide a comparison between the grassland (*Control, Minimum, Chemical* and *Mechanical*) and *Maize* treatments because NEL is a comparable energy value for dairy cattle feeding.

Statistical analysis

Statistical analyses were performed using R 3.2.1 (R Development Core Team, 2016). An analysis of variance (ANOVA) was conducted to analyse the effects of the treatment and year (treatments: *Control*, *Minimum*, *Chemical*, and *Mechanical*) and/or cultivation period (treatments: *Control* and *Maize*) on the cumulative N_2O fluxes, N fertiliser-related N_2O fluxes and the N_{ua} values. Where ANOVA indicated the differences, Tukey's HSD test was used as a *post hoc* evaluation for pair-wise comparisons of all the tests. The variance homogeneity and approximate normality of the residuals were checked by diagnostic plots.

To identify a change in the N_{min} content (0-90 cm) during the winter (i.e. the difference between pre-winter N_{min} and post-winter N_{min} values for the respective winters of 2013/2014 and 2014/2015) in individual treatments, a pairwise t-test was applied. Furthermore, the differences in pre-winter N_{min} content (0-90 cm) were compared between the treatments for the samples from 2013, 2014 and 2015. To ensure a multiple testing correction, the p-values were adjusted for the false discovery rate according to Benjamini and Hochberg (1995).

To analyse the effects of the treatment and year on the DM yield, plant N removal, energy (NEL) yield and NEL yield-related N_2O fluxes for the grassland plots, a two-factorial ANOVA was calculated. The *Maize* plots were compared per harvest year on the basis of the plant N removal, energy (NEL) yield and NEL yield-related N_2O fluxes.

For all the tests, the significance level was set to $p \leq 0.05$.

Generalised additive models

To investigate the relationship of N_2O fluxes to explanatory variables, generalised additive models (GAM) were applied, as implemented in the R package *mgcv* version 1.8-11 (Wood and Augustin, 2002; Wood, 2011). These models can test non-linear relationships in a non-parametric way by fitting additive smoother terms in which the degree of smoothing is determined by the penalised maximum likelihood estimation. The N_2O fluxes were log transformed, which is a common prerequisite for analysing N_2O data due to its skewed distribution (Folorunso and Rolston, 1984). Additionally, an offset of 20 µg N_2O m^{-2} h^{-1} was used to keep most of the negative fluxes in the dataset, except for the three most negative fluxes of the Histic Gleysol because they most likely represent the variation around zero resulting from measurement uncertainty. The three removed fluxes were regarded as the possible true N_2O uptake, and it was considered unlikely that the uptake could be explained by the same relationships as the emissions. However, three values were not sufficient to model the uptake adequately.

The model quality was assessed using diagnostic plots with a focus on variance homogeneity and the approximate normality of residuals and using diagnostic checks (as implemented in the R package), which test whether the basis dimension for the smooths is adequate. NO_3^--N content and soil moisture (i.e. WFPS for the Plaggic Anthrosol and gravimetric water content for the Histic Gleysol) were included as model parameters because they are known to be key controls of N_2O fluxes. Moreover, we also included the CO_2 flux as a proxy for microbial and plant respiratory activity (Deppe et al., 2016), due to the fact that the related O_2 consumption affects N_2O fluxes as a result of the O_2 impact on nitrification and denitrification dynamics. The inclusion of the NH_4^+-N content, soil temperature, and the groundwater level (available once per site), did not improve the model. An attempt was also made to fit a GAM with a power variance function, as implemented in the R package *nlme* version 3.1-124 (Pinheiro and Bates, 2000), to offer a better explanation for the large variation in high N_2O fluxes. This finding resulted in a shift of the NO_3^- and soil moisture optima to higher NO_3^--N content, but it did not improve the model; therefore, the data are not shown.

2.3 Results

2.3.1 Meteorological and hydrological data

At the Plaggic Anthrosol site, the annual precipitation during the hydrological year (1 November to 30 October) was 648 mm in 2014 and 736 mm in 2015. For the Histic Gleysol, the values were 732 mm in 2014 and 668 mm in 2015. Both winters were relatively mild, with only 18 days (winter 2013/2014) or six days (winter 2014/2015) when the mean air temperatures were below 0 °C. The minimum recorded temperature at 5 cm soil depth was 0 °C at both sites.

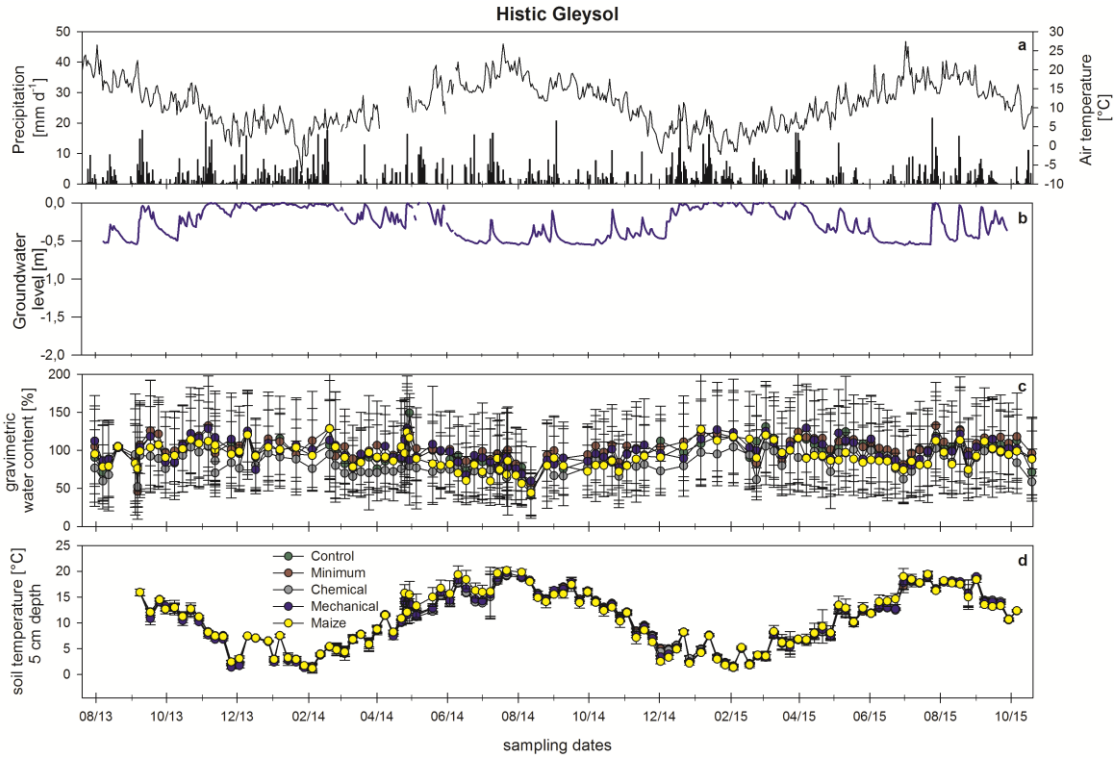

Figure 2-1: Time course of (a) precipitation and air temperature, (b) groundwater level, (c) gravimetric water content and (d) soil temperature for the Histic Gleysol site. Error bars indicate the standard deviations of the mean (n=4)

The Histic Gleysol was characterised by a high groundwater level of -0.5 m to 0 m (Figure 2-1). This level resulted in high water saturation in the topsoil for extended periods, leading to gravimetric water content of up to 200% on some sampling days. Differences in the gravimetric soil water content between treatments were not significant. In the Plaggic Anthrosol, the groundwater level varied between -2.5 m in the summer and autumn to -0.9 m during the winter. The soil WFPS at this site ranged between 20 and 60% in all the treatments.

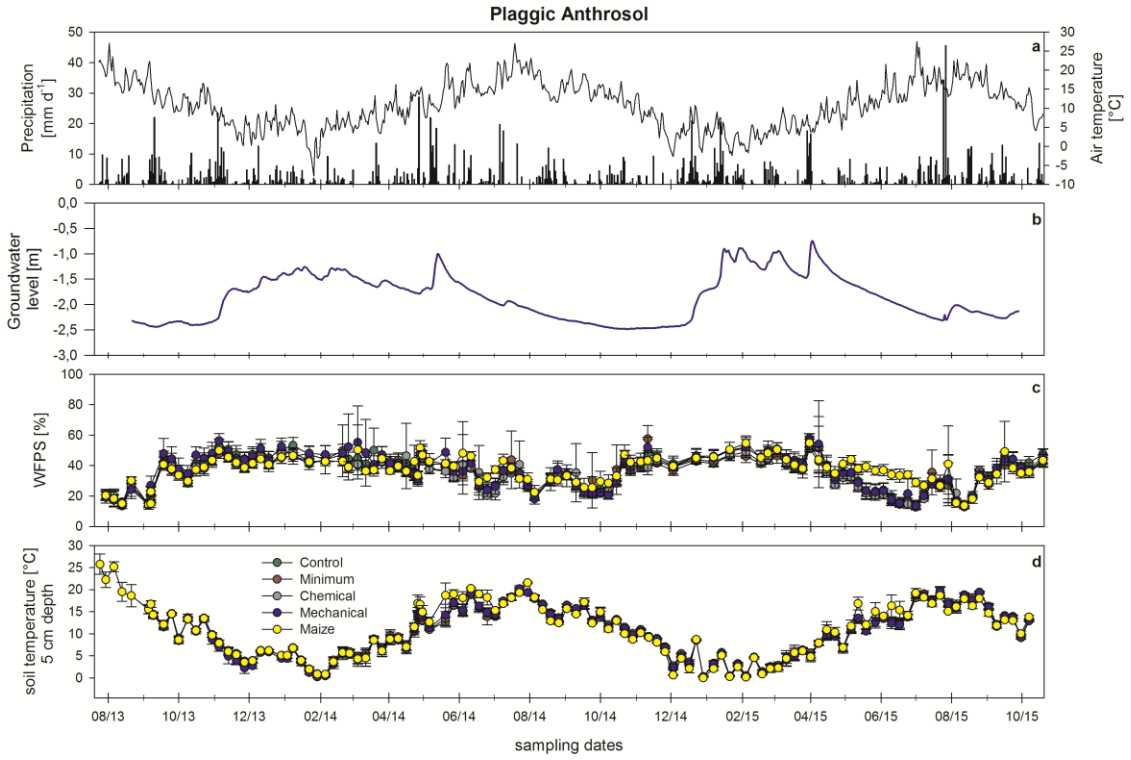

Figure 2-2: Time course of (a) precipitation and air temperature, (b) groundwater level, (c) WFPS and (d) soil temperature for the Plaggic Anthrosol site. Error bars indicate the standard deviations of the mean (n=4)

2.3.2 Soil mineral nitrogen

The dynamics of the soil mineral N (N_{min}) content in the 0-30 cm topsoil layer are shown in Figure 2-3 for the Histic Gleysol and in Figure 2-4 for the Plaggic Anthrosol. The N_{min} content (0-30 cm) increased following grassland renewal (*Minimum*, *Chemical* and *Mechanical* treatments) in the autumn of 2013. For the Plaggic Anthrosol, the NO_3^--N content in particular was elevated for the first two months after grassland renewal, resulting in greater N_{min} content of 47±17 kg N ha^{-1} in the *Chemical* treatment and 53±14 kg N ha^{-1} in the *Mechanical* treatment than the 17±7 kg N ha^{-1} in the *Control* plots. The NO_3^--N content (0-30 cm) from the Histic Gleysol strongly varied between the four replications per treatment, while the differences between the treatments were relatively small. For the period from September to October 2013 (i.e. the period after grassland renewal), the N_{min} content (0-30 cm) amounted to 51±20 kg N ha^{-1} on average in the *Chemical* treatment, 46±18 kg N ha^{-1} in the *Mechanical* treatment and 32±17 kg N ha^{-1} in the *Control* treatment.

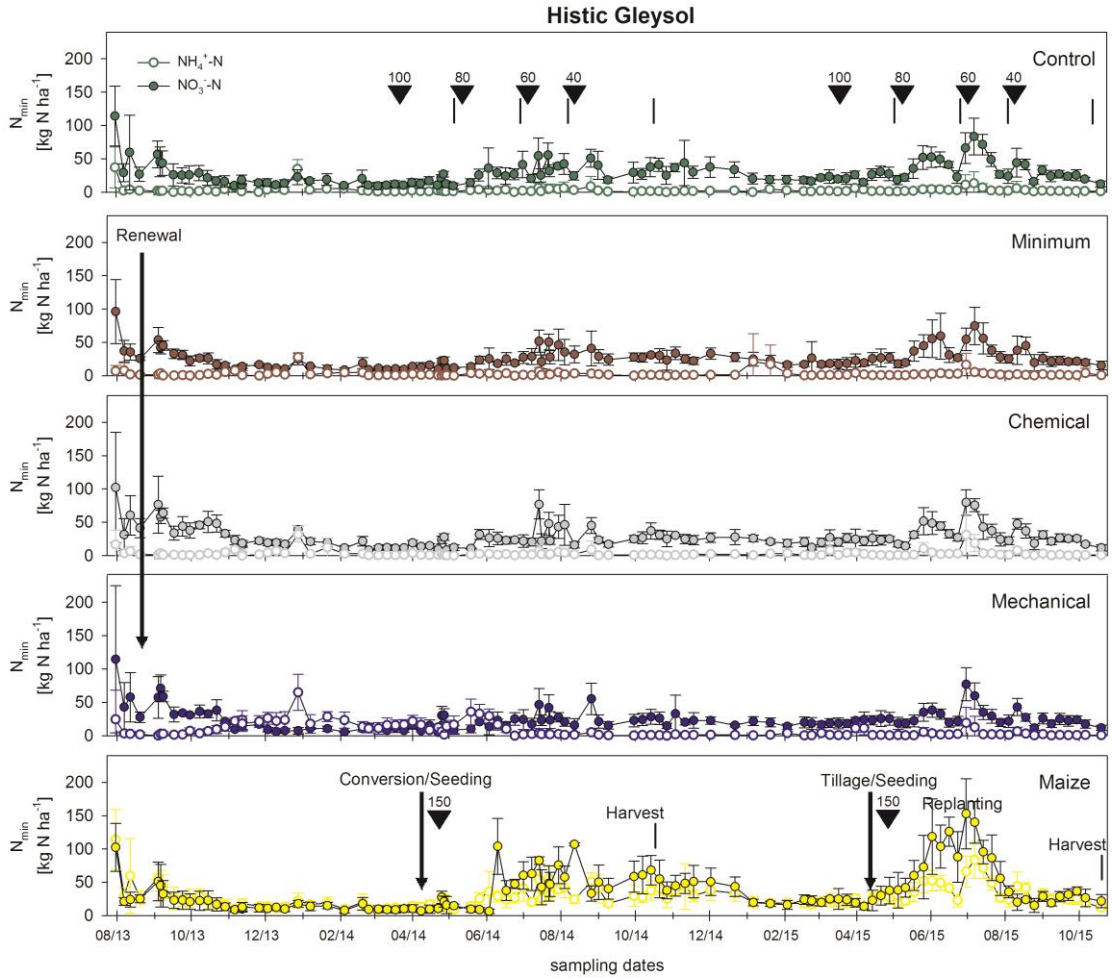

Figure 2-3: Time course of soil NO_3^--N and NH_4^+-N content (0-30 cm topsoil layer) in all the treatments at the Histic Gleysol site. Dates of N fertilisation (black triangles with kg N ha^{-1}) and grass cuts (black lines) were the same for the following treatments: *Control, Minimum, Chemical* and *Mechanical,* which are shown for illustration purposes only in the first panel. N fertilisation was different for the *Maize* plots. Error bars indicate the standard deviations of the mean (n=4)

Grassland conversion to maize cropping in combination with N fertilisation at 150 kg N ha^{-1} in the spring of 2014 led to the highest N_{min} content in the 0-30 cm soil layer in both soils, while a lag time of approximately 1.5 months was obtained. The NO_3^--N content (0-30 cm) in the *Maize* plots increased by up to 104±41 kg N ha^{-1} in the Histic Gleysol and by 175±23 kg N ha^{-1} in the Plaggic Anthrosol. In 2015, the increase in N_{min} content (0-30 cm) after grassland break-up, maize planting and N fertilisation occurred earlier and was stronger, but it also decreased more quickly than in 2014. Generally, the application of N fertiliser led to short-lived peaks in the N_{min} content (0-30 cm) in all the treatments.

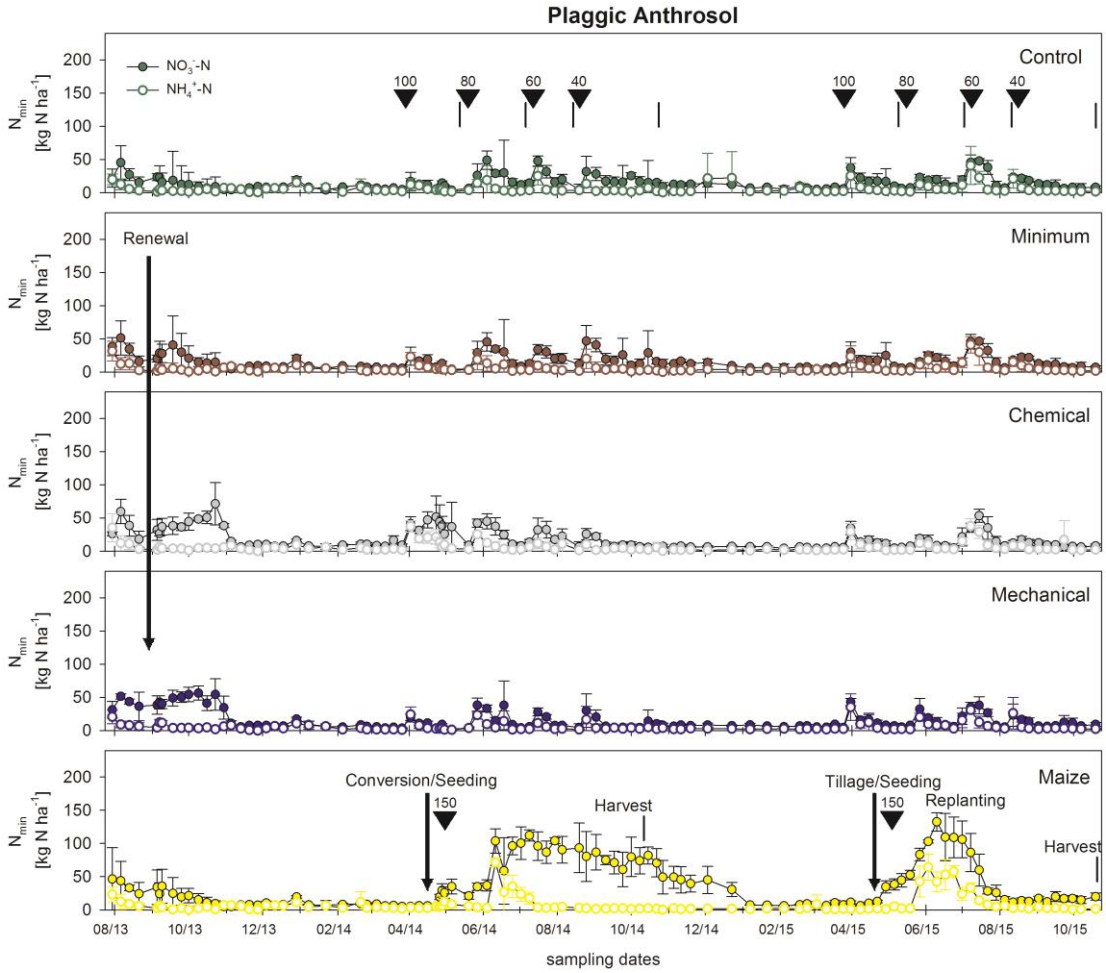

Figure 2-4: Time course of soil NO_3^--N and NH_4^+-N content (0-30 cm topsoil layer) in all treatments at the Plaggic Anthrosol site. Dates of N fertilisation (black triangles with kg N ha^{-1}) and grass cuts (black lines) were the same for the following treatments: *Control, Minimum, Chemical* and *Mechanical,* which are shown for illustration purposes only in the first panel. The N fertilisation was different for the *Maize* plots. Error bars indicate the standard deviations of the mean (n=4)

Depth profiles of N_{min} from 0-90 cm were taken pre-winter in autumn (October), close to the start of the leaching period, and post-winter, in the spring (February) of both years (Figure 2-5). In the first pre-winter sampling (2013) after grassland renewal, the *Chemical* and *Mechanical* treatments showed high N_{min} content (0-90 cm) at both sites. At the Plaggic Anthrosol site, the pre-winter N_{min} content (0-90 cm) of these treatments (88±7 and 104±11 kg N ha^{-1} for the *Chemical* and *Mechanical* treatments, respectively) was significantly higher than that of the *Control* treatment (44±5 kg N ha^{-1}) (see * in Figure 2-5). Furthermore, the change in N_{min} content during the winter (i.e. the difference between pre-winter N_{min} and post-winter N_{min} content) was considerable, and the pre-winter N_{min} content (0-90 cm) was reduced by 80% (see arrows in Figure 2-5). At the Histic Gleysol site, the N_{min} content (0-90 cm) was generally lower than that for the Plaggic Anthrosol. However, the pre-winter N_{min} content (0-90 cm) of the *Chemical* and *Mechanical* treatments during the first year of grassland renewal was

significantly greater than that for the *Control* plots. The decline in N_{min} content (0-90 cm) over the winter was also significant here for the *Chemical* and *Mechanical* treatments.

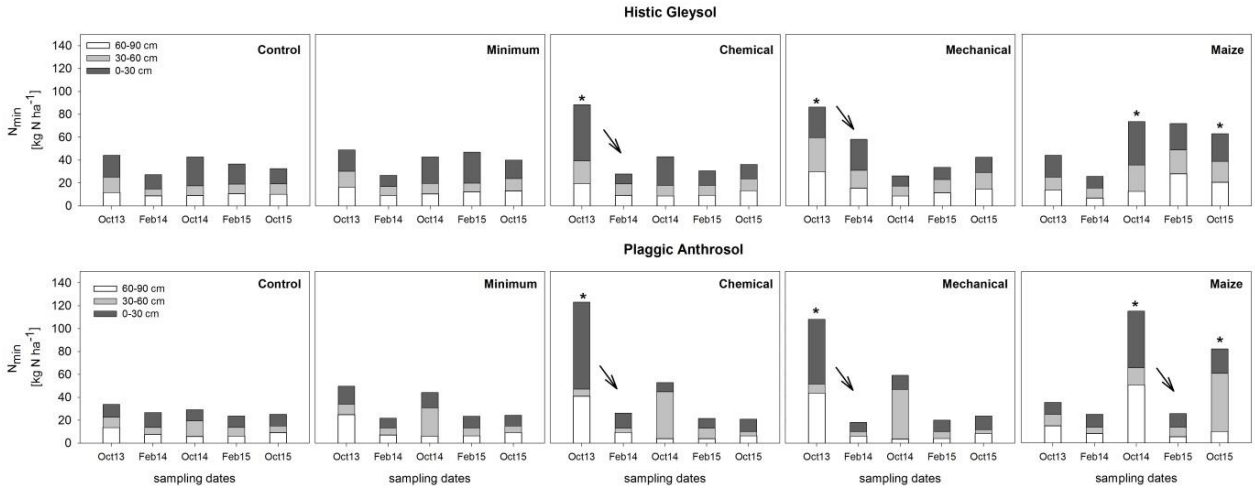

Figure 2-5: Pre-winter (October) and post-winter (February) N_{min} content for all treatments (n=4). Various colours are used for the different soil depths (0-30, 30-60 and 60-90 cm). Significant differences in pre-winter N_{min} content between the treatments are marked by *. Arrows indicate a significant change in the N_{min} content over the winter for the respective treatments.

The conversion of grassland to maize cropping in 2014 led to increased N_{min} content (0-90 cm) after harvest at both sites. At the Plaggic Anthrosol site, a significant decline between the pre-winter N_{min} content (2014) and post-winter N_{min} content (2015) was obtained, while this pattern was not found for the Histic Gleysol. At the Histic Gleysol site, the N_{min} content (0-90 cm) varied at the same elevated level of 69±30 kg N ha^{-1} from October 2014 to October 2015.

2.3.3 N_2O emissions

The N_2O emissions differed significantly between the two investigated soils (Table 2-3a and 2-3b), with a generally higher level at the Histic Gleysol. At this site, the *Mechanical* treatment showed a distinct N_2O emission peak (single N_2O fluxes up to 1.6 kg N ha^{-1} day^{-1}) following grassland renewal in September of 2013 (Figure 2-6).

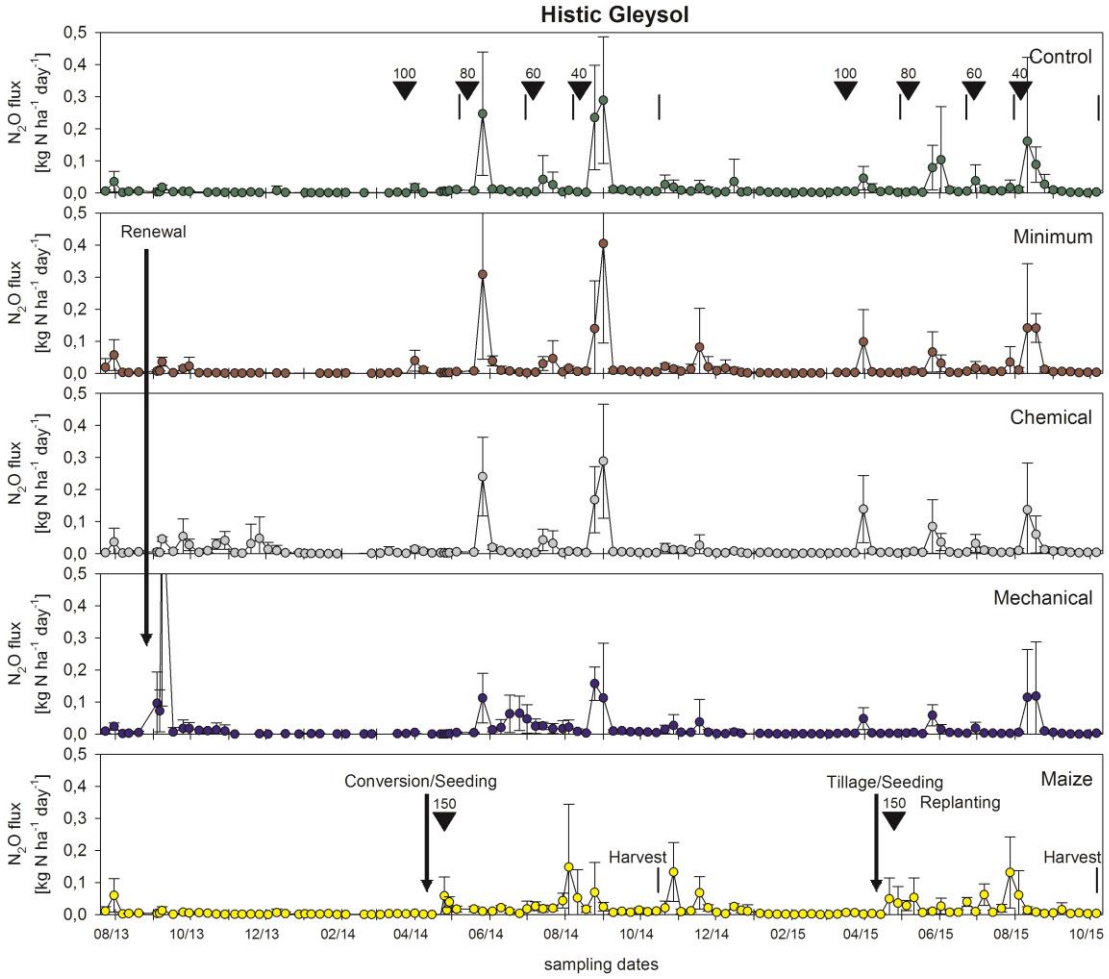

Figure 2-6: Time course of N_2O fluxes in treatments at the Histic Gleysol site. Dates of N fertilisation (black triangles with kg N ha^{-1}) and grass cuts (black lines) were the same for the following treatments: *Control, Minimum, Chemical* and *Mechanical,* which are shown for illustration purposes only in the first panel. The N fertilisation was different for the *Maize* plots. Error bars indicate the standard deviations of the mean (n=4)

This response was not observed in the *Minimum* and *Chemical* treatments. In the Plaggic Anthrosol, the N_2O fluxes following grassland renewal increased, but at a lower level of up to 0.02±0.01 kg N ha^{-1} day^{-1} in the *Chemical* and *Mechanical* treatments (Figure 2-7). Its background fluxes were also generally lower than those of the Histic Gleysol. When cumulative N_2O fluxes were compared within the first eight weeks following grassland renewal for the Histic Gleysol, a tendency for N_2O emissions to increase with the intensity of sward disturbance was evident; the N_2O fluxes increased in the order *Minimum* (0.7±0.4 kg N ha^{-1})

< *Chemical* (1.7±0.5 kg N ha^{-1}) < *Mechanical* (5.6±4.1 kg N ha^{-1}). The same pattern did not occur in the Plaggic Anthrosol. Here, the N_2O emissions were lower for this time period than for the Histic Gleysol, but only N_2O fluxes in the *Mechanical* (1.3±0.4 kg N ha^{-1}) and *Chemical* (1.0±0.3 kg N ha^{-1}) treatments were significantly higher than in the *Control* treatment. During the first year after grassland renewal, individual N_2O peak emissions followed N fertiliser application during the spring and summer, often in combination with heavy rainfall events (>5 mm day^{-1}). This finding was also observed in the second year. Increased N_2O fluxes were not found during the winter.

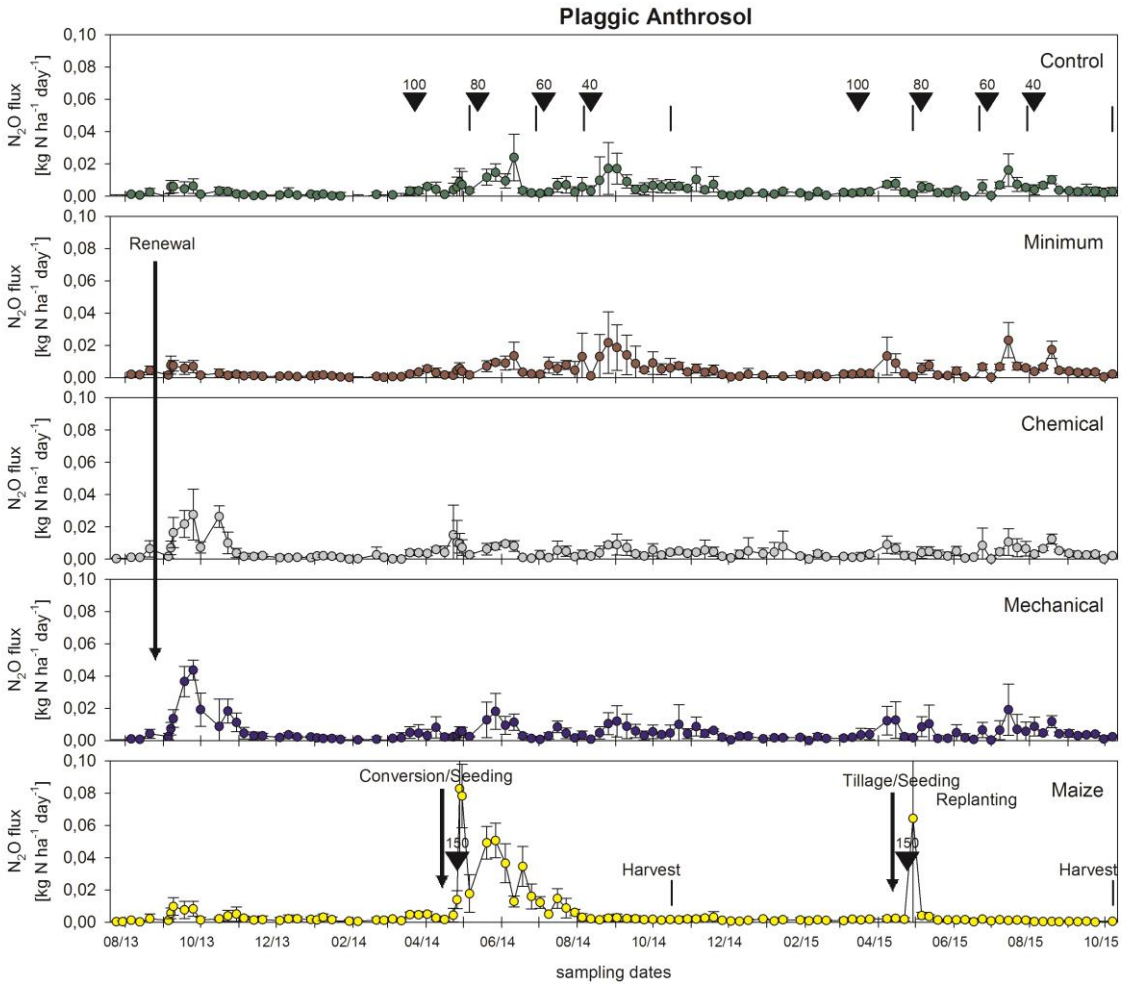

Figure 2-7: Time course of N_2O fluxes in treatments at the Plaggic Anthrosol site. Dates of N fertilisation (black triangles with kg N ha^{-1}) and grass cuts (black lines) were the same for the following treatments: *Control, Minimum, Chemical* and *Mechanical,* which are shown for illustration purposes only in the first panel. The N fertilisation was different for the *Maize* plots. Error bars indicate the standard deviations of the mean (n=4)

Following grassland conversion to maize cropping, including sward destruction, soil tillage and sowing in spring, small peaks in the N_2O fluxes of similar magnitude were observed in both soils (up to 0.1 kg N ha^{-1} day^{-1}). In the Plaggic Anthrosol, elevated N_2O fluxes lasted for approximately two months following the conversion of grassland in 2014, with average N_2O

fluxes of 0.04±0.01 kg N ha^{-1} day^{-1}. In 2015, there was only one single N_2O peak of 0.06±0.13 kg N ha^{-1} day^{-1} after the tillage and planting of maize on the Plaggic Anthrosol.

Annual N_2O fluxes of the grassland treatments are given in Table 2-3a. At the Plaggic Anthrosol site, no significant treatment effect was found on the annual N_2O fluxes; differences in the N_2O emissions between the different forms of renewal and between the years were not significant. At the Histic Gleysol site, the annual N_2O fluxes in the first year (2013-2014) were higher than in the second year (2014-2015), but there were also no significant differences between the renewal treatments. The same pattern was also obtained for N fertiliser-related N_2O fluxes at both sites (Table A2-3a, Supplementary data).

Table 2-3a: Cumulative N_2O fluxes of the grassland treatments per year (September 2013 to 2014 and September 2014 to 2015). Different superscript letters indicate significant differences in the grassland treatments (*Minimum*, *Chemical* and *Mechanical*) in comparison to permanent grassland (*Control*) for the respective sites. Values shown are the mean of treatment replicates ± one standard deviation (n=4)

	2013-2014	**2014-2015**
	N_2O flux kg N ha^{-1} $year^{-1}$	N_2O flux kg N ha^{-1} $year^{-1}$
Histic Gleysol		
Control	6.26±3.10 [a]	6.54±3.92 [a]
Minimum	7.32±3.89 [a]	6.04±1.34 [a]
Chemical	7.96±2.21 [a]	5.26±1.55 [a]
Mechanical	9.88±4.55 [a]	4.33±2.05 [a]
Plaggic Anthrosol		
Control	1.48±0.80 [a]	1.50±0.44 [a]
Minimum	1.51±0.70 [a]	1.67±0.50 [a]
Chemical	1.94±0.61 [a]	1.47±0.83 [a]
Mechanical	2.47±0.99 [a]	1.70±0.98 [a]

The N_2O emissions from grassland conversion to maize cropping cannot be directly compared with the grassland renewal treatments because they differed in terms of the date (renewal in September 2013 and conversion to maize cropping in May of the following year). Furthermore, the *Maize* plots were maintained as grassland from September to ploughing in April 2014, and they were left fallow after harvest and planted for the second period in spring 2015. The effect of the land-use change from grassland to maize cropping was evaluated by comparing the *Maize* treatment with permanent grassland (*Control* treatment) in Table 2-3b. A comparison of the cumulative N_2O fluxes for the two cultivation periods of *Zea mays* L. revealed no differences between the *Maize* treatment and the *Control* treatment in the Histic Gleysol. There was also no annual effect, and the N_2O fluxes for the first year of maize cropping (2014) were not higher than those in 2015. At the Plaggic Anthrosol site, the cumulative N_2O fluxes in the *Maize* plots were greater during the first cultivation period (2.93±0.35 kg N ha^{-1} 168 $days^{-1}$)

than the second cultivation period (0.41±0.45 kg N ha^{-1} 172 $days^{-1}$); however, the difference was not significant. Apart from the N_2O fluxes based on the area (ha), fertiliser-related N_2O fluxes were also calculated (Table A2-3a and A2-3b, Supplementary data). This finding is relevant because the N fertilisation was not the same for all the treatments, i.e. the *Maize* treatment (150 kg N ha^{-1}) received much less N fertiliser than the grassland treatments (280 kg N ha^{-1}). Here, a similar pattern was noted for the maize cultivation periods in 2014 and 2015, while the annual N_2O fluxes related to N fertiliser were significantly different for the Plaggic Anthrosol. This finding occurred because maize fluxes related to the area trended lower than grassland fluxes related to the area. Furthermore, relative differences in NEL yield-related N_2O fluxes between maize and renewal treatments were even smaller than the respective differences in the fluxes related to the area (Table 2-3b and 2-4). In the Plaggic Anthrosol, NEL yield-related N_2O emissions differed only between the *Maize* treatment and permanent grassland in the first year following conversion from grassland to maize cropping (Table 2-4).

Table 2-3b: Cumulative N_2O fluxes of the *Maize* treatment per cultivation period (May to October 2014 and 2015) and on an annual basis for the first year following grassland conversion to maize cropping (April 2014 to May 2015) in comparison to permanent grassland (*Control*). Different superscript letters indicate significant differences between treatments for the respective sites. Values shown are the mean of treatment replicates ± one standard deviation (n=4)

	2014[1]	**2015**[2]	**2014-2015**
	N_2O flux kg N ha^{-1} $period^{-1}$	N_2O flux kg N ha^{-1} $period^{-1}$	N_2O flux kg N ha^{-1} $year^{-1}$
Histic Gleysol			
Control	7.31±4.16 [a]	4.81±4.18 [a]	4.13±1.89 [a]
Maize	4.37±1.85 [a]	3.94±1.71 [a]	3.27±1.20 [a]
Plaggic Anthrosol			
Control	1.38±0.77 [b]	0.76±0.30 [b]	0.95±0.45 [b]
Maize	2.93±0.35 [a]	0.41±0.45 [b]	1.46±0.14 [b]

[1] The *Maize* cultivation period in 2014 was 168 days.

[2] The *Maize* cultivation period in 2015 was 172 days.

2.3.4 Response of N_2O fluxes to soil variables

The applied generalised additive model (GAM, see Supplementary data: Tables A2-4 and A2-5) explained 26% of the variance in the log-scaled N_2O fluxes at the Histic Gleysol and 48% at the Plaggic Anthrosol site. The treatment effect was highly significant for both soils (Table A2-4 and A2-5), whereas a block effect occurred only at the Plaggic Anthrosol site ($p<10^{-7}$). The following variables were significant and thus improved the goodness of fit of the GAM for predicting the N_2O fluxes from both soils ($p<10^{-6}$) as follows: the soil moisture

(i.e. the gravimetric water content for the Histic Gleysol and WFPS for the Plaggic Anthrosol), NO_3^--N content and microbial activity (as represented by the microbial and plant respiratory activity as a proxy). The interaction between the soil moisture and NO_3^- availability in the soil significantly affected the N_2O fluxes in all treatments. For the Histic Gleysol, large N_2O fluxes coincided with water saturation in the topsoil, i.e. a groundwater level near the surface and NO_3^--N content of 100-150 kg N ha^{-1} (Figure A2-1) in all treatments. However, high N_2O fluxes were particularly scarce in the dataset, resulting in high uncertainty in the prediction of high emission rates (Figure A2-1). For the Plaggic Anthrosol in which the N_2O fluxes were generally low, slightly increased N_2O fluxes coincided with lower soil moisture (for WFPS of approximately 20-40%) and NO_3^--N content of 50-100 kg ha^{-1} (Figure A2-2). However, there was a tendency to observe higher N_2O fluxes with increasingly available NO_3^- in the *Chemical* and *Maize* treatments.

2.3.5 Plant growth, nitrogen uptake and yield-related N_2O emissions

Grassland treatments

At the Histic Gleysol, the dry matter (DM) yields of the grassland plots were high, ranging from 13.2±0.4 to 15.6±0.6 Mg ha^{-1} in 2014 and from 12.9±1.1 to 14.0±1.4 Mg ha^{-1} in 2015 (Table 2-4). The DM yields on the Plaggic Anthrosol site were significantly lower and ranged from 7.8±0.2 to 10.2±1.8 Mg ha^{-1} in 2014 and from 9.4±1.0 to 10.4±1.0 Mg ha^{-1} in 2015. The DM yields were significantly higher in 2014 than in 2015 for the Histic Gleysol, while differences at the Plaggic Anthrosol site were not significant (site comparison data are not shown).

The DM yields differed between the grassland treatments in single years. For the Plaggic Anthrosol, the DM yields of 7.8±0.2 Mg ha^{-1} in the *Chemical* treatment were significantly lower than in the *Control*, *Minimum and Mechanical* treatments in 2014. Accordingly, plant N removal and energy yield (GJ NEL ha^{-1}) were also smaller in the *Chemical* treatment. In 2015, the DM, energy yield, and plant N removal from grassland treatments were similar, with no significant differences. For the Histic Gleysol, significant treatment effects were observed for the DM and energy yield in 2014, and the DM yields of the improved grassland (*Minimum* treatment) were smaller than those of the *Mechanical* treatment. At both sites, the differences between grassland treatments in DM yield, energy yields and plant N removal in 2015 were not significant. NEL-related N_2O emissions, as calculated from the net energy yield for lactation

(NEL) and annual N_2O emissions, were not significantly different between the grassland treatments at both sites (Table 2-4).

Maize treatment

The DM yields in the *Maize* treatment were 16.2±1.8 Mg ha^{-1} in 2014 and 17.3±1.1 Mg ha^{-1} in 2015 on the Histic Gleysol and 18.8±0.3 Mg ha^{-1} in 2014 and 20.7±1.8 Mg ha^{-1} in 2015 on the Plaggic Anthrosol (Table 2-4). The differences in yields between the sites were significant. The plant N removal (kg N ha^{-1}) with the harvested biomass differed strongly between the *Maize* treatment and the permanent grassland. On the Histic Gleysol, the plant N removal was significantly lower from the *Maize* treatment than from the *Control* treatment in both years. This finding also applied to the Plaggic Anthrosol in 2014, while in 2015, the plant N removal was not significantly different (260.1±20.6 for the *Control* treatment and 232.4±22.9 for the *Maize* treatment). The energy yields (GJ NEL ha^{-1}) of maize were 20% higher than that of the grassland *Control* on the Histic Gleysol. However, the respective NEL yield-related N_2O emissions were not significantly affected by the different energy yields; there were no treatment or annual effects at this site. For the Plaggic Anthrosol, the difference in energy (NEL) yields between maize and grassland was even greater than on the Histic Gleysol and amounted to 57% higher energy yields from the *Maize* treatment in 2015. This finding was also reflected in the NEL yield-related N_2O emissions (23.91±5.18 g N_2O GJ^{-1} and 7.73±7.90 g N_2O GJ^{-1} for the *Control* and *Maize* treatments, respectively).

Table 2-4: Dry matter yields (DM), plant N removal with harvested biomass, net energy yield for lactation (NEL) and NEL yield-related N_2O fluxes per treatment and year. Different superscript letters indicate significant differences between treatments (*Control*, *Minimum*, *Chemical* and *Mechanical*) and year. Capital letters indicate significant differences between the *Control* and *Maize* treatments and year. Values shown are the mean of treatment replicates ± one standard deviation (n=4)

	2014				2015			
	DM yield	Plant N removal	Energy (NEL) yield	NEL yield-related N_2O fluxes	DM yield	Plant N removal	Energy (NEL) yield	NEL yield-related N_2O fluxes
	Mg ha^{-1}	kg N ha^{-1}	GJ ha^{-1}	g N_2O GJ^{-1}	Mg ha^{-1}	kg N ha^{-1}	GJ ha^{-1}	g N_2O GJ^{-1}
Histic Gleysol								
Control	14.2±1.0 ^{ab}	315.7±30.2 ^{a} ^{AB}	79.8±5.5 ^{ab} ^{A}	74.84±39.02 ^{a} ^{A}	12.9±1.1 ^{b}	329.6±15.9 ^{a} ^{A}	77.8±6.9 ^{b} ^{A}	29.59±16.26 ^{a} ^{A}
Minimum	13.2±0.4 ^{ab}	305.9±19.8 ^{a}	77.4±2.4 ^{b}	87.56±51.06 ^{a}	14.0±1.4 ^{ab}	327.6±50.7 ^{a}	83.6±8.2 ^{ab}	30.71±17.51 ^{a}
Chemical	15.2±1.4 ^{ab}	328.9±27.7 ^{a}	88.7±7.2 ^{ab}	94.14±32.12 ^{a}	14.0±1.0 ^{ab}	323.4±32.9 ^{a}	83.2±6.8 ^{ab}	35.99±11.74 ^{a}
Mechanical	15.6±0.6 ^{a}	328.0±18.1 ^{a}	92.0±3.8 ^{a}	124.12±54.94 ^{a}	13.1±0.5 ^{b}	281.1±24.6 ^{a}	80.4±2.2 ^{ab}	48.31±15.40 ^{a}
Maize	16.2±1.8 ^{B}	188.3±24.3 ^{B}	101.2±11.5 ^{B}	43.63±13.15 ^{A}	17.3±1.1 ^{B}	203.9±14.9 ^{B}	101.5±7.4 ^{B}	26.75±4.48 ^{A}
Plaggic Anthrosol								
Control	10.2±1.8 ^{a}	260.0±31.6 ^{ab} ^{A}	52.9±8.2 ^{a} ^{A}	78.84±46.12 ^{a} ^{A}	9.8±0.9 ^{a}	260.1±20.6 ^{ab} ^{A}	57.7±5.5 ^{a} ^{A}	23.91±5.18 ^{a} ^{A}
Minimum	9.8±1.0 ^{a}	288.7±31.6 ^{a}	52.9±4.9 ^{a}	75.13±19.43 ^{a}	9.4±1.0 ^{a} ^{a}	261.3±25.1 ^{ab}	55.8±6.5 ^{a}	30.52±12.40 ^{a}
Chemical	7.8±0.2 ^{a}	206.9±3.3 ^{b}	45.1±0.6 ^{a}	64.5±21.49 ^{a}	9.7±1.6 ^{a} ^{a}	251.4±39.1 ^{ab}	58.7±8.3 ^{a}	25.25±13.54 ^{a}
Mechanical	9.6±0.7 ^{a}	243.0±18.2 ^{ab}	55.3±4.8 ^{a}	55.15±25.17 ^{a}	10.4±1.0 ^{a} ^{a}	263.2±13.4 ^{ab}	63.4±4.7 ^{a}	28.52±16.28 ^{a}
Maize	18.8±0.3 ^{B}	206.8±14.8 ^{B}	126.3±5.8 ^{B}	69.13±22.96 ^{A}	20.7±1.8 ^{A}	232.4±22.9 ^{A}	127.9±10.5 ^{B}	7.73±7.90 ^{B}

2.3.6 Unaccounted-for N of the N budget

The estimate of unaccounted-for N (i.e. N_{ua}, Eq.1) is shown for the two periods 2013/2014 and 2014/2015, both sites in Figure 2-8 and in detail in Table A2-6 (Supplementary data).

For the Histic Gleysol, the N_{ua} values did not differ between treatments and years. The picture from the Plaggic Anthrosol was different, with a generally wider range in N_{ua} (-103 to +207 kg N ha^{-1}) and significant differences between the treatments in 2013/2014. The *Maize* treatment showed a large N surplus (143±39 kg N ha^{-1}), indicating high N mineralisation, whereas the negative N_{ua} values of the *Chemical* treatment (-98±4 kg N ha^{-1}) indicated large losses. In 2014/2015, the differences between treatments were smaller, ranging from -62 kg N ha^{-1} to +99 kg N ha^{-1} (*Maize*) in the Plaggic Anthrosol.

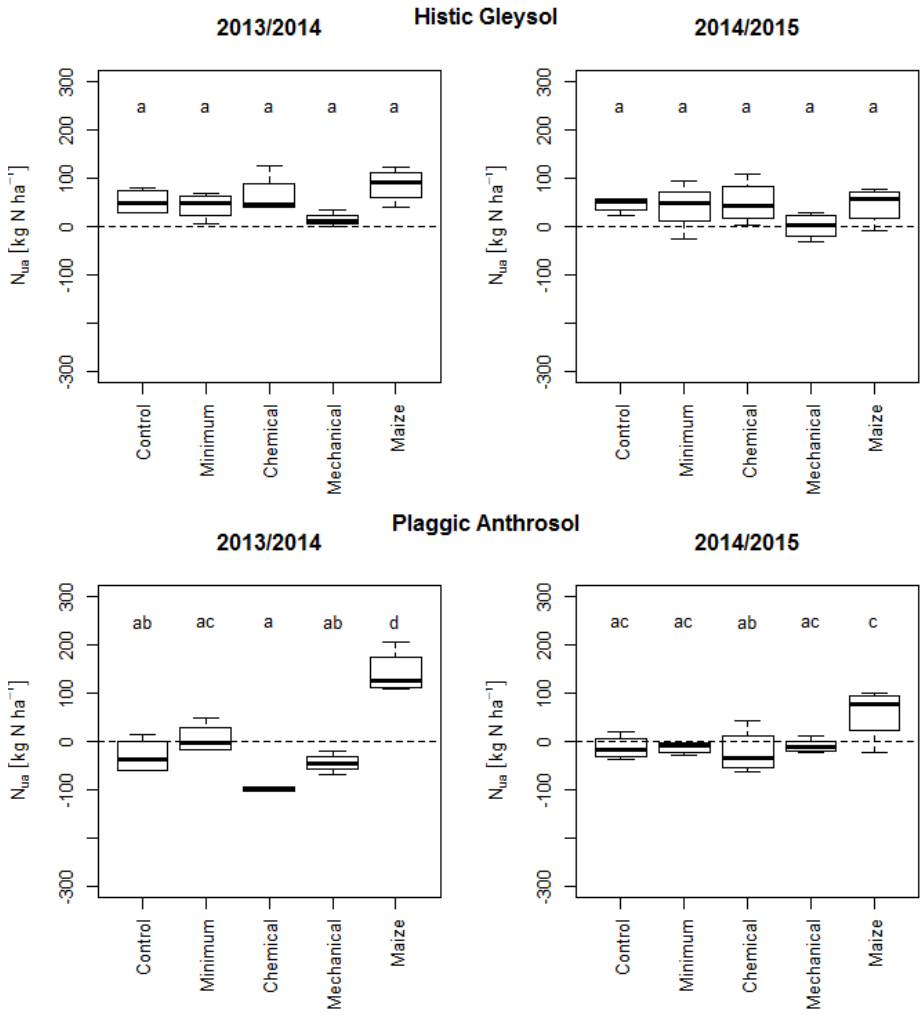

Figure 2-8: Unaccounted-for N of the N budget (i.e. N_{ua}, Eq. 2-1) in kg N ha^{-1} of the Histic Gleysol and of the Plaggic Anthrosol for the periods 2013/2014 and 2014/2015. Different superscript letters indicate significant treatment differences per site and period. Error bars indicate the standard deviations of the mean (n=4)

2.4 Discussion

To the authors' knowledge, the present study is the first attempt to monitor N_2O fluxes following grassland renewal for a period of more than two years. An initial effect on N_2O emissions was found following grassland renewal for the two investigated sites (Histic Gleysol and Plaggic Anthrosol), but this effect did not last for the entire sampling period.

2.4.1 N_2O emissions

Fertilised grasslands are important sources of N_2O production (Dobbie and Smith, 2003; Jones et al., 2005; Soussana et al., 2007), and N_2O losses can increase following the break-up of grassland, as has been shown in several studies (Table 2-1). In the present study, no renewal effect was observed on an annual basis for the two years studied here at either of the investigated sites (Histic Gleysol and Plaggic Anthrosol). The cumulative N_2O fluxes of the renewal treatments (1.97±0.82 kg N ha^{-1} $year^{-1}$ at the Plaggic Anthrosol and 8.39±3.52 kg N ha^{-1} $year^{-1}$ at the Histic Gleysol) during the first year were within the range of previously reported N_2O fluxes after grassland renewal (Table 2-1). The lack of treatment effects on annual fluxes was probably due to the variability of N_2O fluxes induced by the spatial variability of soil properties in combination with the huge impact of management effects as shown by the clear response in N_2O fluxes to grass cutting and the associated N fertiliser application. Those factors apparently masked the smaller impact from grassland renewal treatments.

Site comparison

The present study was conducted at two sites with different soil types and SOM content, due to the fact that most of the studies on N_2O emissions after grassland renewal involved clay or loamy soils (Table 2-1), and because knowledge of the effect of grassland renewal on N_2O production in soils with higher C content was scarce. N_2O fluxes in the Histic Gleysol were up to tenfold higher than on the sandy Plaggic Anthrosol. This difference might be explained by the generally higher initial amounts of available C and N in the Histic Gleysol, which led to larger N transformation rates in the soil.

Seasonal variation in N_2O fluxes

Seasonal variations were observed in the N_2O emission time series (Figure 2-6 and 2-7), with N_2O peaks following N fertilisation during the growing period from March to October. This variation might be partly explained by the combination of rainfall events and higher

temperatures during the summer months, leading to increased microbial activity, and hence N turnover in the soil and consequently, N_2O emission. Similarly, Jones et al. (2005) reported the highest N_2O release within seven to 20 days following N fertiliser application from grasslands. Distinct N_2O emission peaks during winter were caused by frost-thaw-cycles, which governed the large N_2O losses in the grassland renewal studies by Merbold et al. (2014) and Biegemann (2014), and they were not observed in the present study, probably due to the mild winters during the study years of 2013/2014 and 2014/2015.

Treatment effects

It was hypothesised that N_2O emissions after grassland renewal are enhanced compared to those of permanent grassland. This idea was only partly supported by the present results because there were no treatment effects at either site on an annual basis (Table 2-3a). However, a significant short-term increase in N_2O fluxes was observed, lasting for a period of two months after the ploughing of permanent grassland in the present experiment. This short-term effect has been observed before (Davies et al., 2001; Velthof et al., 2010; MacDonald et al., 2011; Cowan et al., 2016; Drewer et al., 2016; Krol et al., 2016). On an annual basis, it seems that the prevailing soil conditions (i.e. the SOM content and water saturation) had a much greater influence on N_2O emissions than the management effects (i.e. different treatments) at the two investigated sites.

Furthermore, it was assumed that there would be an increase in N_2O emissions with increasing sward and soil disturbance, and thus it was expected that the N_2O fluxes would increase in the order of keeping and improving the old sward (*Minimum* treatment) < renewal by chemical sward destruction (*Chemical* treatment) < renewal by chemical and mechanical sward destruction (*Mechanical* treatment). This order was confirmed for the first two months after renewal. For the *Chemical* and *Mechanical* treatments, the increase in N_2O fluxes was probably the result of a combination of (i) small plant N uptake directly after the ploughing of the old grass sward (see section 2.4.4) and (ii) an increased mineralisation of organic C and N (see section 2.4.3).

It should be noted that the N_2O fluxes were highly variable between the individual chambers within the same treatment, resulting in large standard deviations in the annual fluxes. This finding reflects the well-known high spatial variability of factors that control the N_2O release in soil-plant systems (Smith et al., 1998; Schaufler et al., 2010), which might have masked the moderate treatment effects. Furthermore, temporal variability should be taken into account as

another uncertainty due to the fact that a potential error can occur during weekly measurements, as found by Rowlings et al. (2015) with an associated error of up to 34% of the sub-daily mean in humid tropical pastures. Nevertheless, Flessa et al. (2002) promoted weekly N_2O measurements in combination with event-related sampling to estimate the cumulative N_2O emission. With the present data, it might be possible that besides the spatial heterogeneity, the temporal variability of N_2O fluxes also increased the uncertainty in the determination of annual fluxes.

Finally, a question arises as to whether grassland renewal and its various practices should be considered in greenhouse gas emission inventories. No significant differences were found in N fertiliser-related fluxes between grassland treatments at either of the sites. Moreover, N fertiliser-related fluxes were even more uniform than the fluxes related to the area. Only the *Maize* treatment in comparison with the permanent grassland significantly differed during the first year for the Plaggic Anthrosol. In contrast to previous reports (Baggs et al., 2003; Pinto et al., 2004), the present data therefore do not show significant management effects of N_2O fluxes, which might be due to the site heterogeneity, the limited number of measurements and/or the lack of large management effects. This finding shows that the common concept of using fixed default values for fertiliser-related N_2O emission factors to calculate emission inventories that are applied irrespective of the management practice (IPCC, 2006) might be the best approximation, at least for some sites. This assertion is also supported by the close consistency of IPCC default values with N_2O fluxes after grassland renewal at Easter Bush, Scotland (Cowan et al., 2016; Drewer et al., 2016).

2.4.2 Environmental controls and involved processes of N_2O emissions

In the experiments in this study, the two sites significantly differed in their N_2O emissions, while treatment effects were visible only immediately after grassland disturbance. A question remains regarding the extent to which these results can be generalised and how the N_2O fluxes were affected by the change in individual control factors. A variety of factors have been proposed as potentially affecting N_2O emission after grassland ploughing and subsequent changes in vegetation, i.e. the development of new grasses and/or the growing of maize. Soil tillage causes changes in (i) soil porosity, aeration and moisture (Yamulki and Jarvis, 2002), (ii) soil temperatures might increase (MacDonald et al., 2010) due to the lack of plant cover, and (iii) NH_4^+ and NO_3^- are formed by mineralisation and by nitrification in interaction with the dynamics of plant N uptake.

Under aerobic conditions, nitrification is the primary N_2O production pathway, with NH_4^+ as the main source (Wrage et al., 2001). With decreasing O_2 availability, the N_2O production pathways shift towards denitrification and nitrifier denitrification, which might be the primary pathway at the often water-saturated Histic Gleysol. To distinguish between NH_4^+ and NO_3^--derived N_2O emissions and to quantify the N_2 fluxes as the primary end product of the denitrification process, an ^{15}N labelling experiment was conducted from May to July in the first year of the study (2014) at both sites (Buchen et al., 2016). The Histic Gleysol exhibited high denitrification rates (ranging between 22 to 53 kg N ha^{-1} on average within 44 days), and the total N_2O+N_2 fluxes were dominated by N_2 (94%, 95%, and 92% in the *Control*, *Minimum*, and *Maize* treatments, respectively). The dominance of denitrification and the almost complete reduction of N_2O to N_2 was attributed to the high moisture and C_{org} content in the Histic Gleysol and the fact that the soil was often partially waterlogged. Based on those measured N_2O+N_2 fluxes, denitrification losses of probably more than 100 kg N ha^{-1} $year^{-1}$ were assumed. If these N losses *via* denitrification are added to the rough calculation of the fate of plant-available N, it becomes clear that the considerable mineralisation of organic matter must have occurred in the soil. In contrast, N_2 fluxes in the sandy Plaggic Anthrosol were undetectable (i.e. the concentrations of soil-derived N_2 were <1.8 ppm), which could be attributed to a low denitrification activity because of low soil water content, lower C_{org} content and high O_2 availability (Buchen et al., 2016).

The applied GAM confirmed the expected relevance of the soil moisture; in combination with NO_3^- availability, this factor emerged as the most important driving variable of N_2O fluxes for both soils. The GAM identified differences in the control of N_2O release between the two sites, with optimal WFPS content of 20-40% for the Plaggic Anthrosol and an optimal gravimetric water content of >150% for the Histic Gleysol at 50-100 kg available N ha^{-1}. In the Histic Gleysol, the groundwater level was higher than -0.2 m for half of the year (2014), which resulted in high water saturation and favourable conditions for N_2O reduction to N_2. Moreover, large amounts of soil C in combination with increased NO_3^-/NH_4^+ concentrations are known to enhance denitrification (Senbayram et al., 2012). Against this backdrop, the variance in N_2O fluxes explained by these factors (26%) on the Histic Gleysol appears to be relatively low. Several factors might have contributed to this trend, namely unaccountable losses *via* N_2 during the investigation periods, environmental controls that were not included in the applied GAM including soil aeration, soil compaction and/or grassland species composition, and finally, the spatial heterogeneity of the Histic Gleysol site. The applied GAM gave a better

explanation for the Plaggic Anthrosol (48%), probably due to having more homogenous soil conditions and because the N_2O reduction to N_2 was much lower.

2.4.3 Mineral N dynamics

Indications for mineralisation based on weekly data

The N_{min} content in the upper soil layer (0-30 cm) increased by 48% over a two-month period following grassland renewal (treatments: *Chemical* and *Mechanical*) at both sites (Figure 2-3 and 2-4), which resulted from enhanced N mineralisation, reduced plant N uptake and soil aeration following the disturbance of permanent grassland. Keeping and improving the old sward in the *Minimum* treatment did not increase the N_{min} content, but the chemical sward killing and direct seeding (*Chemical* treatment) as well as chemical killing in combination with ploughing (*Mechanical* treatment) led to significantly higher N_{min} content due to greater soil disturbance and higher N mineralisation. Similar results were reported by Velthof et al. (2010), who found an average of 46-77 kg N ha^{-1} higher pre-winter N_{min} content in the renewed grassland than in the reference plots (permanent grassland). No difference in pre-winter N_{min} was observed between the *Chemical* and *Mechanical* treatments in the present experiment. However, the conversion of grassland to maize cropping (*Maize* treatment) together with the application of N fertiliser increased the N_{min} content under maize for a longer period during the summer and resulted in high pre-winter N_{min} content (Figure 2-5) at the Plaggic Anthrosol. N mineralisation plus N fertilisation (150 kg N ha^{-1}) resulted in considerable, positive N_{ua} values of 143±39 kg N ha^{-1} during the first year, which was much higher than it was under the grassland treatments (Figure 2-8).

Unaccounted-for N of the N budget

Because mineralisation was not directly measured in the present study, the unaccounted-for N of the N budget (N_{ua}, Eq.2-1) was calculated as a best estimate for the amount of N derived from mineralisation that ended up in the N_{min} pool or harvested plant biomass at the end of the vegetation period. These soil system budgets use the N_{ua} to estimate uncertainties in nutrient management, and they are frequently applied in farming systems (Allison, 1955; Watson and Atkinson, 1999; Oenema et al., 2003; Meisinger et al., 2008). Negative N_{ua} values indicate unaccounted-for N leaching and/or gaseous N losses, while positive N_{ua} values indicate high N mineralisation.

In the present study, both positive and negative N_{ua} values were identified. During the first year following grassland renewal, large losses were indicated by negative N_{ua} values at the Plaggic Anthrosol for the *Chemical* and *Mechanical* treatments. Furthermore, a high positive N_{ua} value was calculated in the *Maize* treatment at 143±39 kg N ha^{-1}, which is clearly in excess of the known range of atmospheric deposition in this region (approximately 15 kg N ha^{-1} $year^{-1}$, UBA (2009)), thus indicating high N mineralisation. The latter was also reflected in the high pre-winter N_{min} content (up to 140 kg N ha^{-1}) during the first winter after grassland conversion to maize cropping. During the second maize cropping period, the absolute values of N_{ua} were smaller, indicating that the N_{min} dynamics in the soil-plant system was more balanced. The Histic Gleysol site is known for its potential for large gaseous N losses, as substantial fluxes of N_2 and N_2O (a total of 19.7 to 63.6 kg N ha^{-1} 40 $days^{-1}$) have been measured in the field in early summer (Buchen et al., 2016). This finding might explain why the calculation of N_{ua} led to positive values, due to the mineralisation potential of this soil, but lower than expected. Moreover, gaseous losses might have masked an increase in the mineralisation of organic N more or less completely.

Risk of NO_3^- leaching

The present results and the findings of other studies (Table 2-1) support the hypothesis that grassland renewal leads to an increased risk of NO_3^- leaching, in particular, in the Plaggic Anthrosol. To determine the N_{min} losses during the winter, the N_{min} (0-90 cm) was determined close to the start of the leaching period (pre-winter), and again in early spring before plant growth and plant N uptake began (post-winter) (Figure 2-5). When gaseous N losses are small, the change in N_{min} content during the winter can be used as a robust indicator for NO_3^- leaching in winter, which applies to the Plaggic Anthrosol because the mineralisation and immobilisation rates are slow at low temperatures (Herbst et al., 1982). However, for the Histic Gleysol, the potential denitrification loss was large due to high waterlogging because denitrification in saturated soils is known to be intense even at low temperatures (Well et al., 2003) and the N_{min} change in the winter was therefore difficult to interpret. For the Plaggic Anthrosol, the difference in the N_{min} content in the upper 90 cm soil layer before and after winter was therefore used as a maximum estimate for NO_3^- leaching into groundwater during winter, but it accounts for the fact that the true NO_3^- leaching could be lower due to other NO_3^- losses or transformations. The N_{min} loss in winter is known to vary between years (Kayser et al., 2011; Kayser et al., 2015), which can be attributed to weather effects, late mineralisation during mild winters and the fact that N_{min} sampling just represents one point in time (Kayser et

al., 2015). The direct applicability of this method was shown by Seidel et al. (2009), who found NO_3^- leaching losses of 70% of pre-winter N_{min} following grassland renewal and Kayser et al. (2008) with 100% N loss in comparison with pre-winter N_{min} due to grassland conversion to maize cropping on a Plaggic Anthrosol in the first year. At the Plaggic Anthrosol site of our study, the N_{min} content decreased by approximately 80% during the first winter, which indicates potential N losses *via* NO_3^- leaching in this sandy soil.

In the present study and in earlier studies (Scholefield et al., 1993; Shepherd et al., 2001; Seidel et al., 2009), an increased risk of NO_3^- leaching was observed only for the first winter following grassland renewal. Nevertheless, a potential risk of NO_3^- leaching was also present during the second year because high rainfall occurred (Figure 2-1 and 2-2), but the N_{min} loss was lower in the second winter and not significant. Studies measuring the NO_3^- leaching losses *in situ* by suction cups or using lysimeter approaches determined N losses of 35 to 72 kg N ha^{-1} in the first winter following grassland renewal (Shepherd et al., 2001; Seidel et al., 2009). The potential NO_3^- leaching losses seem to be lower when sward disturbance and seeding occur in the spring (Francis et al., 1992; Lloyd, 1992; Francis et al., 1995; Seidel et al., 2009), due to the fact that much more available N can be taken up during the growing period and the new grass sward is well established before the following leaching period (Seidel et al., 2009; Schmeer, 2012).

Grassland conversion to arable land can lead to even higher NO_3^- leaching following grassland renewal, and considerable N losses of up to 104 kg N ha^{-1} have been reported in several studies (Lloyd, 1992; Johnston et al., 1994; Francis et al., 1995; McLenaghen et al., 1996; Djurhuus and Olsen, 1997). The amount of mineralised N was found to increase with the grassland age at the time of conversion and increasing N fertilisation (Whitehead et al., 1990; Velthof and Oenema, 2001), indicating that the combination of these factors enhance the potential for NO_3^- leaching.

In our study, the difference between pre-winter N_{min} content and post-winter N_{min} content in the *Maize* treatment of the Plaggic Anthrosol indicated an apparent NO_3^- leaching loss of 88 kg N ha^{-1} (2014/2015), which is close to the range of findings of Kayser et al. (2008), who reported N losses of 100-220 kg N ha^{-1} from the cultivation of maize in two consecutive years following grassland ploughing on sandy to loamy soils. A reduction in N fertilisation and the planting of a cover crop between two maize cultivation periods are methods for reducing the N surplus and taking up available N after the maize harvest (Köhler et al., 2006; Kayser et al., 2008; Hansen and Eriksen, 2016).

2.4.4 Yields and plant-available nitrogen

It was expected that grassland renewal would lead to higher yields than 15-year-old continuous grassland over the two-year period, as grassland renewal is often used to put in high-yielding grasses and eliminate sward deterioration and soil disturbances; however, neither a yield improvement nor a yield depression occurred after the renewal.

Success in plant development following grassland renewal differed between the two sites and within the investigated treatments. In the autumn of 2013, rapid plant growth in the *Chemical* and *Mechanical* treatments was observed at the Histic Gleysol, apparently due to good water availability. Moreover, maintaining and improving the old sward in the *Minimum* treatment resulted in a visibly higher percentage of *Lolium perenne* L. at this site. By contrast, the sandy Plaggic Anthrosol generally had lower water availability and plant growth, and the *Chemical* treatment in particular was weak due to the slow establishment of the new grass through the chemically killed grass sward, which was still decomposing on the surface. This difficulty made a second reseeding necessary in the spring of 2014. This finding indicates that chemical killing and direct seeding might not be the best option for sandy soils. In contrast to the absence of yield effects in our study, Terlikowski and Barszczewski (2015) reported an increase of 39% in dry matter (DM) yields during the first year following grassland renewal at sites with different soil textures of clay, loam and sand with a N fertilisation rate between 120 to 200 kg N ha^{-1}. Similar results with only a short-term increase in the DM yields were observed by Schmeer (2012) and Creighton et al. (2016), who applied an N fertilisation rate of 200 to 230 kg N ha^{-1}, which is a similar range as that of our study. However, studies with an experimental period lasting more than two years report no significant DM yield effects (Hopkins et al., 1995; Velthof et al., 2010; Schmeer, 2012; Biegemann, 2014), which is consistent with the present results.

In the Plaggic Anthrosol, there was low plant N removal resulting from lower plant N content than in the Histic Gleysol (Table 2-4), which can be used as an indicator of N availability in soil. This finding might be partly related to the establishment of the new grass sward, in which much of the N assimilation is invested in roots and stubble development (Velthof and Oenema, 2001). The energy (NEL) yield can be used as an indicator of the forage quality. Overall, the energy yields were higher in the Histic Gleysol, which is generally a more productive site, than in the Plaggic Anthrosol site (Table 2-4). For the first cut of the year, which usually gives the highest proportion of annual grassland yield and is the most important one for the farmer, the results ranged from 5.4 to 6.3 MJ NEL kg^{-1} DM^{-1} at both sites (data not shown). In productive

grassland in northwest Germany, energy concentrations in forage from first cuts are usually higher than 6.0 MJ NEL kg^{-1} DM^{-1} (Treyse et al., 2008; Benke and Kayser, 2009), and the lower values in our study indicate that the time of the grass cutting was probably not optimal.

Furthermore, grassland conversion to maize cropping in the spring was more challenging on the Histic Gleysol because large rainfall events following maize sowing and limited accessibility to agricultural machinery resulted in lower DM yields, plant N removal and energy (NEL) yields per ha^{-1} at this site (Table 2-4). By contrast, the soil moisture conditions along with higher C and N availability from the decomposition of the old grass sward promoted maize growth on the Plaggic Anthrosol and produced higher yields.

2.5 Conclusions

The results of the present study showed no evidence that the grassland renewal technique had an effect on the annual N_2O losses. Grassland renewal was thus not a significant source of direct N_2O emissions at either experimental site during the two years under study. There was only a short two-month period of significantly increased N_2O fluxes. Those grassland renewal techniques that are based on the destruction of the old grass sward resulted in an increased net N release of N_{min} in the first year, indicating a higher risk of NO_3^- leaching and thus potential losses *via* indirect N_2O emissions. With respect to N_2O mitigation and the prevention of NO_3^- leaching, it is recommended to target the rapid development of the new grass sward, which will then act as an effective N sink. After the destruction of the grass sward during grassland renewal or conversion to arable land, N fertilisation should account for enhanced N mineralisation and should generally be significantly reduced. One objective for grassland renewal is to improve the quality and quantity of the yield. However, no positive effect of this type was found at either site. In view of the potential N losses to the environment, management strategies should therefore carefully balance the advantages and disadvantages of grassland renewal.

Chapter 3

Fluxes of N_2 and N_2O and contributing processes in summer after grassland renewal and grassland conversion to maize cropping on a Plaggic Anthrosol and a Histic Gleysol

Abstract

Grassland renewal and grassland conversion to arable land are common agricultural practices on intensively used grassland sites, especially in north-western Europe. However, grassland ploughing can cause a flush of soil organic nitrogen (N) mineralisation due to soil disturbance during tillage and decomposition of stubble and roots from the old grass sward. This is known to result in enhanced nitrous oxide (N_2O) emissions, but information about the underlying microbial processes, especially the role of N_2O reduction to N_2 *via* denitrification, is scarce. Therefore we applied the ^{15}N gas flux method *in situ* to grassland recently ploughed under for maize cropping, renewed grassland and permanent grassland on a Histic Gleysol and a Plaggic Anthrosol which differed in organic matter content and drainage. We used needle injection of ^{15}N-labelled KNO_3^- at three different depths in the soil to achieve homogeneous label distribution. Fluxes of N_2O and N_2, mineral N concentration and ^{15}N enrichment of these were measured for 44 days after label addition. Overall, no differences in N_2O and N_2 emissions were found between grassland conversion/renewal and permanent grassland. N_2 emissions increased up to 9115 g N ha^{-1} day^{-1} on a single sampling day following grassland conversion to maize cropping on the Histic Gleysol, leading to a great contribution of denitrification when $N_2O/(N_2+N_2O)$ ratio was low. However, heterogeneity of ^{15}N label distribution proved to be a major difficulty in the water-saturated Histic Gleysol and caused potential uncertainty in identification of various production pathways. Lower gaseous losses and higher nitrification potential were detected in the Plaggic Anthrosol, indicating a higher threat of possible leaching of excess mineral N following grassland conversion/renewal.

This chapter has been published by Buchen, C., Lewicka-Szczebak, D., Fuß, R., Helfrich, M., Flessa, H., Well, R., 2016. Fluxes of N_2 and N_2O and contributing processes in summer after grassland renewal and grassland conversion to maize cropping on a Plaggic Anthrosol and a Histic Gleysol. Soil Biology and Biochemistry 101, 6-19. doi:10.1016/j.soilbio.2016.06.028.

3.1 Introduction

Grassland comprises 19.51% (EUROSTAT, 2013) of the total land cover in the European Union (EU-27) and is an important resource for livestock farming. Grassland renewal and conversion of grassland to arable land can lead to considerable nitrogen (N) losses from soil (Davies et al., 2001) due to increased mineralisation of nitrogenous compounds in soil organic matter and in the grass sward. This initial period of high mineral N release is followed by a period with little or no N uptake by plants (Smit and Velthof, 2010; Velthof et al., 2010). These conditions can lead to increased nitrate (NO_3^-) leaching and gaseous N emissions by nitrification and denitrification in soil (Krol et al., 2016). Under anoxic conditions in particular, there can be pronounced denitrification, i.e. microbial reduction of nitrate and nitrite (NO_2^-) to the gases nitric oxide (NO), nitrous oxide (N_2O) and dinitrogen (N_2) (Knowles, 1982; Tiedje, 1982). Since N_2O is a potent greenhouse gas (IPCC, 2007) and a precursor for stratosphere ozone depletion (Ravishankara et al., 2009), its emissions need to be mitigated by adjusting agricultural management activities. To this end, it is important to understand the processes involved and, in particular, to know the fraction of N_2O reduced to N_2 before being released from soil. A number of studies have already identified ploughing of grassland as an important source of N_2O emissions (Grandy and Robertson, 2006), especially in combination with fertiliser application (Mori and Hojito, 2007; Velthof et al., 2010; MacDonald et al., 2011). However, due the complex system controlling N_2O fluxes (e.g. Müller and Clough (2014)) and the interaction of management effects with physical, chemical and biotic factors depending on site properties and climate, it is still not possible to generalise and predict such effects reliably. To better assess annual effects and potential seasonal changes and generate a solid basis for future N cycle models, it is necessary to understand the underlying processes of N_2O transformation, including formation of the end product of denitrification, i.e. N_2. Nitrogen in the form of N_2 is very challenging to quantify (Groffman et al., 2006; Van Groenigen et al., 2015), particularly because of its high atmospheric background concentrations. Hence, information on the effects of grassland renewal and grassland conversion to arable land on N_2 production and on the $N_2O/(N_2+N_2O)$ ratio of denitrification is scarce. No previous field study has investigated processes related to N_2O and N_2 formation and the resulting emission rates following grassland renewal or grassland conversion to arable land. Hence there is still a need to clarify these effects in different soils.

There are only two applicable methods for direct quantification of soil N_2 fluxes under field conditions: the acetylene (C_2H_2) inhibition technique (Yoshinari and Knowles, 1976) and the

^{15}N gas flux method (Hauck and Melsted, 1956). Inhibition of N_2O reduction to N_2 by using C_2H_2 has major disadvantages (Felber et al., 2012), most notably that the C_2H_2 catalyses oxidation of NO in the presence of oxygen (Bollmann and Conrad, 1997; Nadeem et al., 2013a, b). Thus ^{15}N analysis of gas fluxes after addition of ^{15}N labelled nitrate appears to be the only viable method, although it requires homogeneous ^{15}N labelling to produce precise results (Boast et al., 1988; Arah, 1992). The ^{15}N gas flux method also enables the apportionment of N_2O fluxes to different species of mineral N, e.g. based on the difference between ^{15}N enrichment of emitted N_2O and extracted NO_3^- to quantify NO_3^--derived fluxes (Stevens et al., 1997). Moreover, using an extended ^{15}N gas flux approach, the non-random distribution of N_2 and N_2O isotopologues can be taken into account in order to identify the formation of hybrid N_2 and/or N_2O, e.g. from co-denitrification or anammox (Spott and Stange, 2007, 2011). However, non-homogeneity in ^{15}N labelling can lead to a bias in the calculations, because the ^{15}N enrichment of extracted NO_3^- and of the active NO_3^- pool undergoing N_2 and N_2O formation can differ. This discrepancy has been shown to increase drastically over time during incubation of $^{15}NO_3^-$-labelled soil after NH_4^+ fertilisation (Deppe et al., 2017), an effect attributed in that study to non-homogeneity of tracer dilution as a result of small-scale heterogeneity in nitrification.

Field studies on denitrification under different land uses conducted using the ^{15}N gas flux method are summarised in a review by Stevens and Laughlin (1998). However, only a few field studies using ^{15}N tracing to measure N_2O and N_2 at grassland sites have been carried out so far. A first field application with perennial ryegrass was performed on small-scale plots by Rolston et al. (1976), with continued studies in the following years (Rolston et al., 1978; Rolston et al., 1982). Investigations on the effect of soil pH on N_2O and N_2 emissions and the denitrifying community were conducted by Čuhel et al. (2010). Recently, Baily et al. (2012) investigated emissions over 12 days following ^{15}N tracer use on various occasions over the course of one year, while Tauchnitz et al. (2015) determined N_2 emissions following rewetting of peat sites and Sgouridis and Ullah (2015) investigated N_2 emissions across different land use types. The ^{15}N labelling technique not only provides the opportunity to determine gaseous N losses due to denitrification, but also provides information about other N transformation processes that influence the formation and turnover of N_2O (i.e. nitrification, dissimilatory nitrate reduction to ammonium, immobilisation) and plant N uptake. Ploughing of existing grassland increases carbon (C) and N mineralisation (Davies et al., 2001) and also increases the availability of organic matter to microbes, thus favouring denitrification (Luo et al., 1999). Furthermore, an increase in soil porosity and aeration (Yamulki and Jarvis, 2002), along with

the change in oxygen supply brought about by soil tillage, can lead to enhanced nitrification, which is the dominant process of N_2O production under oxic conditions (Wolf and Russow, 2000). Such tillage-induced changes in organic C availability, mineral N concentration and soil porosity can result in changes in total denitrification activity and also in large variations in the relative proportions of N lost as N_2 and N_2O during the denitrification process (Mathieu et al., 2006; Baily et al., 2012; Tauchnitz et al., 2015). In a study on the saturated zone of organic grassland soils, *in situ* measurements using the ^{15}N push-pull approach showed intense denitrification, with N_2 as the main end product (Well et al., 2001; Well et al., 2003). Furthermore, co-metabolic denitrification (i.e. co-denitrification), where hybrid N_2O and/or N_2 is formed from two different N precursor compounds, can produce significant proportions of these gases under anoxic conditions, as shown in ^{15}N tracer studies by Spott and Stange (2011). Apart from denitrification and nitrification, N_2O losses *via* dissimilatory nitrate reduction (DNRA) may also occur under strict anaerobic conditions (Tiedje, 1988). Furthermore, enhanced N losses can occur *via* N leaching following grassland renewal (McLenaghen et al., 1996; Djurhuus and Olsen, 1997; Seidel et al., 2007; Seidel et al., 2009; Velthof et al., 2010).

To date, the ^{15}N gas flux method has not been applied in the field to investigate processes related to N_2O and N_2 formation and the resulting emission rates following grassland renewal or grassland conversion to arable land for different soils. Therefore, we conducted a study on the effects on N_2O fluxes of grassland renewal and grassland conversion to maize cropping on two soils with contrasting organic matter content and soil moisture (a well-drained sandy Plaggic Anthrosol and a Histic Gleysol) in Northern Germany. The complete study consisted of three parts, aimed at: (i) quantifying the field fluxes and the controlling processes; (ii) using isotopomer values of emitted N_2O to determine the relevance of N_2O turnover processes; and (iii) using the ^{15}N gas flux method *in situ* to quantify processes and fluxes of N_2 and N_2O and to provide reference data for the isotopomer approach. Here we describe part (iii). In addition to the need to complement parts (i) and (iii), the objective of this study were: (i) to determine the dynamics of N_2O emissions, N_2 emissions, the $N_2O/(N_2+N_2O)$ ratio of denitrification and the contributing processes and controls following ploughing of permanent grassland for maize cropping and renewal of grassland, in comparison with permanent grassland; (ii) to analyse the effects of two soils with different organic matter content and drainage on these processes; and (iii) to use an extended ^{15}N gas flux approach to evaluate the formation of hybrid N_2 and/or N_2O and determine the potential bias from non-homogeneous ^{15}N-labelling.

Two different time slots were selected after ploughing of grassland (directly after ploughing for maize cropping and 7 months after ploughing for grassland renewal) for analysis of N_2 and N_2O emissions dynamics and related processes in periods with immediate and former influences of grassland ploughing. The hypotheses tested were that: (1) N_2O and N_2 emissions are strongly enhanced by ploughing of grassland in comparison with permanent grassland, (2) denitrification is the dominant N_2O-producing process in the Histic Gleysol, whereas nitrification is favoured in the Plaggic Anthrosol, due to their differing soil properties; and (3) the bias in determining process rates from ^{15}N data arising from non-homogeneity in ^{15}N labelling increases over time due to heterogeneous dilution of the ^{15}N tracer by nitrification.

3.2 Material & methods

3.2.1 Study site

The field study was established on two grassland sites located in Ihausen (53°15'N, 7°50'E, 2 m a.s.l.) and Wehnen (53°10'N, 8°2'E, 10 m a.s.l.), northwest of Oldenburg, Lower Saxony, Germany. These agricultural sites represent two typical soil types with different organic matter content in the region.

The first site was established on a Histic Gleysol with a pH value of 5.8 ($CaCl_2$), a high soil organic matter content of 320 g kg^{-1} soil organic carbon (SOC) and a concentration of 20 g kg^{-1} total nitrogen (TN) in the 0-30 cm topsoil layer. The 30-year mean air temperature at the Ihausen study site is 9.5 °C and mean annual precipitation amounts to 752 mm (data from the nearby German Weather Service station at Friesoythe). The second site was established on a Plaggic Anthrosol with 91% sand, 6% silt and 4% clay in the 0-30 cm layer. This soil had a pH value of 5 ($CaCl_2$), a SOC content of 20 g kg^{-1} and a TN content of 2 g kg^{-1}. Mean long-term precipitation at this site is 760 mm and mean air temperature is 9.9 °C (data from a nearby station at the Chamber of Agriculture research site, Lower Saxony). Cumulative precipitation at both sites was 55 mm during our sampling period, which ran from May to July 2014 (Figure 3-1).

Before this study, both sites were managed as permanent grassland for at least 15 years by local farmers. During the last decades, the grassland in Ihausen was managed by mowing and fertilised with approx. 360 kg N ha^{-1} of fermentation residues, whereas the grassland in Wehnen was managed by grazing and received less fertiliser with 250 kg N ha^{-1} as a mixture of organic and mineral fertiliser. In 2013, a randomised field block trial with different grassland renewal treatments (plot size 9 m x 10 m) and a grassland to cropland conversion treatment,

each replicated four times, were established at both sites. We selected the following three treatments, which represent typical agricultural practices for the area, for the present study: (i) 15-year-old grass sward ("*Control*"); (ii) grassland renewal ("*Renewal*") by chemical killing of the sward with glyphosate, followed by cutting and mixing with a rotary cultivator, ploughing (25 cm depth), seedbed preparation and sowing of a new grass mix (54% *Lolium perenne* L., 20% *Festuca pratensis*, 17% *Phleum pratense L.*, 10% *Poa pratensis* L.). In accordance with local agricultural practice, grassland renewal (ploughing of the old sward to sowing) was carried out at the end of summer (September 2013). The third treatment (iii) was grassland conversion to maize cropping ("*Maize*") by chemical killing of the sward with glyphosate, followed by cutting and mixing with a rotary cultivator, ploughing (25 cm depth), seedbed preparation and sowing of *Zea mays* L. In accordance with local agricultural practice, grassland conversion to maize cropping (ploughing of the old sward to sowing) was carried out in spring (May 2014). The grassland treatments (*Control*, *Renewal*) were fertilised in March 2014 with calcium ammonium nitrate at a rate of 100 kg N ha^{-1}. The first cut followed in May 2014. We chose the period after cutting and fertilisation for our analyses, since this is the only period within the growing season where the ^{15}N tracer can be applied as fertiliser without increasing the total amount of mineral N in the system. Daily precipitation (mm) and air temperature (°C) were recorded by a climate station at each site. In addition, groundwater wells were installed and equipped with water level loggers (Type Diver, Eijkelkamp Agrisearch Equipment, Netherlands) for continuous water level monitoring.

3.2.2 Experimental design and ^{15}N application

Two weeks prior to the experiment, i.e. at the end of May 2014, polyvinyl chloride (PVC) cylinders (15 cm diameter, 35 cm height, 5 mm wall thickness) with sharpened edges were inserted to a depth of 30 cm in a random location in each replicate plot (n = 4) of the *Control* and *Renewal* treatments. For the *Maize* treatment, larger PVC columns (30 cm diameter, 35 cm height, 5 mm wall thickness) were used and placed in the seed row, i.e. with inclusion of one maize plant per micro-plot. The first grass cut/maize sowing was performed prior to installation.

Prior to ^{15}N application, composite topsoil samples (0-10, 10-20, 20-30 cm layers) were taken from each plot to assess mineral N background concentration and calculate the required ^{15}N fertiliser application dose. On 25 May, the soil columns were fertilised with 0.98 g ^{15}N-labelled KNO_3 fertiliser (~60 at%) per column for the *Control* and the *Renewal* treatments and 7.36 ^{15}N-labelled KNO_3 fertiliser (~60 at%) g per column for the *Maize* treatment, resulting in

a fertiliser equivalent of 80 kg N ha^{-1} for the *Control* and *Renewal* plots and 150 kg N ha^{-1} for the *Maize* plots. These different N fertilisation rates for grassland and maize were according to typical local agricultural management practice. The tracer was dissolved in distilled water and then applied by injection *via* steel capillaries. For guidance and equidistant positioning of injection capillaries, we used a plastic template perforated with 12 holes for the small columns and 48 holes for the larger columns. Injection was performed using a peristaltic pump (Ismatec BVP, Wertheim, Germany) with 24 flexible tubes (inner diameter: 1.65 mm), each connected to a steel capillary with a lateral opening (inner diameter: 0.7 mm). The capillaries were inserted though the grid to a defined depth and 2 mL tracer solution were applied simultaneously per injection point to ensure homogeneous horizontal distribution of the ^{15}N fertiliser. By applying only 2 mL per injection point, the increase in water content was equivalent to less than 3% water-filled pore space (WFPS) at both sites (Wu et al., 2011). To approximate a uniform vertical distribution, the ^{15}N tracer solution was applied at three different depths (5, 15 and 25 cm). According to Wu et al. (2011), the bias of non-homogeneity can be reduced by label addition through 38 injections at different depths. In order to achieve this optimal three-dimensional homogeneous distribution of the ^{15}N-labelled NO_3^- solution, we used 36 injections in the smaller columns and 144 injections in the larger columns.

3.2.3 Soil sampling and analysis

Soil samples were taken one week prior to the experiment around the soil columns and weekly in the soil columns during the experiment. Soil samples from the columns were taken using a Goettinger boring rod with diameter 18 mm and 14 mm slots (Nietfeld GmbH, Quakenbrück, Germany). Boreholes were sealed by inserting a closed sand-filled PVC pipe with the same diameter as the bore. Thus soil sampling resulted in a loss of soil volume of approximately 7% and 2% in the 15 cm and 30 cm diameter cores, respectively. Hence, the potential impact of soil sampling losses on measured N fluxes was small and neglected in our calculations. In order to minimise soil disturbance by soil sampling, just one sample was taken per micro-plot on each sampling occasion and divided into three sections (0-10 cm, 10-20 cm, 20-30 cm). At the end of the experiment, soil cores were taken out completely, divided into the three assigned depths and homogenised. Soil moisture content was determined gravimetrically after drying the soil at 105 °C to constant weight. WFPS was calculated from the gravimetric water content and soil bulk density, which was determined in advance for each plot using undisturbed soil samples taken with stainless steel cylinders (100 cm^3). WFPS was also determined for the organic soil (Histic Gleysol), but due to high spatial heterogeneity in SOC and in bulk density,

pore space estimates from intact core measurements prior to the field experiment were not representative for samples of weekly water content measurement. WFPS calculated from water content, bulk density and SOC reached values of 120% and was thus considered inaccurate. At the beginning and end of the experiment, soil NO_3^- and NH_4^+ were extracted by shaking 75 g soil in 300 mL 0.0125 mol $CaCl_2$ solution (ratio 1:4) at room temperature for one hour. At the same time, soil pH was determined by shaking 5 g fresh soil in 25 mL 0.01 mol $CaCl_2$ solution for one hour and using a pH meter (FE20, Mettler Toledo, Urdorf, Switzerland). For soil samples collected between the start and end of the experiment, the extraction ratio of N_{min} analysis was changed to 1:10, as only approx. 10-15 g soil material were available per layer. The NO_3^- and NH_4^+ concentrations in the extracts were determined using a photometric continuous flow analyser (SA 5000, Skalar Analytical B.V., Netherlands). Soil temperature (5 cm depth) was measured in each plot using a hand-held digital thermometer during the gas sampling procedure.

Isotopic analysis of NO_3^- and NH_4^+

The ^{15}N abundance in NO_3^- (a_{NO3}-) and NH_4^+ (a_{NH4+}) was determined according to the procedure described in Stange et al. (2007), whereby NO_3^- was reduced to NO by vanadium chloride ($V(III)Cl_3$) and NH_4^+ was oxidised to N_2 by sodium hypobromite (BrNaO). The NO and N_2 obtained were then analysed using a quadrupole mass spectrometer (GAM 200, InProcess Instruments, Bremen, Germany). The analytical precision was determined by repeated measurements of standards (1 at%, 5 at%, 50 at%, 75 at%) and was consistently around 1.2%.

3.2.4 Gas sampling and analysis

Chamber sampling

Fluxes of N_2O were determined using the closed chamber method (Hutchinson and Mosier, 1981) in opaque PVC chambers with a volume of 4.4179 dm³ (diameter 15 cm, height 20 cm) for grassland plots and 17.6715 dm³ (diameter 30 cm, height 20 cm) for *Maize* plots. Chambers were closed and sealed with air-tight rubber bands for 120 minutes on each sampling occasion. Sampling was always performed in the morning hours on the Histic Gleysol and later in the day on the Plaggic Anthrosol.

Headspace sampling was performed at sampling intervals of 0, 20, 40, 60 minutes in evacuated glass vials (20 mL) using a 30 mL syringe. After closing for 120 minutes, duplicate headspace

samples were taken in evacuated screw-cap exetainers (12 mL). One of the duplicates was analysed by gas chromatography and the other by isotope ratio mass spectroscopy (IRMS). Gas samples were taken on days 1, 3, 5, 7, 8 and 9 and thereafter weekly until day 44 after application of the ^{15}N tracer solution.

N_2O analysis and flux calculation

Measurements of N_2O concentrations in the 20 mL samples (0 to 60 minutes sampling) were carried out with a gas chromatograph (GC 2014, Shimadzu, Duisburg, Germany) equipped with an electron capture detector (ECD) and an autosampler (Loftfields Analytical Solutions, Neu Eichenberg, Germany). The analytical precision was determined weekly by repeated measurements of standard gases (300 ppb N_2O) and was consistently around 6.4 ppb (2%).

The N_2O concentration after 120 minutes (N_2O_{120}) of closure time was analysed using an Agilent 7890A chromatograph (Agilent, Santa Clara, United States) equipped with a micro-ECD and a PAL GC auto-sampler (CTC Analytics AG, Zwingen, Switzerland). The precision of the gas analysis, expressed as the coefficient of variation for repeated determinations of standard gases, was <1% for N_2O.

Flux rates of total N_2O, i.e. including fluxes from ^{15}N-labelled and non-labelled sources, were calculated from ordinary linear regression of the five consecutive samples over time using the R-package *gasfluxes* (Fuß, 2015) and the following equation:

$$\boldsymbol{N_2Oflux_{total}} = \frac{\mathbf{d}\boldsymbol{C}}{\mathbf{d}\boldsymbol{t}} * \frac{\boldsymbol{V}}{\boldsymbol{A}} \qquad \textbf{Eq. 3-1}$$

, where N_2Oflux_{total} is the flux rate in µg N_2O-N m^{-2} h^{-1}, C is N_2O mass concentration in µg N m^{-3} (C_{N2O}) corrected by the chamber temperature according to the ideal gas law, t is closing time of the chamber, V is volume of the chamber in m^3 and A is covered soil area in m^2.

Isotopic analysis of N_2 and N_2O

Gas samples collected after 120 minutes were analysed for isotopologues of N_2 and N_2O using a modified GasBench II preparation system coupled to a MAT 253 isotope ratio mass spectrometer (Thermo Scientific, Bremen, Germany) according to Lewicka-Szczebak et al. (2013). In this set-up, N_2O is converted to N_2 prior to analysis, which allows simultaneous measurement of stable isotope ratios ^{29}R ($^{29}N_2/^{28}N_2$) and ^{30}R ($^{30}N_2/^{29}N_2$), of N_2, of the sum of denitrification products (N_2+N_2O) and of N_2O. The analytical detection limit of the calculated N_2 flux from the ^{15}N labelled pool was approx. 257 µg N m^{-2} h^{-1}.

Calculation of N_2O and N_2 fluxes and apportionment to different N pools

The ^{15}N enrichment of the active NO_3^- pool undergoing N_2 and/or N_2O formation (a_p) can be different from a_{NO3}- because the denitrification products (N_2 and N_2O) are typically produced at anaerobic microsites. Here, a_p was calculated from the non-random distribution of N_2 and/or N_2O isotopologues (Mulvaney, 1984; Arah, 1992) using equations given by Spott et al. (2006). These include calculation of the fraction of N_2 or N_2O evolved from this pool (f_p) as:

$$f_p = \frac{a_m - a_{bgd}}{a_p - a_{bgd}} \quad \textbf{Eq. 3-2}$$

, where $a_m$is measured ^{15}N abundance of N_2 or N_2O:

$$a_m = \frac{^{29}R + 2 * ^{30}R}{2(1 + ^{29}R + ^{30}R)} \quad \textbf{Eq. 3-3}$$

a_{bgd} is measured ^{15}N abundance of atmospheric background N_2;

a_p is calculated ^{15}N abundance of the active ^{15}N-labelled pool:

$$a_p = \frac{^{30}x_m - a_{bgd} * a_m}{a_m - a_{bgd}} \quad \textbf{Eq. 3-4}$$

, where $^{30}x_m$ is the measured fraction of *m/z* 30 in N_2 and converted N_2O:

$$^{30}x_m = \frac{^{30}R}{1 + ^{29}R + ^{30}R} \quad \textbf{Eq. 3-5}$$

The same calculations were used for N_2, N_2+N_2O and for N_2O, resulting in respective values for fractions (f_{p_N2}, f_{p_N2+N2O}, f_{p_N2O}) from the ^{15}N labelled pool and for the respective ^{15}N abundances of the active N pools *(*a_{p_N2}, a_{p_N2+N2O}, a_{p_N2O}). These equations were used when both ^{29}R and ^{30}R of samples were significantly different from the standard (chamber air at t_0). In cases where only either ^{29}R or ^{30}R was significant, we used the simplified equations including best estimates of a_p (Spott et al., 2006), taken from ^{15}N analysis of NO_3^-, e.g. a_{NO3}-. We assumed that the ^{15}N enrichment of the total NO_3^- pool in the soil (a_{NO3}-) was identical to the extractable NO_3^- pool, ^{15}N enrichment of which was quantified by ^{15}N analysis of extracted NO_3^-.

N_2O fluxes from the labelled NO_3^- pool in µg N_2O-N m^{-2} h^{-1} were calculated as:

$$N_2Oflux_L = f_{p\_N2O} * N_2Oflux_{total} \quad \textbf{Eq. 3-6}$$

For sampling events where f_{p_N2O} was not measurable, the N_2O flux emitted from the labelled NO_3^- pool (N_2Oflux_L) was set to 0 for calculations, assuming that no N_2O from the labelled NO_3^- pool was emitted.

The N_2 flux (N_2flux_L) emitted from the labelled NO_3^- pool was obtained as:

$$C_{N2\_L} = f_{p\_N2} * C_{sample} \quad \text{Eq. 3-7}$$

, where the atmospheric concentration of N_2 (0.7809 m^3 m^{-3}) was used as an approximation for C_{N2_sample}, since the contribution of soil-derived N_2 to the sample concentration in field flux studies is negligible (e.g. Mulvaney (1984)). The N_2flux_L was then calculated similarly to the total N_2O flux (Eq. 3-1), assuming that the increase in the emitted N_2 (C_{N2_L}) was also linear as shown for C_{N2O}. Linearity of fluxes during 120 minutes was checked by comparing measurements after 60 and 120 minutes conducted on two separate days. Due to limited IRMS capacity, this check was not possible for all sampling days. From this sample set, eight comparisons were considered valid, since all values were above the detection limit. The ratio between C_{N2_L} for 120- and 60-minute samples was 1.97±0.93 and thus not significantly different from the assumed doubling of concentration. The detection limit of the N_2 concentrations derived by the ^{15}N analyses was determined from the variation in R^{29} and R^{30} values of measured air standards (1 σ) and amounted to 1.8 ppm N_2.

Due to the occurrence of C_{N2_L} values below the detection limit, several gaps existed in the datasets. To enable calculation of cumulative fluxes, these gaps were filled using a value of half the C_{N2_L} detection limit (0.9 ppm) if denitrification was indicated by substantial N_2O fluxes, giving final N_2O concentrations >550 ppb from gas chromatography measurements. For sampling events with lower total N_2O fluxes, N_2flux_L was set at 0, assuming that denitrification was negligible.

The contribution of hybrid N_2 (f_{H_N2}) and N_2O (f_{H_N2O}) was estimated from comparison of a_{p_N2} and a_{p_N2O} with a_{NO3}- values obtained from ^{15}N analysis of NO_3^- in soil extracts. If $a_p < a_{NO3}$- , this can be due to combination of two N sources, labelled and non-labelled, to form N_2O or N_2 (Spott and Stange, 2007). To quantify the fractions of hybrid (f_{H_N2}, f_{H_N2O}) and non-hybrid (f_{NH_N2}, f_{NH_N2O}) N_2 or N_2O, we used the equations given by Spott and Stange (2011), where the fractions of total NO_3^--derived fluxes of N_2 and N_2O are equal to the sum of hybrid and non-hybrid fluxes:

$$f_{p\_N2O} = f_{H\_N2O} + f_{NH\_N2O} \quad \text{Eq. 3-8a}$$

$$f_{p\_N2} = f_{H\_N2} + f_{NH\_N2}$$ **Eq. 3-8b**

Eqs. 3.8a and 3.8b only represent the hybrid N fluxes where one N atom originates from labelled NO_2^- formed from labelled NO_3^- by the first step of denitrification. Hybrid fluxes from non-labelled NO_2^-, e.g. from nitrification, are thus not included.

Based on the calculations above, we defined the following types of N_2O and N_2 fluxes:

Total N_2O flux obtained from gas chromatography analysis:

N_2Oflux_{total} (see Eq. 3-1)

Non-hybrid flux emitted from the labelled NO_3^- pool:

$$N_2Oflux_{L\_NH} = f_{NH\_N2O} * N_2Oflux_{total}$$ **Eq. 3-9a**

$$N_2flux_{L\_NH} = f_{NH\_N2} * N_2flux_L$$ **Eq. 3-9b**

Hybrid flux:

$$N_2Oflux_{L\_H} = f_{H\_N2O} * N_2Oflux_{total}$$ **Eq. 3-10a**

$$N_2flux_{L\_H} = f_{H\_N2} * N_2flux_L$$ **Eq. 3-10b**

For simplicity, we assigned hybrid flux to the flux from the ^{15}N labelled pool, despite one atom being derived from the non-labelled sources.

Total flux from the labelled NO_3^- pool:

$$N_2Oflux_L = N_2Oflux_{L\_H} + N_2Oflux_{L\_NH}$$ **Eq. 3.11a**

$$N_2flux_L = N_2flux_{L\_H} + N_2flux_{L\_NH}$$ **Eq. 3.11b**

N_2O flux from non-labelled N pools:

$$N_2Oflux_{NL} = N_2Oflux_{total} - N_2Oflux_L$$ **Eq. 3-12**

For the definition of N_2 fluxes we had to take into account the fact that we were unable to quantify total soil-emitted N_2, since the emissions of N_2 from non-labelled sources, e.g. NO_2^- or NO_3^- from nitrification, cannot be quantified based on our ^{15}N tracing approach. Hence all fluxes are defined in relation to the N_2 flux derived from the labelled NO_3^- pool (N_2flux_L).

Combining N_2 and N_2O values, we defined the $N_2O/(N_2+N_2O)$ ratio of denitrification using the following definition:

$$\boldsymbol{N_2Oflux_L/(\,N_2flux_L + N_2Oflux_L)} \qquad \textbf{Eq. 3-13}$$

3.2.5 Data treatment and statistical analysis

All calculations were performed using R 3.2.0. (R Development Core Team, 2016).

Statistical analysis

Treatment differences in cumulative fluxes for the replicate plots were tested by analysis of variance (ANOVA). Variance homogeneity and approximate normality of residuals were checked by diagnostic plots. If ANOVA indicated differences, a Tukey-HSD test was performed for pair-wise comparisons. The level of significance was set to $p<0.05$ for all tests. Mean fluxes were calculated by linear interpolation. Because the number of gap-filling data for N_2 and N_2O from the labelled NO_3^- pool increased during the experimental period, average fluxes were calculated and compared based on two different periods: the total experimental period (44 days) including all gap-fillings and the first 23 days, including less than 50% of gap-filling data.

Partial correlation

Since N_2O and N_2 emissions are usually driven by more than one factor and these relationships can be expected to be nonlinear, we used Spearman partial correlation analysis (*pcor*) as implemented in R package *ppcor* version 1.0 (Kim, 2015). We tested the $N_2Ofluxes_{total}$ and $N_2fluxes_L$ as well as f_{p_N2O} and the $N_2O/(N_2+N_2O)$ ratio of denitrification in sum and for each treatment against: NO_3^--N content (0-30 cm depth), NH_4^+-N content (0-30 cm depth), soil temperature (5 cm depth), groundwater level and soil moisture. Soil moisture was represented by gravimetric water content (0-30 cm depth) for the Histic Gleysol and by WFPS (0-30 cm depth) for the Plaggic Anthrosol.

Generalised additive models

Relationships of $N_2Ofluxes_{total}$ to explanatory variables were further investigated using generalised additive models (GAM) as implemented in the R package *mgcv* version 1.8-7 (Wood and Augustin, 2002; Wood, 2011). Such models can represent nonlinear relationships in a nonparametric way by fitting additive smoother terms, whereby the degree of smoothing is determined by penalised maximum likelihood estimation. N_2O fluxes were log-transformed,

which is a common prerequisite for analysing N_2O data because of their skewed distribution (Folorunso and Rolston, 1984). Model quality was assessed using diagnostic plots with the focus on variance homogeneity and approximate normality of residuals. Due to the fact that the driving variables were measured on selected dates, the GAM could only be applied to 70 of 132 N_2O data points. Due to the small number of observations above the detection limit, $N_2fluxes_L$ could not be investigated with GAM.

Beta regression model

The change in the $N_2O/(N_2+N_2O)$ ratio of denitrification during the first 23 sampling days was tested by fitting a beta regression model (R package *betareg* version 3.0-5; Cribari-Neto and Zeileis (2010) to the data). Such a generalised linear model is appropriate for data that are restricted to the interval (0, 1). It presents the data as a beta distribution with a parameterisation using mean and a precision parameter. The mean is linked by the logit function to a linear model, for which we used sampling date and treatment as linear predictors. The precision parameter was modelled in dependence on treatments, date and block. Likelihood ratio tests (R package *lmtest* version 0.9-34; Zeileis and Hothorn (2002)) were employed to compare nested models and thereby assess the significance of parameters.

Gross nitrification rates

Gross nitrification rates (n) in µg N g^{-1} dry soil were calculated based on the pool dilution approach, i.e. from the measured dilution of the added $^{15}NO_3^-$ by production of non-labelled NO_3^- *via* nitrification, according to Kirkham and Bartholomew (1954):

$$\boldsymbol{n} = \frac{(\boldsymbol{C_{NO3-t0} - C_{NO3-ti}})}{\boldsymbol{ti - t0}} * \frac{\boldsymbol{log(a_{NO3-t0}/(a_{NO3-ti})}}{\boldsymbol{log(C_{NO3-t0}/C_{NO3-ti})}} \qquad \textbf{Eq. 3-14}$$

, where C is the concentration of NO_3^--N at different times, marked by the subscript (t_0 or t_i) indicating the time period between the sampling dates and α for the ^{15}N excess enrichment in soil NO_3^-.

3.3 Results

3.3.1 Meteorological data and environmental parameters

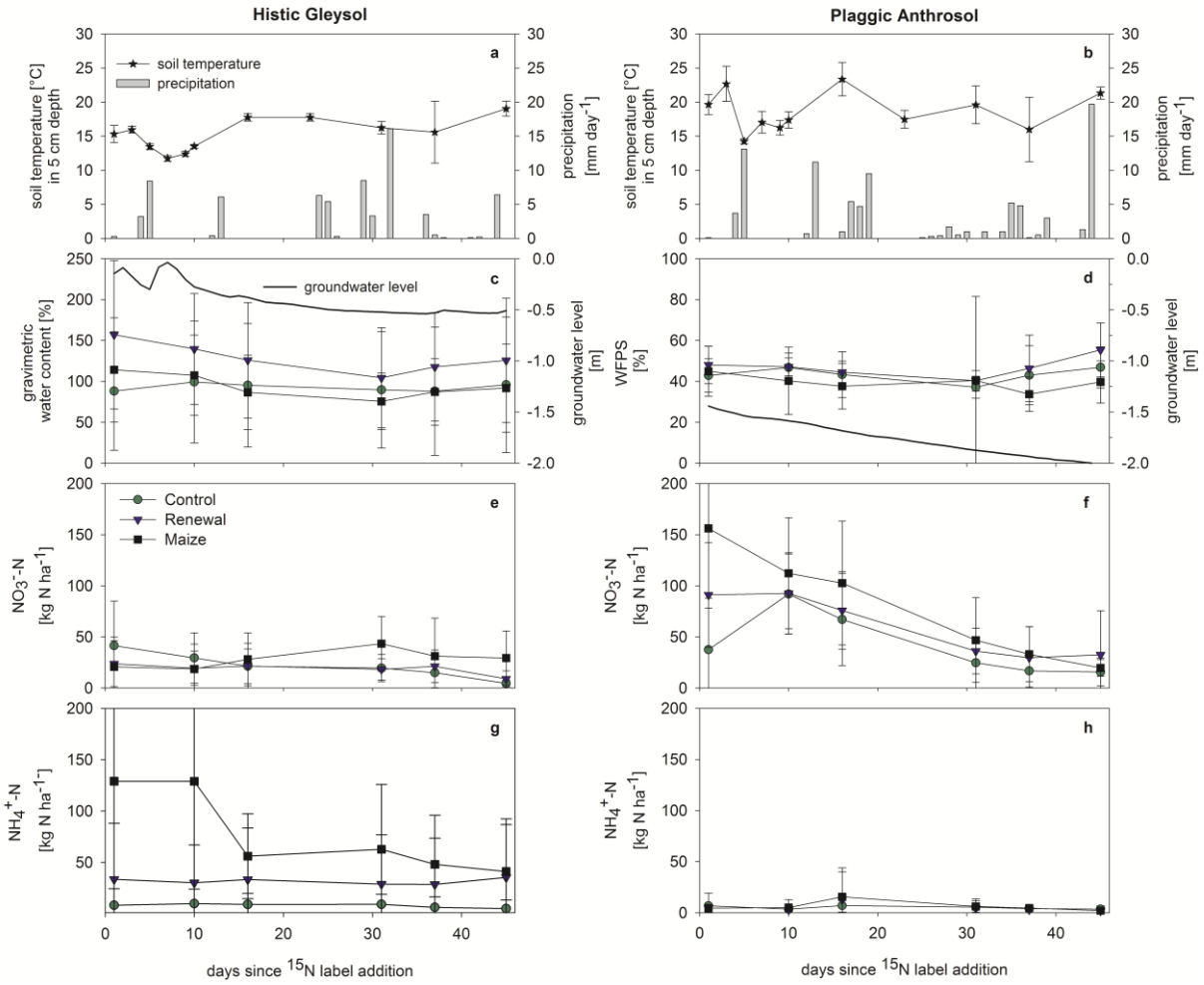

Figure 3-1: (a, b) Soil temperature during gas sampling and daily precipitation, (c) groundwater level and gravimetric water content for the Histic Gleysol, (d) WFPS for the Plaggic Anthrosol, (e, f) NO_3^--N concentration and (g, h) NH_4^+-N concentration. Error bars indicate standard deviation of the mean (n = 4)

The two study sites are located 30 km apart. Precipitation was distributed differently at the two sites (Figure 3-1a and b), with numerous precipitation events up to 10-15 mm during the whole sampling period and a higher precipitation period after four weeks, particularly at the Histic Gleysol site, whereas the Plaggic Anthrosol received more precipitation one week earlier. The Histic Gleysol is strongly influenced by the groundwater level, fluctuating between 0 and -0.5 m. Almost full saturation during the first 10 days and decreasing groundwater levels during the rest of the sampling period led to high gravimetric water contents of up to 200% on some sampling days. Overall, the gravimetric water content differed slightly between the treatments, with a tendency for higher values in the *Renewal* treatment. In the Plaggic Anthrosol, the WFPS of all treatments was in the vicinity of 40-50%. The groundwater level

was below the rooting zone (>1.5 m) at this site and thus did not affect water content in the topsoil at this site.

The two soils also showed differing mineral N dynamics. The Histic Gleysol exhibited high NH_4^+-N concentration (>100 kg N ha^{-1}), especially in the *Maize* treatment (up to 128.9 kg N ha^{-1}), while NO_3^--N concentrations were 4.5-43.3 kg N ha^{-1}. Mineral N in the Plaggic Anthrosol was dominated by NO_3^--N (15.6-156.2 kg N ha^{-1}), while the NH_4^+-N concentration was quite low (<15.4 kg N ha^{-1}). The generally higher NO_3^- concentrations in the *Maize* treatment can be explained by the higher fertilisation rate in that treatment (150 kg N ha^{-1}) compared with the grassland treatments (80 kg N ha^{-1}) and slower plant N uptake by the recently sown maize plants than by the grass.

3.3.2 N_2O and N_2 fluxes and ^{15}N enrichment

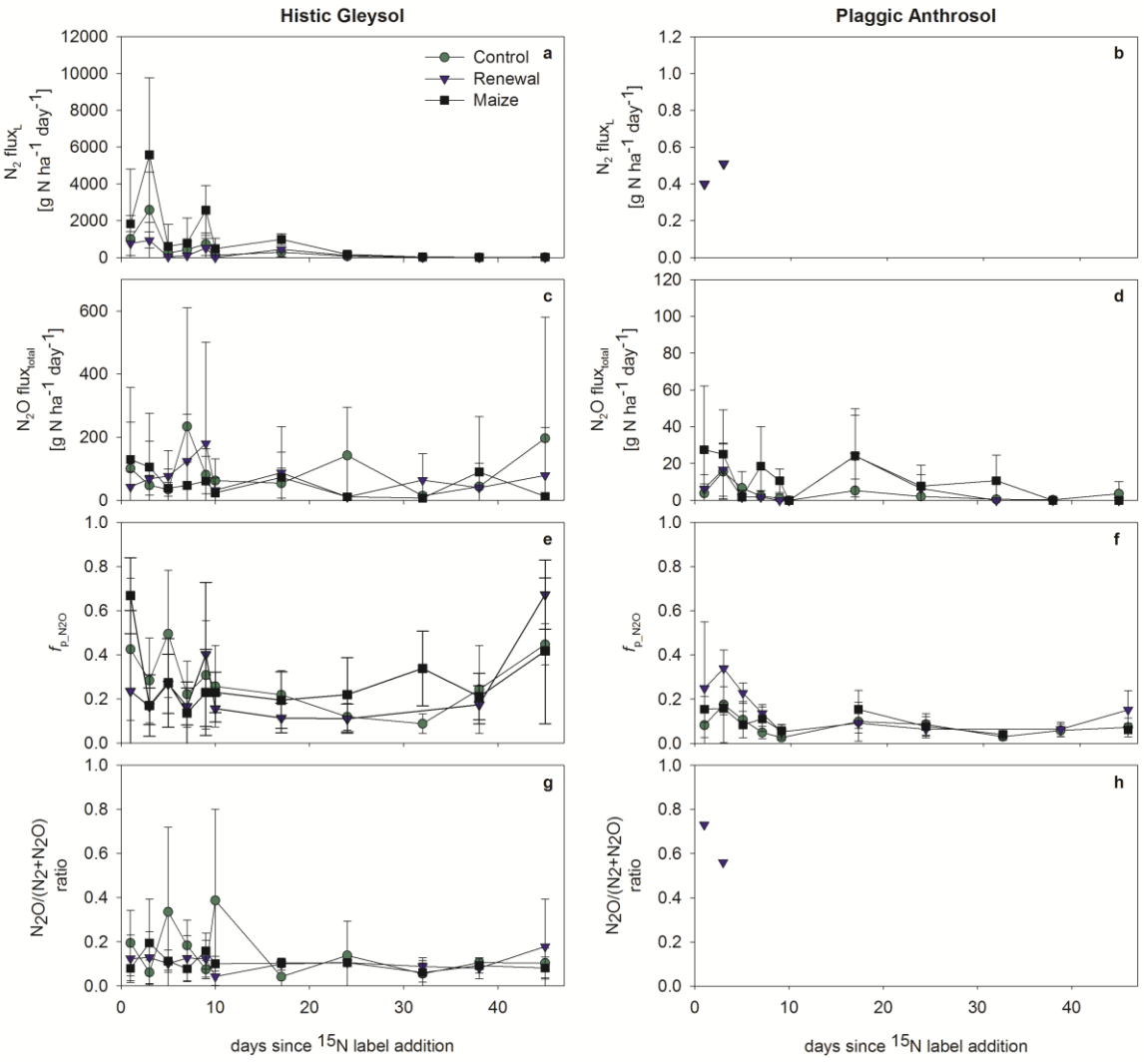

Figure 3-2: (a, b) Daily $N_2fluxes_L$, (c, d) $N_2Ofluxes_{total}$, (e, f) (f_{p_N2O}) from the active labelled NO_3^- pool and (g, h) $N_2O/(N_2+N_2O)$ ratio of denitrification per treatment following ^{15}N label addition at day 0. Error bars indicate standard deviation of the mean. Averages of samples with detectable R^{30} and R^{29} values (n =1 to 4)

The N_2 fluxes derived from the active labelled NO_3^- pool (N_2flux_L) of the Plaggic Anthrosol were below the detection limit (<1.8 ppm), with the exception of block B of the *Renewal* treatment, which exhibited measurable $N_2fluxes_L$ on sampling days 1 and 3 (0.40 and 0.51 g N per ha^{-1} day^{-1}, respectively; Figure 3-2b). In contrast, distinct N_2 emission peaks were observed from the Histic Gleysol following ^{15}N fertiliser application, reaching up to 9115 g N ha^{-1} day^{-1} in the *Maize* treatment on day 3 (Figure 3-2a). After that, $N_2fluxes_L$ declined rapidly within 10 days to very low values and after 27 sampling days they were close to the detection limit.

Total N_2O fluxes ($N_2Ofluxes_{total}$) differed between the two soils (Figure 3-2c and 3-2d). $N_2Ofluxes_{total}$ varied between 0 and 794 g N ha^{-1} day^{-1} for the Histic Gleysol and were about 10-fold lower for the Plaggic Anthrosol. Significant differences were not observed between the treatments. An increase in N_2O production after day 40 apparently occurred after heavy rainfall events, with up to 27 mm on the Histic Gleysol and up to 25 mm on the Plaggic Anthrosol, during the last three days of the experiment.

The fraction of soil-emitted N_2O derived from the active ^{15}N-labelled NO_3^- pool (f_{p_N2O}) varied between 0 and 0.83 in the Histic Gleysol and 0 and 0.5 in the Plaggic Anthrosol (Figure 3-2e and 3-2f). There was a rapid decrease in f_{p_N2O} for the Plaggic Anthrosol within the first 10 days, whereas for the Histic Gleysol, fluctuations were observed and there was a larger range of values, which became an increase after high precipitation during the last days of the experiment.

The time course of a_{p_N2}, a_{p_N2O} and a_{NO3}- values was plotted to explore different aspects of N transformation (Figure 3-3). The fraction of hybrid N_2 and/or N_2O is obtained from the difference between a_{NO3}- and a_{p_N2} and/or a_{p_N2O}, where positive values of these differences provide evidence of hybrid formation. Agreement of a_{p_N2} and a_{p_N2O} is an indicator of homogeneity in ^{15}N labelling (Stevens et al., 1997), which is a prerequisite for quantifying hybrid N_2 and/or N_2O (Spott and Stange, 2007). Decreasing trends in a_{p_N2}, a_{p_N2O} and a_{NO3}- indicated increasing dilution of the total and actively denitrifying NO_3^- pools, e.g. resulting from nitrification.

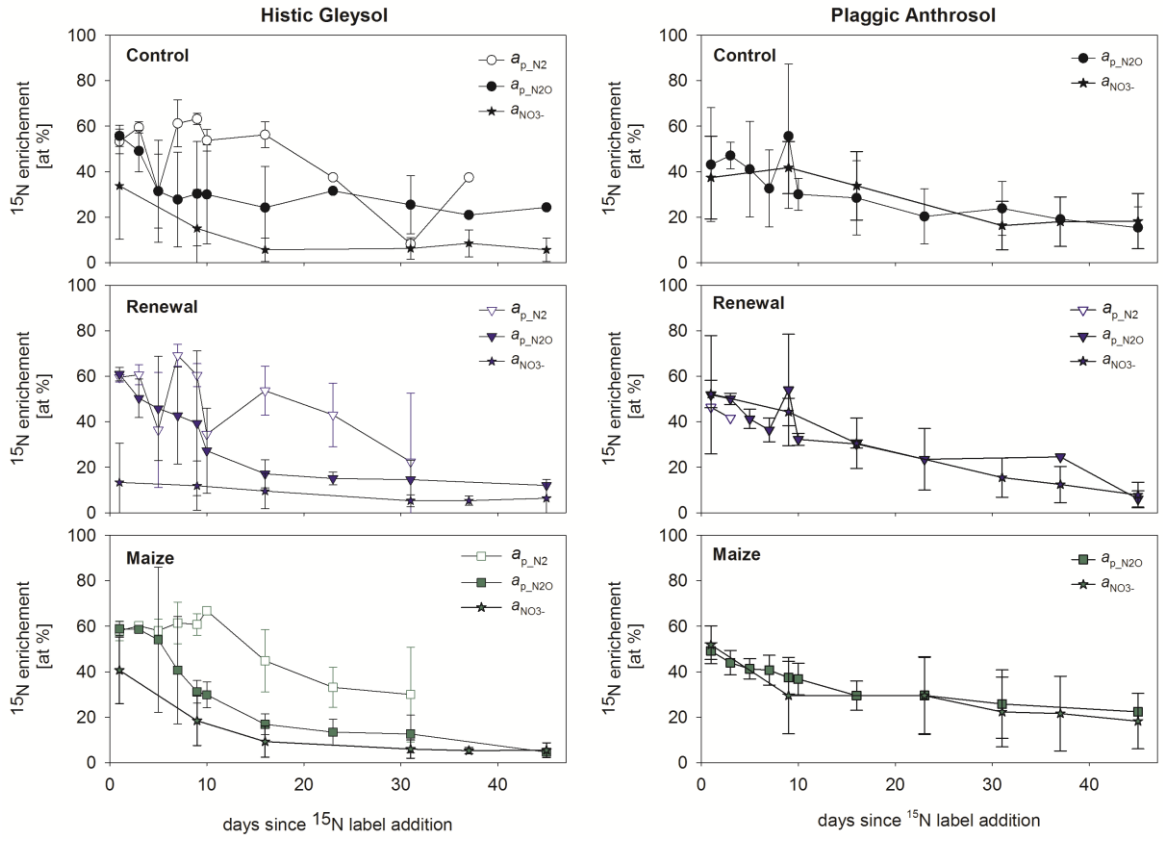

Figure 3-3: ^{15}N enrichment of the labelled N pool emitting N_2 (a_{p_N2}), N_2O (a_{p_N2O}) in headspace samples and ^{15}N enrichment of NO_3^- in soil extracts (a_{NO3}-) per treatment on both soil types. Mean of samples with detectable R^{30} and R^{29} values (n= 1 to 4). Error bars indicate standard deviation of the mean

For the Histic Gleysol, a_{NO3}- was always lower than a_p, indicating substantial differences in enrichment of the total and active NO_3^- pools and hence precluding calculation of hybrid N_2 and N_2O. Non-homogeneity was further supported by differences between a_{p_N2} and a_{p_N2O}. On the first sampling day after application of ^{15}N fertiliser, the ^{15}N enrichment of a_{p_N2} and a_{p_N2O} was close to 60 at%, and within the following days a_{p_N2O} declined more rapidly than a_{p_N2}, which stayed close to initial levels until day 10. For the Plaggic Anthrosol, a_{p_N2} values in the *Renewal* treatment were only available for the two first sampling events and were slightly below a_{p_N2O} values, which were initially close to the ^{15}N enrichment of the added tracer solution (60 at%). In all treatments, a_{p_N2O} and a_{NO3}- overlapped during the entire experimental period, suggesting homogeneity in ^{15}N-labelling and absence of hybrid N_2O. In both soils, all ^{15}N values decreased with time, indicating ongoing nitrification. However, while a_{NO3}- always displayed steadily decreasing trends, a_{p_N2} and a_{p_N2O} values showed some fluctuations, indicating variability in the actively denitrifying NO_3^- pools.

Changes in the $N_2O/(N_2+N_2O)$ ratio of denitrification are shown in Figure 3-2g and 3-2h. Since N_2*fluxes*$_L$ could only be quantified on sampling days 1 and 3 in the Plaggic Anthrosol, we were only able to calculate the $N_2O/(N_2+N_2O)$ ratio of denitrification for those two days (values of

0.73 and 0.56, respectively). Values for the Histic Gleysol were highly variable, ranging from 0 to 0.98. The $N_2O/(N_2+N_2O)$ ratio of denitrification for each block per treatment is shown in Figure A3-1 (Supplementary data). In the *Control* and *Renewal* treatments, variations tended to increase with time, since block C and block D, respectively, exhibited extremely large fluctuations between days 9 and 16. Only the *Maize* treatment stayed at constantly low $N_2O/(N_2+N_2O)$ ratio of denitrification, coinciding with higher N_2 emissions during the sampling period. The fitted beta regression model indicated a decrease in $N_2O/(N_2+N_2O)$ ratio over time (23 sampling days), but differences between the treatments were not significant based on the limited number of available values and large variation between the individual values.

Mean values of N_2Oflux_{total} and N_2flux_L for the first 23 days are given in Table 3-1 and for the entire sampling period in Table A3-6 (Supplementary data). For N_2Oflux_{total}, N_2Oflux_L and N_2flux_L from the Histic Gleysol, there were no significant differences between the three treatments, but there was a tendency for higher $N_2fluxes_L$ and $N_2Ofluxes_L$ in the *Maize* treatment. The mean $N_2O/(N_2+N_2O)$ ratio of denitrification of cumulated fluxes over time ranged between 0.01 and 0.14 for all plots. The average $N_2O/(N_2+N_2O)$ ratio of denitrification was highest for the *Control* and lowest for *Maize*, but differences between treatments were not significant.

Table 3-1: Mean total N_2O fluxes (N_2Oflux_{total}), N_2O fluxes (N_2Oflux_L) and N_2 fluxes (N_2flux_L) from the active labelled NO_3^- pool and the $N_2O/(N_2+N_2O)$ ratio of denitrification, calculated from the mean fluxes per plot, over a 23-day period for the Histic Gleysol and Plaggic Anthrosol. Superscript letters indicate significant differences between the treatments and soil sites at significance level p<0.05. Values shown are mean of treatment replicates ± one standard deviation (n=4, except n=3, marked by *)**

Treatments	N_2Oflux_{total}	N_2Oflux_L	N_2flux_L	$N_2O/(N_2+N_2O)$ ratio of denitrification
	kg N ha^{-1}	kg N ha^{-1}	kg N ha^{-1}	
Histic Gleysol				
Control	2.02±1.56 ^{a*}	0.47±0.50 ^{a*}	21.10±13.52 ^{a*}	0.07±0.07 ^{a}
Renewal	0.67±0.83 ^{a}	0.24±0.42 ^{a}	12.66±8.92 ^{a}	0.03±0.06 ^{a}
Maize	1.89±0.93 ^{a}	0.76±0.48 ^{a}	40.21±21.47 ^{a}	0.02±0.01 ^{a}
Plaggic Anthrosol				
Control	0.27±0.09 ^{a}	0.02±0.02 ^{a}	bd	NA
Renewal	0.37±0.11 ^{a}	0.04±0.02 ^{a}	bd	NA
Maize	0.66±0.27 ^{a}	0.07±0.08 ^{a}	bd	NA

bd below detection limit; *NA* not applicable

**Due to a limited number of N_2 flux values above the detection limit towards the end of the experiment, total N gas fluxes were calculated for two periods: (i) over the first 23 sampling days, with at least two values per treatment above the detection limit (Table 3-1) and for the entire 44 day sampling period (see Table A3-6).

No significant treatment effects were found for the mean fluxes from the Plaggic Anthrosol. Cumulative $N_2 fluxes_L$ could not be determined, because fluxes were mostly below the detection limit. For the $N_2 Ofluxes_{total}$ and $N_2 Ofluxes_L$, a site effect was found ($p \leq 0.1$) for the first 23 days of sampling, with lower values from the Plaggic Anthrosol.

3.3.3 Partial correlation of N_2O and N_2 emissions with soil variables

For the Histic Gleysol, a significant correlation between fluxes and groundwater level (R^2 = 0.51-0.67) was found. Interestingly the soil moisture content, i.e. gravimetric water content, was strongly negatively correlated with N_2O, whereas N_2 was not correlated with moisture. Other important variables with mostly significant correlations were the NO_3^--N and the NH_4^+-N concentrations in both soils. Soil temperature was only significantly correlated with the $N_2 Ofluxes_{total}$ from the Plaggic Anthrosol. Since partial correlation tables stratified by treatment gave a similar picture, they are not shown.

Table 3-2: Partial Spearman's (R^2) correlation of mean total N_2O fluxes ($N_2 Oflux_{total}$), N_2 fluxes ($N_2 flux_L$) and N_2+N_2O fluxes ($(N_2+N_2O)flux_L$) from the active labelled NO_3^- pool, and f_{p_N2O} with potential driving variables

Spearman's R	$N_2 Oflux_{total}$	f_{p_N2O}	$N_2 flux_L$	$(N_2+N_2O)flux_L$
Histic Gleysol				
n	70	42	42	42
NO_3^- content	0.65 **	0.30	0.26	0.27
NH_4^+ content	0.51 **	0.26	0.33	0.45 **
Gravimetric water content	-0.64 **	-0.39 **	0.05	0.06
Soil temperature	0.23	0.35	-0.23	-0.17
Groundwater level	0.67 **	0.67 **	0.54 **	0.51 **
Plaggic Anthrosol				
n	71	37	0	0
NO_3^- content	0.22 *	0.25	NA	NA
NH_4^+ content	-0.24*	-0.03	NA	NA
WFPS	0.09	0.32	NA	NA
Soil temperature	0.36*	0.32	NA	NA
Groundwater level	0.13	-0.09	NA	NA

NA not applicable

* and ** indicate $p<0.05$ and $p<0.01$ level of significance, respectively

We applied a generalised additive model (GAM) to the total N_2O flux dataset to further investigate the effect of driving variables. NO_3^--N, NH_4^+-N, soil temperature and soil moisture content (WFPS for the Plaggic Anthrosol and gravimetric water content for the Histic Gleysol) were selected as driving variables, since these are known to be key controllers of N_2O emissions. Results from ANOVA analyses of N_2O emissions for both sites are given in Tables

A3-7 and A3-8 (Supplementary data). The ANOVA results for the parametric terms for the Histic Gleysol GAM showed that N_2O emissions were significantly dependent on block. In addition, there was a significant interaction of treatment and block, i.e. treatment effects depended on block. Moreover, there was a significant impact of NO_3^--N content and groundwater level. The smoother of groundwater level shows a general increase of N_2O emissions with increasing groundwater levels, but non-changing emissions between about -43 and -27 cm. However, data points for wet conditions were particularly sparse. Groundwater level was used instead of soil moisture, because it proved to be more significant.

The corresponding GAM results for the Plaggic Anthrosol showed significant dependence on treatment and block, whereas the interaction of treatment and block was less important than in the Histic Gleysol, i.e. treatment effects were more similar between blocks. A significant contribution of NO_3^- availability to N_2O emissions was also observed, whereas the impact of soil moisture, in this case represented by WFPS, was negligible. In the Plaggic Anthrosol, soil temperature improved the model according to adjusted R^2 and was not removed by the penalised regression, even though the individual smoother terms were not significant. Shrinkage smoothers stratified by treatment (Figure A3-3) showed differences in temperature dependency between the treatments, with a linear effect for the *Control* and *Maize* treatments. In the *Renewal* treatment, an increase was evident after a temperature maximum of 26 °C was reached, but this effect was driven by just a few data points. In summary, it is apparent that substrate availability (NO_3^--N) and soil moisture in the Histic Gleysol and substrate availability (NO_3^--N) and soil temperature in the Plaggic Anthrosol were the important drivers governing $N_2Ofluxes_{total}$, which is in agreement with the findings from the partial correlation analysis. It should be noted that in both soils, more than 50% of the N_2O emissions could be explained by the GAM.

3.3.4 Contributing processes

Gross nitrification

Gross nitrification rates were calculated per sampling interval (Table A3-8) and on average of the 5 sampling intervals in Table 3-3. Average rates ranged from 0.21±2.38 to 0.87±4.03 mg NO_3^--N kg^{-1} dry soil day^{-1} in the Plaggic Anthrosol (Table 3-3). Tests of differences on the average values between the three sampling depths were unable to identify more and less active soil zones of nitrification. But for single sampling intervals, significant differences between treatments and depths were found.

Table 3-3: Gross nitrification rates per soil layer and average of the 5 sampling intervals for the Plaggic Anthrosol. Different superscript letters indicate significant differences for the respective treatment at significance level p<0.05. Means from treatment replicates ± standard deviation (n=4)

	Gross nitrification rates				
Treatment	mg NO_3^--N kg^{-1} dry soil day^{-1}			kg N ha^{-1} day^{-1}	
Sampling depth	**0-10 cm**	**10-20 cm**	**20-30 cm**	**0-30 cm**	
Control	0.38±2.01	0.47±1.68	0.21±2.38	1.46±4.83	a
Renewal	0.55±1.20	0.84±1.55	0.57±1.66	2.70±3.51	a
Maize	0.87±4.03	0.60±1.93	0.68±1.99	2.90±6.36	a

3.4 Discussion

3.4.1 Impact of grassland disturbance on N_2O and N_2 fluxes

Total N_2O fluxes ($N_2Ofluxes_{total}$) increased during the first days following fertiliser application for both soil types investigated (Histic Gleysol and Plaggic Anthrosol). This is similar to findings by Jones et al. (2005) that the highest N_2O release from grasslands occurs within seven to 20 days following fertiliser application, with a return to close to background levels thereafter. However, the two different soil types studied here varied widely in their N_2O losses, with 10-fold higher $N_2Ofluxes_{total}$ from the Histic Gleysol (up to 611 g N ha^{-1} day^{-1}) than from the Plaggic Anthrosol (up to 50 g N ha^{-1} day^{-1}) for both grassland treatments. Total denitrification losses, i.e. $N_2+N_2Ofluxes_L$ emitted from the active N-labelled NO_3^- pool, were high for the Histic Gleysol soil (up to 33% of ^{15}N-labelled fertiliser applied). In the Plaggic Anthrosol, denitrification losses were lower (at most 0.11% of ^{15}N fertiliser applied was emitted as N_2O), particularly as N_2 fluxes were only detectable in two single samples (Figure 3-2b).

A source of uncertainty in NO_3^--derived N_2 and N_2O fluxes might be the unknown proportion of downward diffusion of labelled N_2 and N_2O due to the existing concentration gradients to the non-labelled subsoil. This effect had been proposed as a possible source of bias in experiments using the C_2H_2 inhibition technique (Mahmood et al., 1998). It can lead to underestimation of denitrification by the soil cover method (Ryden et al., 1987; Arah et al., 1991), especially with extended enclosure time of the chamber (Healy et al., 1996). Because gas diffusivity was much larger in the sandy Plaggic Anthrosol due to its larger air-filled porosity (Moldrup et al., 2000), it can be assumed that this bias was much larger for that soil than for the Histic Gleysol, where subsoil diffusivity was low due to the high groundwater level. It is thus possible that the observation of low or undetectable $N_2fluxes_L$ was in part due to this effect.

In contrast to the large differences in N_2O and N_2 emissions pattern between the two soil types, there were few significant variations in $N_2Ofluxes_{total}$ between the three treatments (Table 3-1 and Table A3-6). This lack of treatment effect is in contrast to findings in a number of previous studies (Davies et al., 2001; Ball et al., 2007; Mori and Hojito, 2007; Velthof et al., 2010) that ploughing of grassland and N fertiliser application at the same time lead to strongly increased N_2O emissions. Similarly, no significant differences in $N_2Ofluxes_L$ were found between the treatments. The fact that there was always N_2O derived from NO_3^- as well as N_2O from other sources demonstrates a contribution from several N_2O-producing pathways, but their share of N_2Oflux_{total} was not significantly altered by grassland ploughing. We did not observe the large short-term N_2O increase after ploughing of permanent grassland reported by MacDonald et al. (2011) and Krol et al. (2016), or even peak emissions for 10 to 15 days (Davies et al., 2001; Velthof et al., 2010). However, total denitrification fluxes (N_2+$N_2Ofluxes_L$) exhibited some clear treatment effects on the Histic Gleysol, as single $N_2fluxes_L$ of up to 9397 g N ha^{-1} day^{-1} were noted for the *Maize* treatment in the first days after fertiliser application, but lower fluxes of at most 4825 and 2389 g N ha^{-1} day^{-1} for the *Control* and *Renewal* treatments, respectively. This flux increase may have resulted from a combination of three factors: (i) high availability of mineral N from fertilisation of the maize (150 kg N ha^{-1}); (ii) initially low N uptake of the maize seedlings; and (iii) mobilisation of SOM and resulting mineralisation of organic C and N due to the recent ploughing. No impact from ploughing in the previous year in the *Renewal* treatment was observed for total N_2O or total denitrification fluxes from either soil type. Moreover, for the Plaggic Anthrosol no treatment differences in $N_2Ofluxes_{total}$ or $N_2Ofluxes_L$ were found. Therefore, the hypothesis of strongly increased N_2O emissions following grassland conversion to arable land was not confirmed for our sites and study period. However, it is important to note that all N fluxes were highly variable between the individual chambers within the same treatment, as shown by the block effect on N_2O in the GAM (Table A3-7). This reflects the well-known high spatial variability of factors controlling N_2O fluxes in soil-plant systems (Smith et al., 1998; Schaufler et al., 2010), which might have masked moderate treatment effects.

3.4.2 Treatment effects on type and magnitude of N_2O processes

In general, it is assumed that denitrification is the dominant N transformation process in soils with a high soil water content, as in the Histic Gleysol studied here, while nitrification is likely to dominate under oxic conditions (Wrage et al., 2001). However, the fraction of soil-emitted N_2O derived from the active labelled NO_3^- pool (f_{p_N2O}) was highly variable (0-0.87, see

Figure 3-1e) in the Histic Gleysol, showing that both NH_4^+-derived N_2O from nitrification and nitrifier denitrification and NO_3^--derived N_2O from denitrification contributed to the flux. The significant contribution of autotrophic or heterotrophic nitrification and/or nitrifier denitrification was attributable to the fraction of N_2O emitted from sources other than the labelled NO_3^- pool (0.13-1). Moreover, it has to be considered that temporarily saturated soil conditions can lead to a potential contribution of dissimilatory nitrate reduction to ammonium (DNRA) to the N_2 and N_2O fluxes, as shown by various studies (Rückauf et al., 2004; Sgouridis et al., 2011; Tauchnitz et al., 2015). ^{15}N enrichment of NH_4^+, which was detected on the second and third sampling day (up to 11 at% and 8 at%, respectively) indicates that DNRA or immobilisation (i.e. assimilatory NO_3^- reduction) and subsequent remobilisation occurred at the study site (Rütting et al., 2011).

The calculation of hybrid N_2 and N_2O ($N_2Oflux_{L\_H}$; $N_2flux_{L\_H}$) according to Spott and Stange (2011) yielded negative values, since a_{NO3}- was always smaller than a_{p_N2} and a_{p_N2O} (see Figure 3-3). Hybrid processes such as co-denitrification and anaerobic ammonium oxidation (Anammox) would result in the opposite relationship. To explain the observations, it has to be considered that a_{NO3}- reflects the average ^{15}N enrichment of NO_3^- extracted from a soil sample, whereas a_{p_N2} and a_{p_N2O} reflect the specific ^{15}N enrichment of the NO_3^- pool undergoing denitrification, i.e. the NO_3^- at denitrifying microsites (Mulvaney, 1984). One possible explanation is spatial heterogeneity of ^{15}N enrichment of NO_3^- whereby the denitrifying (presumably anaerobic) microsites are closer to the enrichment of added NO_3^-, while the aerobic domains are not denitrifying and thus do not emit gaseous denitrification products. However, the latter might be more diluted in ^{15}N enrichment due to more intense nitrification, resulting in lower ^{15}N enrichment of NO_3^- in the bulk soil (Well et al., 2015; Deppe et al., 2017). Moreover, at high moisture content the lag time between production and emission of N_2 and N_2O could result in a similar pattern if the ^{15}N pool were significantly diluted due to nitrification during this lag time, which could be the case at high soil moisture content when gas diffusivity is low. Due to this apparent heterogeneity in the ^{15}N pool enrichment, the potential contribution of hybrid N fluxes cannot be confirmed or rejected. Overall, this observation suggests that non-homogeneity of ^{15}N pool labelling leads to underestimation of the denitrification flux, which can produce a relative error of up to 24% according to Arah (1992) and Van den Heuvel et al. (1988).

In the Histic Gleysol, the lower part of the 30 cm deep ^{15}N-labelled topsoil was initially water-saturated due to the high groundwater level (see Figure 3-1c). High *in situ* denitrification

rates in the saturated zone of organic grassland soils have been reported previously (Well et al., 2001; Well et al., 2003) and have been explained by abundance of organic C (Well et al., 2005) and absence of oxygen due to high respiration and low diffusivity (Well et al., 2001). However, limited diffusive gas exchange also results in transient accumulation of denitrification products in the soil solution (Well et al., 2001; Tauchnitz et al., 2015), leading to a substantial lag time between production and emissions and favouring N_2O reduction to N_2. Hence we cannot rule out the possibility that N_2 accumulation in the saturated zone led to underestimation of denitrification during the first nine days after ^{15}N-labelling, since accumulated N_2 might have been preferentially emitted during declining groundwater levels (Weymann et al., 2009), which might have been incompletely captured due to the infrequent measurements. The co-occurrence of the Histic Gleysol layer with high groundwater levels thus explains the high fluxes with low $N_2O/(N_2+N_2O)$ ratio of denitrification, but also illustrates the need to take dissolved denitrification products in saturated soil layers into account and indicates that total denitrification losses might have been even higher than reported in Table 3-1 and Table A3-6. The $N_2O/(N_2+N_2O)$ ratio of denitrification was usually less than 0.2 and highly variable due to large spatial variability in the N_2O and $N_2fluxes_L$ (see different blocks in Figure A3-1). Similar total ranges have been reported in earlier grassland studies (Smith and Arah, 1990; Mathieu et al., 2006; Čuhel et al., 2010; Baily et al., 2012) and recently by Sgouridis and Ullah (2015), with the $N_2O/(N_2+N_2O)$ ratio of denitrification ranging from 0 to 0.08 within different land use types. Comparisons of the $N_2O/(N_2+N_2O)$ ratio of denitrification of the different treatments within the first 24 hours with values reported by Mathieu et al. (2006) for a similar time range revealed considerably lower mean values in our experiment, with 0.19±0.14 (*Control*), 0.09±0.12 (*Renewal*) and 0.27±0.11 (*Maize*) for the Histic Gleysol. The intensive N_2O reduction to N_2 was apparently responsible for the lack of a short-term N_2O peak, as reported in previous studies (Baily et al., 2012). However, in the *Maize* treatment we observed a large N_2+N_2O response in the first two weeks after ploughing and fertilisation. This confirmed enhancement of denitrification in this treatment, probably mainly induced by the ploughing. It can be assumed that the impact of fertilisation was less important, because NO_3^- concentrations in the *Maize* treatment were not higher than in the *Control* and Renewal treatments, which exhibited lower N_2+N_2O fluxes in this period. It is known that ploughing grassland leads to enhanced decomposition of soil organic matter, favouring the formation of anaerobic microsites in the soil and thus denitrification (Folorunso and Rolston, 1984; Myrold and Tiedje, 1985; Parkin, 1987). Moreover, denitrification "hotspots" induced by decomposing plant residues (Parkin, 1987) may be highly relevant due to heterogeneous incorporation of the

sward. Such "hotspots" might be responsible for the observed large spatial variability in the $N_2fluxes_L$ (e.g. 0.70-9.11 kg N ha^{-1} on sampling day 2 in the *Maize* treatment) from the Histic Gleysol. In contrast, almost all N_2O emitted from the Plaggic Anthrosol was derived from non-labelled (N_2Oflux_{NL}) soil N pools (see Table 3-1). Hence nitrification and nitrifier denitrification dominated the emissions due to the prevailing oxic conditions in that well-aerated soil (Dail et al., 2001).

Furthermore, we showed that $N_2Ofluxes_{L\_H}$ were insignificant in the Plaggic Anthrosol, as there was good agreement between a_{NO3}- and a_{p_N2O} (see Figure 3-3). Thus spatial heterogeneity effects on ^{15}N enrichment, as assumed in the Histic Gleysol, were apparently not so relevant for the Plaggic Anthrosol. This was presumably due to a combination of two factors that result from the sandy texture: (i) high hydraulic conductivity, and thus a lower probability of preferential flow of the injected tracer, and (ii) good soil aeration, and thus absence of anaerobic microsites where dilution of the tracer due to nitrification could be lower.

3.4.3 Impact of controlling factors on N_2, N_2O fluxes and contributing processes

The impact of grassland renewal or conversion to arable land can affect the processes responsible for N_2 and N_2O emissions, since several controlling factors are altered by sward incorporation and the subsequent change in vegetation, i.e. aeration of the soil structure, changes in moisture and groundwater levels caused by the water demand of plants, electron donors for denitrification and enhanced O_2 consumption by rhizodeposition and organic matter decomposition, as well as formation of NH_4^+ and NO_3^- through mineralisation as substrates of nitrification and denitrification and the changes caused by plant N uptake (Müller and Clough, 2014). These treatment factors co-occur with site and climate effects.

Nitrification and denitrification were strongly influenced by the shallow groundwater level (0-0.2 m) in the Histic Gleysol during the first nine sampling days (Figure 3-1a). Under such saturated conditions, the expected $N_2O/(N_2+N_2O)$ ratio of denitrification is close to zero, as reported by Tauchnitz et al. (2015) and confirmed by our observations. Looking at the first three days following ^{15}N label addition, $N_2Ofluxes_{total}$ increased immediately, whereas the highest $N_2fluxes_L$ were measured on the third day. This lag phase between N_2O and N_2 emission peaks has been observed in previous short-term studies by Clough et al. (1998) and Mathieu et al. (2006). They explained the delay by soil water acting as a sink for N_2O and/or the time required for the reduction of N_2O to N_2. Dendooven and Anderson (1994) explained

the lag time by the different enzymes involved in the production and consumption of N_2O under anaerobic conditions and a typical delay in production of N_2O reductase. Furthermore, the N_2O release in saturated soils is limited by inhibited gas diffusivity. A second slight increase in N_2 and N_2O fluxes between day 10 and 20 coincided with increasing soil temperature and a larger rainfall event (>15 mm at both sites), which in combination probably increased denitrification rates. The observation that denitrification is higher and the $N_2O/(N_2+N_2O)$ ratio of denitrification is lower in Gleysols compared with mineral soils, with N_2 fluxes increasing and $N_2O/(N_2+N_2O)$ ratio of denitrification further decreasing during wetting phases, is in agreement with earlier observations by Rückauf et al. (2004); Jørgensen et al. (2012) and Tauchnitz et al. (2015).

In the Plaggic Anthrosol, there was no effect of groundwater level (which was below 2 m) or WFPS on N_2O fluxes and their contributing processes. As the Plaggic Anthrosol is characterised by WFPS around 40-50%, and thus good soil aeration, it has limited potential for denitrification (Bouwman et al., 2002), whereas these conditions are optimal for nitrification (Davidson et al., 1991). Nevertheless, denitrification was detected, since some of the N_2O originated from the active ^{15}N-labelled NO_3^--pool ($N_2Ofluxes_L$) and $N_2fluxes_L$ were above the detection limit (1.8 ppm) in two individual samplings. Since N_2+N_2O emissions were initially high following fertiliser application, mineral N content was an important driving factor controlling N_2O emissions, as also indicated by the results from partial correlation analysis (see Table 3-2) and the GAM for $N_2Ofluxes_{total}$. In addition, an interaction between soil moisture and NO_3^- availability was found in the Histic Gleysol, as reported previously by Abdalla et al. (2009) for grassland soils. In general, however, mineral N values in the Histic Gleysol were highly variable, with NO_3^--N values between 0.25 and 56.21 kg N ha^{-1} and NH_4^+-N values between 0 and 178.33 kg N ha^{-1} on the first sampling day. This variability of NO_3^--N and NH_4^+-N values might be explained by DNRA and associated immobilisation (i.e. assimilatory NO_3^- reduction) or mineralisation (Rütting et al., 2011). The latter are known to be rapid and intense in organic horizons (Berntson and Aber, 2000; Dail et al., 2001; Rückauf et al., 2004). Moreover, we showed that up to 10% of NO_3^- was transformed by DNRA (see section 3.4.2).

The role of nitrification and nitrifier denitrification in N_2O emissions can be evaluated based on the gross nitrification rates obtained from the pool dilution calculations. For the Histic Gleysol the large heterogeneity at this site and the limited mineral N sampling, with one bore sample per soil plot and sampling day, limited the precision in calculation of gross nitrification, whereas values were more robust for the Plaggic Anthrosol due to its lower heterogeneity. The

percentage of N_2O emitted from NH_4^+ oxidation per unit NO_3^- produced is reported to range from 0.1 to 1.8% (Goodroad and Keeney, 1984; Flessa et al., 1996; Well et al., 2008). We calculated N_2O yields based on average values for the 5 sampling intervals in our 44-day study period using fluxes from NH_4^+ oxidation (N_2Oflux_{NL} obtained by the difference between N_2Oflux_{total} and N_2Oflux_L given in Table A3-6) and gross nitrification rates for 0-30 cm soil depth (Table 3-3). For the Plaggic Anthrosol, N_2O yield was 0.9±0.7, 0.4±0.1 and 0.7±0.4 (n=4) for the *Control*, *Reseed* and *Maize* treatments, respectively, and thus within the range quoted in the literature. We assumed that the observed nitrification in the Plaggic Anthrosol reflected higher mineralisation, since no NH_4^+ fertiliser was added and the NH_4^+ concentrations were constantly at a low level during the experiment.

Because organic C availability is expected to be a potential driver of denitrification fluxes (Firestone et al., 1980; Luo et al., 1999), increasing organic C availability by ploughing the soil and thus incorporating dead plant material might explain the high denitrification fluxes in the *Maize* treatment on the Histic Gleysol. Although we did not measure C availability in this study, it is well established that conversion of grassland to arable land by ploughing inevitably leads to substantial mobilisation of organic C due to the destruction of the grass sward and its subsequent decomposition (Davies et al., 2001; Grandy and Robertson, 2006). Furthermore, the balance between electron donors (microbe-available organic C) and acceptors (N oxides) in soil is changed by organic matter mobilisation, favouring N_2O reduction (Smith and Arah, 1990) with increasing electron donor abundance, which further explains the low $N_2O/(N_2+N_2O)$ ratio of denitrification in the Histic Gleysol and the indication of lowest values in the *Maize* treatment.

3.5 Conclusions

In a novel application of the ^{15}N gas flux method, we investigated the dynamics of N_2O and N_2 emissions and contributing processes *in situ* following ploughing of grassland or grassland renewal compared with undisturbed permanent grassland. We found no significant increase in N_2O and N_2 emissions following grassland conversion for maize cropping on either soil studied (Histic Gleysol, Plaggic Anthrosol). Thus the postulated effects of grassland ploughing could not be confirmed, or were not strong enough to be identified, under our experimental conditions (44 days with four replicates), presumably due to the large spatial variability between replicates, especially for the Histic Gleysol. There was a significant site effect, with higher N_2O emissions and higher contribution of denitrification to the total flux in the organic Histic Gleysol compared with the sandy Plaggic Anthrosol, which we attributed to substantial

differences in organic matter content and water content/drainage. Intense N_2O reduction to N_2 prevented an increase in N_2O fluxes despite high denitrification rates. We were able to identify various processes contributing to N_2 and N_2O emissions with the ^{15}N tracing approach used. The results showed that multiple pathways are involved in the effects of grassland disturbance, since we obtained information about NO_3^- formation by nitrification, N_2O production from nitrification/nitrifier denitrification, heterotrophic denitrification and co-denitrification, N_2O reduction and NH_4^+ production by DNRA. However, the data for several of these pathways were fragmentary due to limited precision and/or low sampling frequency, while co-denitrification could not be verified in the Histic Gleysol due to spatial ^{15}N heterogeneity. This incompleteness demonstrates the potential for future improvement in unravelling N processes and their control by improving sampling and analysis and applying more sophisticated and multiple stable isotope approaches, e.g. including N_2O isotopomers and multiple stable isotope tracing approaches.

Chapter 4

Estimating N_2O processes during grassland renewal and grassland conversion to maize cropping using N_2O isotopocules

Abstract

Grassland is an important resource of livestock farming. Common agricultural practices on grasslands are grassland renewal and grassland conversion to maize cropping. However, grassland break-up can lead to a flush of mineral nitrogen (N_{min}) from decomposition of the old grass sward and the decomposition of soil organic matter (SOM) accumulated during the grassland period. The increased carbon (C) and nitrogen (N) mineralisation can result in enhanced nitrous oxide (N_2O) emissions. In the present study, we analysed N_2O emitted from two soils (Plaggic Anthrosol and Histic Gleysol) with different SOM contents and groundwater levels following grassland break-up. For the first time, we used stable isotope analyses of soil-emitted N_2O ($\delta^{18}O_{N2O}$, $\delta^{15}N^{bulk}_{N2O}$ and $\delta^{15}N^{SP}_{N2O}$ = intramolecular distribution of ^{15}N within the linear N_2O molecule) with a novel isotopocule mapping approach to simultaneously estimate the magnitude of N_2O reduction to N_2 and the fraction of N_2O originating from the bacterial denitrification pathway or fungal denitrification and/or nitrification. This approach is based on endmember areas of isotopic values for the N_2O produced from different sources reported in the literature. For this purpose, we calculated two main scenarios with different assumptions for N_2O produced: N_2O is reduced to N_2 before residual N_2O is mixed with N_2O of various sources (Scenario a) and vice versa (Scenario b). Based on this, we applied seven different scenario variations, where we evaluated the range of possible values for the potential N_2O production pathways (heterotrophic bacterial denitrification and/or nitrifier denitrification and fungal denitrification and/or nitrification). This was done by using a range of isotopic endmember values and assuming different fractionation factors of N_2O reduction in order to find the most reliable scenario. Our observations indicate bacterial heterotrophic denitrification and/or nitrifier denitrification as the main source of N_2O production, with a significant contribution of N_2O reduction to N_2 rather than nitrification (i.e. hydroxylamine oxidation) and fungal denitrification throughout the entire study period. A tendency to a higher contribution of N_2O reduction to N_2 could be displayed for the often water-saturated Histic Gleysol, while a lower N_2O reduction potential was found for the Plaggic Anthrosol. For two samples, we attempt to validate our results from the isotopocule mapping approach with a parallel ^{15}N tracing study at the field scale, as conditions of soil moisture, nitrate (NO_3^-) availability and N_2O flux were similar.

This chapter is intended for submission to Biogeoscience. Authors: Buchen, C., Lewicka-Szczebak D., Flessa, H., Well, R.

4.1 Introduction

During the last decades, livestock farming in north-western Europe has undergone a continuous intensification. Grassland renewal is a common agricultural management practice to keep swards higher-yielding and profitable. Moreover, large areas of permanent grassland have even been converted to arable land. Grassland break-up can lead to considerable nitrogen (N) losses from soil induced by increased mineralisation of nitrogen (N) and carbon (C) during the decomposition of organic matter in soil and in the grass sward after grassland break-up (Davies et al., 2001). Then, the combination of increased C and N mineralisation and a low or even lacking plant N uptake can lead to increased gaseous N emissions *via* nitrification and denitrification (Velthof et al., 2010; Necpalova et al., 2013; Krol et al., 2016). Pronounced denitrification can occur, in particular under anoxic conditions, i.e. the microbial reduction of nitrate (NO_3^-) and nitrite (NO_2^-) to the gases: nitric oxide (NO), nitrous oxide (N_2O) and dinitrogen (N_2) (Knowles, 1982; Tiedje, 1982), while nitrification, i.e. ammonia oxidation *via* hydroxylamine and NO_2^- to NO_3^- is regarded as the most important process under strict aerobic conditions. Including nitrifier denitrification, i.e. reduction of NO_2^- to N_2O or N_2 by autotrophic ammonia oxidisers (nitrifiers), which mostly occurs under low oxygen conditions or high NO_2^- concentrations (Wrage et al., 2001; Kool et al., 2011); these processes are considered to be major pathways of N_2O emission. Besides this, several other N_2O and N_2 production pathways exist, such as fungal denitrification (Laughlin and Stevens, 2002), co-denitrification (Spott and Stange, 2011), heterotrophic nitrification (Laughlin et al., 2008; Zhang et al., 2015), dissimilatory NO_3^- reduction to ammonium (DNRA) (Rütting et al., 2011) and anaerobic ammonium oxidation (Anammox) (Long et al., 2013); a complete overview of currently known N_2O production pathways is given elsewhere (Butterbach-Bahl et al., 2013). N_2O is known to be an important greenhouse gas (IPCC, 2013) and a major precursor for ozone depletion (Ravishankara et al., 2009). Therefore, N_2O emissions need to be mitigated by adjusting agricultural management practices. To this end, it is necessary to understand the N_2O processes involved, as well as the contribution of N_2O reduction to N_2. The share of N_2 is mostly unknown because it is challenging to quantify N_2 emissions due to high atmospheric background concentrations of 78% (Groffman et al., 2006; Van Groenigen et al., 2015).

To overcome this problem, several methods have been used for the direct quantification of soil N_2 fluxes under field conditions: the acetylene (C_2H_2) inhibition technique (Yoshinari and Knowles, 1976) and the ^{15}N gas flux method (Hauck and Melsted, 1956). The inhibition of N_2O reduction to N_2 by C_2H_2 has major disadvantages (Felber et al., 2012), since C_2H_2

catalyses the oxidation of NO to NO_2 in the presence of oxygen (Bollmann and Conrad, 1997; Nadeem et al., 2013a, b). Hence, the ^{15}N analysis of gas fluxes after the addition of ^{15}N labelled substrate appears to be the only viable method and was already applied on the studied field sites in order to quantify the processes and fluxes of N_2 and N_2O (Buchen et al., 2016). But also the ^{15}N gas flux method has its limitations: homogenous labelling is required (Boast et al., 1988; Arah, 1992), the method is expensive, can only be applied in fertilised systems, and application of ^{15}N-labelled fertiliser leads to a disturbance of the system (Groffman et al., 2006). Furthermore, the study period is limited to the time frame of ^{15}N label turn-over (Decock and Six, 2013).

Hence, natural abundance isotopic analysis of the four most abundant isotopocules of N_2O species ($^{14}N^{14}N^{16}O$, $^{14}N^{15}N^{16}O$, $^{15}N^{14}N^{16}O$, $^{14}N^{14}N^{18}O$) is a promising alternative to assess N_2O production pathways, because it is a non-invasive method with much lower costs, which increases the potential for a more widespread use. Three isotopic signatures of N_2O can be determined using this method: $\delta^{18}O$ of oxygen ($\delta^{18}O_{N2O}$), $\delta^{15}N$ bulk nitrogen ($\delta^{15}N^{bulk}_{N2O}$) and the intramolecular distribution of ^{15}N in N_2O, specified as "site preference" ($\delta^{15}N^{SP}_{N2O}$), i.e. the difference in $\delta^{15}N_{N2O}$ between the central ($\delta^{15}N^{\alpha}_{N2O}$) and the peripheral ($\delta^{15}N^{\beta}_{N2O}$) N atom of linear N_2O molecule (Brenninkmeijer and Röckmann, 1999; Toyoda and Yoshida, 1999). $\delta^{15}N^{SP}_{N2O}$ is considered to be indicative for the source process (high $\delta_0{}^{15}N^{SP}_{N2O}$ values indicate fungal denitrification and/or nitrification (in the remainder referred to as fungal denitrification / nitrification), while low $\delta_0{}^{15}N^{SP}_{N2O}$ values specify heterotrophic bacterial denitrification and/or nitrifier denitrification (in the remainder referred to as heterotrophic bacterial denitrification / nitrifier denitrification, Table 4-1) and is independent of substrate isotopic composition (Ostrom and Ostrom, 2011). This property enables $\delta^{15}N^{SP}_{N2O}$ values to be used to differentiate between N_2O production pathways, e.g. nitrification and denitrification (Sutka et al., 2006) and different microbial communities, e.g. fungal or bacterial denitrifiers (Sutka et al., 2008; Rohe et al., 2014), because $\delta^{15}N^{bulk}_{N2O}$ and $\delta^{18}O_{N2O}$ are affected by the isotopic composition of N_2O precursors (NO_2^-, NH_4^+, NO_3^- and H_2O) and also N_2O production pathways (nitrification or denitrification). Until now, $\delta^{15}N^{SP}_{N2O}$ has been used in pure culture studies to determine the range of isotopic signatures for the various pathways (Sutka et al., 2003; Toyoda et al., 2005; Sutka et al., 2006; Ostrom et al., 2007; Rohe et al., 2014). In addition, soil incubation studies were conducted to derive information under more natural conditions (Well et al., 2006; Well et al., 2008; Köster et al., 2013a; Köster et al., 2013b; Lewicka-Szczebak et al., 2014), whereby most available data on this topic has been summarised by Toyoda et al. (2015). However, in the course of the denitrification process

isotopic signatures of $\delta^{15}N^{SP}_{N2O}$, $\delta^{15}N^{bulk}_{N2O}$ and $\delta^{18}O_{N2O}$ are altered during N_2O reduction to N_2 (Decock and Six, 2013), and the extent of this change depends particularly on the residual, unreduced N_2O fraction ($r_{N2O} = y_{N2O}/(y_{N2}+y_{N2O})$ with y: mole fraction) and the net isotope effect of N_2O reduction (η_{red}). N_2O reduction can be calculated from the isotopic enrichment of the residual N_2O, based on the isotopic signature before reduction (δ_0) and η_{red} (Lewicka-Szczebak et al., 2014). δ_0 values depend on the processes themselves, while different soil conditions, e.g. moisture, diffusivity, temperature and N fertilisation have an indirect impact. Also η_{red} values may vary depending upon environmental conditions, process rates or substrate variability, as the η_{red} values represent the interaction between complex sequences of chemical and physical processes, i.e. η_{red} values result from the combination of intrinsic isotope effects of diffusion and enzymatic reduction (Ostrom et al., 2007). Moreover, complete reduction of N_2O n to N_2 in isolated micro-niches like dead-end pores leads to lowering of η_{red} values (Well et al., 2012). $\eta_{red}{}^{15}N^{bulk}_{N2O}$ and $\eta_{red}{}^{18}O_{N2O}$ values are quite variable, while for $\eta_{red}{}^{15}N^{SP}_{N2O}$ values, the range from -7.7 to -2.3‰ was recently confirmed under anoxic as well as under oxic conditions by Lewicka-Szczebak et al. (2015). Thus $\eta_{red}{}^{15}N^{SP}_{N2O}$ values can be expected to serve as a suitable calculation basis for field studies. Therefore, we applied the N_2O isotopocule mapping approach (Lewicka-Szczebak et al., 2017), where calculations are based on the relation between $\delta^{18}O_{N2O}$ and $\delta^{15}N^{SP}_{N2O}$ values and which allows a simultaneous estimation of the contribution of different N_2O production pathways and the r_{N2O} value. This approach is a further development of an isotopocule mixing approach first used by Zou et al. (2014).

Applying the N_2O isotopocule mapping approach, we aimed to quantify N_2O reduction to N_2 using natural abundance isotopocules of emitted N_2O to determine the relevance of N_2O turnover processes following grassland renewal and grassland conversion, which is part (3) within a complex field study on two soils with contrasting soil organic matter content and groundwater level (Histic Gleysol and Plaggic Anthrosol). In part (1) we quantified the field fluxes and their controlling processes following grassland renewal and grassland conversion to maize cropping (Buchen et al., submitted). In part (2) we measured the processes related to N_2O and N_2 formation by using the ^{15}N gas flux method (Buchen et al., 2016). To complete parts (1) and (2), the aims of the present study were: (i) to validate the isotopocule mapping approach using an independent dataset (^{15}N tracing experiment of part (2)), (ii) to quantify the contribution of N_2O reduction to N_2 and bacterial / fungal denitrification to the total N_2O flux, (iii) to evaluate seasonal changes of N_2O formation and reduction processes. The quantification of N_2O transformation processes using N_2O isotopocules is based on a study period of more

than one year from August 2013 (i.e. before grassland renewal) until November 2014 (i.e. harvest of the first maize cropping period following grassland conversion).

4.2 Material & methods

4.2.1 Site description

Investigations were carried out on two grassland sites, both northwest of Oldenburg, Lower Saxony, Germany. The study sites were located in Ihausen (53°15' N, 7°50' E, 2 m a.s.l.) and Wehnen (53°10' N, 8°2' E, 10 m a.s.l.) and represent two local soil types with differences in soil organic matter content (SOM) and groundwater level.

The first site (Ihausen) was established on a Histic Gleysol with a mean pH value of 5.8 ($CaCl_2$) and a high SOM content of up to 320 g kg^{-1} soil organic carbon (SOC) and a concentration of 20 g kg^{-1} total nitrogen (TN) in the 0-30 cm soil layer. This site was strongly influenced by the groundwater level, fluctuating between 0 and -0.6 m in 2013 to 2014. The annual average long-term air temperature and precipitation were 9.5 °C and 752 mm (German Weather Service station at Friesoythe; period 1984-2014).

The second site (Wehnen) was established on a Plaggic Anthrosol with a soil texture of 91% sand, 6% silt and 4% clay at 0-30 cm topsoil layer. Further soil properties were a pH value of 5.0 ($CaCl_2$), a SOC content of 20 g kg^{-1} and a TN content of 2 g kg^{-1}. At this site, the groundwater level was always below the rooting zone (-1.5 m) and thus did not affect the water content at this site. The mean long-term precipitation at this site is 760 mm, while the mean air temperature is 9.9 °C (nearby weather station at the experimental site of Chamber of Agriculture, Lower Saxony). More detailed information are given in Buchen et al. (submitted).

Both sites were managed for at least 15 years as permanent grassland by local farmers. In 2013, a randomised field block trial with different grassland renewal treatments and grassland conversion to maize cropping, replicated four times each, was established at both sites. The plot size was 90 m². Briefly, the following renewal treatments were implemented: (i) "*Minimum*", i.e. keeping and improving the old sward by direct sowing with uniform seed of 100% *Lolium perenne* L., (ii) "*Chemical*", i.e. chemical sward killing with glyphosate followed by direct sowing of a new grass mix (54% *Lolium perenne* L., 20% *Festuca pratensis*, 17% *Phleum pratense* L., 10% *Poa pratensis* L.), (iii) "*Mechanical*", i.e. chemical killing of the sward with glyphosate followed by cutting and mixing with a rotary cultivator, mouldboard ploughing (depth of 25 cm), seedbed preparation and sowing of the new grass

mixture. In addition we established the treatments (iv) "*Maize*", i.e. the conversion of permanent grassland to arable land for maize cropping by chemical killing of the sward with glyphosate followed by cutting and mixing with a rotary cultivator, mouldboard ploughing (25 cm depth), seedbed preparation and sowing of *Zea mays* L. and (v) "*Control*", i.e. permanent grassland.

In accordance with local agricultural practice in this region, grassland renewal (*Minimum*, *Chemical* and *Mechanical* treatments) was carried out by the end of summer (September 2013), while grassland conversion to maize cropping (*Maize* treatment) was delayed to spring 2014. Grassland treatments were fertilised with calcium ammonium nitrate at a rate of 100, 80, 60, 40 kg N ha^{-1} $year^{-1}$. The grassland treatments were cut four times per year. The *Maize* treatment received 150 kg N ha^{-1} (NPK-fertiliser) to sowing and was harvested in October. A detailed summary of all agricultural management practices at the two sites is given in Buchen et al. (submitted).

4.2.2 Soil sampling

Throughout the year, composite soil samples (0-30 cm) per plot were taken for the determination of soil NO_3^- and its isotopic composition ($\delta^{18}O_{NO3-}$ and $\delta^{15}N^{bulk}_{NO3-}$) using a Goettinger gouge auger with a diameter of 18 mm and 14 mm slot (Nietfeld GmbH, Quakenbrück, Germany). Soil NO_3^- was extracted according to VDLUFA (2002) (section 6.1.4.) (600 mL 0.0125 mol $CaCl_2$ solution, 150 g field fresh-sieved soil, shaken for 1 h) and measured photometrically with a Nanocolor photometer (Macherey and Nagel, Düren, Germany), as described in detail in Buchen et al. (submitted). Subsamples were used for the determination $\delta^{18}O$ in soil water ($\delta^{18}O_{H2O}$). Soil moisture content was determined gravimetrically after drying a subsample at 105 °C to constant weight. WFPS was calculated from the gravimetric water content and soil bulk density, which was determined in advance for each plot using undisturbed soil samples taken with stainless steel cylinders (100 cm^3). Reliable WFPS values could not be determined for the Histic Gleysol soil because of the high spatial heterogeneity in SOC contents and bulk density at this site. WFPS calculated from water content, bulk density and SOC contents reached values of 120% and was thus considered inaccurate (Buchen et al., 2016).

4.2.3 N_2O sampling and analysis

N_2O fluxes were determined using the closed chamber method weekly from August 2013 to November 2014 (Hutchinson and Mosier, 1981). Gas samples were collected 0, 20, 40,

60 minutes after chamber closure by flushing septum capped vials (volume of 20 mL) with air from the chamber following the procedure described in Buchen et al. (submitted). With each gas sampling the chamber temperature and soil temperature were measured.

N_2O analyses were carried out with two gas chromatographs (GC 2014, Shimadzu, Kyoto, Japan, modified according to Loftfield et al. (1997), and CP-3800 GC, Varian, Walnut Creek, USA) equipped with ECD detectors and coupled with autosampler systems. The analytical precision was determined weekly by repeated measurements of standard gases (300 ppb N_2O) and was consistently <2% (6.4 ppb).

4.2.4 N_2O isotopocule sampling and analysis

Samples for N_2O isotopocule analysis were taken weekly 60 minutes after chamber closure from chamber air and from free-air in 120 mL crimp neck vials sealed with butyl septa. We ensured a 25-fold exchange of the vial volume by chamber air and a final over pressure which was maintained until and checked prior to gas analysis. Selection for isotopocule analysis was based on a monthly interval, as well as on selected events with high N_2O fluxes following management events, i.e. grassland renewal and grassland conversion to maize cropping, as well as N fertilisation events. In total, 300 isotopocule samples were analysed for the Histic Gleysol and 320 isotopocule samples for the Plaggic Anthrosol.

N_2O isotopocule samples were analysed using a Delta V isotope ratio mass spectrometer (IRMS, Thermo Scientific, Bremen, Germany), coupled to an automatic preparation system with Precon + Trace GC Isolink (Thermo Scientific, Bremen, Germany), as described previously by Lewicka-Szczebak et al. (2014). Briefly, isotopocule values were obtained by measuring m/z 44, 45 and 46 of the intact N_2O^+ ions, as well as m/z 30 and 31 of NO^+ fragment ions, simultaneously, to determine average $\delta^{15}N$ of N_2O ($\delta^{15}N^{bulk}{}_{N2O}$), $\delta^{15}N^{\alpha}{}_{N2O}$ ($\delta^{15}N_{N2O}$ of the central N position of the N_2O molecule) and $\delta^{18}O_{N2O}$ (Toyoda and Yoshida, 1999), while $\delta^{15}N^{\beta}{}_{N2O}$ values ($\delta^{15}N_{N2O}$ of the peripheral N position of the N_2O molecule) were calculated based on the following equation:

$$\boldsymbol{\delta^{15}N^{bulk}{}_{N2O} = \frac{\delta^{15}N^{\alpha}{}_{N2O} + \delta^{15}N^{\beta}{}_{N2O}}{2}} \qquad \textbf{Eq. 4-1}$$

The difference between the central ($\delta^{15}N^{\alpha}{}_{N2O}$) and peripheral ($\delta^{15}N^{\beta}{}_{N2O}$) position within the linear N_2O molecule has been defined as ^{15}N site preference ($\delta^{15}N^{SP}{}_{N2O}$) (Brenninkmeijer and Röckmann, 1999; Toyoda and Yoshida, 1999). The scrambling factor of 0.096 has been taken into account (Röckmann et al., 2003). The ratios of $^{15}N/^{14}N$ or $^{18}O/^{16}O$ in the molecules of a

sample (R_{sample}) were compared to corresponding ratios of reference materials ($R_{standard}$) (i.e. atmospheric N_2 and Vienna Standard Mean Ocean Water (V-SMOW):

$$\delta X = \frac{R_{sample} - R_{standard}}{R_{standard}} * 1000 \qquad \text{Eq. 4-2}$$

, where X = $^{15}N^{bulk}$, $^{15}N^{\alpha}$, $^{15}N^{\beta}$, or ^{18}O. All delta values (δ) are expressed in permil (‰). The analytical precision, given as standard deviation (1σ) of the internal standards for measurements of $\delta^{15}N_{N2O}$, $\delta^{18}O_{N2O}$ and $\delta^{15}N^{SP}{}_{N2O}$ was typically better 0.1, 0.2, and 0.5‰, respectively. Pure N_2O (Westfalengas, Münster, Germany; purity >99.995) was calibrated for isotopocule values by Toyoda and Yoshida in the laboratory of Tokyo Institute of Technology (Toyoda and Yoshida, 1999) and used as a reference gas.

4.2.5 Determination of precursor compounds

$\delta^{15}N$ and $\delta^{18}O$ in soil nitrate and soil water

Every three months, the isotopic composition of NO_3^- in soil extract ($\delta^{15}N^{bulk}{}_{NO3-}$, $\delta^{18}O_{NO3-}$) was determined using the bacterial denitrifier method (Sigman et al., 2001; Casciotti et al., 2002). The analytical precision of the bacterial denitrifier method determined as standard deviation (1σ) of the international standards was typically 0.5‰ for $\delta^{18}O_{NO3-}$ and 0.2‰ for $\delta^{15}N^{bulk}{}_{NO3-}$.

Parallel to the determination of soil NO_3^- isotopes, a subsample from soil sampling was used for soil water extraction following the method described by Königer et al. (2011). Samples of extracted soil water ($\delta^{18}O_{H2O}$) were analysed with a laser spectrometer using cavity ringdown spectroscopy (CRDS) (Picarro, model L1115-I, Picarro Inc., Santa Clara, USA). The analytical precision (1σ) was below 0.1‰ and the overall error associated with the soil water extraction method (1σ) of five sample replicates was below 0.5‰.

In between the sampling at three month intervals, missing values were calculated by linear interpolation. Because $\delta^{15}N^{bulk}{}_{NO3-}$ and $\delta^{18}O_{NO3-}$ of soil NO_3^- and $\delta^{18}O_{H2O}$ of soil water were not determined before November 2013, missing values were filled with the annual average value ($\delta^{15}N^{bulk}{}_{NO3-}$: Plaggic Anthrosol: 0.40±1.98‰ and Histic Gleysol: 0.93±2.41‰; $\delta^{18}O_{H2O}$ from soil water extraction: Plaggic Anthrosol: -6.84±1.46‰ and Histic Gleysol: -6.86±0.95‰) for the respective sampling site.

4.2.6 Data processing and statistical analysis

Calculation of the isotopic signature of soil-emitted N_2O

During chamber air sampling, the collected N_2O is a mixture of atmospheric and soil-emitted N_2O. Thus, the δ value of soil-emitted N_2O was calculated using a basic isotope mixing model, as described by Well et al. (2006):

$$\boldsymbol{\delta_{soil-emitted}} = \frac{(\boldsymbol{\delta_{mix}} * \boldsymbol{C_{mix}} + \boldsymbol{\delta_{air}} * \boldsymbol{C_{air}})}{\boldsymbol{C_{mix}} - \boldsymbol{C_{air}}} \qquad \textbf{Eq. 4-3}$$

, where $\delta_{soil\text{-}emitted}$ = isotopic composition ($\delta^{15}N^{bulk}_{N2O}$, $\delta^{18}O_{N2O}$ or $\delta^{15}N^{SP}_{N2O}$) of the soil-emitted N_2O; δ_{mix} = isotopic composition ($\delta^{15}N_{N2O}$, $\delta^{18}O_{N2O}$ or $\delta^{15}N^{SP}_{N2O}$) of the chamber air sample in ‰; δ_{air} = isotopic composition ($\delta^{15}N_{N2O}$, $\delta^{18}O_{N2O}$ or $\delta^{15}N^{SP}_{N2O}$) of the free-air sample in ‰; C_{mix} = N_2O concentration of the chamber sample in ppb, C_{air} = N_2O concentration of the air sample in ppb. C_{mix} values were taken from gas chromatographic analysis after 60 minutes of chamber closure. C_{air} values were calculated as average over the three lowest C_{mix} concentrations per sampling day to achieve a representative composition of C_{air} concentrations depending on occurring management events, and/or N fertilisation, while δ_{air} values were calculated as an average of the three air samples. This was done because initial N_2O concentrations from the chamber were rather variable and sometimes lower than N_2O concentrations of the free-air samples. Nevertheless, we used the free-air samples as a best estimate for δ_{air} values, as initial chamber samples were not analysed for stable isotopes.

The $\delta_{soil\text{-}emitted}$ values obtained from small C_{mix} values (<385 ppb) were not used for further data analysis, because δ_{mix} was close to δ_{air} within the precision of the analysis and the propagated error in the calculation of $\delta_{soil\text{-}emitted}$ was large (>4‰). This has led to an even reduced final dataset of 148 samples for the Histic Gleysol and 129 samples for the Plaggic Anthrosol. To define the threshold of <385 ppb, we conducted a Monte-Carlo simulation for error propagation of $\delta_{soil\text{-}emitted}$ using $\delta^{15}N^{SP}_{N2O}$ values, because $\delta^{15}N^{SP}_{N2O}$ values have the highest measurement uncertainty. For the Monte-Carlo simulation, we used annual mean values from both sites: δ_{mix} = 18.44±0.50‰, δ_{air} = 18.37±0.50‰ and C_{air} = 320±5 ppb.

Isotopocule mapping approach to estimate the magnitude of N_2O reduction to N_2 and to identify N_2O source processes

We used the isotopocule mapping approach (Figure 4-1b) introduced by Lewicka-Szczebak et al. (2017) to simultaneously estimate the magnitude of N_2O reduction to N_2 and the admixture of bacterial denitrification (i.e. heterotrophic denitrification / nitrifier denitrification) of

soil-emitted N_2O in our samples. To calculate the residual, unreduced N_2O fraction (r_{N2O}) and the N_2O fraction from bacterial denitrification (f_B), the reduction and mixing lines were calculated based on the endmember values reported in the literature (Table 4-1) for the isotopic values of N_2O produced from different pathways (δ_0: initial isotopic signature of N_2O before reduction).

Table 4-1: $\delta_0{}^{15}N^{SP}{}_{N2O}$ and $\delta_0{}^{18}O_{N2O/H2O}$ values for different N_2O production pathways with the appropriate minimum, maximum and mean[1] of endmember values (adapted from Lewicka-Szczebak et al. (2017)) used in the isotopocule mapping approach

Process	$\delta_0{}^{15}N^{SP}{}_{N2O}$ (‰)			$\delta_0{}^{18}O_{N2O/H2O}$ (‰)			Reference
	Min	Max	Mean[1]	Min	Max	Mean[1]	
Heterotrophic bacterial denitrification	-7.5	3.7	-3.9	17.4	21.4	21.0	Sutka et al. (2006); Toyoda et al. (2005); Lewicka-Szczebak et al. (2014); Lewicka-Szczebak et al. (2016)
Nitrifier Denitrification	-13.6	1.9		19.8	26.5		Frame and Casciotti (2010); Sutka et al. (2006)
Fungal denitrification[2]	30.2	39.3	34.8	40.6	51.9	43.6	Maeda et al. (2015); Rohe et al. (2014); Sutka et al. (2008)
Nitrification	32.0	38.7		35.6	55.2		Frame and Casciotti (2010); Heil et al. (2014); Sutka et al. (2006)

[1] Mean value of minimum and maximum values for both endmember values (i.e. heterotrophic bacterial denitrification and nitrifier denitrification; fungal denitrification and nitrification)

[2] A study by Rohe et al. (2014) indicated also lower $\delta_0{}^{15}N^{SP}{}_{N2O}$ values for individual fungal species (e.g. *C. funicola* with an $\delta_0{}^{15}N^{SP}{}_{N2O}$ value of 21.9 ‰). For calculations we discarded these values, as only values of strains with higher N_2O production rates (>10 mg N_2O g^{-1} fungal biomass) are accepted as in recent studies by Maeda et al. (2015) and Lewicka-Szczebak et al. (2017)

Large differences in $\delta_0{}^{15}N^{SP}{}_{N2O}$, indicated from pure culture studies, allow the distinction of bacterial denitrification (lower $\delta_0{}^{15}N^{SP}{}_{N2O}$ values) from fungal denitrification and nitrification (both with higher $\delta_0{}^{15}N^{SP}{}_{N2O}$ values). However, high $\delta_0{}^{15}N^{SP}{}_{N2O}$ cannot exclusively be taken as an indicator of nitrification as there is some overlap in $\delta_0{}^{15}N^{SP}{}_{N2O}$ with fungal denitrification (Sutka et al., 2008). Furthermore, $\delta_0{}^{18}O_{N2O/H2O}$ can also be utilised, as lower endmember values are assigned for heterotrophic bacterial denitrification / nitrifier denitrification and higher ones for fungal denitrification / nitrification (Rohe et al., 2014; Lewicka-Szczebak et al., 2016). Because reported endmember values of heterotrophic bacterial denitrification and nitrifier denitrification are similar, and there are too few data to justify the assumption of different values (Toyoda et al. (2005); Sutka et al. (2006); Frame and Casciotti (2010); Lewicka-Szczebak et al. (2014)), both process are represented by a common value. For $\delta^{18}O_{N2O}$, δ_0 values are expressed as relative values in relation to the source, i.e. soil water ($\delta_0{}^{18}O_{N2O/H2O}$), which allows us to reasonably compare the different treatments differing in soil water isotopic

signatures. Conversely, the measured $\delta_0{}^{15}N^{SP}{}_{N2O}$ values could be directly used for calculations, as here δ_0 values are independent of the isotopic signature of the source.

As N_2O reduction is associated with isotope fractionation, we used reported ranges for the net isotope effects of N_2O reduction (η_{red}) for our calculations: $\eta_{red}{}^{15}N^{sp}$: range from -7.7 to -2.3‰ with a mean values of -5.4‰ and $\eta_{red}{}^{18}O_{N2O/H2O}$: range from -17.4 to -12‰ with a mean value of -15‰ (Jinuntuya-Nortman et al., 2008; Well and Flessa, 2009; Lewicka-Szczebak et al., 2014). Although the range of possible η_{red} variations is quite large, it has been recently shown that the mean η_{red} values and typical $\eta_{red}{}^{15}N^{SP}{}_{N2O}/\eta_{red}{}^{18}O_{N2O/H2O}$ ratios are applicable if r_{N2O} >0.1, i.e. if N_2O reduction is not close to completeness, as this was found under both, anoxic and oxic conditions by Lewicka-Szczebak et al. (2015). Due to the variability of the endmember values there are several possible routes of the mixing line, which are situated between the extreme lines (minimum, maximum line, Figure 4-1a). Similar to that, the variability of the $\delta^{15}N^{SP}{}_{N2O}/\delta^{18}O_{N2O/H2O}$ slope yields in a wide range of slopes of the reduction line (minimum slope = 0.19 and maximum slope = 0.44).

Different Scenarios modelled with the isotopocule mapping approach

If we assume bacterial denitrification as the first source of N_2O, we can differentiate between two Scenarios a and b (see Figure 4-1b and Lewicka-Szczebak et al. (2017)):

- **Scenario a**: the N_2O emitted due to bacterial denitrification (i.e. heterotrophic bacterial denitrification / nitrifier denitrification) is ***first reduced to N_2 and then mixed with N_2O*** from the second endmember source. These values are determined using Figure 4-1b following the orange short dashed line: move from the first source on the reduction line to the intercept with the red_mix line and then move up the red_mix line to the sample point.

- **Scenario b**: the N_2O from the endmembers (i.e. heterotrophic bacterial denitrification / nitrifier denitrification and nitrification / fungal denitrification) is ***first mixed and then the mixed N_2O is reduced to N_2.*** These values are determined using Figure 4-1b following the green short dashed line: move from the first source on the mixing line to the intercept with the mix_red line and then move up the mix_red line to the sample point.

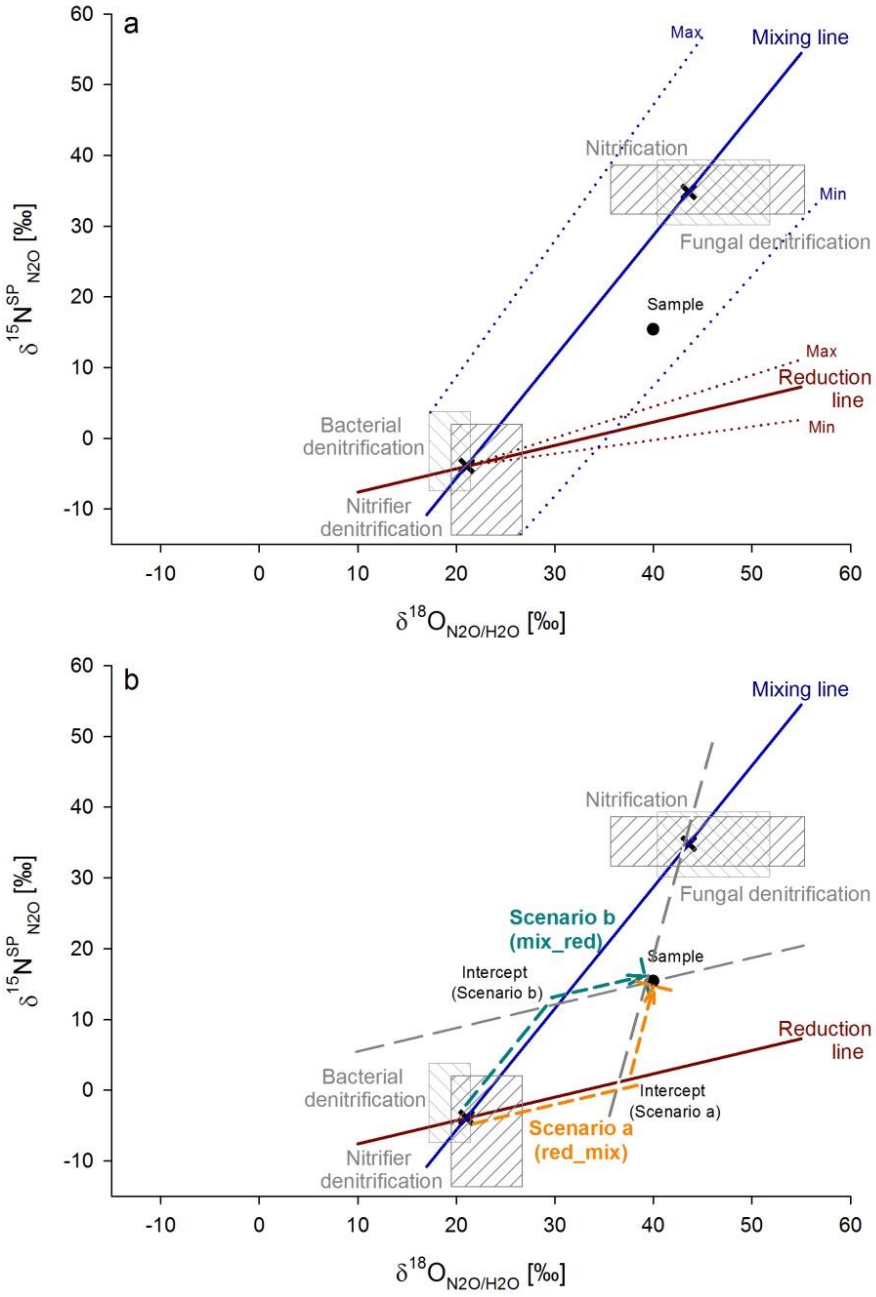

Figure 4-1: Isotopocule map illustrating the simultaneous estimation of N_2O reduction to N_2 and other source processes (modified after Lewicka-Szczebak et al. (2017)

a: Top and bottom crosshatched boxes indicate the expected ranges for heterotrophic bacterial denitrification / nitrifier denitrification (bottom) and nitrification / fungal denitrification (top). Mixing lines were drawn between minimum, maximum (blue dotted lines) and mean (blue solid line) values for both $\delta^{15}N^{SP}_{N2O}$ and $\delta^{18}O_{N2O/H2O}$ of the respective processes. Reduction lines represent minimum and maximum (red dotted lines) and mean routes (red solid line) based on $\eta_{red}{}^{15}N^{SP}_{N2O}/\eta_{red}{}^{18}O_{N2O/H2O}$ ratios (values and references see Table 4-1 and text in section 4.2.6)

b: Short dashed lines illustrate the assumed combination of mixing and reduction assumed in the calculations (see text in section 4.2.6), where Scenario a represents the assumption of "*first reduction, then mixing*" (orange short dashed line) and Scenario b "*first mixing, then reduction*" (green short dashed line)

Based on this approach, we established seven scenario variations (1-7), including different mean, minimum and maximum endmember values of $\delta_0{}^{15}N^{SP}{}_{N2O}$ and $\delta_0{}^{18}O_{N2O/H2O}$ (Table 4-1) and fractionation factors of N_2O reduction to cover the whole potential variations of the N_2O reduced fraction and the admixture of bacterial denitrification.

The following Scenario variations (variation from average values in Scenario 1 are marked in bold) were assigned for Scenario a and b:

1) *Mean mixing line, mean reduction line, mean $\eta_{red}{}^{15}N^{SP}$ values,*

2) ***Maximum mixing line**, mean reduction line, mean $\eta_{red}{}^{15}N^{SP}$ values,*

3) ***Minimum mixing line**, mean reduction line, mean $\eta_{red}{}^{15}N^{SP}$ values,*

4) *Mean mixing line, **minimum reduction line**, mean $\eta_{red}{}^{15}N^{SP}$ values,*

5) *Mean mixing line, **maximum reduction line**, mean $\eta_{red}{}^{15}N^{SP}$ values,*

6) *Mean mixing line, mean reduction line, **minimum $\eta_{red}{}^{15}N^{SP}$ values**,*

7) *Mean mixing line, mean reduction line, **maximum $\eta_{red}{}^{15}N^{SP}$ values**.*

If the samples analysed are located between the mean mixing and reduction lines (Figure 4-1a, Scenario variation 1), we can estimate the impact of fractionation associated with N_2O reduction to N_2 and the admixture of bacterial denitrification from its location. Samples, which are located outside of the area between the mean mixing and mean reduction line could be better calculated using the introduced Scenario variations 2-7. For all samples in the different scenario variations, the following applies: if a sample is located outside of the assigned mixing/reduction areas for the specific Scenario, calculations yielded unrealistic values (i.e. r_{N2O} or f_B values <0 or >1). For the further calculations the values out of the 0 to 1 range were set to 0 or 1, respectively. We further calculated the percentage of samples from the total data set which were out of the 0 to 1 range. In most of the scenario variations, this was less than 10% of the total data set. However, exceptionally high contribution of r_{N2O} or f_B values out of the 0-to-1 range was found for the Scenarios a3/b3 with extremely high calculated r_{N2O} values (46% of the samples in Scenario a3 and 64% in Scenario b3). Furthermore, four samples from the Histic Gleysol and five samples from the Plaggic Anthrosol which were located outside of any endmember values could not be calculated with the present isotopocule mapping approach and were discarded (Figure 4-2). Also some samples, which were located above the

fungal denitrification / nitrification endmember values ($\delta_0{}^{15}N^{SP}_{N2O}$>39‰), indicating a contribution of DNRA (Behrendt et al., 2015), were not considered in our calculations.

N_2O and N_2 flux calculations of microbial processes

Based on r_{N2O} and f_B values calculated from the isotopocule mapping approach, we determined microbial process rates in g N ha^{-1} day^{-1} for different sources, i.e. N_2O reduction to N_2, the proportion heterotrophic bacterial denitrification / nitrifier denitrification and the proportion of fungal denitrification / nitrification:

$$\boldsymbol{N_2O{+}N_2flux} = \frac{\mathbf{1}}{\boldsymbol{r_{N2O}}} * \boldsymbol{N_2Oflux} \qquad \textbf{Eq. 4-4}$$

$$\boldsymbol{N_2flux} = (\boldsymbol{N_2Oflux} + \boldsymbol{N_2flux}) - \boldsymbol{N_2Oflux} \qquad \textbf{Eq. 4-5}$$

N_2O flux emitted from heterotrophic bacterial denitrification / nitrifier denitrification:

$$\boldsymbol{N_2Oflux_{bD}} = \boldsymbol{f_B} * \boldsymbol{N_2Oflux} \qquad \textbf{Eq. 4-6}$$

N_2O flux emitted from fungal denitrification /nitrification:

$$\boldsymbol{N_2Oflux_{fDNi}} = (\mathbf{1} - \boldsymbol{f_B}) * \boldsymbol{N_2Oflux} \qquad \textbf{Eq. 4-7}$$

To calculate microbial process rates, the needed N_2O fluxes were taken from Buchen et al. (submitted). In addition, we had to set a maximum limit for the $N_2{+}N_2O$fluxes to our calculations, to avoid unrealistic high fluxes, which occurred in all scenarios and scenario variations for samples showing almost no N_2O reduction to N_2 (r_{N2O} values <0.01) and a small proportion of the admixture of bacterial denitrification (f_B values <0.16) at the same time. This is due to the fact that r_{N2O} values <0.01 are extremely sensitive for the variability of selected endmember values of $\delta_0{}^{15}N^{SP}_{N2O}$ for fungal denitrification / nitrification. To ensure a realistic $N_2{+}N_2O$ flux limit for the two investigated sites, we selected the maximum measured N_2 fluxes during our parallel ^{15}N tracing study (Histic Gleysol: 9533 g ha^{-1} day^{-1} and Plaggic Anthrosol: 352 g ha^{-1} day^{-1}) (Buchen et al., 2016). This concerns less than 10% of the N_2 fluxes at the Histic Gleysol, except calculations with Scenario a6 with 23%. For the Plaggic Anthrosol most of the flux calculations were below the limit (less than 10%), except Scenario a5 (19%), Scenario a6 (61%) and Scenario b6 (32%).

Statistical analysis

All calculations were performed using R.3.3.1 (R Development Core Team, 2016).

Since N_2O and N_2 emissions are usually driven by more than one factor and these relationships can be expected to be nonlinear, we used Spearman partial correlation analysis (*pcor*) as implemented in R package *ppcor* version 1.0 (Kim, 2015). We tested r_{N2O} values (Scenarios a1 and b1), f_B values (Scenario a1/b1) and N_2O+N_2 flux (Scenarios a1 and b1) against potential driving variables: NO_3^--N content (0-30 cm depth), NH_4^+-N content (0-30 cm depth), soil temperature (5 cm soil depth) and soil moisture. Soil moisture in 0-30 cm soil depth was represented by gravimetric water content for the Histic Gleysol and by WFPS for the Plaggic Anthrosol.

4.3 Results

4.3.1 Isotopocule mapping

Isotopocule values of soil-emitted N_2O per treatment and site are shown in the isotopocule map for samples meeting the minimum concentration criteria (>385 ppb, section 2.5.4). Most of the samples are located between the mean mixing and reduction lines (Figure 4-2), while some samples beyond that area are located within the maximum mixing line and minimum reduction line. From Figure 4-2, we can see variable N_2O reduction rates and besides that, the contribution of heterotrophic bacterial denitrification and the contribution of nitrification / fungal denitrification for both soils. For the Histic Gleysol, the values of all treatments scatter almost within the entire area between mixing and reduction lines, while a clear dominance of only one process for a specific treatment is thus not evident from the map. However, samples of the grassland treatments for the Plaggic Anthrosol appear to be more distant from the fungal denitrification / nitrification area, while samples of the *Maize* treatment tend to scatter more in parallel and closely above the reduction line.

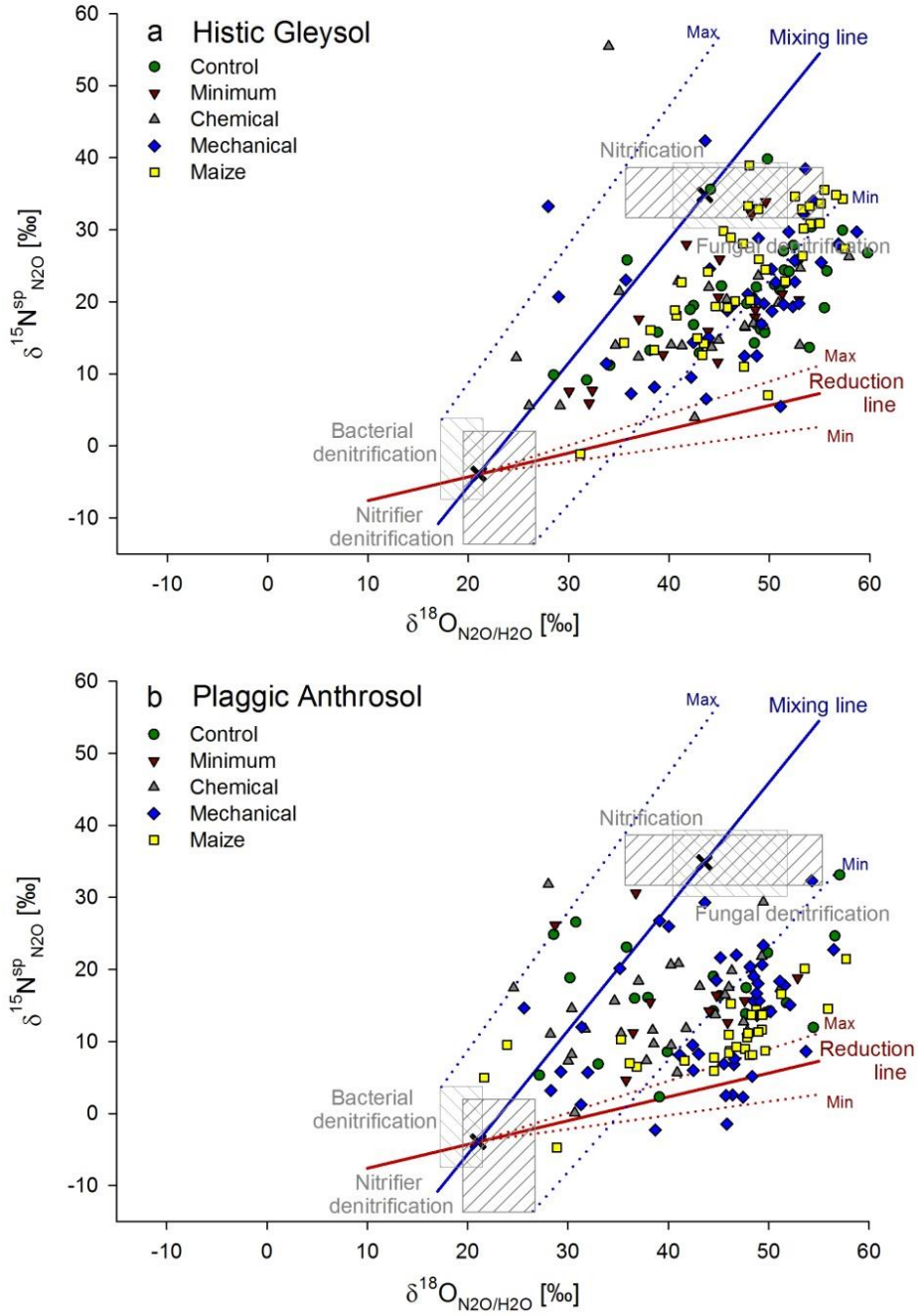

Figure 4-2: Isotopocule values of soil-emitted N_2O plotted per treatment in the isotopocule map ($\delta^{15}N^{SP}_{N2O}$ vs. $\delta^{18}O_{N2O/H2O}$) for a: Histic Gleysol (n=148) and b: Plaggic Anthrosol (n=129). Note that values outside of endmember areas were excluded from calculations

4.3.2 N_2O reduction and source partitioning

The time course of the residual, unreduced N_2O fraction (r_{N2O}) and the N_2O fraction from bacterial denitrification (f_B), based on the calculations of Scenarios a and b (i.e. using average values for η_{red} and endmember areas) are shown for each sampling day in Figure 4-3.

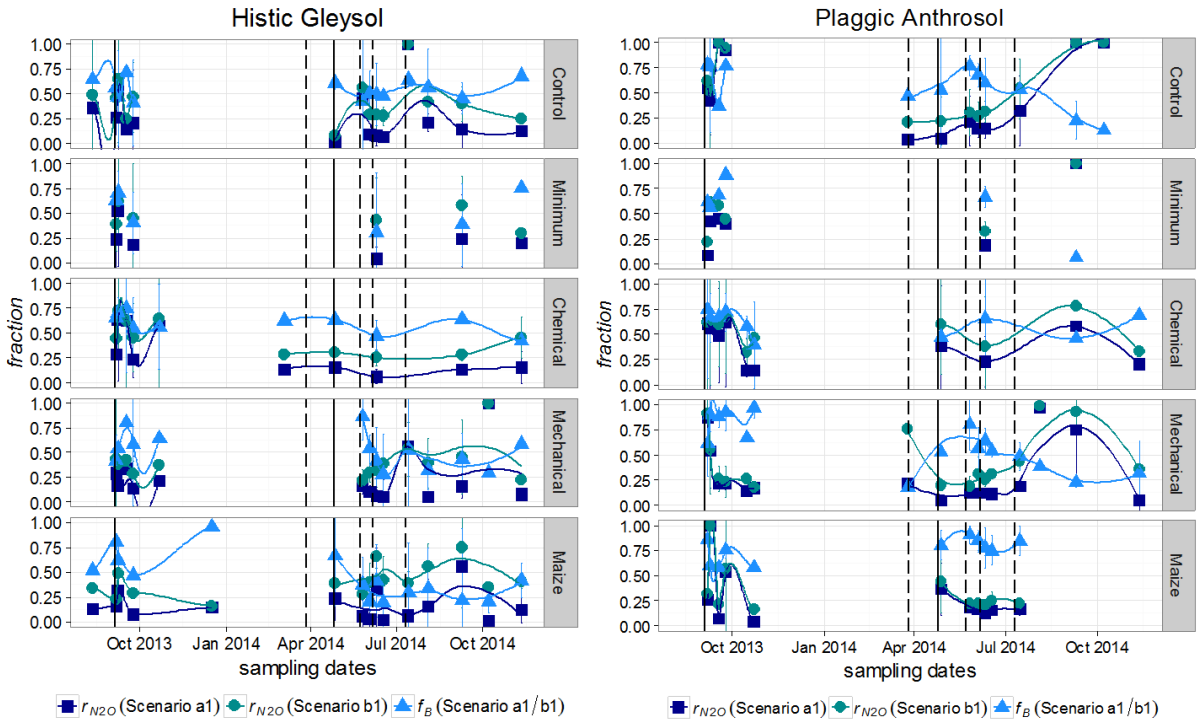

Figure 4-3: Time course of the unreduced, residual N_2O fraction (r_{N2O}) and the N_2O fraction from bacterial denitrification (f_B) based on calculations of Scenario a1 and b1 for the Histic Gleysol and the Plaggic Anthrosol. Dates of grassland renewal and grassland conversion to maize (black lines). N fertilisation rates (100-80-60-40 kg N ha^{-1}) (dashed black lines) were the same for the treatments: *Control, Minimum, Chemical and Mechanical*. N fertilisation was different for the *Maize* plots with 150 kg N ha^{-1}each May. Error bars indicate standard deviation of the mean for sampling dates with n≥2. A non-parametric "loess" smoother was fitted (solid lines) was fitted for illustration purposes, but note that this is not a fit of the true time course of values.

An impact of management events (e.g. grassland renewal and grassland conversion) and N fertilisation on r_{N2O} values and f_B values was visible for both sites. Generally, r_{N2O} values were highly variable and ranged between 0 and 1 for the presented scenarios and at both sites, while f_B values ranged between 0.20 and 0.98 at the Histic Gleysol and between 0.16 and 1.00 at the Plaggic Anthrosol. After grassland renewal in September 2013, average r_{N2O} values for both Scenarios varied on a lower level (0.31±0.28) in the *Mechanical* treatment, whereas higher r_{N2O} values appeared in the *Minimum* (>0.52) and *Chemical* (0.42±0.25) treatment at the Histic Gleysol site. Furthermore, low r_{N2O} values were found in all treatments following N fertilisation in summer 2014, while f_B values decreased during this time period, too. At the Plaggic Anthrosol, a similar trend of r_{N2O} and f_B values following grassland renewal and N fertilisation occurred, while the range of f_B values was smaller during summer 2014 compared to the Histic Gleysol. Low r_{N2O} values (average from June to July 2014: 0.16±0.02 in Scenario a1 and 0.22±0.03 in Scenario b1) and high f_B values (average from June to July 2014: 0.80±0.08 in Scenario a1/b1) were found, especially in the *Maize* treatment following grassland conversion to maize cropping.

4.3.3 N_2O+N_2 fluxes

Based on r_{N2O} values, we calculated the total denitrification losses (i.e. N_2O+N_2 flux) separately for Scenarios a1 and b1 per treatment and for both sites (time courses in Figure 4-4). Similar to the r_{N2O} values (Figure 4-3), N_2O+N_2 fluxes increased after management events and following N fertilisation in summer 2014.

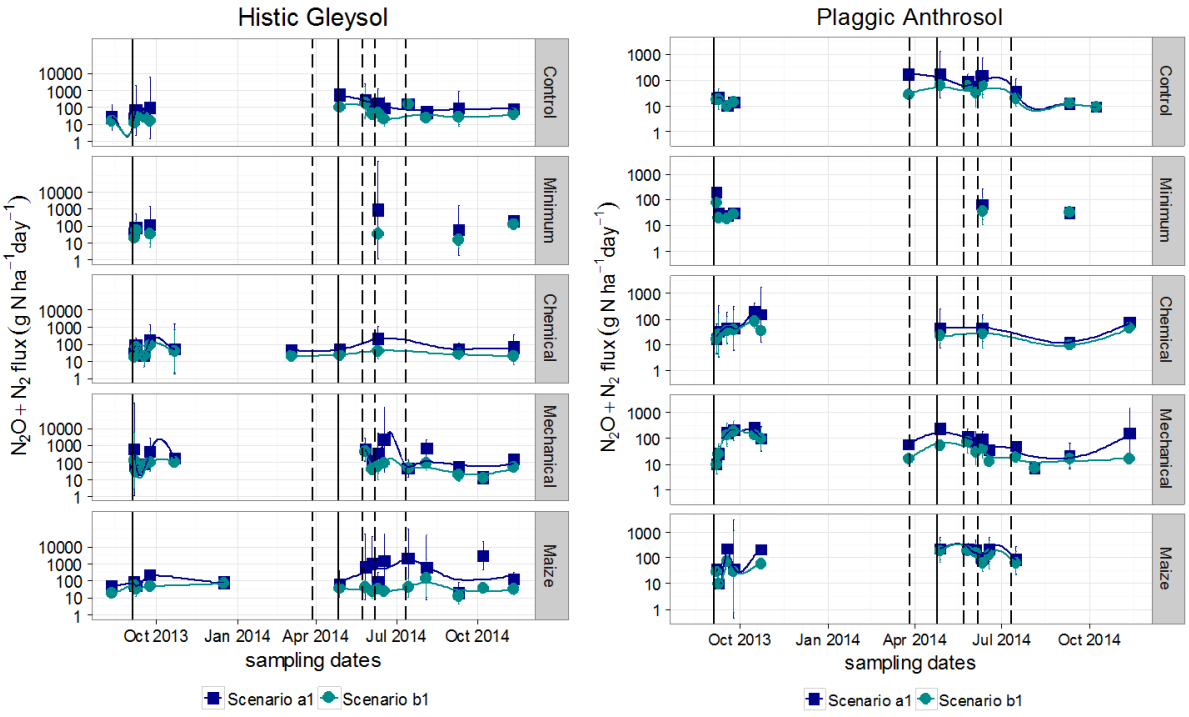

Figure 4-4: Time course of denitrification losses (N_2O+N_2 flux) based on calculations of Scenario a1 and b1 for the Histic Gleysol and the Plaggic Anthrosol. Dates of grassland renewal and grassland conversion to maize (black lines). N fertilisation rates (100-80-60-40 kg N ha^{-1}) (dashed black lines) were the same for the treatments: *Control, Minimum, Chemical and Mechanical*. N fertilisation was different for the *Maize* plots with 150 kg N ha^{-1} each May. Error bars indicate standard deviation of the mean for sampling dates with n≥2. Note the logarithmic scale of N_2O+N_2 fluxes. A non-parametric "loess" smoother was fitted (solid lines) was fitted for illustration purposes, but note that this is not a fit of the true time course of values.

At the Histic Gleysol, N_2O+N_2 fluxes increased up to the estimated maximum of 9533 g N ha^{-1} day^{-1} (Buchen et al., 2016) in the *Mechanical* treatment in September 2013. During this time, N_2O+N_2 fluxes increased on a lower level in the *Chemical* treatment (up to 559 g N ha^{-1} day^{-1} in Scenario a1). Following grassland conversion to maize cropping, high N_2O+N_2 fluxes were measured with a constantly higher calculated N_2O+N_2 flux from Scenario a1 than from Scenario b1 in the *Maize* treatment. Interestingly, the effect of N fertilisation events during summer 2014 was more visible in the *Control* and *Mechanical* treatment than in the *Minimum* and *Chemical* treatment.

The N_2O+N_2 fluxes from the Plaggic Anthrosol revealed a significantly lower level than from the Histic Gleysol. But also here, N_2O+N_2 fluxes increased following grassland renewal and

fluxes up to 252 (Scenario a1) and 266 g N ha^{-1} day^{-1} (Scenario b1) in the *Mechanical* treatment and up to the maximum of 353 g N ha^{-1} day^{-1} (Scenario a1) in the *Chemical* treatment. Grassland conversion to maize cropping led to an increase in N_2O+N_2 fluxes (average: 168±87 g N ha^{-1} day^{-1} in Scenario a1 and 121±68 g N ha^{-1} day^{-1} in Scenario b1) during a period from May 2014 to July 2014, while the *Control* treatment ranged between 98±79 g N ha^{-1} day^{-1} in Scenario a1 and 47±28 g N ha^{-1} day^{-1} in Scenario b1). Between mid July 2014 and the end of the sampling campaign in November 2014, no N_2O+N_2 fluxes were obtained in the *Maize* treatment at the Plaggic Anthrosol, because all sample N_2O concentrations were below the minimum threshold of 385 ppb. Similar to the Histic Gleysol, N fertilisation events affected only the *Control* and *Mechanical* treatment.

In addition to the total denitrification losses, we also calculated process related N_2O fluxes from heterotrophic bacterial denitrification / nitrifier denitrification and fungal denitrification / nitrification, which are shown in a time course per Scenario a1 and b1 in Figure A4-2 and A4-3 (Supplementary data). Generally, mean N_2O fluxes were 50 times lower than N_2 fluxes at the Histic Gleysol and 15 times lower at the Plaggic Anthrosol. For the total N_2O flux in the *Maize* treatment at the Histic Gleysol, a contribution up to 660 g N ha^{-1} day^{-1} from heterotrophic bacterial denitrification / nitrifier denitrification and a contribution of up to 1652 g N ha^{-1} day^{-1} from fungal denitrification / nitrification was found. At the Plaggic Anthrosol, N_2O fluxes from heterotrophic bacterial denitrification / nitrifier denitrification ranged between 5 and 481 g N ha^{-1} day^{-1} and between 0 and 122 g N ha^{-1} day^{-1} for fungal denitrification / nitrification.

4.3.4 Comparison of mean values from different Scenario variations

Mean r_{N2O} values, mean f_B values and the N_2O+N_2 flux for the Scenario variations (1-7) and Scenarios (a,b) for the Histic Gleysol and the Plaggic Anthrosol are given in Table 4-2. It must be noted that mean N_2+N_2O fluxes do not represent mean values for the sites because isotopocule values could only be determined from samples with a N_2O concentration of >385 ppb. A wide range of r_{N2O} values could be noticed within the calculated Scenarios and their variations. Scenario a always yielded higher r_{N2O} values than Scenario b in the scenario variations. A detailed look at the single scenarios revealed the highest r_{N2O} values in extreme scenarios with Scenario a3/b3 (***Minimum mixing line**, mean reduction line, mean* $\eta_{red}{}^{15}N^{SP}$ *values*) and Scenario a4/b4 (*Mean mixing line, **minimum reduction line**, mean* $\eta_{red}{}^{15}N^{SP}$ *values*) for both soils. f_B values were the same for the two Scenarios a and b, but ranged within the scenario variations from 0.22±0.17 to 0.74±0.22 for the Histic Gleysol and from

0.37±0.18 to 0.88±0.16 for the Plaggic Anthrosol. Also for the N_2O+N_2 fluxes a large variation occurred. For the Histic Gleysol, the N_2O+N_2 fluxes ranged between 260±823 and 3278±3851 g N ha^{-1} day^{-1} in Scenario a and on a lower level in Scenario b (33±58 to 322±674 g N ha^{-1} day^{-1}). For the Plaggic Anthrosol, N_2O+N_2 fluxes ranged from 54±53 to 254±141 g N ha^{-1} day^{-1} in Scenario a and 25±24 to 183±139 g N ha^{-1} day^{-1} in Scenario b. An overview of all possible minimum and maximum values of r_{N2O} and f_B in each scenario and per scenario variation is given in Table A4-1 (Supplementary data).

Table 4-2: Mean values of the residual, unreduced N_2O fraction (r_{N2O}), the N_2O fraction from bacterial denitrification (f_B), and the N_2O+N_2 flux for the Scenario variations (1-7) and Scenarios (a and b) for the Histic Gleysol and the Plaggic Anthrosol. Values shown are mean of treatment replicates ± one standard deviation (Histic Gleysol n=148 and Plaggic Anthrosol n=129). Mean N_2+N_2O fluxes do not represent mean values for the sites, because isotopocule values could only be determined from samples with high fluxes

		r_{N2O}		f_B	N_2O+N_2 flux (g N ha^{-1} day^{-1})	
	Scenarios	**Sc.a**	**Sc.b**	**Sc.a/b**	**Sc.a**	**Sc.b**
	Histic Gleysol					
Scenario variations	**1**	0.23±0.27	0.44±0.22	0.49±0.22	889±2256	75±125
	2	0.14±0.14	0.22±0.13	0.74±0.22	590±1535	153±255
	3	0.63±0.40	0.91±0.16	0.22±0.17	922±2573	33±58
	4	0.36±0.27	0.63±0.16	0.43±0.21	566±1904	46±76
	5	0.17±0.25	0.32±0.24	0.54±0.23	1240±2620	124±221
	6	0.12±0.26	0.22±0.25	0.49±0.22	3278±3851	322±674
	7	0.34±0.26	0.57±0.18	0.49±0.22	260±823	52±86
	Plaggic Anthrosol					
Scenario variations	**1**	0.33±0.29	0.43±0.27	0.67±0.21	105±93	64±65
	2	0.22±0.17	0.24±0.19	0.88±0.16	123±96	117±103
	3	0.66±0.35	0.84±0.19	0.37±0.18	55±80	25±24
	4	0.48±0.26	0.62±0.20	0.61±0.19	54±53	35±32
	5	0.26±0.30	0.33±0.30	0.72±0.23	159±126	108±106
	6	0.18±0.31	0.24±0.31	0.67±0.21	254±141	183±139
	7	0.45±0.26	0.56±0.22	0.67±0.21	58±53	41±39

Mean values per treatment are shown in Table A4-2 (Histic Gleysol) and Table A4-3 (Plaggic Anthrosol) in the Supplementary data. Due to variable sample sizes (Histic Gleysol: 17-42 samples and Plaggic Anthrosol: 9-41 samples) in the data set, it must be noted that mean N_2+N_2O fluxes do not represent true treatment means, but can be used as an indicator for trends in the total data set. In general, differences in r_{N2O} and f_B values between the five treatments were very low. Large variation was shown for r_{N2O} values per treatment between the two Scenarios a and b within one scenario variation (for example: r_{N2O} values of the *Maize* treatment at the Plaggic Anthrosol: 0.24±0.24 in Scenario a1 and 0.31±0.23 in Scenario b1), whereas this did not apply for the Histic Gleysol. Also variability between the scenario

variations was large and the calculated N_2O+N_2 fluxes of all scenario variations ranged for example from 40±71 to 3038±3689 g N ha^{-1} day^{-1} in the *Control* treatment at the Histic Gleysol.

4.3.5 Partial correlation of N_2O, N_2 fluxes and fractions with soil variables

For the Histic Gleysol, a significant positive correlation between r_{N2O} values in both Scenario calculations (Scenarios a1 and b1) and NO_3^--N content was found, while the NH_4^+-N content and soil moisture were negatively correlated (Table 4-3). Also f_B values were negatively correlated with the NH_4^+-N content, soil moisture and soil temperature. Furthermore, Spearman's correlation showed an impact of NH_4^+-N content (R^2: 0.31) and soil moisture (R^2: 0.30) on the N_2O+N_2 fluxes in Scenario a1, while this was not observed for Scenario b1.

Table 4-3: Partial Spearman's correlation coefficients (R^2) of the residual, unreduced N_2O fraction (r_{N2O}) (Scenario a1 and b1), the N_2O fraction from bacterial denitrification (f_B), (Scenario a1/b1) and the N_2O+N_2 flux and the N_2 flux (Scenario a1 and b1) with potential driving variables for the Histic Gleysol (n=136) and the Plaggic Anthrosol (n=129)

Spearman's R	r_{N2O}				f_B		N_2O+N_2 flux				N_2 flux			
	Sc.a1		Sc.b1		Sc.a1/b1		Sc.a1		Sc.b1		Sc.a1		Sc.b1	
Histic Gleysol														
NO_3^--N content	0.27	**	0.32	**	0.06		-0.06		0.07		-0.13		-0.09	
NH_4^+-N content	-0.28	**	-0.17	**	-0.20	**	0.31	**	0.02		0.31	**	0.05	
Soil moisture	-0.29	**	-0.20	**	-0.22	**	0.30	**	0.04		0.29	**	0.07	
Soil temperature	-0.09		0.19	**	-0.20	**	0.10		-0.01		0.09		-0.07	
Plaggic Anthrosol														
NO_3^--N content	-0.02		-0.21	**	0.34	**	0.22	**	0.36	**	0.21		0.34	**
NH_4^+-N content	-0.07		0.08		-0.15		-0.13		-0.19	**	-0.12		-0.18	**
Soil moisture	-0.36	**	-0.32	**	0.04		0.42	**	0.37	**	0.41	**	0.38	**
Soil temperature	-0.15		-0.23	**	0.10		0.10		0.16		0.12		0.20	**

** indicate $p<0.05$ level of significance, respectively.

At the Plaggic Anthrosol, r_{N2O} values were negatively correlated with NO_3^--N content, soil moisture und soil temperature in Scenario b1, while Scenario a1 showed only a significant correlation with soil moisture (R^2: -0.36). In contrast to the Histic Gleysol, f_B values were positively correlated with NO_3^--N content at the Plaggic Anthrosol. Also for the N_2O+N_2 fluxes, NO_3^--N content and soil moisture were the positively significantly correlated parameters in Scenario a1, while Scenario b1 showed additionally a negative correlation with NH_4^+-N contents. Generally, the Plaggic Anthrosol shows more significant relations correspondence of N_2O, N_2 fluxes and fractions (r_{N2O}, f_B) with soil variables in Scenario b1, whereas the Histic Gleysol shows a greater consistency with Scenario a1. Overall, soil

moisture and N substrate availability (reflected in NO_3^--N and NH_4^+-N contents) were the most important controlling factors.

4.3.6 Comparison of r_{N2O} values from the ^{15}N labelling experiment and from the isotopocule mapping approach

In a previous study by Buchen et al. (2016), we used the ^{15}N gas flux method *in situ* to quantify fluxes of N_2 and N_2O emitted from ^{15}N labelled NO_3^- and the N_2O flux from non-labelled pools. In the present study, we used isotopocule values of emitted N_2O to determine the relevance of N_2O turnover processes. Hence, we compared r_{N2O} values determined by the ^{15}N labelling experiments (^{15}N) with the r_{N2O} values based on the calculations using the isotopocule mapping approach (Scenarios a1 and b1) on four sampling dates in June 2014 at the Histic Gleysol when both approaches had been employed in parallel.

In general, r_{N2O} values from Scenario a1 and Scenario b1 and r_{N2O} values from the ^{15}N labelling experiment are well matched only on single dates and for single treatments (see framed treatments in Figure 4-5), whereas in other cases poor agreement was observed. Nevertheless, in order to properly compare r_{N2O} values, the parameters controlling the N_2O transformation processes should be similar in both experiments. To achieve equal conditions, the two experiments were located next to each other and treated identically. But the N fertiliser was applied aboveground for the isotopocule sampling as this was part of the two-year field flux study where management was conducted according to farmer's practice, whereas a ^{15}N labelled fertiliser solution had to be injected with needles in the ^{15}N labelling experiment to obtain homogenous labelling. Consequently, N_{min} content and soil moisture was not always similar in natural abundance and ^{15}N tracer plots. We therefore selected the *Maize* treatment on June 2-3, 2014 and the *Mechanical* treatment on June 9-10, 2014 as the best comparable samplings of both experimental approaches, based on the environmental parameters (soil moisture, NO_3^--N content and N_2O flux) of these dates (Table A4-4). For the *Maize* treatment, the calculated r_{N2O} values from Scenario a1 (0.03±0.04) and the ^{15}N labelling experiment (0.02±0.02) matched very well, while the r_{N2O} values from Scenario b1 (0.40±0.09) were significantly higher. This also applies for the *Mechanical* treatment with r_{N2O} values of 0.06±0.04 for Scenario a1, 0.07±0.07 for ^{15}N labelling experiment and 0.32±0.18 for Scenario b1. As shown earlier, r_{N2O} values from isotopocule calculations based on Scenario b1 were always higher than in Scenario a1 (see sections 4.3.2 and 4.3.4). On the sampling dates, on which either NO_3^--N content, soil moisture or N_2O flux differed largely between approaches (Table A4-4), the match of r_{N2O} values was variable. But there was general agreement of all

comparisons in so far as r_{N2O} values of ^{15}N and Scenario a1 were between 0 and 0.5, meaning that both approaches showed that N_2 mostly dominated the NO_3^-derived N_2+N_2O flux or was at least equal to the N_2O flux.

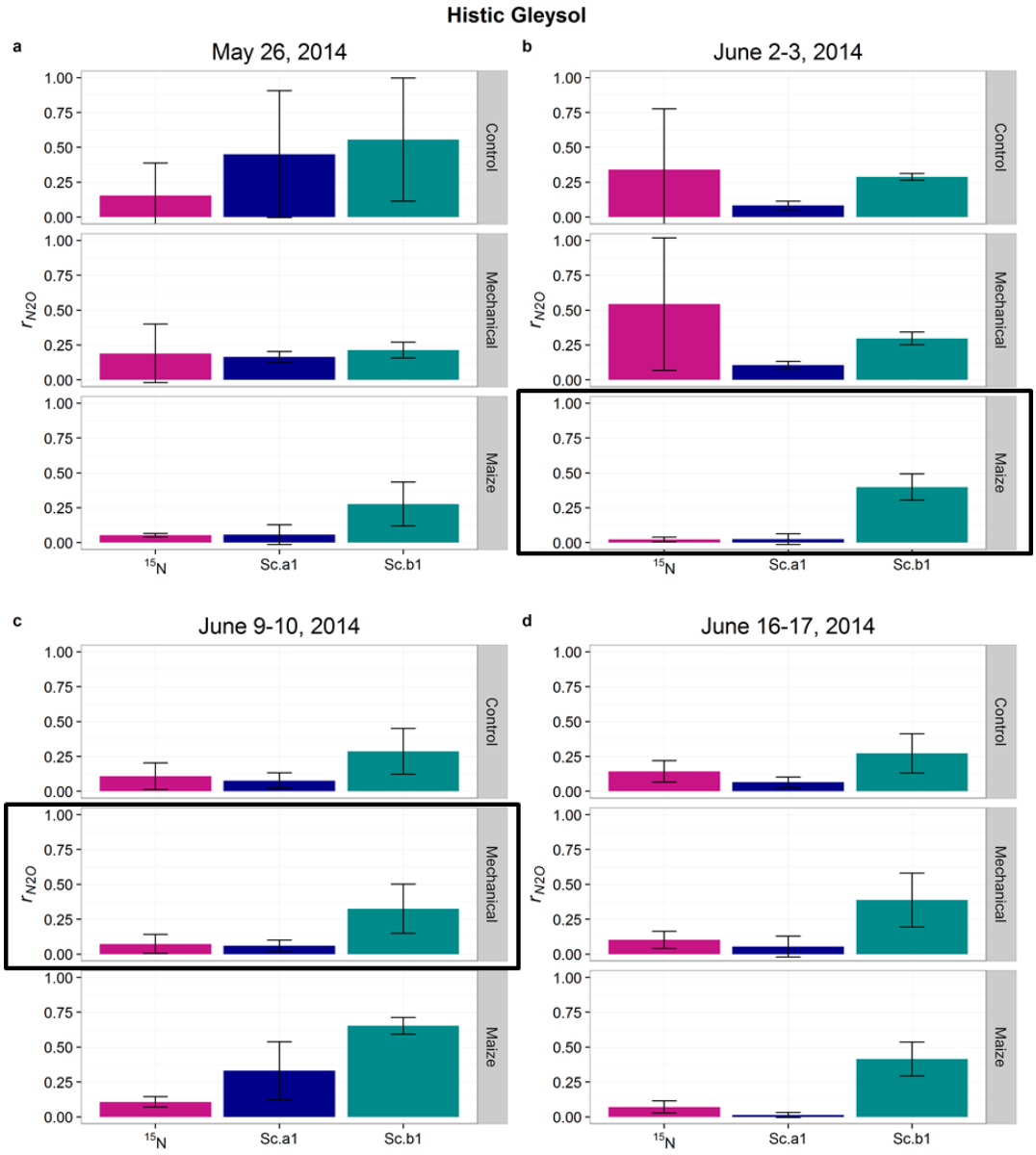

Figure 4-5: Comparison of the residual, unreduced N_2O fraction (r_{N2O}) from the ^{15}N labelling experiments (^{15}N) with the isotopocule mapping approach (Scenario a1 and b1) of the Histic Gleysol for the four parallel sampling dates in June 2014. The 2-day time periods are due to 1-day delayed isotopocule samplings. Error bars represent standard deviations of the mean values (n≥3). Treatments selected for the comparison are framed in black

4.4 Discussion

4.4.1 Scenario calculations and the attempt to validate the isotopocule mapping approach

Isotopocule maps, i.e. plots of $\delta^{15}N^{SP}_{N2O}$ vs. $\delta^{18}O_{N2O}$ and $\delta^{15}N^{SP}_{N2O}$ vs. $\delta^{15}N^{bulk}_{N2O}$ have been previously used to differentiate between the main N_2O production processes (heterotrophic bacterial denitrification / nitrifier denitrification and fungal denitrification / nitrification) (Koba et al., 2009; Zou et al., 2014) and N_2O reduction to N_2 (Well et al., 2012). Recently, Zou et al. (2014) used the isotopocule mapping approach ($\delta^{15}N^{SP}_{N2O}$ vs. $\delta^{15}N^{bulk}_{N2O}$ map) with different ranges for N_2O reduction in order to estimate possible shifts to N_2O from bacterial denitrification, while the present approach went further and used independent estimates of N_2O reduction (Lewicka-Szczebak et al., 2017), in order to simultaneously estimate N_2O reduction to N_2 and various N_2O production pathways. In contrast to Zou et al. (2014) and many other studies (Toyoda et al., 2011; Kato et al., 2013; Toyoda et al., 2015; Wolf et al., 2015), we used $\delta^{15}N^{SP}_{N2O}$ vs. $\delta^{18}O_{N2O}$ map (Well et al., 2012; Lewicka-Szczebak et al., 2014; Lewicka-Szczebak et al., 2015) to overcome the limitations of $\delta^{15}N^{bulk}_{N2O}$, as $\delta^{15}N^{bulk}_{N2O}$ is more variable depending on the substrate isotopic composition (e.g. NO_3^-, NH_4^+, NO_2^-) than $\delta^{18}O_{N2O}$. $\delta^{18}O_{N2O}$ is expected to be more stable due to its almost complete O exchange with H_2O and constant isotope effect during O exchange (Lewicka-Szczebak et al., 2016).

In Figure 4-2, all samples per site are shown in one isotopocule map to estimate N_2O reduction to N_2 and contribution of other sources (i.e. the admixture of bacterial denitrification). This calculation was possible for all samples that were located between the assigned isotopic endmember values taken from literature. Note that by using literature ranges for isotopic endmember values, a recalculation of isotopic values according to the specific substrate is necessary, while only $\delta^{15}N^{SP}_{N2O}$ is independent of the substrate isotopic signature. The required isotopic signature of soil water as a substrate for $\delta^{18}O$ values ($\delta^{18}O_{H2O}$) in the present study was performed by soil water extraction and taken into account. Unfortunately, there is still an uncertainty in determination of the assigned endmember values due to the range of isotopic endmember values (Table 4-1). Therefore, we developed several scenario variations, combining mean, minimum and maximum values for endmember values and isotopic fractionation factors associated with N_2O reduction to cover the entire potential range in the calculation of r_{N2O} and f_B values. This yields the maximum range of possible values irrespective of probability. Hence, a further step in uncertainty estimation is needed for future studies, i.e. by using Monte-Carlo simulation, taking the measurement uncertainty of N_2O

concentrations, the variance and covariance of $\delta^{15}N^{SP}_{N2O}$, $\delta^{18}O_{N2O}$ and $\delta^{15}N^{bulk}_{N2O}$ into account and ensure ranges for the specific endmember values (heterotrophic bacterial denitrification / nitrifier denitrification and fungal denitrification / nitrification) (Wu et al., in preparation). We used values for heterotrophic bacterial denitrification / nitrifier denitrification ($\delta_0{}^{15}N^{SP}_{N2O}$: -3.9‰ and $\delta_0{}^{18}O_{N2O/H2O}$: 21.0‰) with $\delta_0{}^{15}N^{SP}_{N2O}$ values from pure culture studies and $\delta_0{}^{18}O_{N2O/H2O}$ values from controlled soil incubations, where the water exchange is high and the isotope effect between water and formed N_2O is quite stable (Lewicka-Szczebak et al., 2016). For the fungal denitrification / nitrification endmember area, a mean value of $\delta_0{}^{15}N^{SP}_{N2O}$: 34.8‰ vs. $\delta_0{}^{18}O_{N2O/H2O}$: 43.6‰ was taken into account for calculations. These are also afflicted with uncertainties, as a previous study found also lower $\delta_0{}^{15}N^{SP}_{N2O}$ values of 21.9 ‰ for fungal denitrification (Rohe et al., 2014), but since this fungal strain (*C. funicola*) showed less than 100 times lower N_2O production with NO_2^- compared to other species and no N_2O production with NO_3^-, we excluded this from our calculations (Maeda et al., 2015; Lewicka-Szczebak et al., 2016). A further uncertainty is given by the isotopic fractionation factors associated with N_2O reduction, which were recently examined under oxic and anoxic conditions and therefore very likely applicable for field studies unless N_2O reduction is nearly complete (i.e. r_{N2O}<0.1) (Lewicka-Szczebak et al., 2015), and will be evaluated by Wu et al. (in preparation).

In order to answer the question which of the scenarios is the most probable one, it is important to know that not all scenarios are possible for individual samples, depending on their location between the assigned endmember values in the isotopocule map. $\delta^{15}N^{SP}_{N2O}$ and $\delta^{18}O_{N2O/H2O}$ values located outside of the scenario specific endmember areas yielded unrealistic r_{N2O} and f_B values <0 or >1. In particular in Scenario a3/b3 (*Minimum mixing line, mean reduction line, mean* $\eta_{red}{}^{15}N_{SP}$ *values*), 46/64% of the samples of the total data were set to 0 or 1. For a better understanding of a single sample in the various Scenarios (a,b) and Scenario variations (1-7), we plotted a sample of the Maize treatment (September 9, 2014) with a $\delta^{18}O_{N2O/H2O}$ value of 51.5‰ and a $\delta^{15}N^{SP}_{N2O}$ value of 20.0‰, which results in a wide range of r_{N2O} values (0.01-0.78) and f_B values (0.26-0.83) (Figure A4-1). The wide range of r_{N2O} and f_B values demonstrates that the sample yields results between almost complete N_2O reduction to N_2 and a low admixture of bacterial denitrification, as well as the opposite, depending on the specific scenario. While differences between the seven Scenario variations were large, differences between the Scenarios a and b within a scenario variation were slightly lower. But still, a tendency to higher r_{N2O} values (i.e. less N_2O reduction to N_2) from Scenario b (*first mixing, then* N_2O *reduction*) than Scenario a (*first* N_2O *reduction, then mixing*) was visible (Figure 4-3

and Table 4-3). But based on our current knowledge, we consider Scenarios a1 or b1 as the most probable ones for the majority of samples, because by using mean values for endmember areas (Table 4-1), the most suitable values combined from former studies (Toyoda et al., 2005; Sutka et al., 2006; Sutka et al., 2008; Frame and Casciotti, 2010; Heil et al., 2014; Lewicka-Szczebak et al., 2014; Rohe et al., 2014; Maeda et al., 2015) were taken to indicate the most common N_2O production pathways. If we further compare mean N_2O+N_2 fluxes from Scenarios a and b (Table 4-2, A4-3 and A4-4) large differences were visible, which can be explained from the calculations based on the isotopocule map in Figure 4-1b. N_2O+N_2 fluxes are rather similar, as long as Scenarios a and b follow the same reduction line. But if a sample is located closer to the fungal denitrification / nitrification endmember area, the contribution of reduction in Scenario b (*first mixing then reduction*) becomes lower due to the longer distance on the mixing line and a shorter distance on the reduction line.

A first attempt at validation for the isotopocule mapping approach was done by a comparison with a parallel ^{15}N labelling experiment at the Histic Gleysol (Buchen et al., 2016) which is to our knowledge the first field scale comparison of this kind. Unfortunately, we were not able to compare all measured r_{N2O} values from the parallel sampling within the 44 days of the ^{15}N labelling study period with the calculated r_{N2O} values using the isotopocule mapping approach. Although both experiments were fertilised at the same N rate and date, the soil conditions and N_2O fluxes were quite different, due to the differences in fertiliser application. In the ^{15}N labelling study, needle injection of N fertiliser was applied to achieve homogenous label distribution, where N fertiliser (e.g. NO_3^-) could be used directly by soil microbes as a substrate for N_2O production. In the third part of the study (Isotopocules), N fertiliser was applied according to famers' practice aboveground at the entire field, resulting in differences in NO_3^--N and NH_4^+-N concentrations in soil. We expected an maximum increase in water content, equivalent to less than 3% WFPS due to the injection of ^{15}N tracer solution in the labelling experiment and assumed this to have only a short and low impact, but due to the columns inserted at 30 cm depth and heavy rainfall during the beginning of the experiment, the soil within the PVC cylinders of the ^{15}N micro-plots was partly water-saturated, while water from isotopocule sampling plots could flow off more easily. But when soil conditions were comparable (see selected dates in Table A4-4), the results were also similar between calculated r_{N2O} values of Scenario a1 and measured r_{N2O} values during the ^{15}N labelling experiment (Figure 4-5). However, Scenario b1 led to higher r_{N2O} values in the selected treatments, which resulted in a lower correspondence between measured and calculated r_{N2O} values. We showed in our previous study (Buchen et al., 2016), that mean r_{N2O} values were usually less than 0.2

during a study period of 44 days in summer 2014. If we compare those r_{N2O} values with the calculated mean r_{N2O} values (0.17±0.25) (i.e. average of the investigated *Control*, *Mechanical* and *Maize* treatment) of Scenario a1 during this time, mean r_{N2O} values were in good agreement.

4.4.2 Contribution of N_2O reduction to N_2 and other source processes to the total N_2O flux

Earlier studies have shown, that isotopocule analysis are a useful tool to distinguish between the main N_2O production pathways such as heterotrophic bacterial denitrification / nitrifier denitrification or nitrification / fungal denitrification in various environments (Koba et al., 2009; Park et al., 2011; Toyoda et al., 2011; Zou et al., 2014). Using grassland soils under natural abundance incubations, Wrage et al. (2004a) assumed heterotrophic bacterial denitrification / nitrifier denitrification as the most important pathway of N_2O production with a contribution of N_2O reduction due to conditions with small concentrations of N_2O, while reduction of emitted N_2O to N_2 was not measured in this study. The present results, showed a significant contribution of N_2O reduction to N_2 (see low r_{N2O} values Figure 4-3) in Scenario a1/b1 for both sites, which was confirmed by results from the ^{15}N labelling study for the Histic Gleysol (Buchen et al., 2016). In contrast, a good correspondence was not confirmed for the sandy Plaggic Anthrosol, as results from the ^{15}N labelling study showed less N_2O reduction to N_2 (only 2 samples above the N_2 detection limit of 1.8 ppm). This was attributed to low denitrification activity because of low soil water contents, low SOC contents and soil aeration (Buchen et al., 2016). However, results from the isotopocule approach showed a significant contribution of N_2O reduction to N_2 for this site.

Although, r_{N2O} values were low on average, their variability was quite large, especially following grassland renewal and grassland conversion to maize cropping. N fertilisation exhibited a different pattern between more stable r_{N2O} values during summer but increased variability in f_B values at both sites. For instance, r_{N2O} values in the *Chemical* treatment following grassland renewal in 2013 ranged between 0.01-1.00 (Scenario a1) at the Histic Gleysol and 0.04-1.00 (Scenario a1) at the Plaggic Anthrosol within 6 weeks, possibly caused by grassland disturbance. This might be explained by the sward destruction during grassland renewal, which led to a substantial mobilisation of organic C and N and its decomposition, and thus resulting in conditions favouring anaerobic microsites as “hotspots” (Folorunso and Rolston, 1984; Parkin, 1987). This was preferably confirmed for the *Mechanical* treatment (Figure 4-3) at the Plaggic Anthrosol, where higher f_B values (two-month average:

0.86±0.15 of Scenario a1) were found following grassland renewal, which showed a clear dominance of bacterial denitrification. At the Histic Gleysol the two-month average of f_B values in the *Mechanical* treatment accounted only for 0.53±0.19 (Scenario a1), indicating a lower admixture of bacterial denitrification, because the contribution of N_2O reduction was greater. Several other studies already identified heterotrophic bacterial denitrification / nitrifier denitrification as the major N_2O production process in soils by assessing low $\delta^{15}N^{SP}_{N2O}$ values (Opdyke et al., 2009; Ostrom et al., 2010). For example, Opdyke et al. (2009) estimated that 87% of heterotrophic bacterial denitrification / nitrifier denitrification in croplands based on $\delta^{15}N^{SP}_{N2O}$ of soil-emitted N_2O assessed with closed flux chambers, assuming that N_2O reduction was negligible. By interpreting $\delta^{15}N^{SP}_{N2O}$ and assuming negligible N_2O reduction Ostrom et al. (2010) suggested that heterotrophic bacterial denitrification accounted for 53-100% of the total N_2O flux, concluding that heterotrophic bacterial denitrification as the primary source of N_2O production in cultivation of a historically never-tilled grassland soil. Recently, Wolf et al. (2015) determined isotopocule values of soil-emitted N_2O on continuous *in situ* free air measurements above a grassland site. They identified heterotrophic bacterial denitrification as the main source of N_2O production with a significant contribution of N_2O reduction to N_2 in an intensively managed grassland site following a phase of rewetting. This was evaluated from the gradual increase in isotopic composition in a $\delta^{15}N^{SP}_{N2O}/\delta^{18}O$ map, since N-O bonds between lighter isotopes are cleaved preferentially, which lead an increase in $\delta^{15}N^{SP}_{N2O}$, $\delta^{15}N^{bulk}_{N2O}$ and $\delta^{18}O$ in the remaining N_2O. A similar dynamic in soil might be assumable for the Histic Gleysol due to the known fluctuating groundwater levels at this site.

Based on the r_{N2O} and f_B values, we calculated the total denitrification losses (i.e. N_2O+N_2 flux), as well as the N_2O fluxes from heterotrophic bacterial denitrification / nitrifier denitrification and fungal denitrification / nitrification. If we compared N_2O emission and N_2 emission, we found that N_2 fluxes were 50 times greater than the N_2O fluxes at the Histic Gleysol, which underline the great contribution of N_2O reduction to the total denitrification loss. But if we then partitioned the N_2O flux in its sources, we found a higher contribution from fungal denitrification / nitrification than from heterotrophic bacterial denitrification / nitrifier denitrification for the Histic Gleysol. This goes along with low f_B values, which were found at the Histic Gleysol (Table 4-2) and which is also a visible tendency from the isotopocule map in Figure 4-2. Then low f_B values indicate a high contribution of nitrification (i.e. hydroxylamine-derived N_2O) and fungal denitrification. A significant contribution of fungal N_2O had been shown by Lewicka-Szczebak et al. (2017), during He-incubations using the same organic soil. The simultaneous occurrence of fungal denitrification (low f_B values) and heterotrophic

bacterial denitrification (low r_{N2O} values) at the Histic Gleysol might have resulted from low O_2 concentration due to fluctuating groundwater levels, which promotes such processes (Yanai et al., 2007; Zou et al., 2014), while nitrification is likely to be supressed under anaerobic conditions (Kato et al., 2013). As nitrification is generally thought to be less important, this process may become more important under conditions with high O_2 values, low pH values and high organic C contents (Wrage et al., 2001; Guo et al., 2013). Nevertheless, fungal denitrification is so far not distinguishable from nitrification; so that a proportion of nitrification-derived N_2O has to be considered.

Furthermore, the process of co-metabolic denitrification (i.e. co-denitrification) should be considered, as it is known that bacteria and fungi are also able to produce hybrid N_2O and N_2 from NO_2^- and N from another source (i.e. NH_4^+ or organic N) (Spott and Stange, 2011). Until now, there are only a few studies showing a significant contribution of hybrid N_2O and N_2 in natural soils (Laughlin and Stevens, 2002; Long et al., 2013; Selbie et al., 2015). Nevertheless, these studies identified co-denitrification as the main N_2 production process (Long et al., 2013) and Laughlin and Stevens (2002) even demonstrated a contribution of fungal co-denitrification of up to 92% to the N_2 flux in grassland soils. But until now, co-denitrification has not been reported at isotopic natural abundance level so far. In our ^{15}N labelling study, a contribution of hybrid N_2O production processes such as co-denitrification and/or anaerobic ammonium oxidation (Anammox) could not be completely excluded for the Histic Gleysol due to large spatial heterogeneity (Buchen et al., 2016).

Moreover, it has been shown by ^{15}N labelling (Buchen et al., 2016), that dissimilatory NO_3^- reduction to ammonia (DNRA) has added to the possible N_2O production process at the Histic Gleysol, as the site was often temporarily water-saturated throughout the year (Rückauf et al., 2004; Tauchnitz et al., 2015). For two dates (June 1, 2014 and June 9, 2014), DNRA and/or subsequent immobilisation (i.e. assimilatory NO_3^- reduction) (Rütting et al., 2011) occurred at the study site (Buchen et al., 2016). Also some values from the isotopocule mapping approach above the endmember area of fungal denitrification / nitrification support the occurrence of DNRA, which had been shown by Behrendt et al. (2015) for $\delta_0{}^{15}N^{SP}{}_{N2O}$ values >39‰. Overall, the determination of different N_2O production processes is still strained by high number of uncertainties; particularly as potentially more than the displayed processes of the isotopocule mapping approach are involved, which has been shown especially for the Histic Gleysol in previous studies (e.g. co-denitrification, Anammox, DNRA and subsequent immobilisation) (Buchen et al., 2016; Lewicka-Szczebak et al., 2017).

4.4.3 Controlling factors of soil-emitted N_2O+N_2 fluxes and contributing processes

Grassland renewal or grassland conversion to maize cropping can considerably affect N_2O and/or N_2 production processes, since several controlling factors are altered by sward destruction, subsequent decomposition of soil organic matter and changes in vegetation cover. Namely, changes in soil moisture by water demand of plants; changes in soil aeration by soil tillage; changes in electron donors' availability for denitrification and enhanced O_2 consumption by rhizodeposition and organic matter decomposition; changes in substrate availability of NO_3^- and NH_4^+ through mineralisation, as well as changes in plant N uptake can be expected (Davies et al., 2001; Yamulki and Jarvis, 2002; MacDonald et al., 2010), all of which are highly relevant for N_2O turnover (Müller and Clough, 2014). Furthermore, those effects also depend on site and climatic variables. To evaluate the impact of controlling variables on r_{N2O} values and f_B values, we calculated Spearman's correlations with the following parameters: N substrate availability in form of NO_3^--N and NH_4^+-N contents, soil moisture and soil temperature. Here again, N substrate availability has been identified as a major control, governing N_2O+N_2 fluxes (Saggar et al., 2013; Buchen et al., 2016). As f_B values were negatively correlated with NH_4^+-N contents, this might reflect that a significant part of NH_4^+-derived N_2O was emitted *via* nitrification at the Histic Gleysol. Furthermore, r_{N2O} values were significantly correlated with large NO_3^--N contents and high soil moisture. As shown earlier, soil moisture has been identified as another major control of N_2+N_2O production at the Histic Gleysol in the topsoil layer, which is caused by near-surface groundwater levels on this site (Buchen et al., 2016). These observed effects at the Histic Gleysol are thus in line with the well-known enhancement of denitrification by NO_3^- availability and soil moisture (Müller and Clough, 2014).

In the present study, a statistical comparison of average fluxes of the entire study period was not possible due to low and unequal sample size. But the impact of management events was evident in some cases from the time course of N_2O+N_2 fluxes (Figure 4-4). Total denitrification losses (i.e. N_2O+N_2 fluxes in Figure 4-4) increased following grassland renewal (autumn 2013) and grassland conversion to maize cropping (summer 2014), which is comparable to results derived from the ^{15}N labelling study for the Histic Gleysol. Also the grassland treatments (*Control, Chemical* and *Mechanical*) revealed high N_2+N_2O fluxes during the summer period in 2014, which might result from N fertilisation events in combination with changes in soil moisture and higher temperatures. As treatment comparisons are mandatory to

understand the effects of a certain management practices (e.g. grassland renewal) further studies are needed with complete data sets, which improve the determination of soil-emitted N_2O, either by more precise isotopocule measurements and/or by measurements of isotopic composition of soil-air.

4.5 Conclusions

In the present study, we used the isotopocule mapping approach to estimate the magnitude of N_2O reduction to N_2 and the fraction of N_2O originating from the heterotrophic bacterial denitrification pathway, fungal denitrification and or nitrification of soil-emitted N_2O. For both scenarios the unreduced, residual N_2O fraction (r_{N2O} values) ranged between 0 and 1 at both sites, while the N_2O fraction from bacterial denitrification (f_B values) ranged between 0.20 and 0.98 at the Histic Gleysol and between 0.16 and 1.00 at the Plaggic Anthrosol. Based on this, we indicate heterotrophic bacterial denitrification / nitrifier denitrification as the main source of N_2O production with a significant contribution of N_2O reduction to N_2 rather than nitrification (i.e. hydroxylamine oxidation) and fungal denitrification throughout the entire study period. A tendency to a higher contribution of N_2O reduction to N_2 could be displayed for the often water-saturated Histic Gleysol, while a lower reduction potential occurred at the sandy Plaggic Anthrosol. To support those results, we made a first attempt of validation and compared our results with a parallel ^{15}N labelling study at the field scale at the Histic Gleysol. On average r_{N2O} values were in good agreement for two samplings, as conditions of soil moisture, NO_3^- availability and N_2O flux were similar in both studies. A comparison for f_B values was not possible, which reveals the need to further constrain parameters of the isotopocule mapping approach and more validation attempts including f_B values, either by multiple isotope tracing and/or modelling (Müller et al., 2014; Zou et al., 2014). Furthermore, a complex estimation of uncertainties using actual endmember ranges is a prospective challenge. We took the first step by using minimum, maximum and mean values for endmember values of heterotrophic bacterial denitrification / nitrifier denitrification and fungal denitrification / nitrification in our calculation. We did this to cover the ranges of possible r_{N2O} values and f_B values. Moreover, other processes contribute to N_2O turnover in soil besides the processes displayed here in the isotopocule map, indicating a requirement for further natural abundance isotopic research.

Chapter 5

Synthesis and conclusions

Grassland break-up due to grassland management practices like grassland renewal or grassland conversion to arable cropping are common agricultural practices. Nevertheless, they can have a large impact on N losses. In the present thesis, grassland renewal techniques and grassland conversion to maize cropping were studied with respect to N_2O and N_2 emissions, their dynamics and environmental controls. Furthermore mineral N (N_{min}) dynamics were determined to evaluate the potential for NO_3^- leaching following grassland break-up. The combined evaluation of a two-year field trial with *in situ* application of stable isotope approaches (i.e. application of the ^{15}N tracing technique and natural abundance isotope signatures of soil-emitted N_2O) for selected periods, allowed a more comprehensive understanding of N_2O transformation processes, in particular to N_2O reduction to N_2 and the contributing processes to N_2O production for two local agricultural sites. Two soils, which differ in soil organic matter (SOM) content and drainage regime (Plaggic Anthrosol and Histic Gleysol) were chosen in order to allow the evaluation of N losses due to different environmental drivers and to give the possibility to apply the obtained findings to other sites.

5.1 Overview of the main findings

5.1.1 Soil mineral N dynamics and N_2O emissions following grassland renewal

N_2O fluxes and N_{min} dynamics (0-30 cm) were studied for a period of two years following grassland renewal by using different techniques and grassland conversion to maize cropping, while N_{min} profiles (0-90 cm) in autumn (pre-winter) and spring (post-winter) were used to evaluate the N_{min} loss over winter to estimate the potential for NO_3^- leaching. Furthermore the yield effect was investigated. The following results were obtained:

- Grassland renewal and grassland conversion to maize cropping resulted in elevated N_2O fluxes for a two-month period compared to permanent grassland, while no annual effect occurred for the two investigated sites. The net release of N_{min} increased following grassland break-up which is accompanied by an enhanced risk of NO_3^- leaching.
- N_2O emissions increased during the first two months with the degree of sward and soil disturbance: keeping and improving the old sward (*Minimum* treatment) < renewal by

chemical sward destruction and direct sowing (*Chemical* treatment) < renewal by chemical and mechanical sward destruction (*Mechanical* treatment). The N_{min} release during the first winter was highest in the *Chemical*, *Mechanical* and *Maize* treatments.

- N_2O fluxes were site-specific and greater for the C-rich Histic Gleysol, while the risk of NO_3^- leaching was higher for the sandy and well-drained Plaggic Anthrosol.
- Grassland renewal did not influence yield (neither increase, nor depression).

5.1.2 Fluxes of N_2 and N_2O and contributing processes in summer after grassland renewal and grassland conversion to maize cropping on a Plaggic Anthrosol and a Histic Gleysol

During the summer period following grassland conversion to maize cropping, the ^{15}N gas flux method was applied to determine denitrification losses and contributing processes of N_2O production and consumption by measuring N_2O fluxes, N_2 fluxes, N_{min} contents and their ^{15}N enrichment. The following results were obtained:

- Denitrification losses with partial N_2O reduction to N_2 were high for the Histic Gleysol, while they were rather low at the Plaggic Anthrosol. Mean N_2O+N_2 emissions did not differ between the treatments at the Histic Gleysol, while N_2O emissions were significantly different between the treatments at the Plaggic Anthrosol.
- A contribution of nitrification and nitrifier denitrification was evaluated for the Plaggic Anthrosol, while a potential contribution of N_2O production by NH_4^+ production by DNRA was indicated at the Histic Gleysol.
- Large amounts of available organic C and N, water-saturation and low O_2 availability lead to a higher contribution of denitrification and N_2O reduction to N_2 at the Histic Gleysol than at the Plaggic Anthrosol.
- A contribution of hybrid N_2O and/or N_2 through co-denitrification and/or anammox could neither be confirmed nor rejected due to non-homogeneous ^{15}N-label distribution at the Histic Gleysol. For the Plaggic Anthrosol heterogeneity was minor important.

5.1.3 Estimating N_2O processes during grassland renewal and grassland conversion to maize cropping using N_2O isotopocules

Within the first year following grassland renewal, natural abundance isotopic signatures of soil-emitted N_2O were analysed to identify sources of N_2O emission and evaluate the contribution of N_2O reduction to N_2 to the total N_2O flux. This was carried out by the

application of a novel isotopocule mapping approach. Furthermore available data on N_2O reduction were compared to the results of the ^{15}N tracing experiment (Chapter 3). The following results were obtained:

- If environmental conditions, such as NO_3^- availability, N_2O flux and soil moisture were similar, results of Scenario a1 (i.e. using average values from literature for the setting of the isotopocule mapping approach) agreed with results from the ^{15}N tracing experiment.
- Heterotrophic bacterial denitrification and/or nitrifier denitrification with a contribution of N_2O reduction to N_2 were found as the main source of N_2O production, while fungal denitrification and/or nitrification also contributed to the flux.
- Management events like grassland ploughing resulted in higher N_2O production rates, while seasonal changes throughout the year were hard to identify.
- The identification of treatment effects using the isotopocule mapping approach was difficult, due to unequal sample sizes within the different treatments.

5.2 Impact of grassland break-up on N_2O+N_2 fluxes, mineral N dynamics and yield

5.2.1 Management effects

Similar to various previous studies (Mori and Hojito, 2007; Velthof et al., 2010; MacDonald et al., 2011; Biegemann, 2014), only a short-term increase of N_2O fluxes after grassland renewal and grassland conversion to arable cropping was observed in the present study. The expected annual effect of grassland break-up on N_2O emission was not obtained. However, the present study covered a period of two years for the first time and thereby provided results which can be utilised in the national greenhouse gas inventories and/or to derive mitigation strategies. Previous studies mostly focussed on shorter time periods (section 2.1) and limited sampling intervals might lead to an underestimation of the annual N_2O budget. Biegemann (2014) and Merbold et al. (2014) for instance reported profound contributions of N_2O emissions during winter as a results of freeze/thaw cycling. Such dominant contribution are likely to be missed when only selected time periods are measured (e.g. Krol et al. (2016); Mori and Hojito (2007)). Nevertheless, the present results, which revealed no long-term impact of grassland break-up on N_2O emission, should not be generalised, because it is known that N_2O emissions can be much higher from other soil types and under different environmental/weather conditions.

Moreover, different grassland renewal techniques applied in the present study, represent various agricultural practices of north-western Germany. These techniques differ in intensity of disturbance starting from minimal intervention, such as improving the old sward by resowing (*Minimum* treatment), in comparison to chemical (*Chemical* treatment) and/or mechanical destruction of the sward and soil structure by applying herbicide (e.g. glyphosate) followed by ploughing (*Mechanical* treatment). Impact on N_2O emission between the treatments were only found within a two-month period, while the increase of the degree of sward and soil disturbance within the treatments lead to an increase of N_2O emission.

Apart from N_2O fluxes, also the net N_{min} release increased during the first month after grassland renewal and grassland conversion to maize cropping, which led to a higher risk of NO_3^- leaching losses (i.e. groundwater pollution with NO_3^-) during winter (Section 2.3.2). A conceptual model summarizing the relationship between the impacts of grassland break-up (i.e. N losses) with respect to the time between cultivation and sowing (Velthof and Oenema, 2001) is shown in Figure 5-1. The results indicate that the risk of N losses is lower from grassland renewal than from grassland conversion followed by arable cropping. Moreover, the risk increases if the soil is left fallow after grassland break-up.

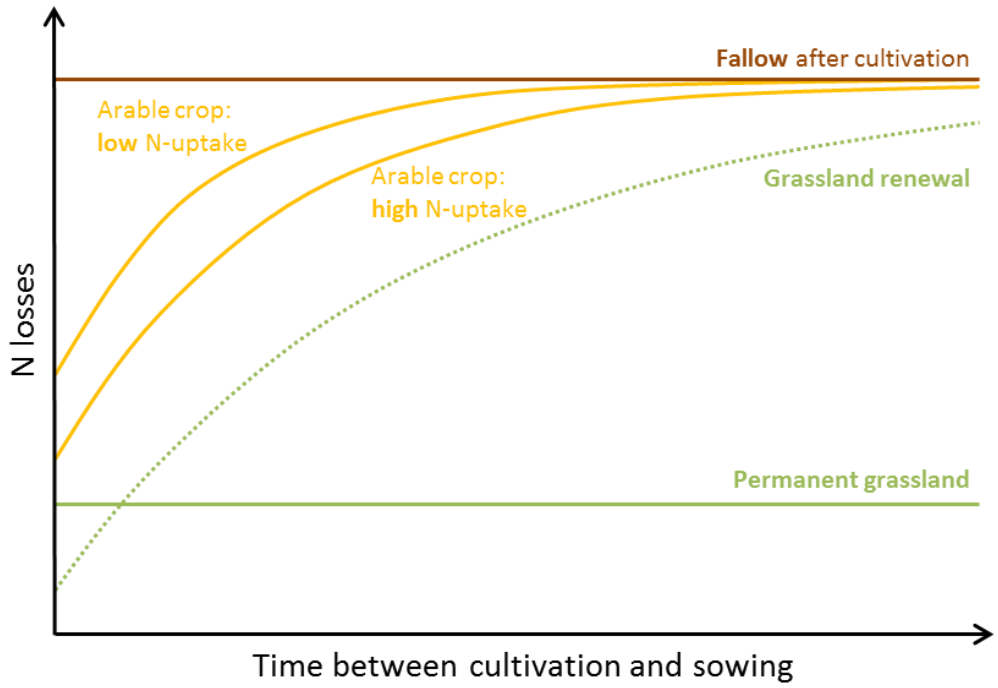

Figure 5-1: Assumed N-losses (N_2O emission and NO_3^- leaching), depending on the time between cultivation and sowing of a new grass/crop after grassland break-up in comparison to permanent grassland (modified after Velthof and Oenema (2001))

In the present study, fields were not left fallow directly after grassland break-up, but they were uncultivated during winter following the first season of maize cultivation after grassland conversion to maize cropping, as it is often the case in maize monocultures. As a result, large amounts of pre-winter N_{min} were determined for the *Maize* treatment at the beginning of the leachate period, while post-winter N_{min} contents were rather low (section 2.3.2) for both sites and within both years under evaluation. For the sandy Plaggic Anthrosol, the change of N_{min} contents over winter can be used as a robust indicator of NO_3^- leaching, as gaseous N losses were small, as well as mineralisation and immobilisation rates are slow at low temperatures (Herbst et al., 1982). However, for the Histic Gleysol the N_{min} change in winter was more difficult to interpret. The potential denitrification loss was large due to high water-saturation and in particular denitrification in saturated soils is known to be intense even at low temperatures (Well et al., 2003) (section 2.4.3). Equipment for direct quantification of leachate e.g. suction cups or lysimeters, was not available for the experimental setup reported here. To prevent the risk of NO_3^- leaching a catch crop (e.g. yellow mustard, Italian ryegrass, winter rye and fodder radish) would be a useful alternative, especially at the sandy Plaggic Anthrosol (Kayser et al., 2008). Growing a catch crop at the Histic Gleysol probably is difficult due to high groundwater levels, paired with complicated accessibility and traffic ability by the farmer. Overall, it has to be stated that it is necessary to ensure a rapid development of the new grass/crop (i.e. acting as an N sink).

Furthermore, the time of grassland break-up can become more important with respect to minimizing strategies for NO_3^- leaching. While this was not investigated in the present study, previous research (Francis et al., 1992; Lloyd, 1992; Seidel et al., 2009; Velthof et al., 2010; Biegemann, 2014) suggested that grassland renewal in spring lead to a lower NO_3^- leaching potential, as the new grass sward provides a good ground cover and takes up considerable amounts of available N_{min} within the growing period (Francis et al., 1995). However, grassland renewal in spring can lead to significant lower yields during the first cut, so that this option is rarely applied by farmers. But overall, moving the time of grassland renewal from autumn to spring might be the best alternative for light/sandy soils (Seidel et al., 2009).

5.2.2 Environmental drivers

Since the study was carried out on two sites with different SOM content and drainage regime, differences in the level of N_2O and N_2 emissions and between the present N_2O production and consumption processes were expected. It has become evident that N_2O emissions at the Histic Gleysol were up to tenfold higher than at the Plaggic Anthrosol (Chapter 2 and 3).

In particular water-saturation due to high groundwater-levels (often only -0.2 m) at the Histic Gleysol leads to high N losses *via* denitrification. Further this might be further enhanced by the large amount of available organic C, especially following grassland break-up and the simultaneous occurrence of anoxic conditions due to high microbial respiration and low oxygen diffusivity. Moreover, the input of C and N by decomposing plant residues of the incorporated grass sward can lead to the formation of denitrification "hotspots" (Parkin, 1987). Statistically, the impact of environmental controlling factors was investigated by application of generalised additive model (GAM) (Chapter 3 and 4) and partial correlations (Chapter 4 and 5). The obtained results indicated that N_2O fluxes were mainly controlled by NO_3^- availability and soil moisture (i.e. gravimetric water content). Large rainfall events during summer when the groundwater level was lower in combination with increasing soil temperature might also have affected N_2O production in soil, especially as the temperature impact on enzymatic processes involved in N_2O production is well known (Butterbach-Bahl et al., 2013).

For the Plaggic Anthrosol, the applied GAM and partial correlations revealed also a major impact of NO_3^- availability and soil moisture to the N_2O flux, while soil temperature had to be added during summer periods (section 3.3.3). In comparison to the Histic Gleysol, soil moisture varied on a lower level of 20-60% WFPS at the Plaggic Anthrosol, while the groundwater was below the rooting zone, so that the soil could be characterised as well-aerated and thus emitting less N_2O. This sandy soil was more likely to loose N *via* NO_3^- leaching due to its high permeability, so that N_{min} was easily transported to deeper layers and could be subsequently leached out into the groundwater. Previous studies have shown that this risk is further increased due to the flush of available N after grassland break-up, especially for old, grazed and N fertilised grassland sites with high C and N contents (Velthof and Oenema, 2001; Kayser et al., 2008).

Further the effect of different environmental drivers, such as N_{min} availability, organic C contents and soil moisture on N_2O fluxes was shown to be much larger than management practices (i.e. different treatments). Hence there was also feedback of grassland management on soil properties, as grassland renewal (i.e. grassland ploughing (*Mechanical* treatment) or chemical killing (*Chemical* treatment)) had an impact on C/N availability due to an increase of mineralisation. This demonstrates that effects of soil type, soil properties, environmental drivers and grassland management on N losses should be based on long-term experiments to obtain a more comprehensive understanding. Furthermore, risk assessment using weather data

should be included in the evaluation of different grassland management practices (e.g. what is the risk during wet and mild winter on sites with a high NO_3^- leaching potential) (Velthof and Oenema, 2001).

5.2.3 Yield effects and famer's potential benefit

To evaluate the famer's potential benefit of grassland renewal, quantity and quality of harvested biomass were investigated within the first part of the study (Chapter 2).

Neither a yield increase, nor a yield depression following grassland renewal was observed, which confirms previous results reported by Hopkins et al. (1995), Velthof et al. (2010), Schmeer (2012) and Biegemann (2014). Also the plant N content and the energy (NEL) yield, which are used as indicators for quality improvement, did not differ between grassland renewal treatments and continuous grassland. Even though exact data on the frequency of grassland renewal are lacking for Germany, Biegemann (2014) assumed that in many cases grassland renewal is carried out more often than necessary. The author claimed that grassland renewal is done because its practice is part of the common farming systems rather than due to rational reasons (Biegemann, 2014). When asking the Chamber of Agriculture across Germany a north-south difference in the application of grassland renewal techniques was found. While chemical and/or mechanical sward destruction are a more common management practice in the northern regions of Germany, farmers in the southern parts of Germany prefer minimal procedures like rejuvenation and resowing practices (personal communication). Nevertheless, grassland renewal is the one and only appropriate method and will increase the farmer's benefit, if the grass sward is in really poor condition. To avoid unnecessary grassland renewal, the Chamber of Agriculture, Lower Saxony for example provides a spreadsheet where farmers can evaluate typical damage patterns in the composition of the sward and necessary measures, which can be applied in the following, are recommend (Chamber of Agriculture, 2016).

In the present study, the field was fertilised according to local practice with 280 kg N ha^{-1} for the grassland treatments and 150 kg N ha^{-1} for the *Maize* treatment, because N mineralisation following grassland disturbance is not yet taken into account in current fertiliser recommendations and this lead to large pre-winter N_{min} contents at the end of the vegetation period. An option to increase the farmer's benefit and at the same time to reduce the amount of pre-winter N_{min} would be the adjustment of the N-input *via* fertilisation by taking the amount of available N_{min} into account. This will probably also reduce gaseous N losses *via* N_2O and N_2, as Velthof et al. (2010) showed that, N_2O emissions increased with increasing N application

rate (0 <120 < 300kg N ha^{-1} $year^{-1}$). In particular after break-up and management (i.e. cuts, N fertilisation) it was found that the investigated grassland sites were also able to convert a large part of N_2O into N_2 (Chapter 3 and 4). Although N_2 emissions are not environmentally damaging, they still represent a significant economic N loss (i.e. as plant-available N) for the farmer. Until now, exact data on N fertilisation following grassland renewal are rare, only recommendations of location adapted N fertilisation due to the Code of Good Agricultural Practice, can be found. A first attempt of a tool including an economic evaluation of grassland renewal, a nitrogen balance and a recommendation on whether to resow or not, was provided by the "Grassland Renovation Guide" of the University of Wageningen. This program calculates the costs/benefits of grassland renewal, depending on factors such as costs, present content of desirable grasses and clover, soil type, groundwater level, irrigation and N fertilisation level (Hoving, 2007). Unfortunately the "Grassland Renovation Guide" is no longer available at the listed webpage, as well as information about the application in agricultural consultation is lacking.

5.3 Determination of N_2O processes

5.3.1 Methodological aspects

As the first part of the study (Chapter 2) was used to investigate the annual N_2O budget and potential NO_3^- leaching losses, *in situ* application of two individual stable isotope approaches during selected time periods provided the opportunity for a more comprehensive understanding of N_2O production and consumption processes (Chapter 3 and 4). This was done to better understand key components of the N-cycle in order to develop mitigation strategies to prevent direct and indirect N_2O emission.

The quantification of N_2 emissions, hybrid N_2O/N_2 production and the contribution of the (N_2O/N_2+N_2O) ratio of denitrification and nitrification was possible by the application of the ^{15}N tracing approach (Chapter 3). This study gave evidence of large total denitrification losses (N_2O+N_2) from the labelled NO_3^- pool within the summer period in 2014 and following grassland conversion to maize cropping, in particular for the Histic Gleysol (up to 33% of ^{15}N labelled fertiliser applied); while total denitrification losses were much lower for the Plaggic Anthrosol. A contribution of hybrid N_2O and N_2 due to co-denitrification or anaerobic ammonium oxidation (Anammox) was excluded for the Plaggic Anthrosol, while in-homogeneous label distribution in the water-saturated Histic Gleysol led to large uncertainties in the identification of these processes (section 3.3.2). Moreover, a low precision of this

method has to be added to the discussion of advantages and disadvantages of the method, as the detection limit for N_2 concentrations was set >1.8 ppm for IRMS analysis. Heterogeneity in label distribution also complicated the determination of nitrification for the Histic Gleysol. This further promotes the difficulties and uncertainties arising from the application of the ^{15}N tracing approach, as in-homogenous pool labelling are known to result in a bias of N_2 fluxes of up to 24% (Van den Heuvel et al., 1988; Arah, 1992). A better label distribution might be achieved by increasing the number of injections of the labelled compounds and injection depths. Due to much more homogenous label distribution at the Plaggic Anthrosol, nitrification could be quantified. Results reflected a high mineralisation potential as no NH_4^+ fertiliser was used and NH_4^+ contents during the experiment were rather low. A high contribution of N_2O fluxes from other N sources than the labelled NO_3^- pool indicates the occurrence of several other N_2O production pathways, but this share was not altered by grassland break-up. In the present study, identification of other N_2O production pathways was limited, because only one N pool (i.e. NO_3^- pool) was labelled with ^{15}N. Triple isotope labelling of the different N pools (e.g. NO_2^-, NO_3^-, NH_4^+) would have been necessary to determine all N_2O production pathways, using this labelling method (Müller et al. 2014). Moreover, experimental time was limited due to possible rapid label turnover (approximately 20 days).

Using natural abundance stable isotope signatures of soil-emitted N_2O within the third part of the study (Chapter 4) improved our understanding of N_2O sources. This method allows distinguishing N_2O produced during bacterial denitrification from N_2O originating from fungal denitrification and/or nitrification. A limitation in using natural abundance stable isotope signatures of soil-emitted N_2O in comparison to the applied ^{15}N tracing approach is that the (N_2O/N_2+N_2O) ratio of denitrification cannot be measured directly. This needs to be estimated based on fractionation factors for N_2O reduction and isotopic values of N_2O produced from different pathways (heterotrophic bacterial denitrification / nitrifier denitrification and fungal denitrification / nitrification), as applied in the isotopocule mapping approach (Section 4.2.6). A quite range of range of uncertainties has to be taken into account though. With that approach, a qualitative determination of bacterial and fungal denitrification is only possible by taking fractionation and the variability of fraction factors into account. A first attempt to estimate uncertainty was done in the present study by the application of minimum, maximum and mean values during calculations. The wide range of applied values lead also to a large variability in the (N_2O/N_2+N_2O) ratio of denitrification (i.e. the residual, unreduced N_2O fraction: r_{N2O} values) and soil-emitted N_2O due to bacterial denitrification (f_B values) within different tested scenarios (section 4.3.4). However, a response of management events (i.e. grassland break-up,

cuts and N fertilisation) was clearly visible, although treatment comparisons were not possible due to unequal sample sizes. To confirm the findings of the isotopocule mapping approach, a first step of validation (i.e. with two samples) was done by a comparison of (N_2O/N_2+N_2O) ratio of denitrification measured with the ^{15}N tracing experiment with values calculated using the isotopocule mapping approach using average values of fractionation factors and isotopic endmember values (Scenario a1) (section 4.3.6). This comparison was done only for two flux measurements (two sampling events of two treatments, respectively) were conditions of soil moisture, NO_3^- availability and N_2O flux were similar in both experimental events. Results were in good agreement, indicating that the isotopocule mapping approach yields reasonable results at least under certain conditions. This first comparison at the field scale is a further step towards a more reliable source identification of N_2O processes under natural conditions. However, the limited precision of natural abundance stable isotope signatures of soil-emitted N_2O due to high atmospheric background concentrations as well as the variability of fractionation factors and isotopic endmember values are still a further challenge that needs to be solved. Anyhow, a major advantage using natural abundance stable isotope signatures of soil-emitted N_2O is the potential for its long-term application, as no label addition is required. Furthermore, the application of this method does not require application of isotope tracers and is thus feasible under standard field management operations, e.g. surface application of N fertilisation is possible. As both methods need further improvement, in particular in dealing with uncertainties the combination of natural abundance stable isotope signatures of soil-emitted N_2O with improved stable isotope tracing approaches, e.g. using triple isotope labelling would be a great chance to get reliable results for N_2O turnover processes.

5.3.2 Impact of heterogeneity at the field scale

The three studies within this thesis were conducted at the field scale in order to quantify N losses under natural conditions and display grassland renewal/conversion effects due to local practice. However, such experiments refer to various uncertainties at different scales.

At the field scale, spatial variability due to natural dynamics, microbial processes and differences in soil properties led to a high variability in N_2O and N_2 fluxes. High spatial variability could have prevented the detection of small differences between the different treatments, as variations within the specific treatments were large. For the Histic Gleysol spatial variability of fluxes probably resulted from heterogeneity in C and N contents throughout the entire field trial in combination with changing groundwater levels, thus leading to a high uncertainty in the determination of grassland break-up effects. Measured N_2O+N_2

fluxes were highly variable between the individual chambers within the same treatment, which resulted in large standard deviations of the cumulative fluxes. This might have masked also moderate treatment effects. However, no treatment effects were determined for the sandy Plaggic Anthrosol too, although soil properties (e.g. C and N content, WFPS, pH) were a lot more homogenous on this site. Even if variations of measured N_2O fluxes within the field experiments were rather high, these results were still comparable with other studies (Velthof et al., 2010; Biegemann, 2014; Krol et al., 2016).

Moreover, small-scale heterogeneity of N_2O production and consumption in soil microsites lead to spatial variability. In particular, the presence of light available SOM in combination with anoxic conditions can result in the development of denitrification "hotspots" (Parkin, 1987), which lead to high variability in natural denitrification rates. As "hotspots" of N_2O production are linked to specific environmental conditions, further research is needed to evaluate the effect of environmental drives, such as C_{org} content, O_2 availability, soil temperature, pH and N availability (NO_3^-, NO_2^-, and NH_4^+). All these parameters however, are accompanied with a variety of uncertainties. This might be challenging under field conditions, especially as environmental drivers cannot be controlled. Laboratory studies on the other hand offer a greater potential to determine specific uncertainties of an environmental driver. A combination of both approaches hence will be necessary to gather insight into the "real life processes".

Apart from spatial variability, also the known temporal variability of N_2O+N_2 fluxes might have increased uncertainty in the determination of treatment effects within the presented studies. Measurement frequencies, ranged from daily to weekly to better represent the temporal variability within the applied management practices (e.g. grassland break-up, cuts, N fertilisation). The measurement frequency of N_2O fluxes within the first part of the study (Chapter 2) was weekly in general, while the frequency was increased to every two days following grassland renewal and grassland conversion to maize cropping. During the ^{15}N tracing experiment (Chapter 3), N_2O+N_2 fluxes from the labelled NO_3^- pool were measured every two days during the first week and weekly afterwards. N_2O samples for isotopocule analysis (Chapter 4) were taken also weekly and analysed based on N_2O fluxes and with a higher frequency after grassland break-up and within the ^{15}N tracing experiment. To account for the annual N_2O budget, Flessa et al. (2002) showed that weekly measurements of N_2O fluxes complemented by additional event-related measurements can provide an accurate estimate. Nevertheless, a potential error could occur due the sampling frequency, as Rowlings

et al. (2015) found an associated error up to 34% of the sub-daily mean in humid tropical pastures due to weekly measurements.

Furthermore, the applied measurement technique (i.e. closed chamber approach) has to deal with a variety of uncertainties, which were introduced in section 1.5. Briefly, chamber fluxes are just measured over a certain number of enclosed areas, which ranged from a small area of 20 cm² for the N_2O+N_2 measurements (Chapter 3) to a larger area of 310 cm² for the N_2O measurements (Chapter 2). Therefore, it is necessary to reduce uncertainty by taking a practical number of flux measurements and the use of large chambers, which cover a representative soil area. Within the ^{15}N tracing experiment the representativeness of soil area was further limited by the size of soil columns (i.e. 15 cm diameter for the grassland plots and 30 cm for the maize plots). Labelling of larger soil columns (>30 cm diameter) would have been a great advantage, but would have been also associated with higher costs for ^{15}N label addition.

Nevertheless, diffusion barriers, structural heterogeneity, bioturbation, zones with overlapping nitrification and denitrification, temporal variations, and many more phenomena are still present in soil, (Groffman et al., 2006) so that ideal conditions for homogenous isotope mixing are hardly to be realised at the field scale.

If N_2O+N_2 fluxes are extrapolated to a farm, field or even regional scale, the upscaling under large spatial variability of N_2O sources often resulted in significant uncertainty (Velthof et al., 1996). These uncertainties could be reduced by identifying hotpots of N_2O+N_2 fluxes and determining the causes of these increased emissions (Cowan et al., 2015). Identifying areas in which N_2O fluxes are significantly increased in comparison to the majority of the experimental site, the overall uncertainty of the results might be reduced by the definition of different emission factors (Cowan et al., 2015). But even if the determined N_2O+N_2 fluxes of the three experiments conducted within the course of this thesis have to be treated with caution due to only two investigated sites with variable flux estimates, the obtained results provide a potential data basis for upscaling by the so called “bottom up” approach and are likely to be seen as a first step towards a better integration of grassland renewal in the greenhouse gas emission inventories.

5.4 Conclusions and further implications

After grassland renewal and grassland conversion to maize cropping, the effect of grassland break-up on N_2O emission only lasted for a period of two months at the two investigated sites. An impact on the annual N_2O emission budget was not obtained. This shows, that the common

concept of using fixed default values for N_2O emission factors to calculate emission inventories, which are applied irrespective of management practice might be the best approximation that could be used right now at least for some sites. Nevertheless, the effect of grassland renewal on N_2O emission is very site specific, which underlines the need of further studies on various sites and also for investigations for longer periods of time, so that diverse collected data can be used as a suitable basis for calculation of greenhouse gas inventories.

Apart from the direct N_2O emission, the contribution of indirect N_2O emission due to fertiliser NO_3^- leaching should not be neglected, as following grassland break-up large amounts of mineral N at the end of the vegetation period increased the risk of NO_3^- leaching, in particular for sandy soils like the Plaggic Anthrosol. This underlines the importance of a rapid development of a new grass/crop or either a catch crop, which could then act as a N sink. Moreover, the amount of mineral N from increased N mineralisation should be taken into account when applying N fertiliser to minimize the risk of N losses and improve N use efficiency of agricultural systems.

A first step towards a better understanding of N_2O production and consumption processes was achieved by the application of two independent stable isotope approaches at the field scale. It has been found that N_2O fluxes were mainly driven by bacterial denitrification (heterotrophic bacterial denitrification and/or nitrifier denitrification) with partial reduction of N_2O to N_2 in particular at the often water-saturated Histic Gleysol, while for the Plaggic Anthrosol a higher fraction of N_2O from nitrification was obtained. Nevertheless, various uncertainties in the determination of single processes demonstrate the further need for research on other sites under different environmental conditions, ideally with employment of isotopic methods during the entire study period.

The best option to minimize the loss of nitrogen is still the preservation of permanent grassland. For that reason, effort, consequences and use of grassland renewal should be carefully considered. To minimise the need of grassland renewal, an aim for farmers should be to rather improve and adapt grassland management, instead of trying to balance management practices favouring sward deterioration.

References

Abdalla, M., Jones, M., Smith, P., Williams, M., 2009. Nitrous oxide fluxes and denitrification sensitivity to temperature in Irish pasture soils. Soil Use and Management 25, 376-388.

Allison, F., 1955. The Enigma of Soil Nitrogen Balance Sheets, In: Norman, A.G. (Ed.), Advances in Agronomy. Academic Press, pp. 213-250.

Ammann, C., Spirig, C., Leifeld, J., Neftel, A., 2009. Assessment of the nitrogen and carbon budget of two managed temperate grassland fields. Agriculture, Ecosystems & Environment 133, 150-162.

Arah, J., 1992. New formulae for mass spectrometric analysis of nitrous oxide and dinitrogen emissions. Soil Science Society of America Journal 56, 795-800.

Arah, J., Smith, K., Crichton, I., Li, H., 1991. Nitrous oxide production and denitrification in Scottish arable soils. Journal of Soil Science 42, 351-367.

Baggs, E., 2008. A review of stable isotope techniques for N_2O source partitioning in soils: recent progress, remaining challenges and future considerations. Rapid Communications in Mass Spectrometry 22, 1664-1672.

Baggs, E., Philippot, L., 2010. Microbial terrestrial pathways to nitrous oxide, In: Smith, K. (Ed.), Nitrous Oxide and Climate Change. Earthscan Publications, London, pp. 4-35.

Baggs, E., Stevenson, M., Pihlatie, M., Regar, A., Cook, H., Cadisch, G., 2003. Nitrous oxide emissions following application of residues and fertiliser under zero and conventional tillage. Plant and Soil 254, 361-370.

Baily, A., Watson, C., Laughlin, R., Matthews, D., McGeough, K., Jordan, P., 2012. Use of the ^{15}N gas flux method to measure the source and level of N_2O and N_2 emissions from grazed grassland. Nutrient Cycling in Agroecosystems 94, 287-298.

Ball, B., Watson, C., Crichton, I., 2007. Nitrous oxide emissions, cereal growth, N recovery and soil nitrogen status after ploughing organically managed grass/clover swards. Soil Use and Management 23, 145-155.

Behrendt, U., Well, R., Giesemann, A., Ulrich, A., Augustin, J., 2015. Isotopologue signatures of nitrous oxide produced by nitrate-ammonifying bacteria isolated from soil, EGU General Assembly Conference Abstracts, p. 8017.

Benjamini, Y., Hochberg, Y., 1995. Controlling the false discovery rate: a practical and powerful approach to multiple testing. Journal of the Royal Statistical Society. Series B (Methodological), 289-300.

Benke, M., Kayser, M., 2009. Research into practice: the role of research and agricultural advisory service, In: Taube, F. (Ed.), Modelling forage production systems. Schriftenreihe des Instituts für Pflanzenbau und Pflanzenzüchtung, Christian-Albrechts-Universität zu Kiel, pp. 137–143.

Berntson, G.M., Aber, J.D., 2000. Fast nitrate immobilization in N saturated temperate forest soils. Soil Biology and Biochemistry 32, 151-156.

Biegemann, T., 2014. Grünlandumbruch und Neuansaat: kurz- und langfristige Effekte auf Treibhausgasemissionen und Ertragsleistungen von Grünlandbeständen. Dissertation. Institut für Pflanzenbau und Pflanzenzüchtung, Christian-Albrechts-Universität zu Kiel (in German).

Blackmer, A., Bremner, J., 1978. Inhibitory effect of nitrate on reduction of N_2O to N_2 by soil microorganisms. Soil Biology and Biochemistry 10, 187-191.

Boast, C., Mulvaney, R., Baveye, P., 1988. Evaluation of nitrogen-15 tracer techniques for direct measurement of denitrification in soil: I. Theory. Soil Science Society of America Journal 52, 1317-1322.

Bollag, J., Tung, G., 1972. Nitrous oxide release by soil fungi. Soil Biology and Biochemistry 4, 271-276.

Bollmann, A., Conrad, R., 1997. Acetylene blockage technique leads to underestimation of denitrification rates in oxic soils due to scavenging of intermediate nitric oxide. Soil Biology and Biochemistry 29, 1067-1077.

Bouwman, A., 1996. Direct emission of nitrous oxide from agricultural soils. Nutrient Cycling in Agroecosystems 46, 53-70.

Bouwman, A., Boumans, L., Batjes, N., 2002. Emissions of N_2O and NO from fertilized fields: Summary of available measurement data. Global Biogeochemical Cycles 16, 1058.

Braker, G., Conrad, R., 2011. Diversity, structure, and size of N_2O-producing microbial communities in soils -what matters for their functioning? Advances in Applied Microbiology Volume 75, 33-70.

Brenninkmeijer, C., Röckmann, T., 1999. Mass spectrometry of the intramolecular nitrogen isotope distribution of environmental nitrous oxide using fragment-ion analysis. Rapid Communications in Mass Spectrometry 13, 2028-2033.

Buchen, C., Benke, M., Flessa, H., Fuß, R., Gensior, A., Helfrich, M., Kayser, M., Well, R., submitted. Soil mineral N dynamics and N_2O emission following grassland renewal. Agriculture, Ecosystem & Environment.

Buchen, C., Lewicka-Szczebak, D., Fuß, R., Helfrich, M., Flessa, H., Well, R., 2016. Fluxes of N_2 and N_2O and contributing processes in summer after grassland renewal and grassland conversion to maize cropping on a Plaggic Anthrosol and a Histic Gleysol. Soil Biology and Biochemistry 101, 6-19.

Butterbach-Bahl, K., Baggs, E., Dannenmann, M., Kiese, R., Zechmeister-Boltenstern, S., 2013. Nitrous oxide emissions from soils: how well do we understand the processes and their controls? Philosophical Transactions of the Royal Society B: Biological Sciences 368, 20130122.

Casciotti, K., Sigman, D., Hastings, M., Böhlke, J., Hilkert, A., 2002. Measurement of the oxygen isotopic composition of nitrate in seawater and freshwater using the denitrifier method. Analytical Chemistry 74, 4905-4912.

Chamber of Agriculture, 2016. Grünlandbestände fit halten - Neuansaaten nur nach Bedarf. Chamber of Agriculture, Lower Saxony, Oldenburg, pp. https://www.lwk-niedersachsen.de/index.cfm/portal/pflanze/nav/278/article/29779.html (Accessed November 29713, 22016).

Cowan, N., Levy, P., Famulari, D., Anderson, M., Drewer, J., Carozzi, M., Reay, D., Skiba, U., 2016. The influence of tillage on N_2O fluxes from an intensively managed grazed grassland in Scotland. Biogeosciences 13, 4811-4821.

Cowan, N., Norman, P., Famulari, D., Levy, P., Reay, D., Skiba, U., 2015. Spatial variability and hotspots of soil N_2O fluxes from intensively grazed grassland. Biogeosciences 12, 1585-1596.

Creighton, P., Kennedy, E., Hennessy, D., O'Donovan, M., 2016. Impacts of sward renewal method with perennial ryegrass (*Lolium perenne*) on dry matter yield, tiller density and nitrate leaching. American Journal of Plant Sciences 7, 684.

Cribari-Neto, F., Zeileis, A., 2010. Beta Regression in R. Journal of Statistical Software 34, 1-24.

Čuhel, J., Šimek, M., Laughlin, R., Bru, D., Chèneby, D., Watson, C., Philippot, L., 2010. Insights into the effect of soil pH on N_2O and N_2 emissions and denitrifier community size and activity. Applied and Environmental Microbiology 76, 1870-1878.

Dail, D., Davidson, E., Chorover, J., 2001. Rapid abiotic transformation of nitrate in an acid forest soil. Biogeochemistry 54, 131-146.

Dalal, R., Wang, W., Robertson, G., Parton, W., 2003. Nitrous oxide emission from Australian agricultural lands and mitigation options: a review. Soil Research 41, 165-195.

Davidson, E., Hart, S., Shanks, C., Firestone, M., 1991. Measuring gross nitrogen mineralization, and nitrification by ^{15}N isotopic pool dilution in intact soil cores. Journal of Soil Science 42, 335-349.

Davies, M., Smith, K., Vinten, A., 2001. The mineralisation and fate of nitrogen following ploughing of grass and grass-clover swards. Biology and Fertility of Soils 33, 423-434.

Decock, C., Six, J., 2013. How reliable is the intramolecular distribution of ^{15}N in N_2O to source partition N_2O emitted from soil? Soil Biology and Biochemistry 65, 114-127.

Dendooven, L., Anderson, J., 1994. Dynamics of reduction enzymes involved in the denitrification process in pasture soil. Soil Biology and Biochemistry 26, 1501-1506.

Deppe, M., Well, R., Giesemann, A., Spott, O., Flessa, H., 2017. Soil N_2O fluxes and related processes in laboratory incubations simulating ammonium fertilizer depots. Soil Biology and Biochemistry 104, 68-80.

Deppe, M., Well, R., Kücke, M., Fuß, R., Giesemann, A., Flessa, H., 2016. Impact of CULTAN fertilization with ammonium sulfate on field emissions of nitrous oxide. Agriculture, Ecosystems & Environment 219, 138-151.

DESTATIS, 1995. Statistisches Jahrbuch 1995 für die Bundesrepublik Deutschland.

DESTATIS, 2016. Dauergrünland nach Art der Nutzung im Zeitvergleich. Statistisches Bundesamt, Wiesbaden, pp. https://www.destatis.de/DE/ZahlenFakten/Wirtschaftsbereiche/LandForstwirtschaftFischerei/FeldfruechteGruenland/Tabellen/ZeitreiheDauergruenlandNachNutzung.html (Accessed September 22, 2016).

DIN ISO 11277, 2002. Soil quality - determination of particle size distribution in mineral soil material - method by sieving and sedimentation. DIN Deutsches Institut für Normung eV, Beuth (in German).

Djurhuus, J., Olsen, P., 1997. Nitrate leaching after cut grass/clover leys as affected by time of ploughing. Soil Use and Management 13, 61-67.

Dobbie, K., Smith, K., 2003. Nitrous oxide emission factors for agricultural soils in Great Britain: the impact of soil water-filled pore space and other controlling variables. Global Change Biology 9, 204-218.

Drewer, J., Anderson, M., Levy, P.E., Scholtes, B., Helfter, C., Parker, J., Rees, R., Skiba, U., 2016. The impact of ploughing intensively managed temperate grasslands on N_2O, CH_4 and CO_2 fluxes. Plant and Soil, 1-16.

Eickenscheidt, T., Heinichen, J., Augustin, J., Freibauer, A., Drösler, M., 2014. Nitrogen mineralization and gaseous nitrogen losses from waterlogged and drained organic soils in a black alder (*Alnus glutinosa* (L.) Gaertn.) forest. Biogeosciences 11, 2961-2976.

European Parliament and Council, 2013. Regulation (EU) No 1307/2013 of the European Parliament and of the Council of 17 December 2013 establishing Rules for Direct Payments to Farmers under Support Schemes within the Framework of the Common Agricultural Policy and Repealing Council Regulation (EC) No 637/2008 and Council Regulation (EC) No 73/2009. Official Journal of the European Communities L347, 608-670.

EUROSTAT, 2013. Land cover and land use, landscape (LUCAS) database EUROSTAT, the statistical office of the European Union, Luxembourg, pp. http://ec.europa.eu/eurostat/web/lucas/data/database (Accessed November 18, 2015).

Felber, R., Conen, F., Flechard, C., Neftel, A., 2012. Theoretical and practical limitations of the acetylene inhibition technique to determine total denitrification losses. Biogeosciences 9, 4125-4138.

Firestone, M., Firestone, R., Tiedje, J., 1980. Nitrous oxide from soil denitrification: factors controlling its biological production. American Association for the Advancement of Science 208, 749-751.

Flechard, C., Ambus, P., Skiba, U., Rees, R., Hensen, A., van Amstel, A., Dasselaar, A., Soussana, J., Jones, M., Clifton-Brown, J., Raschi, A., Horvath, L., Neftel, A., Jocher, M., Ammann, C., Leifeld, J., Fuhrer, J., Calanca, P., Thalman, E., Pilegaard, K., Di Marco, C., Campbell, C., Nemitz, E., Hargreaves, K., Levy, P., Ball, B.C., Jones, S., van de Bulk, W., Groot, T., Blom, M., Domingues, R., Kasper, G., Allard, V., Ceschia, E., Cellier, P., Laville, P., Henault, C., Bizouard, F., Abdalla, M., Williams, M., Baronti, S., Berretti, F., Grosz, B., 2007. Effects of climate and management intensity on nitrous oxide emissions in grassland systems across Europe. Agriculture, Ecosystems & Environment 121, 135-152.

Flessa, H., Pfau, W., Dörsch, P., Beese, F., 1996. The influence of nitrate and ammonium fertilization on N_2O release and CH_4 uptake of a well-drained topsoil demonstrated by a soil microcosm experiment. Zeitschrift für Pflanzenernährung und Bodenkunde 159, 499-503.

Flessa, H., Ruser, R., Schilling, R., Loftfield, N., Munch, J., Kaiser, E., Beese, F., 2002. N_2O and CH_4 fluxes in potato fields: automated measurement, management effects and temporal variation. Geoderma 105, 307-325.

Folorunso, O., Rolston, D., 1984. Spatial variability of field-measured denitrification gas fluxes. Soil Science Society of America Journal 48, 1214-1219.

Frame, C., Casciotti, K., 2010. Biogeochemical controls and isotopic signatures of nitrous oxide production by a marine ammonia-oxidizing bacterium. Biogeosciences 7, 2695-2709.

Francis, G., 1995. Management practices for minimising nitrate leaching after ploughing temporary leguminous pastures in Canterbury, New Zealand. Journal of Contaminant Hydrology 20, 313-327.

Francis, G., Haynes, R., Sparling, G., Ross, D., Williams, P., 1992. Nitrogen mineralization, nitrate leaching and crop growth following cultivation of a temporary leguminous pasture in autumn and winter. Nutrient Cycling in Agroecosystems 33, 59-70.

Francis, G., Haynes, R., Williams, P., 1995. Effects of the timing of ploughing in temporary leguminous pastures and two winter cover crops on nitrogen mineralization, nitrate leaching and spring wheat growth. Journal of Agricultural Science 124, 1-9.

Fry, B., 2006. Stable isotope ecology. Springer Science & Business Media, LLC, New York, NY, USA.

Fuß, R., 2015. R-package: *gasfluxes*, pp. https://bitbucket.org/ecoRoland/gasfluxes (Accessed December 30, 2015).

GfE, 2008. New Equations for Predicting Metabolisable Energy of Grass and Maize Products for Ruminants. Proceedings of the Society of Nutrition Physiology 17, 191-198.

Giani, L., Makowsky, L., Mueller, K., 2014. Plaggic Anthrosol: Soil of the Year 2013 in Germany: An overview on its formation, distribution, classification, soil function and threats. Journal of Plant Nutrition and Soil Science 177, 320-329.

Goodroad, L., Keeney, D., 1984. Nitrous oxide production in aerobic soils under varying pH, temperature and water content. Soil Biology and Biochemistry 16, 39-43.

Grandy, A., Robertson, G., 2006. Initial cultivation of a temperate-region soil immediately accelerates aggregate turnover and CO_2 and N_2O fluxes. Global Change Biology 12, 1507-1520.

Groffman, P., Altabet, M., Böhlke, J., Butterbach-Bahl, K., David, M., Firestone, M., Giblin, A., Kana, T., Nielsen, L., Voytek, M., 2006. Methods for measuring denitrification: diverse approaches to a difficult problem. Ecological Applications 16, 2091-2122.

Guo, J., Peng, Y., Wang, S., Ma, B., Ge, S., Wang, Z., Huang, H., Zhang, J., Zhang, L., 2013. Pathways and organisms involved in ammonia oxidation and nitrous oxide emission. Critical Reviews in Environmental Science and Technology 43, 2213-2296.

Hansen, E., Eriksen, J., 2016. Nitrate leaching in maize after cultivation of differently managed grass-clover leys on coarse sand in Denmark. Agriculture, Ecosystems & Environment 216, 309-313.

Hassink, J., 1994. Effects of soil texture and grassland management on soil organic C and N and rates of C and N mineralization. Soil Biology and Biochemistry 26, 1221-1231.

Hauck, R., Melsted, S., 1956. Some aspects of the problem of evaluating denitrification in soils. Soil Science Society of America Journal 20, 361-364.

Hauck, R., Melsted, S., Yankwich, P., 1958. Use of N-isotope distribution in nitrogen gas in the study of denitrification. Soil Science 86, 287.

Healy, R., Striegl, R., Russell, T., Hutchinson, G., Livingston, G., 1996. Numerical evaluation of static-chamber measurements of soil - atmosphere gas exchange: identification of physical processes. Soil Science Society of America Journal 60, 740-747.

Heil, J., Wolf, B., Brüggemann, N., Emmenegger, L., Tuzson, B., Vereecken, H., Mohn, J., 2014. Site-specific ^{15}N isotopic signatures of abiotically produced N_2O. Geochimica et Cosmochimica Acta 139, 72-82.

Herbst, F., Bufe, J., GARZ, J., Hagemann, O., 1982. Simple methods for assessing nitrate loss from winter leaching. Archiv für Acker und Pflanzenbau - Archives of Agronomy and Soil Science 26, 665-672.

Hofstra, N., Bouwman, A., 2005. Denitrification in agricultural soils: summarizing published data and estimating global annual rates. Nutrient Cycling in Agroecosystems 72, 267-278.

Höper, H., 2002. Carbon and nitrogen mineralisation rates of fens in Germany used for agriculture. A review, Wetlands in Central Europe. Springer, pp. 149-164.

Hopkins, A., Murray, P., Bowling, P., Rook, A., Johnson, J., 1995. Productivity and nitrogen uptake of ageing and newly sown swards of perennial ryegrass (*Lolium perenne* L.) at different sites and with different nitrogen fertilizer treatments. European Journal of Agronomy 4, 65-75.

Hoving, I., 2007. Economy of grassland renovation: a model approach, In: Taube, F., Conijn, J. (Eds.), Grassland resowing and grass-arable crop rotations.Third and fourth workshop of the EGF working group., Wageningen Plant Research International, pp. 73-76.

Huber, P., Ronchetti, E., 1981. Robust Statistics. Wiley Series in Probability and Mathematical Statistics. New York, NY, USA: Wiley-IEEE 52, 54.

Hutchinson, G., Mosier, A., 1981. Improved soil cover method for field measurement of nitrous oxide fluxes. Soil Science Society of America Journal 45, 311-316.

IPCC, 2006. IPCC Guidelines for National Greenhouse Gas Inventories. Prepared by the National Greenhouse Gas Inventories Programme, Eggleston HS., Buendia L., Miwa K., Ngara T. and Tanabe K., IGES, Japan.

IPCC, 2007. Climate Change 2007: The Physical Science Basis. , In: Solomon, S., Qin, D., Manning, M., Chen, Z., Marquis, Averyt, M., Tignor, M., Miller, H. (Eds.), Contribution of Working Group I to the Fourth Assessment Report of the Intergovernmental Panel on Climate Change, Cambridge University Press, Cambridge, United Kingdom and New York, NY, USA.

IPCC, 2013. Climate Change 2013: The Physical Science Basis. , In: Stocker, T., Qin, D., Plattner, K., Tignor, M., Allen, S., Boschung, J., Nauels, A., Xia, Y., Bex, V., Midgley, P. (Eds.), Contribution of Working Group I to the Fifth Assessment Report of the Intergovernmental Panel on Climate Change, Cambridge University Press, Cambridge, United Kingdom and New York, NY, USA.

IPCC, 2014. 2013 Revised Supplementary Methods and Good Practice Guidance Arising from the Kyoto Protocol. Hiraishi, T., Krug, T., Tanabe, K., Srivastava, N., Baasansuren, J., Fukuda, M. and Troxler, TG., IPCC, Switzerland.

IUSS Working Group, 2006. WRB, 2006. World reference base for soil resources FAO, Rome, Italy.

Jarvis, S., Stockdale, E., Shepherd, M., Powlson, D., 1996. Nitrogen mineralization in temperate agricultural soils: processes and measurement, In: Donald, L.S. (Ed.), Advances in Agronomy. Academic Press, pp. 187-235.

Jinuntuya-Nortman, M., Sutka, L., Ostrom, P., Gandhi, H., Ostrom, N., 2008. Isotopologue fractionation during microbial reduction of N_2O within soil mesocosms as a function of water-filled pore space. Soil Biology and Biochemistry 40, 2273-2280.

Johnston, A., McEwen, J., Lane, P., Hewitt, M., Poulton, P., Yeoman, D., 1994. Effects of one to six year old ryegrass-clover leys soil nitrogen and on the subsequent yields and fertilizer nitrogen requirements of the arable sequence winter wheat, potatoes, winter wheat, winter beans (*Vicia faba*) grown on a sandy loam soil. Journal of Agricultural Science 122, 73-89.

Jones, S., Rees, R., Skiba, U., Ball, B., 2005. Greenhouse gas emissions from a managed grassland. Global and Planetary Change 47, 201-211.

Jørgensen, C., Struwe, S., Elberling, B., 2012. Temporal trends in N_2O flux dynamics in a Danish wetland – effects of plant-mediated gas transport of N_2O and O_2 following changes in water level and soil mineral-N availability. Global Change Biology 18, 210-222.

Kammann, C., Grünhage, L., Müller, C., Jacobi, S., Jäger, H., 1998. Seasonal variability and mitigation options for N_2O emissions from differently managed grasslands. Environmental Pollution 102, 179-186.

Karman, A., Van Boeckl, M., 1986. Evaluation of the Kjeldahl factor for conversion of nitrogen content of milk and milk products to protein content. Netherlands Milk and Dairy Journal 40, 315-336.

Kato, T., Toyoda, S., Yoshida, N., Tang, Y., Wada, E., 2013. Isotopomer and isotopologue signatures of N_2O produced in alpine ecosystems on the Qinghai–Tibetan Plateau. Rapid Communications in Mass Spectrometry 27, 1517-1526.

Kayser, M., Benke, M., Isselstein, J., 2011. Little fertilizer response but high N loss risk of maize on a productive organic-sandy soil. Agronomy for Sustainable Development 31, 709-718.

Kayser, M., Breitsameter, L., Benke, M., Isselstein, J., 2015. Nitrate leaching is not controlled by the slurry application technique in productive grassland on organic–sandy soil. Agronomy for Sustainable Development 35, 213-223.

Kayser, M., Seidel, K., Müller, J., Isselstein, J., 2008. The effect of succeeding crop and level of N fertilization on N leaching after break-up of grassland. European Journal of Agronomy 29, 200-207.

Keeney, D., Fillery, I., Marx, G., 1979. Effect of temperature on the gaseous nitrogen products of denitrification in a silt loam soil. Soil Science Society of America Journal 43, 1124-1128.

Kim, S., 2015. R-package *ppcor*: An R Package for a Fast Calculation to Semi-partial Correlation Coefficients. Communications for Statistical Applications and Methods 22, 665-674.

Kirkham, D., Bartholomew, W., 1954. Equations for following nutrient transformations in soil, utilizing tracer data: I. Soil Science Society of America Journal 18, 33-34.

Knowles, R., 1982. Denitrification. Microbiological Reviews 46, 43-70.

Koba, K., Osaka, K., Tobari, Y., Toyoda, S., Ohte, N., Katsuyama, M., Suzuki, N., Itoh, M., Yamagishi, H., Kawasaki, M., Kim, S., Yoshida, N., Nakajima, T., 2009. Biogeochemistry of nitrous oxide in groundwater in a forested ecosystem elucidated by nitrous oxide isotopomer measurements. Geochimica et Cosmochimica Acta 73, 3115-3133.

Köhler, K., Duynisveld, W., Böttcher, J., 2006. Nitrogen fertilization and nitrate leaching into groundwater on arable sandy soils. Journal of Plant Nutrition and Soil Science 169, 185-195.

Kool, D., Dolfing, J., Wrage, N., Van Groenigen, J., 2011. Nitrifier denitrification as a distinct and significant source of nitrous oxide from soil. Soil Biology and Biochemistry 43, 174-178.

Köster, J., Well, R., Dittert, K., Giesemann, A., Lewicka-Szczebak, D., Mühling, K., Herrmann, A., Lammel, J., Senbayram, M., 2013a. Soil denitrification potential and its influence on N_2O reduction and N_2O isotopomer ratios. Rapid Communications in Mass Spectrometry 27, 2363-2373.

Köster, J., Well, R., Tuzson, B., Bol, R., Dittert, K., Giesemann, A., Emmenegger, L., Manninen, A., Cárdenas, L., Mohn, J., 2013b. Novel laser spectroscopic technique for continuous analysis of N_2O isotopomers–application and intercomparison with isotope ratio mass spectrometry. Rapid Communications in Mass Spectrometry 27, 216-222.

Krol, D., Jones, M., Williams, M., Richards, K., Bourdin, F., Lanigan, G., 2016. The effect of renovation of long-term temperate grassland on N_2O emissions and N leaching from contrasting soils. Science of the Total Environment 560–561, 233-240.

Küstermann, B., Munch, J., Hülsbergen, K.-J., 2013. Effects of soil tillage and fertilization on resource efficiency and greenhouse gas emissions in a long-term field experiment in Southern Germany. European Journal of Agronomy 49, 61-73.

Laughlin, R., Stevens, R., 2002. Evidence for fungal dominance of denitrification and codenitrification in a grassland soil. Soil Science Society of America Journal 66, 1540-1548.

Laughlin, R., Stevens, R., Müller, C., Watson, C., 2008. Evidence that fungi can oxidize NH_4^+ to NO_3^- in a grassland soil. European Journal of Soil Science 59, 285-291.

Leiber-Sauheitl, K., Fuß, R., Voigt, C., Freibauer, A., 2014. High CO_2 fluxes from grassland on histic Gleysol along soil carbon and drainage gradients. Biogeosciences 11, 749-761.

Lewicka-Szczebak, D., Augustin, J., Giesemann, A., Well, R., 2017. Quantifying N_2O reduction to N_2 based on N_2O isotopocules – validation with independent methods (helium incubation and ^{15}N gas flux method). Biogeosciences 14, 711-732.

Lewicka-Szczebak, D., Dyckmans, J., Kaiser, J., Marca, A., Augustin, J., Well, R., 2016. Oxygen isotope fractionation during N_2O production by soil denitrification. Biogeosciences 13, 1129-1144.

Lewicka-Szczebak, D., Well, R., Bol, R., Gregory, A., Matthews, G., Misselbrook, T., Whalley, W., Cardenas, L., 2015. Isotope fractionation factors controlling isotopocule signatures of soil-emitted N_2O produced by denitrification processes of various rates. Rapid Communications in Mass Spectrometry 29, 269-282.

Lewicka-Szczebak, D., Well, R., Köster, J., Fuß, R., Senbayram, M., Dittert, K., Flessa, H., 2014. Experimental determinations of isotopic fractionation factors associated with N_2O production and reduction during denitrification in soils. Geochimica et Cosmochimica Acta 134, 55-73.

Lewicka-Szczebak, D., Well, R., Giesemann, A., Rohe, L., Wolf, U., 2013. An enhanced technique for automated determination of ^{15}N signatures of N_2,(N_2+N_2O) and N_2O in gas samples. Rapid Communications in Mass Spectrometry 27, 1548-1558.

Lloyd, A., 1992. Nitrate leaching under arable land ploughed out from grass, Proceedings, the Fertiliser Society No. 330.

Loftfield, N., Flessa, H., Augustin, J., Beese, F., 1997. Automated gas chromatographic system for rapid analysis of the atmospheric trace gases methane, carbon dioxide, and nitrous oxide. Journal of Environmental Quality 26, 560-564.

Long, A., Heitman, J., Tobias, C., Philips, R., Song, B., 2013. Co-occurring anammox, denitrification, and codenitrification in agricultural soils. Applied and Environmental Microbiology 79, 168-176.

Luo, J., Tillman, R., Ball, P., 1999. Factors regulating denitrification in a soil under pasture. Soil Biology and Biochemistry 31, 913-927.

MacDonald, J., Angers, D., Rochette, P., Chantigny, M., Royer, I., Gasser, M., 2010. Plowing a poorly drained grassland reduced soil respiration. Soil Science Society of America Journal 74, 2067-2076.

MacDonald, J., Rochette, P., Chantigny, M., Angers, D., Royer, I., Gasser, M., 2011. Ploughing a poorly drained grassland reduced N_2O emissions compared to chemical fallow. Soil and Tillage Research 111, 123-132.

Maeda, K., Spor, A., Edel-Hermann, V., Heraud, C., Breuil, M.-C., Bizouard, F., Toyoda, S., Yoshida, N., Steinberg, C., Philippot, L., 2015. N_2O production, a widespread trait in fungi. Scientific Reports 5.

Mahmood, T., Malik, K., Shamsi, S., Sajjad, M., 1998. Denitrification and total N losses from an irrigated sandy-clay loam under maize–wheat cropping system. Plant and Soil 199, 239-250.

Mathieu, O., Lévêque, J., Hénault, C., Milloux, M., Bizouard, F., Andreux, F., 2006. Emissions and spatial variability of N_2O, N_2 and nitrous oxide mole fraction at the field scale, revealed with ^{15}N isotopic techniques. Soil Biology and Biochemistry 38, 941-951.

McLenaghen, R., Cameron, K., Lampkin, N., Daly, M., Deo, B., 1996. Nitrate leaching from ploughed pasture and the effectiveness of winter catch crops in reducing leaching losses. New Zealand Journal of Agricultural Research 39, 413-420.

Meisinger, J., Calderon, F., Jenkinson, D., 2008. Soil nitrogen budgets. Nitrogen in agricultural systems, 505-562.

Merbold, L., Eugster, W., Stieger, J., Zahniser, M., Nelson, D., Buchmann, N., 2014. Greenhouse gas budget (CO_2, CH_4 and N_2O) of intensively managed grassland following restoration. Global Change Biology 20, 1913-1928.

Moldrup, P., Olesen, T., Schjønning, P., Yamaguchi, T., Rolston, D., 2000. Predicting the gas diffusion coefficient in undisturbed soil from soil water characteristics. Soil Science Society of America Journal 64, 94-100.

Mori, A., Hojito, M., 2007. Grassland renovation increases N_2O emission from a volcanic grassland soil in Nasu, Japan. Soil Science and Plant Nutrition 53, 812-818.

Müller, C., Clough, T., 2014. Advances in understanding nitrogen flows and transformations: gaps and research pathways. Journal of Agricultural Science 152, 34-44.

Müller, C., Kammann, C., Ottow, J., Jäger, H., 2003. Nitrous oxide emission from frozen grassland soil and during thawing periods. Journal of Plant Nutrition and Soil Science 166, 46-53.

Müller, C., Laughlin, R., Spott, O., Rütting, T., 2014. Quantification of N_2O emission pathways via a ^{15}N tracing model. Soil Biology and Biochemistry 72, 44-54.

Mulvaney, R., 1984. Determination of ^{15}N-labeled dinitrogen and nitrous oxide with triple-collector mass spectrometers. Soil Science Society of America Journal 48, 690-692.

Myrold, D.D., Tiedje, J.M., 1985. Diffusional constraints on denitrification in soil. Soil Science Society of America Journal 49, 651-657.

Nadeem, S., Dörsch, P., Bakken, L., 2013a. Autoxidation and acetylene-accelerated oxidation of NO in a 2-phase system: implications for the expression of denitrification in ex situ experiments. Soil Biology and Biochemistry 57, 606-614.

Nadeem, S., Dörsch, P., Bakken, L., 2013b. The significance of early accumulation of nanomolar concentrations of NO as an inducer of denitrification. FEMS Microbiology Ecology 83, 672-684.

Necpalova, M., Casey, I., Humphreys, J., 2013. Effect of ploughing and reseeding of permanent grassland on soil N, N leaching and nitrous oxide emissions from a clay-loam soil. Nutrient Cycling in Agroecosystems 95, 305-317.

Nitsch, H., Osterburg, B., Roggendorf, W., Laggner, B., 2012. Cross compliance and the protection of grassland–illustrative analyses of land use transitions between permanent grassland and arable land in German regions. Land Use Policy 29, 440-448.

Oenema, O., Kros, H., de Vries, W., 2003. Approaches and uncertainties in nutrient budgets: implications for nutrient management and environmental policies. European Journal of Agronomy 20, 3-16.

Opdyke, M., Ostrom, N., Ostrom, P., 2009. Evidence for the predominance of denitrification as a source of N_2O in temperate agricultural soils based on isotopologue measurements. Global Biogeochemical Cycles 23.

Osterburg, B., Laggner, B., Nitsch, H., Roggendorf, W., Röder, N., Pötsch, E., Krautzer, B., Hopkins, A., 2011. Analysis of grassland conversion into arable land in Northwest Germany, Grassland Farming and Land Management Systems in Mountainous Regions. Proceedings of the 16th Symposium of the European Grassland Federation, Gumpenstein, Austria, 29th-31st August, 2011. Agricultural Research and Education Center (AREC) Raumberg-Gumpenstein, pp. 350-352.

Osterburg, B., Nitsch, H., Laggner, B., Roggendorf, W., 2010. Auswertung von Daten des Integrierten Verwaltungs- und Kontrollsystems zur Abschätzung von Wirkungen der EU-Agrarreform auf Umwelt und Landschaft. Arbeitsberichte aus der vTI-Agrarökonomie 07, 1-95 (in German).

Ostrom, N., Ostrom, P., 2011. The isotopomers of nitrous oxide: analytical considerations and application to resolution of microbial production pathways, Handbook of Environmental Isotope Geochemistry. Springer, pp. 453-476.

Ostrom, N., Pitt, A., Sutka, R., Ostrom, P., Grandy, A., Huizinga, K., Robertson, G., 2007. Isotopologue effects during N_2O reduction in soils and in pure cultures of denitrifiers. Journal of Geophysical Research 112, G02005.

Ostrom, N., Sutka, R., Ostrom, P., Grandy, A., Huizinga, K., Gandhi, H., von Fischer, J., Robertson, G., 2010. Isotopologue data reveal bacterial denitrification as the primary source of N_2O during a high flux event following cultivation of a native temperate grassland. Soil Biology and Biochemistry 42, 499-506.

Papen, H., Von Berg, R., Hinkel, I., Thoene, B., Rennenberg, H., 1989. Heterotrophic nitrification by *Alcaligenes faecalis*: NO_2^-, NO_3^-, N_2O, and NO production in exponentially growing cultures. Applied and Environmental Microbiology 55, 2068-2072.

Park, S., Pérez, T., Boering, K., Trumbore, S.E., Gil, J., Marquina, S., Tyler, S., 2011. Can N_2O stable isotopes and isotopomers be useful tools to characterize sources and microbial pathways of N_2O production and consumption in tropical soils? Global Biogeochemical Cycles 25.

Parkin, T., 1987. Soil microsites as a source of denitrification variability. Soil Science Society of America Journal 51, 1194-1199.

Pedersen, A., 2015. R-package *HMR*: *Flux Estimation with Static Chamber Data*, R package version 0.4.1. http://CRAN.R-project.org/package=HMR.

Pedersen, A., Petersen, S., Schelde, K., 2010. A comprehensive approach to soil-atmosphere trace-gas flux estimation with static chambers. European Journal of Soil Science 61, 888-902.

Philippot, L., Hallin, S., Schloter, M., 2007. Ecology of denitrifying prokaryotes in agricultural soil. Advances in Agronomy 96, 249-305.

Pinheiro, J., Bates, D., 2000. Mixed-effects models in S and S-PLUS. Springer, New York.

Pinto, M., Merino, P., Del Prado, A., Estavillo, J., Yamulki, S., Gebauer, G., Piertzak, S., Lauf, J., Oenema, O., 2004. Increased emissions of nitric oxide and nitrous oxide following tillage of a perennial pasture. Nutrient Cycling in Agroecosystems 70, 13-22.

Poeplau, C., Don, A., Vesterdal, L., Leifeld, J., Van Wesemael, B., Schumacher, J., Gensior, A., 2011. Temporal dynamics of soil organic carbon after land-use change in the temperate zone–carbon response functions as a model approach. Global Change Biology 17, 2415-2427.

R Development Core Team, 2016. A language and environment for statistical computing. Version: 3.3.1. R Foundation for Statistical Computing, Vienna, Austria.

Ravishankara, A., Daniel, J., Portmann, R., 2009. Nitrous oxide (N_2O): the dominant ozone-depleting substance emitted in the 21st century. Science 326, 123-125.

Rees, R., Augustin, J., Alberti, G., Ball, B., Boeckx, P., Cantarel, A., Castaldi, S., Chirinda, N., Chojnicki, B., Giebels, M., Gordon, H., Grosz, B., Horvath, L., Juszczak, R., Kasimir Klemedtsson, A., Klemedtsson, L., Medinets, S., Machon, A., Mapanda, F., Nyamangara, J., Olesen, J., Reay, D., Sanchez, L., Sanz Cobena, A., Smith, K., Sowerby, A., Sommer, M., Soussana, J., Stenberg, M., Topp, C., van Cleemput, O., Vallejo, A., Watson, C., Wuta, M., 2013. Nitrous oxide emissions from European agriculture: an analysis of variability and drivers of emissions from field experiments. Biogeosciences 10, 2671-2682.

Reheul, D., Vliegher, A., Bommelé, L., Carlier, L., 2007. The comparison between temporary and permanent grassland, Permanent and Temporary Grassland: Plant, Environment and Economy. Proceedings of the 14th Symposium of the European Grassland Federation, Ghent, Belgium, 3-5 September 2007. Belgian Society for Grassland and Forage Crops, pp. 1-13.

Röckmann, T., Kaiser, J., Brenninkmeijer, C., Brand, W., 2003. Gas chromatography/isotope-ratio mass spectrometry method for high-precision position-dependent ^{15}N and ^{18}O measurements of atmospheric nitrous oxide. Rapid Communications in Mass Spectrometry 17, 1897-1908.

Rohe, L., Anderson, T., Braker, G., Flessa, H., Giesemann, A., Lewicka-Szczebak, D., Wrage-Mönnig, N., Well, R., 2014. Dual isotope and isotopomer signatures of nitrous oxide from fungal denitrification–a pure culture study. Rapid Communications in Mass Spectrometry 28, 1893-1903.

Rolston, D., Fried, M., Goldhamer, D., 1976. Denitrification measured directly from nitrogen and nitrous oxide gas fluxes. Soil Science Society of America Journal 40, 259-266.

Rolston, D., Hoffman, D., Toy, D., 1978. Field Measurement of Denitrification: I. Flux of N_2 and N_2O. Soil Science Society of America Journal 42, 863-869.

Rolston, D., Sharpley, A., Toy, D., Broadbent, F., 1982. Field measurement of denitrification: III. Rates during irrigation cycles. Soil Science Society of America Journal 46, 289-296.

Rösemann, C., Haenel, H., Dämmgen, U., Freibauer, A., Wulf, S., Eurich-Menden, B., Döhler, H., Schreiner, C., Bauer, B., Osterburg, B., 2015. Calculations of gaseous and particulate emissions from German agriculture 1990-2013: Report on methods and data (RMD) Submission 2015.

Roth, K., 2006. Bodenkartierung und GIS-basierte Kohlenstoffinventur von Graslandböden: Untersuchungen an den ETH-Forschungsstationen Chamau und Früebüel (ZG, Schweiz). Geographisches Institut der Universität Zürich (in German).

Rowlings, D., Grace, P., Scheer, C., Liu, S., 2015. Rainfall variability drives interannual variation in N_2O emissions from a humid, subtropical pasture. Science of the Total Environment 512, 8-18.

Rückauf, U., Augustin, J., Russow, R., Merbach, W., 2004. Nitrate removal from drained and reflooded fen soils affected by soil N transformation processes and plant uptake. Soil Biology and Biochemistry 36, 77-90.

Rütting, T., Boeckx, P., Müller, C., Klemedtsson, L., 2011. Assessment of the importance of dissimilatory nitrate reduction to ammonium for the terrestrial nitrogen cycle. Biogeosciences 8, 1779-1791.

Ryden, J., Skinner, J., Nixon, D., 1987. Soil core incubation system for the field measurement of denitrification using acetylene-inhibition. Soil Biology and Biochemistry 19, 753-757.

Saggar, S., Jha, N., Deslippe, J., Bolan, N., Luo, J., Giltrap, D., Kim, D., Zaman, M., Tillman, R., 2013. Denitrification and N_2O:N_2 production in temperate grasslands: Processes, measurements, modelling and mitigating negative impacts. Science of the Total Environment 465, 173-195.

Schaufler, G., Kitzler, B., Schindlbacher, A., Skiba, U., Sutton, M., Zechmeister-Boltenstern, S., 2010. Greenhouse gas emissions from European soils under different land use: effects of soil moisture and temperature. European Journal of Soil Science 61, 683-696.

Schmeer, M., 2012. Der Einfluss von Bodenverdichtung sowie Grünlanderneuerung auf Stickstoffemissionen und Ertragsleistungen von Futterbausystemen. Dissertation. Institut für Pflanzenbau und Pflanzenzüchtung, Christian-Albrechts-Universität zu Kiel (in German).

Scholefield, D., Tyson, K., Garwood, E., Armstrong, A., Hawkins, J., Stone, A., 1993. Nitrate leaching from grazed grassland lysimeters: effects of fertilizer input, field drainage, age of sward and patterns of weather. Journal of Soil Science 44, 601-613.

Seidel, K., Kayser, M., Müller, J., Isselstein, J., 2009. The effect of grassland renovation on soil mineral nitrogen and on nitrate leaching during winter. Journal of Plant Nutrition and Soil Science 172, 512-519.

Seidel, K., Müller, J., Kayser, M., Isselstein, J., 2007. The effect of fertilizer type and level of N fertilization before and after grassland renewal on N leaching losses. Journal of Agronomy and Crop Science 193, 30-36.

Seitzinger, S., Harrison, J.A., Böhlke, J., Bouwman, A., Lowrance, R., Peterson, B., Tobias, C., Drecht, G.V., 2006. Denitrification across landscapes and waterscapes: a synthesis. Ecological Applications 16, 2064-2090.

Selbie, D., Lanigan, G., Laughlin, R., Di, H., Moir, J., Cameron, K., Clough, T., Watson, C., Grant, J., Somers, C., Richards, K., 2015. Confirmation of co-denitrification in grazed grassland. Scientific Reports 5, 17361.

Senbayram, M., Chen, R., Budai, A., Bakken, L., Dittert, K., 2012. N_2O emission and the $N_2O/(N_2O:N_2)$ product ratio of denitrification as controlled by available carbon substrates and nitrate concentrations. Agriculture, Ecosystems & Environment 147, 4-12.

Sgouridis, F., Heppell, C., Wharton, G., Lansdown, K., Trimmer, M., 2011. Denitrification and dissimilatory nitrate reduction to ammonium (DNRA) in a temperate re-connected floodplain. Water Research 45, 4909-4922.

Sgouridis, F., Ullah, S., 2015. The relative magnitude and controls of in situ N_2 and N_2O fluxes due to denitrification in natural and semi-natural terrestrial ecosystems using ^{15}N tracers. Environmental Science & Technology 49, 14110-14119.

Shepherd, M., Hatch, D., Jarvis, S., Bhogal, A., 2001. Nitrate leaching from reseeded pasture. Soil Use and Management 17, 97-105.

Sigman, D., Casciotti, K., Andreani, M., Barford, C., Galanter, M., Böhlke, J., 2001. A bacterial method for the nitrogen isotopic analysis of nitrate in seawater and freshwater. Analytical Chemistry 73, 4145-4153.

Smit, A., Velthof, G., 2010. Comparison of indices for the prediction of nitrogen mineralization after destruction of managed grassland. Plant and Soil 331, 139-150.

Smith, K., Thomson, P., Clayton, H., McTaggart, I., Conen, F., 1998. Effects of temperature, water content and nitrogen fertilisation on emissions of nitrous oxide by soils. Atmospheric Environment 32, 3301-3309.

Smith, K.A., Arah, J., 1990. Losses of nitrogen by denitrification and emissions of nitrogen oxides from soils, Proceedings-Fertiliser Society No. 299.

Soussana, J., Allard, V., Pilegaard, K., Ambus, P., Amman, C., Campbell, C., Ceschia, E., Clifton-Brown, J., Czobel, S., Domingues, R., Flechard, C., Fuhrer, J., Hensen, A., Horvath, L., Jones, M., Kasper, G., Martin, C., Nagy, Z., Neftel, A., Raschi, A., Baronti, S., Rees, R., Skiba, U., Stefani, P., Manca, G., Sutton, M., Tuba, Z., Valentini, R., 2007. Full accounting of the greenhouse gas (CO_2, N_2O, CH_4) budget of nine European grassland sites. Agriculture, Ecosystems & Environment 121, 121-134.

Spott, O., Russow, R., Apelt, B., Stange, C., 2006. A ^{15}N-aided artificial atmosphere gas flow technique for online determination of soil N_2 release using the zeolite Köstrolith SX6®. Rapid Communications in Mass Spectrometry 20, 3267-3274.

Spott, O., Stange, C., 2007. A new mathematical approach for calculating the contribution of anammox, denitrification and atmosphere to an N_2 mixture based on a ^{15}N tracer technique. Rapid Communications in Mass Spectrometry 21, 2398-2406.

Spott, O., Stange, C., 2011. Formation of hybrid N_2O in a suspended soil due to co-denitrification of NH_2OH. Journal of Plant Nutrition and Soil Science 174, 554-567.

Stange, C., Spott, O., Müller, C., 2009. An inverse abundance approach to separate soil nitrogen pools and gaseous nitrogen fluxes into fractions related to ammonium, nitrate and soil organic nitrogen. European Journal of Soil Science 60, 907-915.

Stange, C., Spott, O., Russow, R., 2013. Analysis of the coexisting pathways for NO and N_2O formation in Chernozem using the ^{15}N-tracer SimKIM-Advanced model. Isotopes in Environmental and Health Studies 49, 503-519.

Stange, F., Spott, O., Apelt, B., Russow, R., 2007. Automated and rapid online determination of ^{15}N abundance and concentration of ammonium, nitrite, or nitrate in aqueous samples by the SPINMAS technique. Isotopes in Environmental and Health Studies 43, 227-236.

Stehfest, E., Bouwman, L., 2006. N_2O and NO emission from agricultural fields and soils under natural vegetation: summarizing available measurement data and modeling of global annual emissions. Nutrient Cycling in Agroecosystems 74, 207-228.

Stevens, R., Laughlin, R., 1998. Measurement of nitrous oxide and di-nitrogen emissions from agricultural soils. Nutrient Cycling in Agroecosystems 52, 131-139.

Stevens, R., Laughlin, R., Atkins, G., Prosser, S., 1993. Automated determination of nitrogen-15-labeled dinitrogen and nitrous oxide by mass spectrometry. Soil Science Society of America Journal 57, 981-988.

Stevens, R., Laughlin, R., Burns, L., Arah, J., Hood, R., 1997. Measuring the contributions of nitrification and denitrification to the flux of nitrous oxide from soil. Soil Biology and Biochemistry 29, 139-151.

Sutka, R., Adams, G., Ostrom, N., Ostrom, P., 2008. Isotopologue fractionation during N_2O production by fungal denitrification. Rapid Communications in Mass Spectrometry 22, 3989-3996.

Sutka, R., Ostrom, N., Ostrom, P., Gandhi, H., Breznak, J., 2003. Nitrogen isotopomer site preference of N_2O produced by *Nitrosomonas europaea* and *Methylococcus capsulatus* Bath. Rapid Communications in Mass Spectrometry 17, 738-745.

Sutka, R.L., Ostrom, N., Ostrom, P., Breznak, J., Gandhi, H., Pitt, A., Li, F., 2006. Distinguishing nitrous oxide production from nitrification and denitrification on the basis of isotopomer abundances. Applied and Environmental Microbiology 72, 638-644.

Taube, F., Gierus, M., Hermann, A., Loges, R., Schönbach, P., 2014. Grassland and globalization - challenges for north-west European grass and forage research. Grass and Forage Science 69, 2-16.

Tauchnitz, N., Spott, O., Russow, R., Bernsdorf, S., Glaser, B., Meissner, R., 2015. Release of nitrous oxide and dinitrogen from a transition bog under drained and rewetted conditions due to denitrification: results from a [^{15}N] nitrate–bromide double-tracer study. Isotopes in Environmental and Health Studies 51, 300-321.

Terlikowski, J., Barszczewski, J., 2015. The effectiveness of permanent grassland renovation under different soil and climatic conditions. Journal of Research and Applications in Agricultural Engineering 60, 112-119.

Tiedje, J., 1982. Denitrification. Methods of Soil Analysis. Part 2 - Chemical and Microbiological Properties, 1011-1026.

Tiedje, J., 1988. Ecology of denitrification and dissimilatory nitrate reduction to ammonium. Biology of Anaerobic Microorganisms 717, 179-244.

Tiedje, J., Sexstone, A.J., Parkin, T., Revsbech, N., 1984. Anaerobic processes in soil. Plant and Soil 76, 197-212.

Tiley, G., Frame, J., 1991. Improvement of upland permanent pastures and lowland swards by surface sowing methods. Proceedings of a Conference of the European Grassland Federation, 89-94.

Toyoda, S., Mutobe, H., Yamagishi, H., Yoshida, N., Tanji, Y., 2005. Fractionation of N_2O isotopomers during production by denitrifier. Soil Biology and Biochemistry 37, 1535-1545.

Toyoda, S., Yano, M., Nishimura, S., Akiyama, H., Hayakawa, A., Koba, K., Sudo, S., Yagi, K., Makabe, A., Tobari, Y., 2011. Characterization and production and consumption processes of N_2O emitted from temperate agricultural soils determined via isotopomer ratio analysis. Global Biogeochemical Cycles 25.

Toyoda, S., Yoshida, N., 1999. Determination of nitrogen isotopomers of nitrous oxide on a modified isotope ratio mass spectrometer. Analytical Chemistry 71, 4711-4718.

Toyoda, S., Yoshida, N., Koba, K., 2015. Isotopocule analysis of biologically produced nitrous oxide in various environments. Mass Spectrometry Reviews.

Treyse, K., Kelm, M., Mehrtens, H., Taube, F., 2008. Ein Indikatoransatz zur Bewertung der Nachhaltigkeit von intensiv genutzten Grünlandbestanden. Berichte über Landwirtschaft 86, pp. 79-102 (in German).

UBA, 2009. Crititical N loads - map service http://gis.uba.de/website/depo1/. Umweltbundesamt, Dessau-Roßlau (Acessed July 15, 2016).

Ussiri, D., Lal, R., 2012. Soil emission of nitrous oxide and its mitigation. Springer Science & Business Media, LLC, New York, NY, USA.

Van den Heuvel, R., Mulvaney, R., Hoeft, R., 1988. Evaluation of nitrogen-15 tracer techniques for direct measurement of denitrification in soil: II. Simulation studies. Soil Science Society of America Journal 52, 1322-1326.

Van Groenigen, J., Huygens, D., Boeckx, P., Kuyper, T., Lubbers, I., Rütting, T., Groffman, P., 2015. The soil N cycle: new insights and key challenges. Soil 1, 235-256.

VDLUFA, 2002. Methodenbuch I. Die Untersuchung von Böden (Handbook: Soil Analysis), Darmstadt (in German).

VDLUFA, 2013. Methodenbuch III. Die chemische Untersuchung von Futtermitteln (Handbook: Animal Nutrition), Darmstadt (in German).

Vellinga, T., Hoving, I., 2011. Maize silage for dairy cows: mitigation of methane emissions can be offset by land use change. Nutrient Cycling in Agroecosystems 89, 413-426.

Vellinga, T., Van den Pol-van Dasselaar, A., Kuikman, P., 2004. The impact of grassland ploughing on CO_2 and N_2O emissions in the Netherlands. Nutrient Cycling in Agroecosystems 70, 33-45.

Velthof, G., Hoving, I., Dolfing, J., Smit, A., Kuikman, P., Oenema, O., 2010. Method and timing of grassland renovation affects herbage yield, nitrate leaching, and nitrous oxide emission in intensively managed grasslands. Nutrient Cycling in Agroecosystems 86, 401-412.

Velthof, G., Jarvis, S., Stein, A., Allen, A., Oenema, O., 1996. Spatial variability of nitrous oxide fluxes in mown and grazed grasslands on a poorly drained clay soil. Soil Biology and Biochemistry 28, 1215-1225.

Velthof, G., Oenema, O., 2001. Effects of ageing and cultivation of grassland on soil nitrogen. Alterra-rapport No. 399, Netherlands.

Watson, C., Atkinson, D., 1999. Using nitrogen budgets to indicate nitrogen use efficiency and losses from whole farm systems: a comparison of three methodological approaches. Nutrient Cycling in Agroecosystems 53, 259-267.

Weißbach, F., Schmidt, L., Kuhla, S., 1996. Simplified method for calculation of NEL from metabolizable energy, Proceedings of the Society of Nutrition Physiology (Germany). DLG.

Well, R., Augustin, J., Davis, J., Griffith, S., Meyer, K., Myrold, D., 2001. Production and transport of denitrification gases in shallow ground water. Nutrient Cycling in Agroecosystems 60, 65-75.

Well, R., Augustin, J., Meyer, K., Myrold, D., 2003. Comparison of field and laboratory measurement of denitrification and N_2O production in the saturated zone of hydromorphic soils. Soil Biology and Biochemistry 35, 783-799.

Well, R., Buchen, C., Deppe, M., Eschenbach, W., Gattinger, A., Giesemann, A., Krause, H., Lewicka-Szczebak, D., 2015. Non-homogeneity of isotopic labelling in ^{15}N gas flux studies: theory, some observations and possible lessons. Geophysical Research Abstracts 17, 11636.

Well, R., Butterbach-Bahl, K., 2010. Indirect emissions of nitrous oxide from nitrogen deposition and leaching of agricultural nitrogen, In: Smith, K. (Ed.), Nitrous Oxide and Climate Change. Earthscan Publications, London, pp. 162-189.

Well, R., Eschenbach, W., Flessa, H., von der Heide, C., Weymann, D., 2012. Are dual isotope and isotopomer ratios of N_2O useful indicators for N_2O turnover during denitrification in nitrate-contaminated aquifers? Geochimica et Cosmochimica Acta 90, 265-282.

Well, R., Flessa, H., 2009. Isotopologue enrichment factors of N_2O reduction in soils. Rapid Communications in Mass Spectrometry 23, 2996-3002.

Well, R., Flessa, H., Xing, L., Xiaotang, J., Römheld, V., 2008. Isotopologue ratios of N_2O emitted from microcosms with NH_4^+ fertilized arable soils under conditions favoring nitrification. Soil Biology and Biochemistry 40, 2416-2426.

Well, R., Höper, H., Mehranfar, O., Meyer, K., 2005. Denitrification in the saturated zone of hydromorphic soils-laboratory measurement, regulating factors and stochastic modeling. Soil Biology and Biochemistry 37, 1822-1836.

Well, R., Kurganova, I., de Gerenyu, V., Flessa, H., 2006. Isotopomer signatures of soil-emitted N_2O under different moisture conditions - A microcosm study with arable loess soil. Soil Biology and Biochemistry 38, 2923-2933.

Weymann, D., Well, R., von der Heide, C., Böttcher, J., Flessa, H., Duijnisveld, W., 2009. Recovery of groundwater N_2O at the soil surface and its contribution to total N_2O emissions. Nutrient Cycling in Agroecosystems 85, 299-312.

Whitehead, D., Bristow, A., Lockyer, D., 1990. Organic matter and nitrogen in the unharvested fractions of grass swards in relation to the potential for nitrate leaching after ploughing. Plant and Soil 123, 39-49.

Wolf, B., Merbold, L., Decock, C., Tuzson, B., Harris, E., Six, J., Emmenegger, L., Mohn, J., 2015. First on-line isotopic characterization of N_2O emitted from intensively managed grassland. Biogeosciences 12, 1573-1611.

Wolf, I., Russow, R., 2000. Different pathways of formation of N_2O, N_2 and NO in black earth soil. Soil Biology and Biochemistry 32, 229-239.

Wood, S., 2011. Fast stable restricted maximum likelihood and marginal likelihood estimation of semiparametric generalized linear models. Journal of the Royal Statistical Society 73, 3-36.

Wood, S., Augustin, N., 2002. GAMs with integrated model selection using penalized regression splines and applications to environmental modelling. Ecological Modelling 157, 157-177.

Wrage, N., Lauf, J., del Prado, A., Pinto, M., Pietrzak, S., Yamulki, S., Oenema, O., Gebauer, G., 2004a. Distinguishing sources of N_2O in European grasslands by stable isotope analysis. Rapid Communications in Mass Spectrometry 18, 1201-1207.

Wrage, N., Velthof, G., Laanbroek, H., Oenema, O., 2004b. Nitrous oxide production in grassland soils: assessing the contribution of nitrifier denitrification. Soil Biology and Biochemistry 36, 229-236.

Wrage, N., Velthof, G., Van Beusichem, M., Oenema, O., 2001. Role of nitrifier denitrification in the production of nitrous oxide. Soil Biology and Biochemistry 33, 1723-1732.

Wu, D., Lewicka-Szczebak, D., Köster, J., Fuß, R., Well, R., Cárdenas, L., Bol, R., in preparation. Using the correlation between N_2O $\delta^{18}O$ and α position $\delta^{15}N$ as a tool to spot N_2O reduction process during denitrification in soils Journal of Plant Nutrition and Soil Science.

Wu, H., Dannenmann, M., Fanselow, N., Wolf, B., Yao, Z., Wu, X., Brüggemann, N., Zheng, X., Han, X., Dittert, K., 2011. Feedback of grazing on gross rates of N mineralization and inorganic N partitioning in steppe soils of Inner Mongolia. Plant and Soil 340, 127-139.

Yamulki, S., Jarvis, S., 2002. Short-term effects of tillage and compaction on nitrous oxide, nitric oxide, nitrogen dioxide, methane and carbon dioxide fluxes from grassland. Biology and Fertility of Soils 36, 224-231.

Yanai, Y., Toyota, K., Morishita, T., Takakai, F., Hatano, R., Limin, S., Darung, U., Dohong, S., 2007. Fungal N_2O production in an arable peat soil in Central Kalimantan, Indonesia. Soil Science and Plant Nutrition 53, 806-811.

Yoshinari, T., Knowles, R., 1976. Acetylene inhibition of nitrous oxide reduction by denitrifying bacteria. Biochemical and Biophysical Research Communications 69, 705-710.

Zeileis, A., Hothorn, T., 2002. Diagnostic Checking in Regression Relationships. R News 2, 7-10.

Zhang, J., Müller, C., Cai, Z., 2015. Heterotrophic nitrification of organic N and its contribution to nitrous oxide emissions in soils. Soil Biology and Biochemistry 84, 199-209.

Zou, Y., Hirono, Y., Yanai, Y., Hattori, S., Toyoda, S., Yoshida, N., 2014. Isotopomer analysis of nitrous oxide accumulated in soil cultivated with tea *Camellia sinensis* in Shizuoka, central Japan. Soil Biology and Biochemistry 77, 276-291.

Appendix A2 – Supplementary data: Soil mineral N dynamics and N_2O emissions following grassland renewal

Table A2-1: Agricultural management of the treatments on the Histic Gleysol from June 2013 to October 2015 (Table is continued on the next page)

Date	Measures	Treatments	Agents	Application rate
2013-06-10	Implementation of experimental design	All		
2013-07-17	N fertilisation following 2nd cut	All	Calcium ammonium nitrate (15.7% N-NH_3; 9.5% N-NO_3)	60 kg N ha^{-1}
2013-08-25	3rd cut	All		
2013-08-29	Chemical killing	*Chemical, Mechanical*	Round Up Power Flex	3.75 L ha^{-1}
2013-09-02	Rotovating	*Mechanical*		
2013-09-02	Ploughing to 25 cm depth	*Mechanical*		
2013-09-02	Sowing	*Mechanical*	54% *Lolium perenne* L., 20% *Festuca pratensis*, 17% *Phleum pratense* L., 10% *Poa pratensis* L.	40 kg ha^{-1}
2013-09-03	Direct sowing	*Chemical*	54% *Lolium perenne* L., 20% *Festuca pratensis*, 17% *Phleum pratense* L., 10% *Poa pratensis* L.	40 kg ha^{-1}
2013-09-03	Resowing	*Minimum*	100% *Lolium perenne* L.	15 kg ha^{-1}
2013-09-03	Rolling	All		
2013-10-30	4th cut	*Control, Maize*		
2013-11-01	Weed control	All	Ranger	2 L ha^{-1}
2014-03-01	Resowing	*Chemical*	54% *Lolium perenne* L., 20% *Festuca pratensis*, 17% *Phleum pratense* L., 10% *Poa pratensis* L.	20 kg ha^{-1}
2014-03-27	N fertilisation	All grasslands	Calcium ammonium nitrate (15.7% N-NH_3; 9.5% N-NO_3)	100 kg N ha^{-1}
2014-04-16	Chemical killing	*Maize*	Round Up Power Flex	3.75 L ha^{-1}
2014-04-24	Rotovating	*Maize*		
2014-04-24	Ploughing to 25 cm depth	*Maize*		
2014-04-24	Sowing	*Maize*	*Zea mays* L. - variety: *Colisee*	80,000 seeds ha^{-1}
2014-05-22	1st cut	All grasslands		
2014-05-23	N fertilisation	All grasslands	Calcium ammonium nitrate (15.7% N-NH_3; 9.5% N-NO_3)	80 kg N ha^{-1}

2014-06-06	Resowing	*Maize*	*Zea mays* L. - variety: *Colisee* by hand	
2014-06-06	N fertilisation	*Maize*	NPK (ammonium nitrate, triple superphosphate, Korn-Kali)	155 kg N ha^{-1} 77 kg P ha^{-1} 240 kg K ha^{-1}
2014-06-27	Weed control	*Maize*	MILAGRO forte	0.6 L ha^{-1}
2014-06-27	weed control	*Maize*	MILAGRO Peak	20 g ha^{-1}
2014-07-10	2nd cut	All grasslands		
2014-07-11	N fertilisation	All grasslands	Hydrosulfan	60 kg N ha^{-1}
2014-08-21	3rd cut	All grasslands		
2014-08-22	N fertilisation	All grasslands	Hydrosulfan	40 kg N ha^{-1}
2014-10-13	Harvest	*Maize*		
2014-10-15	4th cut	All grasslands		
2015-03-26	N fertilisation	All grasslands	Calcium ammonium nitrate (15.7% N-NH_3; 9.5% N-NO_3)	100 kg N ha^{-1}
2015-04-10	Chemical killing	*Maize*	Durano	3.75 L ha^{-1}
2015-04-27	Rotovating	*Maize*		
2015-04-27	Ploughing to 25 cm depth	*Maize*		
2015-04-27	Sowing	*Maize*	*Zea mays* L. - variety: *Colisee*	80,000 seeds ha^{-1}
2015-05-20	1st cut	All grasslands		
2014-05-20	N fertilisation	All grasslands	Calcium ammonium nitrate (15.7% N-NH_3; 9.5% N-NO_3)	80 kg N ha^{-1}
2015-05-21	N fertilisation	*Maize*	NPK (ammonium nitrate, triple superphosphate, Korn-Kali)	155 kg N ha^{-1} 77 kg P ha^{-1} 240 kg K ha^{-1}
2015-06-03	Weed control	*Maize*	MILAGRO Peak	15 g ha^{-1}
2015-06-03	Weed control	*Maize*	DUAL GOLD	1 L ha^{-1}
2015-06-03	Weed control	*Maize*	CALARIS	1.2 L ha^{-1}
2015-06-09	Resowing	*Maize*	*Zea mays* L. - variety: *Colisee* by hand	
2015-06-24	2nd cut	All grasslands		
2015-06-25	N fertilisation	All grasslands	Calcium ammonium nitrate (15.7% N-NH_3; 9.5% N-NO_3)	60 kg N ha^{-1}
2015-08-07	3rd cut	All grasslands		
2015-08-10	N fertilisation	All grasslands	Calcium ammonium nitrate (15.7% N-NH_3; 9.5% N-NO_3)	40 kg N ha^{-1}
2015-10-13	Harvest	*Maize*		
2015-10-16	4th cut	All grasslands		

Table A2-2: Agricultural management of the treatments on the Plaggic Anthrosol from June 2013 to October 2015 (Table is continued on the next page)

Date	Measures	Treatments	Agents	Application rate
2013-06-10	Implementation of experimental design	All		
2013-07-24	N fertilisation following 2nd cut	All	Calcium ammonium nitrate (15.7% N-NH_3; 9.5% N-NO_3)	60 kg N ha^{-1}
2013-08-29	3rd cut	All		
2013-08-29	Chemical killing	*Chemical, Mechanical*	Round Up Power Flex	3.75 L ha^{-1}
2013-09-02	Rotovating	*Mechanical*		
2013-09-02	Ploughing to 25 cm depth	*Mechanical*		
2013-09-02	Sowing	*Mechanical*	54% *Lolium perenne* L., 20% *Festuca pratensis*, 17% *Phleum pratense* L., 10% *Poa pratensis* L.	40 kg ha^{-1}
2013-09-03	Direct sowing	*Chemical*	54% *Lolium perenne* L., 20% *Festuca pratensis*, 17% *Phleum pratense* L., 10% *Poa pratensis* L.	40 kg ha^{-1}
2013-09-03	Resowing	*Minimum*	100% *Lolium perenne* L.	15 kg ha^{-1}
2013-09-03	Rolling	All		
2013-10-31	4th cut	All, except *Chemical*		
2013-11-01	Weed control	All	Ranger	2 L ha^{-1}
2014-03-01	Resowing	*Chemical*	54% *Lolium perenne* L., 20% *Festuca pratensis*, 17% *Phleum pratense* L., 10% *Poa pratensis* L.	20 kg ha^{-1}
2014-03-27	N fertilisation	All grasslands	Calcium Ammonium-nitrate (15.7% N-NH_3; 9.5% N-NO_3)	100 kg N ha^{-1}
2014-04-16	Chemical killing	*Maize*	Round Up Power Flex	3.75 L ha^{-1}
2014-04-24	Rotovating	*Maize*		
2014-04-24	Ploughing to 25 cm depth	*Maize*		
2014-04-24	Sowing	*Maize*	*Zea mays* L. - variety: *Colisee*	80,000 seeds ha^{-1}
2014-05-19	Weed control	*Maize*	MILAGRO forte	0.6 L ha^{-1}
2014-05-19	Weed control	*Maize*	MILAGRO Peak	20 g ha^{-1}
2014-05-23	1st cut	All grasslands		

2014-05-23	N fertilisation	All grasslands	Calcium ammonium nitrate (15.7% N-NH_3; 9.5% N-NO_3)	80 kg N ha^{-1}
2014-06-06	N fertilisation	*Maize*	NPK (ammonium nitrate, triple superphosphate, Korn-Kali)	155 kg N ha^{-1} 77 kg P ha^{-1} 240 kg K ha^{-1}
2014-07-10	2nd cut	All grasslands		
2014-07-11	N fertilisation	All grasslands	Hydrosulfan	60 kg N ha^{-1}
2014-08-21	3rd cut	All grasslands		
2014-08-22	N fertilisation	All grasslands	Hydrosulfan	40 kg N ha^{-1}
2014-10-08	Harvest	*Maize*		
2014-10-15	4th cut	All grasslands		
2015-03-26	N fertilisation	All grasslands	Calcium ammonium nitrate (15.7% N-NH_3; 9.5% N-NO_3)	100 kg N ha^{-1}
2015-04-10	Chemical killing	*Maize*	Durano	3.75 L ha^{-1}
2015-04-27	Rotovating	*Maize*		
2015-04-27	Ploughing to 25 cm depth	*Maize*		
2015-04-27	Sowing	*Maize*	*Zea mays* L. - variety: *Colisee*	80,000 seeds ha^{-1}
2015-06-03	Weed control	*Maize*	MILAGRO Peak	15 g ha^{-1}
2015-06-03	Weed control	*Maize*	DUAL GOLD	1 L ha^{-1}
2015-06-03	Weed control	*Maize*	CALARIS	1.2 L ha^{-1}
2015-05-20	1st cut	All grasslands		
2014-05-20	N fertilisation	All grasslands	Calcium ammonium nitrate (15.7% N-NH_3; 9.5% N-NO_3)	80 kg N ha^{-1}
2015-05-21	N fertilisation	*Maize*	NPK (ammonium nitrate, triple superphosphate, Korn-Kali)	155 kg N ha^{-1} 77 kg P ha^{-1} 240 kg K ha^{-1}
2015-06-25	2nd cut	All grasslands		
2015-06-25	N fertilisation	All grasslands	Calcium ammonium nitrate (15.7% N-NH_3; 9.5% N-NO_3)	60 kg N ha^{-1}
2015-08-10	3rd cut	All grasslands		
2015-08-10	N fertilisation	All grasslands	Calcium ammonium nitrate (15.7% N-NH_3; 9.5% N-NO_3)	40 kg N ha^{-1}
2015-10-13	Harvest	*Maize*		
2015-10-16	4th cut	All grasslands		

Table A2-3a: Cumulative N fertiliser-related N_2O fluxes (N_2O per N fertiliser in %) of the grassland treatments per year (September 2013 to 2014 and September 2014 to 2015). Different superscript letters indicate significant differences in the grassland treatments (*Minimum*, *Chemical* and *Mechanical*) in comparison to permanent grassland (*Control*) for the respective sites. Values shown are the mean of treatment replicates ± one standard deviation (n=4)

	2013-2014	**2014-2015**
	N_2O per N fertiliser %	N_2O per N fertiliser %
Histic Gleysol		
Control	2.24±1.11 [a]	2.34±1.40 [a]
Minimum	2.61±1.39 [a]	2.16±0.48 [a]
Chemical	2.84±0.79 [a]	1.88±0.55 [a]
Mechanical	3.53±1.63 [a]	1.55±0.73 [a]
Plaggic Anthrosol		
Control	0.53±0.29 [a]	0.53±0.16 [a]
Minimum	0.54±0.25 [a]	0.60±0.18 [a]
Chemical	0.69±0.22 [a]	0.53±0.30 [a]
Mechanical	0.88±0.35 [a]	0.61±0.35 [a]

Table A2-3b: Cumulative N fertiliser-related N_2O fluxes (N_2O per N fertiliser in %) of the *Maize* treatment per cultivation period (May to October 2014 and 2015) and on an annual basis for the first year following grassland conversion to maize cropping (April 2014 to May 2015) in comparison to permanent grassland (*Control*). Different superscript letters indicate significant differences between treatments for the respective sites. Values shown are the mean of treatment replicates ± one standard deviation (n=4)

	2014[1]	**2015[2]**	**2014-2015**
	N_2O per N fertiliser %	N_2O per N fertiliser %	N_2O per N fertiliser %
Histic Gleysol			
Control	2.61±1.48 [a]	1.72±1.49 [a]	1.48±0.68 [a]
Maize	2.92±1.24 [a]	2.62±1.14 [a]	2.18±0.80 [a]
Plaggic Anthrosol			
Control	0.49±0.28 [a]	0.27±0.11 [a]	0.34±0.16 [a]
Maize	1.95±0.23 [b]	0.27±0.30 [a]	0.98±0.10 [b]

[1] The *Maize* cultivation period in 2014 was 168 days.

[2] The *Maize* cultivation period in 2015 was 172 days.

Table A2-4: ANOVA table of a penalised regression generalised additive model (GAM) of log-transformed N_2O emissions depending on linear effects of treatment and block, an interaction of gravimetric water content and NO_3^- concentration per treatment and a smoother of CO_2 flux for the Histic Gleysol

$logN_2O\_flux \sim treat + block + te(NO_3^-, gravimetric\ water\ content, by = treat) + s(CO_2\ flux, bs = "cs", k = 10)$

Parametric terms	**df**	**p-value**
Treatment	4	0.000 **
Block	3	0.735
Approximate significance of smooth terms	**edf**	**p-value**
te(NO_3^-, gravimetric water content): *Control* treatment	6	0.000 **
te(NO_3^-, gravimetric water content): *Minimum* treatment	3	0.000 **
te(NO_3^-, gravimetric water content): *Chemical* treatment	6	0.000 **
te(NO_3^-, gravimetric water content): *Mechanical* treatment	13	0.000 **
te(NO_3^-, gravimetric water content): *Maize* treatment	8	0.000 **
s(CO_2 flux)	6	0.000 **

** indicates p<0.05 level of significance

edf: array of estimated degrees of freedom for the model terms; *te*: function used in definition for tensor smooth terms including several variables within GAM model formulae, *s*: function used in definition of smooth terms with *bs* indicating the smoothing basis used (cs: cubic spline with shrinkage) and *k* as a dimension of the basis used to represent the smoothing term, i.e. a parameter giving a minimum for smoothness of the term

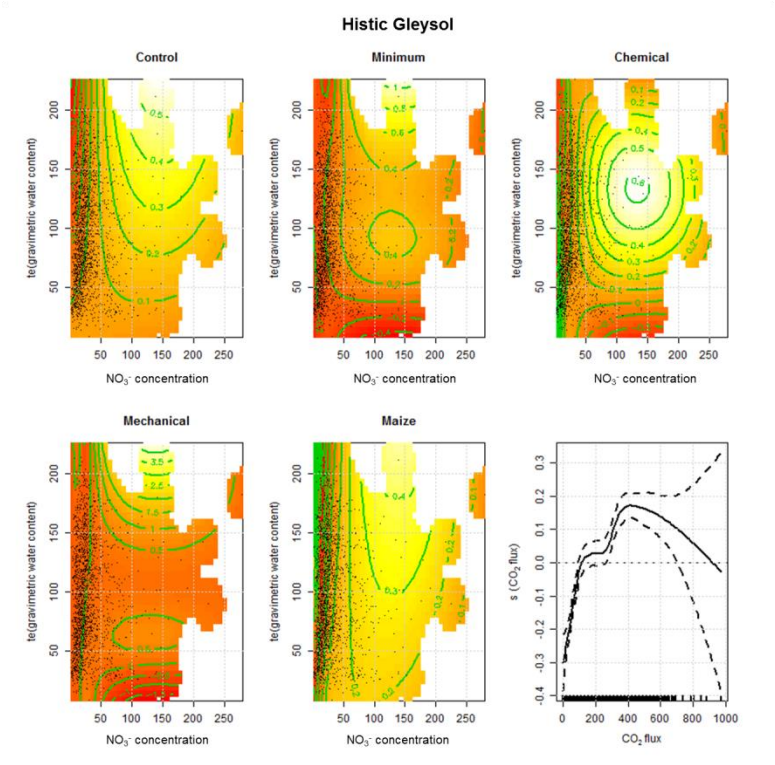

Figure A2-1: GAM model plots of log-scaled N_2O fluxes and explaining parameters. Shown are smoothing terms *te*: gravimetric water content (y-axis) and NO_3^- concentrations (x-axis) and the interaction term *s*: CO_2 flux of the treatments (*Control*, *Minimum*, *Chemical*, *Mechanical* and *Maize*) on the Histic Gleysol. The values in colour or at lines given at the y-axis of the figures represent the values inserted into the equation to calculate the modelled N_2O flux at the respective value-combinations of nitrate, gravimetric water content and CO_2 flux

Table A2-5: ANOVA table of a penalised regression generalised additive model (GAM) of log-transformed N_2O emissions depending on linear effects of treatment and block, an interaction of WFPS and NO_3^- concentration per treatment and a smoother of CO_2 flux for the Plaggic Anthrosol

$logN_2O\_flux \sim treat + block + te(NO_3^-, WFPS, by = treat) + s(CO_2\ flux, bs = "cs", k = 10)$

Parametric terms	**df**	**p-value**
Treatment	4	0.000 **
Block	3	0.000 **
Approximate significance of smooth terms	**edf**	**p-value**
te(NO_3^-, WFPS): *Control* treatment	8	0.000 **
te(NO_3^-, WFPS): *Minimum* treatment	4	0.000 **
te(NO_3^-, WFPS): *Chemical* treatment	12	0.000 **
te(NO_3^-, WFPS): *Mechanical* treatment	8	0.000 **
te(NO_3^-, WFPS): *Maize* treatment	5	0.000 **
s(CO_2 flux)	5	0.000 **

** indicates p<0.05 level of significance

edf: array of estimated degrees of freedom for the model terms; *te*: function used in definition for tensor smooth terms including several variables within GAM model formulae, *s*: function used in definition of smooth terms with *bs* indicating the smoothing basis used (cs: cubic spline with shrinkage) and *k* as a dimension of the basis used to represent the smoothing term, i.e. a parameter giving a minimum for smoothness of the term

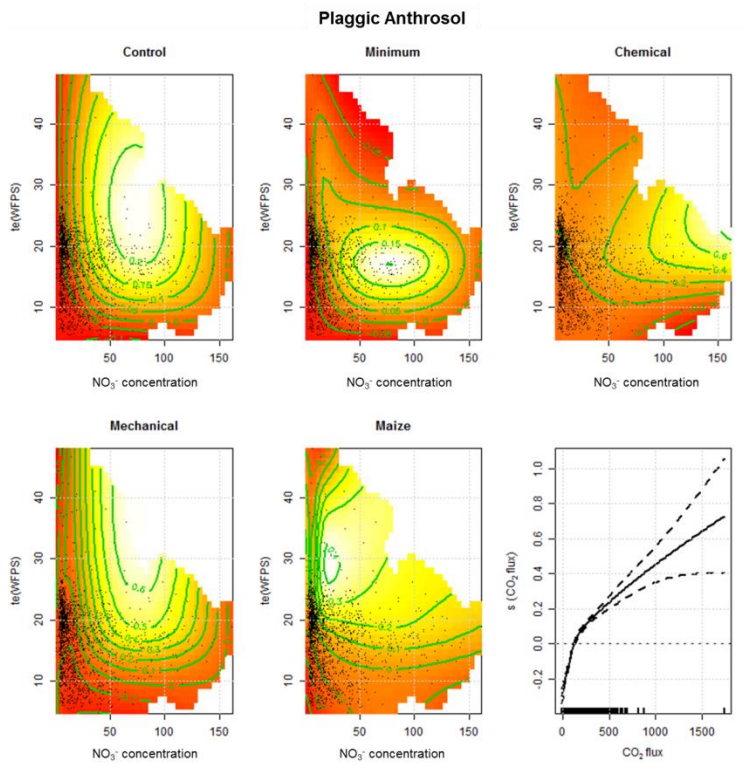

Figure A2-2: GAM model plots of log-scaled N_2O fluxes and explaining parameters. Shown are smoothing terms *te*: WFPS (y-axis) and NO_3^- concentrations (x-axis) and the interaction term *s*: CO_2 flux of the treatments (*Control, Minimum, Chemical, Mechanical* and *Maize*) on the Plaggic Anthrosol. The values in colour or at lines given at the y-axis of the figures represent the values inserted into the equation to calculate the modelled N_2O flux at the respective value-combinations of nitrate, WFPS and CO_2 flux

Table A2-6: Calculation of the unaccounted-for N of the N budget (i.e. N_{ua}, Eq. 2-1) in kg N ha^{-1} of the Histic Gleysol and of the Plaggic Anthrosol for the periods 2013-2014 (February 2013 to October 2014) and 2014-2015 (February 2014 to October 2015). Values shown are the mean of treatment replicates ± one standard deviation (n=4)

	2013-2014			2014-2015		
	A	**B**	**N_{ua}**	**A**	**B**	**N_{ua}**
Histic Gleysol	kg N ha^{-1}			kg N ha^{-1}		
Control	307±2	358±25	51±22	317±2	362±14	46±13
Minimum	307±3	349±21	42±18	327±16	368±45	41±43
Chemical	308±4	372±33	64±29	311±7	360±33	49±39
Mechanical	346±29	360±20	14±-9	321±13	321±27	0±24
Maize	176±7	262±25	86±18	222±46	267±19	45±34
Plaggic Anthrosol						
Control	309±9	278±30	-31±32	299±4	287±21	-13±22
Minimum	305±3	311±27	6±26	303±4	290±10	-13±10
Chemical	321±10	222±8	-98±4	294±2	273±40	-22±40
Mechanical	305±5	261±20	-44±18	298±3	288±13	-9±13
Maize	179±4	321±41	143±39	212±67	270±23	58±48

A: Post-winter N_{min} contents in 0-90 cm soil depth (can be evaluated from Figure 2-5) + added N fertiliser (i.e. 280 kg N ha^{-1} in the grassland treatments and 150 kg N ha^{-1} in the *Maize* treatment)

B: Plant N removal by harvest (see Table 2-4) + pre-winter N_{min} contents at 0-90 cm soil depth (can be evaluated from Figure 2-5)

Appendix A3 – Supplementary data: Fluxes of N_2 and N_2O and contributing processes in summer after grassland renewal and grassland conversion to maize cropping on a Plaggic Anthrosol and a Histic Gleysol

Table A3-1: Soil characteristics of the studied soils at 0-30 cm depth. C_{org}, C/N ratio, pH and bulk density were measured on soil cores on a plot basis (n=20). Texture was analysed from a single soil profile. Mean ± standard deviation. nd = not determined

Soil type	Location	Depth	Sand	Silt	Clay	C_{org}	C/N ratio	pH	Bulk density
		cm	%	%	%	g kg^{-1}		$CaCl_2$	g cm^{-3}
Histic Gleysol	Ihausen	0-10	nd	nd	nd	196.9±96.5	13.5±1.2	5.6±0.5	0.6±0.2
		10-20	nd	nd	nd	191.2±120.3	14.3±1.7	5.5±0.3	0.7±0.3
		20-30	70	24	5	56.4±50.7	14.4±2.8	5.6±0.3	0.9±0.3
Plaggic Anthrosol	Wehnen	0-10	91	6	3	28.1±3.1	14.4±0.8	5.1±0.2	1.3±0.1
		10-20	90	6	4	22.4±3.0	14.4±0.8	4.9±0.4	1.4±0.1
		20-30	91	6	3	18.9±4.3	15.9±2.7	4.9±0.4	1.4±0.1

Table A3-2: Agricultural management practices at the Histic Gleysol site (Ihausen) between June 2013 and July 2014

Date	Measures	Treatments	Agents	Application rate
2013-06-10	Implementation of experimental design	All		
2013-07-17	N fertilisation following 2nd cut	All	Calcium ammonium-nitrate (15.7% N-NH_3; 9.5% N-NO_3)	60 kg N ha^{-1}
2013-08-25	3rd cut	All		
2013-08-29	Chemical killing	*Renewal*	Round Up Power Flex	3.75 L ha^{-1}
2013-09-02	Rotovating	*Renewal*		
2013-09-02	Ploughing to 25 cm depth	*Renewal*		
2013-09-02	Sowing	*Renewal*	54% *Lolium perenne* L., 20% *Festuca pratensis*, 17% *Phleum pratense* L., 10% *Poa pratensis* L.	40 kg ha^{-1}
2013-09-03	Rolling	All		
2013-10-30	4th cut	*Control, Maize*		
2013-11-01	Weed control	All	Ranger	2 L ha^{-1}
2014-03-27	N fertilisation	All grasslands	Calcium ammonium-nitrate (15.7% N-NH_3; 9.5% N-NO_3)	100 kg N ha^{-1}
2014-04-16	Chemical killing	*Maize*	Round Up Power Flex	3.75 L ha^{-1}
2014-04-24	Rotovating	*Maize*		
2014-04-24	Ploughing to 25 cm depth	*Maize*		
2014-04-24	Sowing	*Maize*	*Zea mays* L., variety Colisee	80,000 seeds ha^{-1}
	Installation of PVC cylinders	All		
2014-05-22	1st cut	All grasslands		
2014-05-23	N fertilisation	All grasslands	Calcium ammonium-nitrate (15.7% N-NH_3; 9.5% N-NO_3)	80 kg N ha^{-1}
2014-06-06	Sowing	*Maize*	*Zea mays* L. , variety *Colisee* by hand	
2014-06-06	N fertilisation	*Maize*	NPK (ammonium-nitrate, triple superphosphate, Korn-Kali)	155 kg N ha^{-1} 77 kg P ha^{-1} 240 kg K ha^{-1}
2014-06-27	Weed control	*Maize*	MILAGRO forte	0.6 L ha^{-1}
2014-06-27	Weed control	*Maize*	MILAGRO Peak	20 g ha^{-1}
2014-05-25	^{15}N fertiliser application	All grasslands	Potassium nitrate (~60 at%)	80 kg N ha^{-1}
		Maize	Potassium nitrate (~60 at%)	150 kg N ha^{-1}

Table A3-3: Agricultural management practices at the Plaggic Anthrosol site (Wehnen) between June 2013 and July 2014

Date	Measures	Treatments	Agents	Application rate
2013-06-10	Implementation of experimental design	All		
2013-07-24	N fertilisation following 2nd cut	All	Ammonium-nitrate (15.7% $N\text{-}NH_3$; 9.5% $N\text{-}NO_3$)	60 kg N ha^{-1}
2013-08-29	3rd cut	All		
2013-08-29	Chemical killing	*Renewal*	Round Up Power Flex	3.75 L ha^{-1}
2013-09-02	Rotovating	*Renewal*		
2013-09-02	Ploughing to 25 cm depth	*Renewal*		
2013-09-02	Sowing	*Renewal*	54% *Lolium perenne* L., 20% *Festuca pratensis*, 17% *Phleum pratense* L., 10% *Poa pratensis* L.	40 kg ha^{-1}
2013-09-03	Rolling	All		
2013-10-31	4th cut	All		
2013-11-01	Weed control	All	Ranger	2 L ha^{-1}
2014-03-27	N fertilisation	All grasslands	Ammonium-nitrate (15.7% $N\text{-}NH_3$; 9.5% $N\text{-}NO_3$)	100 kg N ha^{-1}
2014-04-16	Chemical killing	*Maize*	Round Up Power Flex	3.75 L ha^{-1}
2014-04-24	Rotovating	*Maize*		
2014-04-24	Ploughing to 25 cm depth	*Maize*		
2014-04-24	Sowing	*Maize*	*Zea mays* L., variety *Colisee*	80,000 seeds ha^{-1}
	Installation of PVC cylinders	All		
2014-05-19	Weed control	*Maize*	MILAGRO forte	0.6 L ha^{-1}
2014-05-19	Weed control	*Maize*	MILAGRO Peak	20 g ha^{-1}
2014-05-23	1st cut	All grasslands		
2014-05-25	^{15}N fertiliser application	All grasslands	Potassium nitrate (~60 at%)	80 kg N ha^{-1}
		Maize	Potassium nitrate (~60 at%)	150 kg N ha^{-1}

Table A3-4: Summary of N_2O and N_2 forming processes, determined by application of the ^{15}N gas flux method *in situ*

Abbreviation	Processes	Definition of fluxes	Analytical methods	Calculations
N_2Oflux_{total}	• All N_2O forming processes	Sum of all N_2O fluxes	Gas chromatography (section 3.2.4)	Eq. 3-1
N_2Oflux_L [1)] N_2flux_L [1)]	• Heterotrophic denitrification • Co-denitrification • Anammox	N_2O and N_2 fluxes derived from the labelled NO_3^- pool in soil	Isotope ratio mass spectrometry (section 3.2.4)	Eq. 3-2
$N_2Oflux_{L\_NH}$ [1)] $N_2flux_{L\_NH}$ [1)]	• Heterotrophic denitrification	Non-hybrid N_2O and N_2 fluxes derived from the labelled NO_3^- pool in soil	Isotope ratio and quadrupole mass spectrometry (sections 3.2.3 and 3.2.4)	Eq. 3-9a Eq. 3-9b
N_2Oflux_{NL} N_2flux_{NL}	• Nitrification • Nitrifier denitrification	N_2O and N_2 fluxes derived from other pools than the labelled NO_3^-	Isotope ratio mass spectroscopy (section 3.2.4)	Eq. 3-2 [2)]
$N_2Oflux_{L\_H}$ $N_2flux_{L\_H}$	• Co-denitrification • Anammox	Hybrid N_2O and N_2 fluxes derived from the labelled NO_3^- pool in soil	Isotope ratio and quadrupole mass spectrometry (sections 3.2.3 and 3.2.4)	Eq. 3-10a Eq. 3-10b

[1]) Hybrid N fluxes were defined here fluxes derived from the labelled pool, despite the fact that only one of the two N atoms originated from the non-labelled pools.

[2]) N_2flux_{NL}: not quantified

Table A3-5: Mean total N_2O fluxes (N_2Oflux_{total}), N_2O fluxes (N_2Oflux_L) and N_2 fluxes (N_2flux_L) from the active labelled NO_3^- pool and the $N_2O/(N_2+N_2O)$ ratio of denitrification, calculated from the mean fluxes per plot, over a 44-day period for the Histic Gleysol and Plaggic Anthrosol. Superscript letters indicate significant differences between the treatments and soil sites at significance level p<0.05. Values are mean of treatment replicates ± one standard deviation (n=4)

Treatments	N_2Oflux_{total}	N_2Oflux_L	N_2flux_L	$N_2O/(N_2+N_2O)$ ratio of denitrification
	kg N ha^{-1}	kg N ha^{-1}	kg N ha^{-1}	
Histic Gleysol				
Control	3.15±2.31 [a]	0.45±0.51 [a]	49.83±32.57 [a]	0.05±0.06 [a]
Renewal	1.14±1.14 [a]	0.24±0.41 [a]	21.97±19.09 [a]	0.04±0.06 [a]
Maize	4.00±3.11 [a]	1.27±1.33 [a]	52.75±31.37 [a]	0.03±0.03 [a]
Plaggic Anthrosol				
Control	0.38±0.13 [a]	0.02±0.02 [a]	bd	NA
Renewal	0.51±0.21 [a]	0.04±0.02 [a]	bd	NA
Maize	0.83±0.30 [a]	0.07±0.08 [a]	bd	NA

bd below the detection limit; *NA* not applicable

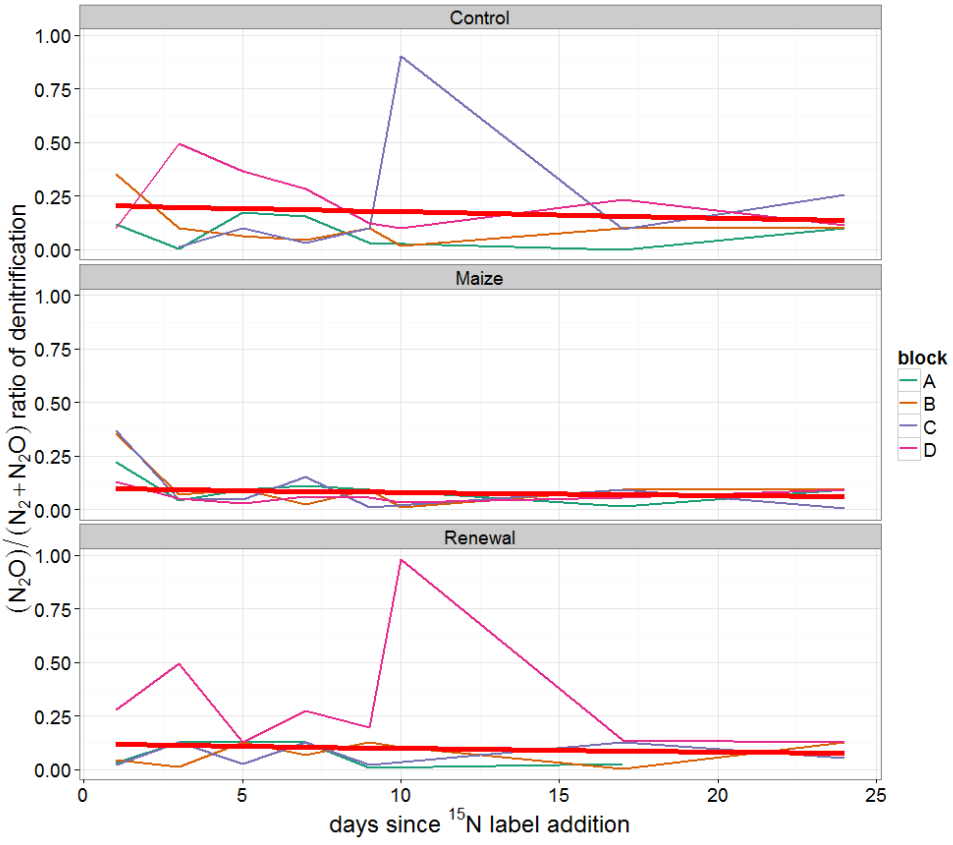

Figure A3-1: $N_2O/(N_2+N_2O)$ ratio of denitrification of each block (different colours) and the different treatments (*Control, Renewal* and *Maize*) over the first 23 sampling days for the Histic Gleysol. Results from the beta regression model are shown in the red line.

Table A3-6: ANOVA table of a penalised regression generalised additive model (GAM) of log-transformed $N_2Ofluxes_{total}$ depending on linear effects of treatment, block and nitrate (NO_3^--N) concentration and a smoother of groundwater level for the Histic Gleysol:

log N_2Oflux_{total} ~ treatment * block + nitrate + s(groundwater level, bs = "cs", k = 5)

Parametric terms	**df**	**p-value**
Treatment	2	0.486
Block	3	0.026 **
Nitrate	1	0.001 **
Treatment:Block	6	0.024 **
Approximate significance of smooth terms	**edf**	**p-value**
s(groundwater level)	3.084	0.000 **

**indicates p<0.05 level of significance

edf: array of estimated degrees of freedom for the model terms; s: function used in definition of smooth terms within GAM model formulae with *bs* indicating the smoothing basis used (cs: cubic spline with shrinkage) and *k* as a dimension of the basis used to represent the smoothing term, i.e. a parameter giving a minimum for smoothness of the term

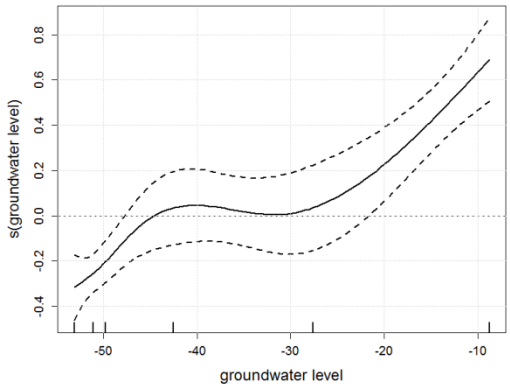

Figure A3-2: Model plot of the interaction term *s*(groundwater level) for the Histic Gleysol

Table A3-7: ANOVA table of a penalised regression generalised additive model (GAM) of log-transformed N_2Oflux_{total} depending on linear effects of treatment, block and nitrate (NO_3^--N) concentration and a smoother of groundwater level for the Plaggic Anthrosol:

log N_2Oflux_{total} ~ treatment * block + WFPS + s(nitrate, bs = "cs", k = 4) + s(soil temperature, bs = "cs", k = 4, by = treatment)

Parametric terms	**df**	**p-value**
Treatment	2	0.002 **
Block	3	0.037 **
WFPS	1	0.186
Treatment:Block	6	0.097
Approximate significance of smooth terms	**edf**	**p-value**
s(nitrate)	2.842	0.001 **
s(soil temperature): *Control* treatment	0.534	0.342
s(soil temperature): *Renewal* treatment	2.584	0.124
s(soil temperature): *Maize* treatment	0.573	0.266

**indicates p<0.05 level of significance

edf: array of estimated degrees of freedom for the model terms; s: function used in definition of smooth terms within GAM model formulae with *bs* indicating the smoothing basis used (cs: cubic spline with shrinkage) and *k* as a dimension of the basis used to represent the smoothing term, i.e. a parameter giving a minimum for smoothness of the term

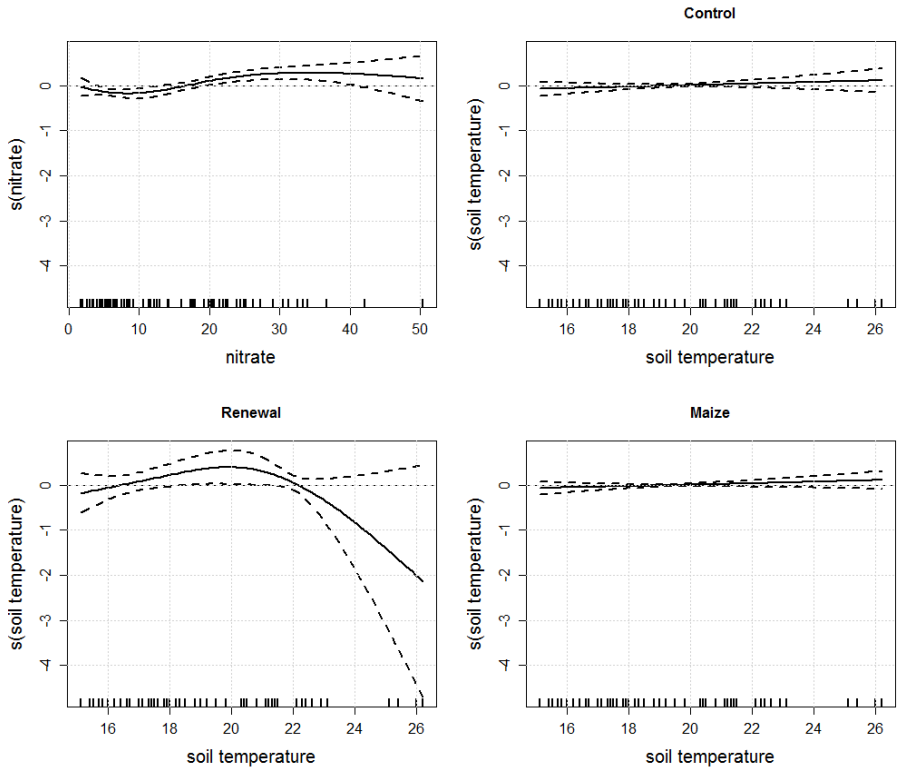

Figure A3-3: Model plot of the interaction terms *s*(nitrate) and *s*(soil temperature) for the three treatments (*Control, Reseed* and *Maize*) on the Plaggic Anthrosol

Table A3-8: Gross nitrification rates per depth and sampling interval for the Plaggic Anthrosol. Different superscript letters indicate significant differences for the respective sampling interval at significance level p <0.05. Means from treatment replicates ± standard deviation (n=4)

	Gross nitrification rate				
Treatment	mg NO_3^--N kg^{-1} dry soil day^{-1}				
Sampling depth	0-10 cm				
Sampling interval	**Day 1 to 8**	**Day 8 to 16**	**Day 16 to 30**	**Day 30 to 38**	**Day 30 to 44**
Control	0.72±1.57 ^{ab}	0.41±0.69 ^{a}	0.14±0.77 ^{b}	0.14±0.47 ^{a}	0.01±0.04 ^{b}
Renewal	0.72±0.30 ^{ab}	1.18±0.76 ^{a}	0.40±0.31 ^{ab}	0.21±0.20 ^{a}	0.02±0.03 ^{b}
Maize	3.18±3.32 ^{a}	0.92±1.54 ^{a}	0.22±0.42 ^{b}	0.04±0.12 ^{a}	-0.01±0.03 ^{b}*
Sampling depth	10-20 cm				
Sampling interval	**Day 1 to 8**	**Day 8 to 16**	**Day 16 to 30**	**Day 30 to 38**	**Day 30 to 44**
Control	0.09±0.37 ^{ab}	0.68±0.55 ^{a}	1.62±0.85 ^{ab}	-0.03±0.07 ^{a}*	0.00±0.01 ^{b}
Renewal	0.51±0.38 ^{ab}	1.24±0.56 ^{a}	1.57±0.50 ^{ab}	0.32±0.26 ^{a}	0.09±0.09 ^{ab}
Maize	1.57±1.03 ^{ab}	0.02±0.35 ^{a}	1.19±0.93 ^{ab}	0.21±0.37 ^{a}	0.02±0.05 ^{b}
Sampling depth	20-30 cm				
Sampling interval	**Day 1 to 8**	**Day 8 to 16**	**Day 16 to 30**	**Day 30 to 38**	**Day 30 to 44**
Control	-1.03±0.93 ^{b}*	0.15±0.20 ^{a}	1.99±0.70 ^{a}	-0.02±0.07 ^{a}*	-0.01±0.02 ^{b}*
Renewal	0.28±0.73 ^{ab}	0.31±0.46 ^{a}	1.62±0.65 ^{ab}	0.29±0.07 ^{a}	0.16±0.09 ^{a}
Maize	0.57±0.46 ^{ab}	0.96±1.36 ^{a}	1.88±0.72 ^{a}	-0.03±0.16 ^{a}*	0.03±0.02 ^{b}

* Negative nitrification rates resulted from an increase of ^{15}N enrichment from the 1st to the 2nd sampling date

Appendix A4 – Supplementary data: Estimating N_2O processes during grassland renewal and grassland conversion to maize cropping using N_2O isotopocules

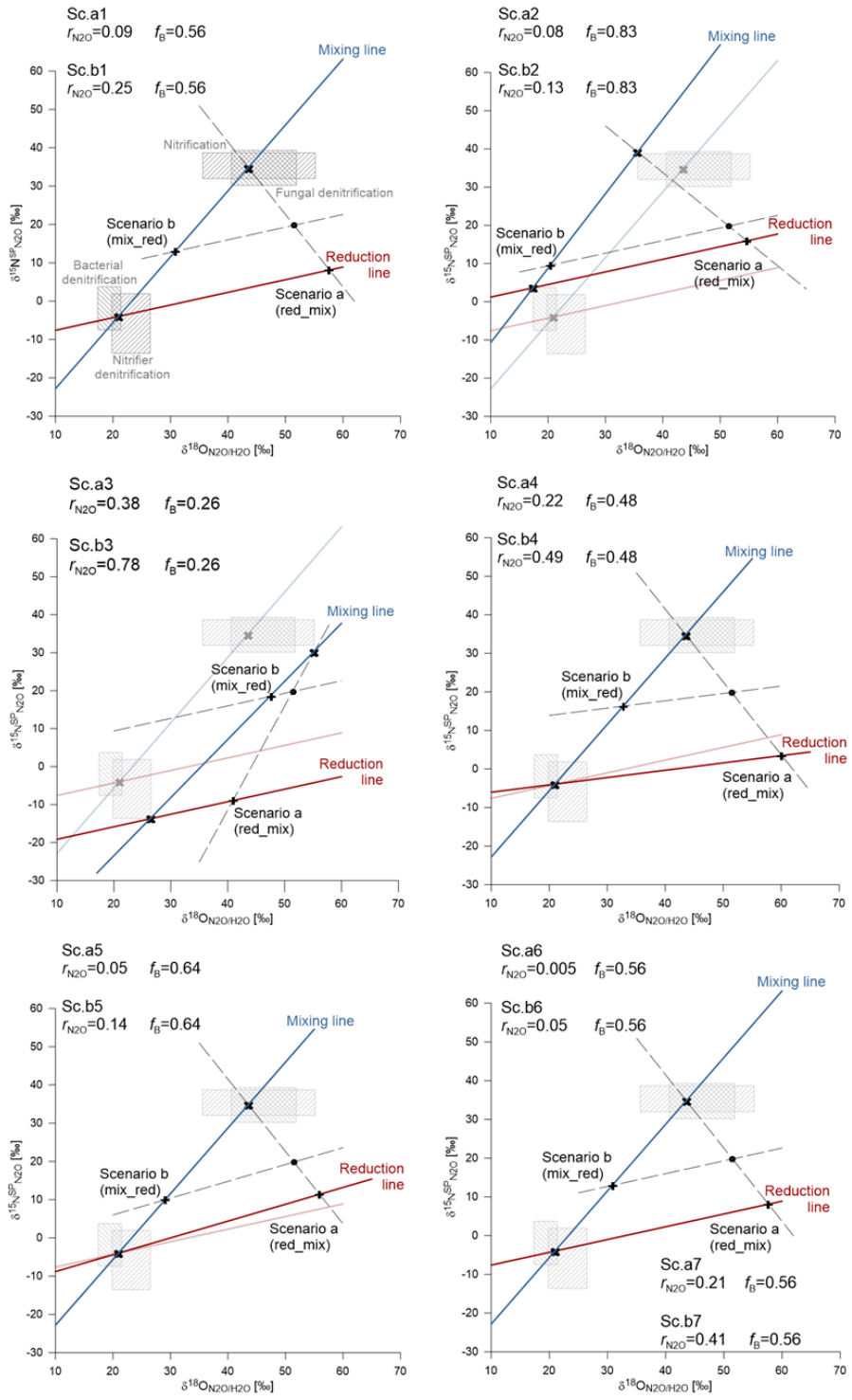

Figure A4-1: Example of scenario variations (Scenario 1-7a and Scenario 1-7b) and the calculated residual, unreduced N_2O fractions or the fractions of N_2O from heterotrophic bacterial denitrification based on one sample of the Maize treatment (September 9, 2014) with a $\delta^{18}O_{N2O/H2O}$ value of 51.5‰ and a $\delta^{15}N^{SP}_{N2O}$ value of 20.0‰

Table A4-1: Minimum and maximum values of the residual, unreduced N_2O fraction (r_{N2O}) and N_2O fraction from heterotrophic bacterial denitrification (f_B) in each Scenario (a and b) and per Scenario variation (1-7) allowing r_{N2O} or f_B values <0 or >1. The share of limited samples is given in percentage of the total data set

		r_{N2O}						f_B		
		Sc.a			Sc.b			Sc.a/b		
		Min	Max	% of total data set	Min	Max	% of total data set	Min	Max	% of total data set
Scenario variation	**Histic Gleysol**									
	1	0.00	2.34E+33	6.76	0.07	1.87	5.41	-0.73	1.02	3.38
	2	0.00	1.95	0.68	0.04	0.79	0.00	-0.53	1.32	14.19
	3	0.00	7.11E+32	45.95	0.21	7.80	64.19	-0.92	0.68	19.59
	4	0.00	1.07E+03	6.76	0.25	1.39	5.41	-0.69	0.90	2.70
	5	0.00	27.43	6.08	0.02	2.46	5.41	-0.77	1.14	4.05
	6	0.00	3.47E+72	6.76	0.00	3.89	5.41	-0.73	1.02	3.38
	7	0.00	4.65E+21	6.76	0.18	1.50	5.41	-0.73	1.02	3.38
Scenario variation	**Plaggic Anthrosol**									
	1	0.00	3.15E+02	8.53	0.12	2.14	8.53	0.06	1.14	3.88
	2	0.01	0.98	0.00	0.07	0.99	0.00	0.31	1.44	46.51
	3	0.00	5.02E+28	42.64	0.34	7.20	49.61	-0.19	0.79	6.98
	4	0.01	9.15	8.53	0.33	1.49	8.53	0.08	1.05	0.78
	5	0.00	2.26E+05	8.53	0.05	3.00	8.53	0.04	1.22	10.85
	6	0.00	2.69E+05	8.53	0.01	5.23	8.53	0.06	1.14	3.88
	7	0.02	41.89	8.53	0.26	1.64	8.53	0.06	1.14	3.88

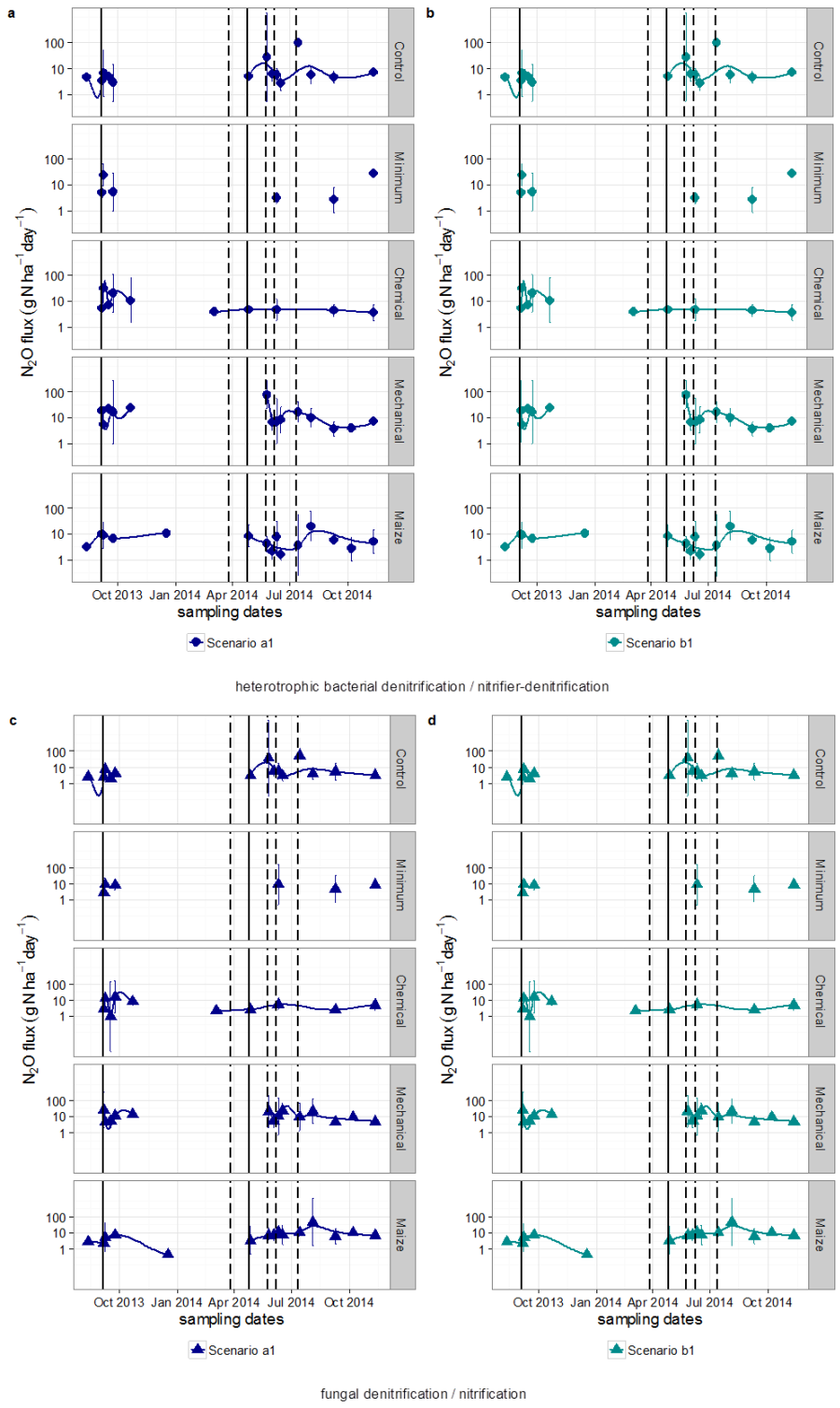

Figure A4-2: Time course of (a, b) N_2O flux from heterotrophic bacterial denitrification / nitrifier denitrification and (c, d) N_2O flux from fungal denitrification / nitrification based on calculations of Scenario a1 and b1 for the Histic Gleysol. Dates of grassland renewal and grassland conversion to maize (black lines). N fertilisation rates (100-80-60-40 kg N ha^{-1}) (dashed black lines) were the same for the treatments: *Control, Minimum, Chemical and Mechanical*. N fertilisation was different for the *Maize* plots with 150 kg N ha^{-1} each May. Error bars indicate standard deviation of the mean for sampling dates with n≥2. A non-parametric "loess" smoother was fitted (solid lines) was fitted for illustration purposes, but note that this is not a fit of the true time course of values

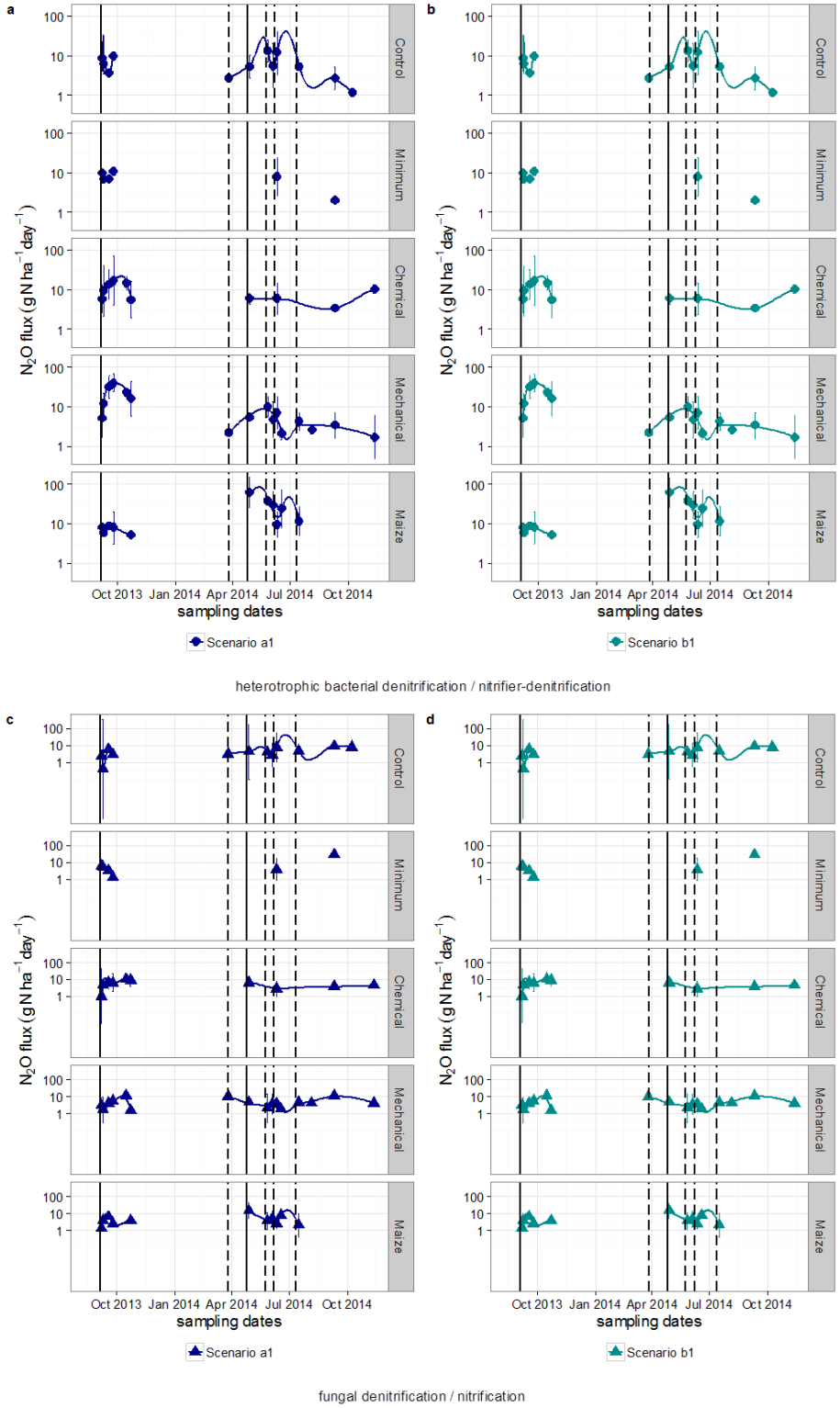

Figure A4-3: Time course of (a, b) N_2O flux from heterotrophic bacterial denitrification / nitrifier denitrification and (c, d) N_2O flux from fungal denitrification / nitrification based on calculations of Scenario a1 and b1 for the Plaggic Anthrosol. Dates of grassland renewal and grassland conversion to maize (black lines). N fertilisation rates (100-80-60-40 kg N ha^{-1}) (dashed black lines) were the same for the treatments: *Control, Minimum, Chemical and Mechanical*. N fertilisation was different for the *Maize* plots with 150 kg N ha^{-1} each May. Error bars indicate standard deviation of the mean for sampling dates with n≥2. A non-parametric "loess" smoother was fitted (solid lines) was fitted for illustration purposes, but note that this is not a fit of the true time course of values

Table A4-2: Mean values of the residual, unreduced N_2O fraction (r_{N2O}), N_2O fraction from heterotrophic bacterial denitrification (f_B) and the N_2O+N_2 flux for the scenario variations (1-7) and Scenarios (a and b) per treatment of the Histic Gleysol. Values shown are mean of treatment replicates ± one standard deviation. Mean N_2+N_2O fluxes do not represent mean values for the sites, because isotopocule values could only be determined from samples with representing high fluxes

Histic Gleysol	r_{N2O}					f_B					N_2O+N_2 flux (g N ha^{-1} day^{-1})				
Treatment	***Control***	***Minimum***	***Chemical***	***Mechanical***	***Maize***	***Control***	***Minimum***	***Chemical***	***Mechanical***	***Maize***	***Control***	***Minimum***	***Chemical***	***Mechanical***	***Maize***
n	33	17	23	33	42	33	17	23	33	42	33	17	23	33	42
Sc. a1	0.24±0.29	0.26±0.24	0.34±0.32	0.22±0.28	0.16±0.2	0.51±0.17	0.51±0.22	0.59±0.15	0.51±0.23	0.39±0.25	196±227	644±2090	134±189	1163±2487	1732±3184
Sc. b1	0.41±0.25	0.5±0.2	0.48±0.27	0.39±0.2	0.44±0.17	0.51±0.17	0.51±0.51	0.59±0.59	0.51±0.51	0.39±0.39	60±85	44±34	58±68	145±202	55±101
Sc. a2	0.13±0.11	0.16±0.12	0.21±0.17	0.13±0.13	0.12±0.16	0.78±0.18	0.77±0.22	0.85±0.13	0.76±0.21	0.63±0.25	470±1646	224±340	163±224	949±1858	784±1804
Sc. b2	0.2±0.13	0.1±0.95	0.25±0.17	0.2±0.13	0.22±0.1	0.78±0.18	0.77±0.22	0.85±0.13	0.76±0.21	0.63±0.25	122±180	66±20	116±139	290±398	116±226
Sc. a3	0.63±0.41	0.67±0.39	0.79±0.3	0.58±0.4	0.56±0.45	0.23±0.13	0.23±0.17	0.29±0.14	0.23±0.19	0.15±0.18	988±2599	946±2475	46±72	1026±2749	1257±3102
Sc. b3	0.87±0.22	0.95±0.09	0.91±0.14	0.89±0.16	0.96±0.11	0.23±0.13	0.23±0.17	0.29±0.14	0.23±0.19	0.15±0.18	32±62	20±15	27±29	52±67	27±66
Sc. a4	0.36±0.28	0.41±0.26	0.48±0.28	0.35±0.27	0.28±0.24	0.45±0.16	0.46±0.22	0.54±0.15	0.45±0.22	0.34±0.24	82±100	226±693	63±80	578±1708	1351±3084
Sc. b4	0.6±0.19	0.68±0.15	0.66±0.19	0.59±0.15	0.64±0.13	0.45±0.16	0.46±0.22	0.54±0.15	0.45±0.22	0.34±0.24	40±71	29±21	38±43	78±99	38±83
Sc. a5	0.19±0.29	0.19±0.21	0.27±0.33	0.14±0.24	0.11±0.18	0.57±0.18	0.55±0.23	0.64±0.16	0.57±0.24	0.44±0.25	358±423	801±2275	234±350	1915±3266	2130±3407
Sc. b5	0.3±0.27	0.39±0.22	0.38±0.3	0.27±0.22	0.32±0.19	0.57±0.18	0.55±0.23	0.64±0.16	0.57±0.24	0.44±0.25	96±121	66±58	91±114	263±391	79±124
Sc. a6	0.13±0.29	0.11±0.16	0.2±0.34	0.12±0.29	0.06±0.16	0.51±0.17	0.51±0.22	0.59±0.15	0.51±0.23	0.39±0.25	3038±3689	2409±3577	1494±2469	4041±4082	4197±4219
Sc. b6	0.21±0.28	0.27±0.21	0.28±0.33	0.17±0.23	0.2±0.19	0.51±0.17	0.51±0.22	0.59±0.15	0.51±0.23	0.39±0.25	290±517	139±151	215±328	736±1202	157±193
Sc. a7	0.34±0.27	0.38±0.24	0.45±0.28	0.33±0.26	0.26±0.22	0.51±0.17	0.51±0.22	0.59±0.15	0.51±0.23	0.39±0.25	81±103	125±272	67±87	314±536	518±1427
Sc. b7	0.54±0.21	0.63±0.17	0.6±0.22	0.53±0.16	0.58±0.14	0.51±0.17	0.51±0.22	0.59±0.15	0.51±0.23	0.39±0.25	44±74	32±23	42±48	92±120	42±87

Table A4-3: Mean values of the residual, unreduced N_2O fraction (r_{N2O}), N_2O fraction from heterotrophic bacterial denitrification (f_B) and the N_2O+N_2 flux for the scenario variations (1-7) and Scenarios (a and b) per treatment of the Plaggic Anthrosol. Values shown are mean of treatment replicates ± one standard deviation. Mean N_2+N_2O fluxes do not represent mean values for the sites, because isotopocule values could only be determined from samples with representing high fluxes

Plaggic Anthrosol	r_{N2O}					f_B					**N_2O+N_2 flux (g N ha^{-1} day^{-1})**				
Treatment	***Control***	***Minimum***	***Chemical***	***Mechanical***	***Maize***	***Control***	***Minimum***	***Chemical***	***Mechanical***	***Maize***	***Control***	***Minimum***	***Chemical***	***Mechanical***	***Maize***
n	22	9	29	41	28	22	9	29	41	28	22	9	29	41	28
Sc. a1	0.39±0.36	0.34±0.28	0.41±0.3	0.29±0.28	0.24±0.24	0.58±0.23	0.61±0.22	0.62±0.17	0.68±0.24	0.79±0.1	82±93	70±67	81±84	102±87	166±97
Sc. b1	0.5±0.31	0.46±0.24	0.54±0.25	0.4±0.27	0.31±0.22	0.58±0.23	0.61±0.22	0.62±0.17	0.68±0.24	0.79±0.1	36±27	38±26	41±29	67±72	116±79
Sc. a2	0.25±0.23	0.19±0.07	0.26±0.19	0.19±0.14	0.2±0.16	0.82±0.21	0.86±0.22	0.87±0.14	0.87±0.17	0.98±0.05	94±96	94±67	103±89	118±85	183±105
Sc. b2	0.3±0.25	0.25±0.16	0.29±0.18	0.15±0.81	0.18±0.17	0.82±0.21	0.86±0.22	0.87±0.14	0.87±0.17	0.98±0.05	70±55	74±52	80±58	119±112	202±118
Sc. a3	0.69±0.39	0.72±0.38	0.89±0.25	0.59±0.35	0.51±0.28	0.29±0.19	0.33±0.15	0.32±0.15	0.38±0.22	0.47±0.09	52±98	58±112	32±63	64±90	68±42
Sc. b3	0.88±0.19	0.92±0.13	0.96±0.1	0.81±0.21	0.7±0.18	0.29±0.19	0.33±0.15	0.32±0.15	0.38±0.22	0.47±0.09	15±8	17±9	19±10	26±25	44±32
Sc. a4	0.51±0.32	0.51±0.24	0.56±0.25	0.44±0.25	0.4±0.2	0.53±0.21	0.56±0.2	0.58±0.16	0.62±0.23	0.71±0.1	47±74	35±25	41±32	52±51	81±52
Sc. b4	0.66±0.22	0.65±0.17	0.71±0.17	0.59±0.2	0.52±0.16	0.53±0.21	0.56±0.2	0.58±0.16	0.62±0.23	0.71±0.1	21±14	24±12	27±17	34±32	61±45
Sc. a5	0.33±0.38	0.27±0.29	0.33±0.31	0.22±0.28	0.18±0.25	0.62±0.26	0.65±0.25	0.66±0.18	0.72±0.25	0.86±0.12	124±124	117±124	117±109	161±122	242±118
Sc. b5	0.41±0.35	0.35±0.28	0.44±0.29	0.3±0.29	0.21±0.24	0.62±0.26	0.65±0.25	0.66±0.18	0.72±0.25	0.86±0.12	61±50	62±52	62±50	114±117	199±117
Sc. a6	0.27±0.4	0.17±0.32	0.24±0.32	0.15±0.27	0.1±0.26	0.58±0.23	0.61±0.22	0.62±0.17	0.68±0.24	0.79±0.1	215±158	207±140	209±152	276±137	315±96
Sc. b6	0.32±0.38	0.25±0.3	0.33±0.31	0.22±0.3	0.13±0.26	0.58±0.23	0.61±0.22	0.62±0.17	0.68±0.24	0.79±0.1	143±130	130±129	120±105	186±146	295±107
Sc. a7	0.49±0.32	0.47±0.24	0.53±0.26	0.41±0.25	0.37±0.21	0.58±0.23	0.61±0.22	0.62±0.17	0.68±0.24	0.79±0.1	50±74	38±27	45±35	54±43	89±58
Sc. b7	0.61±0.25	0.59±0.19	0.66±0.2	0.53±0.22	0.45±0.18	0.58±0.23	0.61±0.22	0.62±0.17	0.68±0.24	0.79±0.1	24±17	27±15	30±19	41±40	72±52

Table A4-4: Potential parameters controlling N_2O transformation processes during the ^{15}N labelling experiment (^{15}N study) and the isotopocule sampling (Scenario a1/b1) for the four parallel sampling dates in June 2014. The 2-day time periods are due to 1-day delayed isotopocule samplings. Values shown are mean of treatment replicates ± one standard deviation. n=3-4. Data compilation from Buchen et al., 2016; Buchen et al.. submitted

	Treatment	***Control***		***Mechanical***		***Maize***	
	Date	**^{15}N study**	**Sc.a1/b1**	**^{15}N study**	**Sc.a1/b1**	**^{15}N study**	**Sc.a1/b1**
NO_3^--N content (kg N ha^{-1})	26 May 2014	39.67±44.5	29.63±15.19	23.72±22.32	20.82±2.22	10.1±17.27	9.07±5.62
	02-03 June2014	27.86±25.94	36.03±30.47	19.40±16.83	13.43±11.98	**9.24±9.12**	**6.49±3.54**
	09-10 June 2014	19.72±17.84	28.94±16.91	**21.46±22.32**	**17.21±10.03**	14.99±15.74	103.98±41.95
	16-17 June 2014	NA	18.92±11.18	NA	12.86±7.92	NA	37.67±15.07
NH_4^+-N content (kg N ha^{-1})	26 May 2014	7.23±16.18	4.95±5.06	32.83±14.26	32.83±14.26	123.46±148.02	44.45±25.39
	02-03 June2014	6.80±7.42	2.90±2.48	29.37±10.41	29.37±10.41	123.16±150.93	47.18±18.02
	09-10 June 2014	6.85±10.84	2.75±2.52	33.32±50.14	12.97±7.37	63.93±51.12	154.35±54.28
	16-17 June 2014	NA	4.48±5.05	NA	9.48±6.99	NA	131.05±41.88
Total N_2O flux (µg m^2 h^{-1})	26 May 2014	198.33±131.37	710.38±598.71	281.74±494.68	469.05±321.56	438.54±710.24	48.57±24.77
	02-03 June2014	259.29±288.02	50.71±11.13	132.74±161.99	55.72±27.54	**98.82±48.77**	**44.16±17.85**
	09-10 June 2014	224.69±197.07	53.22±30.16	**363.73±609.17**	**111.89±104.46**	301.04±336.27	89.86±31.18
	16-17 June 2014	592.14±636.02	25.25±14.12	44.27±47.39	143.43±79.62	45.6±46.89	44.41±22.63
gravimetric water content (%)	26 May 2014	88.08±72.48	67.49±48.74	156.97±90.78	99.64±50.91	114.03±63.85	85.62±59.77
	02-03 June2014	99.29±74.64	87.78±41.53	139.6±67.67	98.09±53.81	**107.4±49.1**	**81.72±37.4**
	09-10 June 2014	95.13±75.54	79.02±58.35	**125.87±70.54**	**81.81±63.59**	86.59±45.35	70.01±37.85
	16-17 June 2014	NA	70.66±50.51	NA	62.97±47.26	NA	60.1±31.67

NA not available

Parameters that were chosen for the comparison of r_{N2O} values from isotopocule calculations and the ^{15}N labelling experiment are marked in bold.

Danksagung

Mein Dank gilt der Deutschen Forschungsgemeinschaft für die Finanzierung dieses Promotionsprojektes im Rahmen des Graduiertenkollegs 1397 „Steuerung von Humus- und Nährstoffhaushalt in der ökologischen Landwirtschaft“.

Ganz besonders danke ich Dr. Reinhard Well für die Betreuung dieses Promotionsprojektes. Jederzeit hast du dir Zeit für Fragen genommen und mich durch deine Erfahrung und fachliche Hilfe in der Umsetzung meiner Ziele unterstützt!

Großer Dank geht auch an Prof. Heinz Flessa, der ebenfalls an der Konzeption des Projektes mitgewirkt hat und mich durch seinen fachlichen Rat maßgeblich unterstützt hat.

Bei Herrn Prof. Rolf Nieder möchte ich mich für die externe Betreuung dieser Promotionsarbeit, seine hilfreichen Ratschläge und für sein Engagement im Promotionsgremium bedanken. Des Weiteren danke ich Herrn Prof. Stephan Weber für die Bereitschaft als Prüfer dieser Arbeit zu fungieren, Frau Prof. Antje Schwalb für die Übernahme des Vorsitzes der Prüfungskommission und Herrn Prof. Harald Biester für die Bereitschaft, gegebenenfalls einzuspringen.

Dr. Anette Giesemann danke ich für die Einführung in das neue Themenfeld der Massenspektrometrie und auch für zahlreiche Diskussionen über Proben, Messungen und Ergebnisse, sowie ein jederzeit offenes Ohr.

Ich möchte mich zudem bei Dr. Mirjam Helfrich für fachliche Ratschläge und aufmunternde Gespräche, bei Dr. Andreas Gensior für fachliche und praktische Hilfe in Sachen Bodenbeprobung und bei Dr. Roland Fuß für seine Hilfe bei statistischen Fragestellungen, bedanken.

Dr. Matthias Benke und seinem Team vom Fachbereich Grünland und Futterbau der Landwirtschaftskammer Oldenburg danke ich für die unkomplizierte und freundliche Zusammenarbeit: Felicitas Kaemena für die Organisation; Stephan Freese und Peter Gatersleben für ihre Hilfe bei der Probenahme von Gas- und Bodenproben; Christian Thomßen, Robert Klippert und dem Team der Versuchsdurchführung Pflanzenbau für die Anlage und Bewirtschaftung der Versuchsflächen; den Landwirten Peter Beeken, Jens Geveke und Hauke Heeren für die Überlassung der Flächen.

Dr. Manfred Kayser danke ich für seine fachliche Unterstützung, viele Telefonate und Diskussionen, sowie dem Laborteam von Uwe Vehlow der Universität Göttingen-Vechta für die Bearbeitung unzähliger N_{min} Proben.

Vom Feld bis zur fertigen Publikation ist es ein weiter Weg und viele helfende Hände wurden benötigt. Für den Einsatz im Feld möchte ich mich ganz besonders bei den beiden Technikern Frank Hegewald, Steffen Scheller und Peter Braunisch bedanken. Weiterhin gilt mein Dank dem Team des Isotopen- und Zentrallabors am Thünen-institut für Agrarklimaschutz, insbesondere Martina Heuer, Ute, Rieß, Kerstin Gilke, Andrea Oehns- Rittgerodt, Sabine Wathsack, Regina Lausch, Ute Tambor, Monika Zerbian und Susanne Behn, die mich bei der Durchführung meiner Versuche und unzähligen Proben unterstützt haben und ohne die es nicht machbar gewesen wäre. Insgesamt durfte ich eine tolle Arbeitsatmosphäre erleben!

Bei Prof. Bernhard Ludwig und Marion Höck möchte ich mich für die Unterstützung am Institut für Umweltchemie der Universität Kassel bedanken, bei der das Graduiertenkolleg angesiedelt war. Mein Dank gilt insbesondere meinen dort lieb gewonnen Kollegiatinnen und Kollegiaten, besonders Anja Nüsse.

Dr. Dominika Lewicka-Szczebak danke ich für ihre fachliche Hilfe und ihre vielfältige Unterstützung bei der Durchführung von Versuchen und dessen Auswertung. Vielen Dank für die schöne Zeit, in der wir uns ein Büro teilen durften.

Bei Dr. Lena Rohe, Dr. Marianna Deppe und Dr. Jasmin Miltz bedanke ich mich für viele freundschaftliche und fachliche Gespräche, gepaart mit vielen Hilfestellungen des täglichen Doktorandenlebens.

Schließlich bedanke ich mich bei meinen Eltern, meiner Schwester, meinen Omis und meinem Freund für eure Unterstützung in allen Lebenslagen und euer Vertrauen in mich!

Curriculum vitae

Personal details

Name	Caroline Buchen
Date of birth	June 3, 1987 in Siegen
Nationality	German

Education

2013 - 2017	**Technical University Braunschweig**, Germany Graduate studies „Geoecology“ Prof. Dr. Rolf Nieder (Institute of Geoecology - Soil Science and Soil Physics)
2013 - 2015	**University of Kassel, Witzenhausen**, Germany Member of the DFG Research Training Group 1397 “Regulation of soil organic matter and nutrient turnover in agriculture”
2009 - 2012	**Justus Liebig University**, **Giessen**, Germany Master of Science in Environmental and Resources Management Master thesis “Automatic quantification of water and nitrogen fluxes in differently managed rice paddy systems” Prof. Dr. Lutz Breuer and Prof. Dr. Hans-Georg Frede (Institute of Landscape Ecology and Resources Management)
2010 - 2011	**University of Natural Resources and Life Science**, **Vienna**, Austria Master program with ERASMUS: Water Management and Environmental Engineering
2006 - 2009	**Justus Liebig University**, **Giessen**, Germany Bachelor of Science in Agricultural Sciences and Environmental Management Bachelor thesis “15 Jahre Kooperation Bergisches Land an der Wiehltalsperre - Wie haben sich Nitratkonzentrationen und –frachten verändert?” Prof. Dr. Hans-Georg Frede and Dr. Martin Bach (Institute of Landscape Ecology and Resources Management)
1996 - 2006	**Hollenberg Gymnasium Waldbröl**, Germany A-level

List of publications

Buchen, C., Lewicka-Szczebak, D., Fuss, R., Helfrich, M., Flessa, H., Well, R., 2016. Fluxes of N_2 and N_2O and contributing processes in summer after grassland renewal and grassland conversion to maize cropping on a Plaggic Anthrosol and a Histic Gleysol." Soil Biology and Biochemistry 101, 6-19.

Heinz, E., Kraft, P., Buchen, C., Frede, H., Aquino, E., Breuer, L., 2013. Set Up of an automatic water quality sampling system in irrigation agriculture. Sensors 14, 212-228.

Selected conference abstracts

Buchen, C., Benke, M., Flessa, H., Gensior, A., Helfrich, M., Kayser, M., Well, R. (2016). Greenhouse gas fluxes and mineral N dynamics following grassland renewal or conversion to arable land. In Book of Abstracts. 19th Nitrogen Workshop, Skara, Sweden (Poster presentation)

Buchen, C., Benke, M., Flessa, H., Gensior, A., Helfrich, M., Kayser, M., Well, R. (2015). Greenhouse gas fluxes and mineral N dynamics following grassland renewal or conversion to arable land. In Book of Abstracts. DFG-Workshop, Witzenhausen (Oral presentation)

Buchen, C., Benke, M., Flessa, H., Gensior, A., Helfrich, M., Kayser, M., Lewicka-Szczebak, D., Well, R. (2015). Einfluss verschiedener Grünlanderneuerungstechniken auf N_2O Emissionen und NO_3^- Dynamik. In DBG Abstracts, Munich (Poster presentation)

Buchen, C., Eschenbach, W., Flessa, H., Giesemann, A., Lewicka-Szczebak, D., & Well, R. (2015). Measuring denitrification after grassland renewal and grassland conversion to cropland by using the ^{15}N gas-flux method. In Geophysical Research Abstracts (Vol. 17, EGU2015-6006) (Oral presentation)

Buchen, C., Benke, M., Helfrich, M., Flessa, H., Kayser, M., Well, R. (2014) Impact of grassland renovation practices on N_2O emissions and nitrate dynamics. In Book of Abstracts. Non CO_2 Greenhouse Gas Symposium, NCGG7, Antwerp (Oral presentation)

Buchen, C., Flessa, H., Giesemann, A., Lewicka-Szczebak, D., Well, R. (2014) Methodenvergleich zur Bestimmung der Denitrifikation im Freiland - ^{15}N Tracertechnik vs. Isotopomere. In Book of Abstracts. ASI-Jahrestagung Munich (Poster presentation)

Buchen, C., Flessa, H., Helfrich, M., Poeplau, C., Well, R. (2013) Nitrogen losses during grassland renovation and conversion to arable land– A review for temperate soils. In Book of Abstracts. Open Science Conference. Greenhouse Gas Management in European Land Use Systems (p. 14) (Poster presentation)

Declaration of Authorship

The three main chapters (3 to 4) of this thesis comprise individual studies intended to be published as the following research papers:

- **Chapter 2**: Soil mineral N dynamics and N_2O emission following grassland renewal is submitted and currently under review in Agriculture, Ecosystems and Environment.
- **Chapter 3**: Fluxes of N_2 and N_2O and contributing processes in summer after grassland renewal and grassland conversion to maize cropping on a Plaggic Anthrosol and a Histic Gleysol is already published in Soil Biology and Biochemistry.
- **Chapter 4**: Estimating N_2O processes during grassland renewal and grassland conversion to maize cropping using N_2O isotopocules is intended for submission in Biogeoscience.

I am the lead author, but not the only author of these three articles. To declare my contribution to the individual phases of the three studies, the following scale was used:

A: I contributed to the work (0-33%)

B: I made a substantial contribution (34-66%)

C: I did the majority of the work independently (67-100%)

It is applied to four categories:

- **Concept:** Drafting of the basic scientific problem and identification of knowledge/research gaps, which will be answerable via analyses or concrete experiments/investigations
- **Planning:** Planning of experiments/analyses and formulation of investigative methodologies, including choice of method and independent methodological development, in such a way that the scientific questions asked can be expected to be answered
- **Execution:** Involvement in the analysis or the concrete experiments/investigation
- **Manuscript:** Presentation, interpretation and discussion of the results obtained in article form

	Concept	**Planning**	**Execution**	**Manuscript**
Chapter 2	A	B	C	C
Chapter 3	A	B	C	C
Chapter 4	A	B	C	C